



AD-A266 384

Technical Report CERC-93-6

April 1993

2

**US Army Corps
of Engineers**
Waterways Experiment
Station

Observations and Modelling of Winds and Waves During the Surface Wave Dynamics Experiment

Report 1

Intensive Observation Period IOP-1

20-31 October 1990

by Michael J. Caruso
Woods Hole Oceanographic Institution

Hans C. Graber
University of Miami

*Robert E. Jensen
Coastal Engineering Research Center*

Mark A. Donelan
Canada Centre for Inland Waters

DTIC
SELECTED
JUL 01 1993
D

Approved For Public Release: Distribution Is Unlimited

93 6 22 054

93-14802

A standard linear barcode is positioned horizontally across the page. To its right, handwritten in black ink, is the number '200'.

Prepared for Headquarters, U.S. Army Corps of Engineers

Under Upgrading of Discrete Spectral Hindcasting Models
Work Unit 32523
Office of Naval Research Contracts N00014-90-J-146
N00014-92-J-1546, and N00014-88-J-1028



The contents of this report are not to be used for advertising, publication, or promotional purposes. Citation of trade names does not constitute an official endorsement or approval of the use of such commercial products.



PRINTED ON RECYCLED PAPER

Observations and Modelling of Winds and Waves During the Surface Wave Dynamics Experiment

Report 1

Intensive Observation Period IOP-1

20-31 October 1990

DTIC QUALITY EVALUATED 5

by Michael J. Caruso

Department of Physical Oceanography
Woods Hole Oceanographic Institution, Woods Hole, MA 02543

Hans C. Graber
Rosenstiel School of Marine and Atmospheric Science
University of Miami, Miami, FL 33149-1098

Robert E. Jensen
Coastal Engineering Research Center
U.S. Army Corps of Engineers
Waterways Experiment Station
3909 Halls Ferry Road, Vicksburg, MS 39180-6199

Mark A. Donelan

National Water Research Institute
Canada Centre for Inland Waters, Burlington, Ontario L7R 4A6, Canada

Accession For	
NTIS	CR&I
DTIC	TAB
Unannounced	
Justification	
By _____	
Distribution / _____	
Availability Codes	
Dist	Avail and/or Special
A-1	

Report 1 of a series

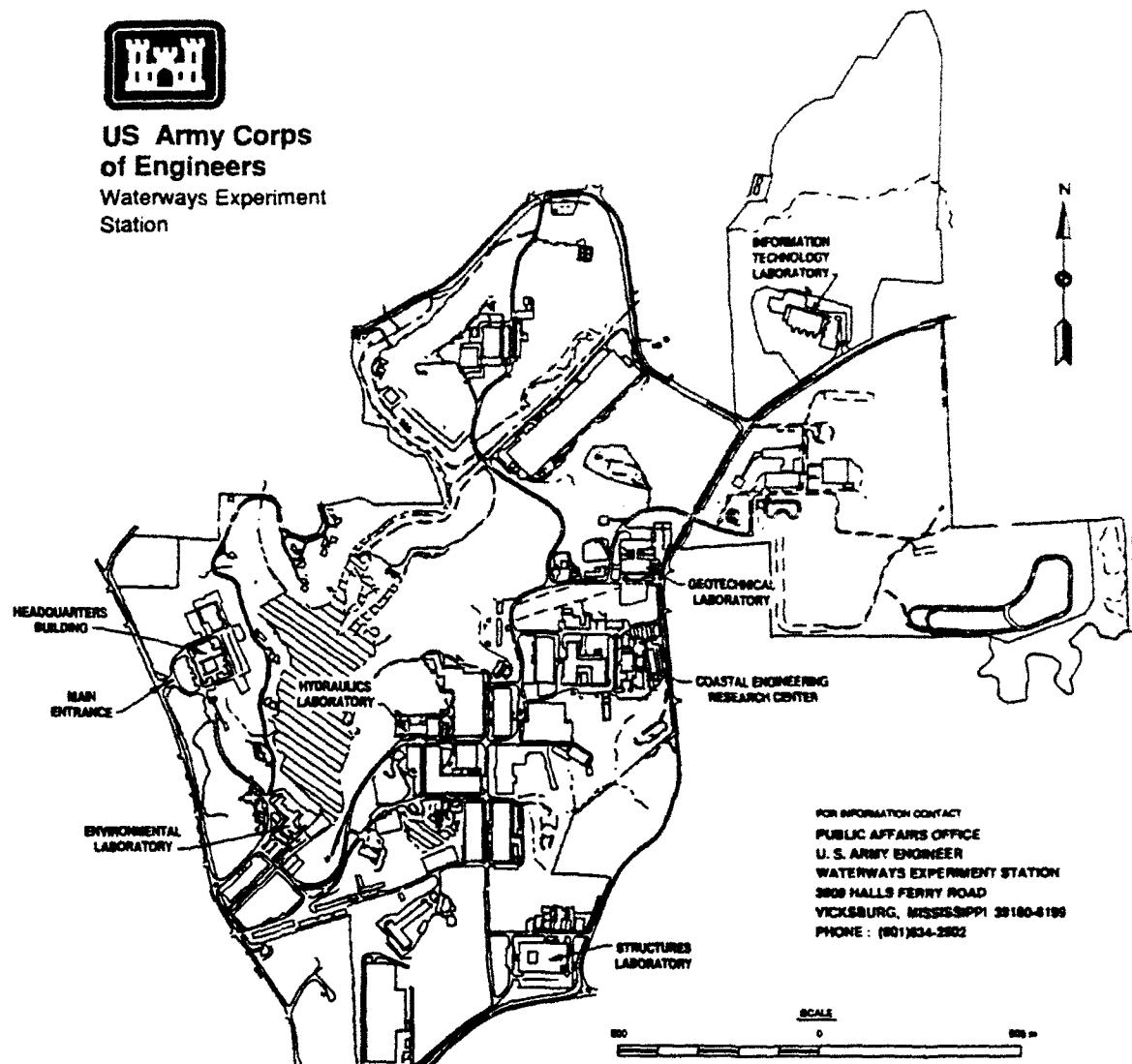
Approved for public release; distribution is unlimited

Prepared for U.S. Army Corps of Engineers
Washington, DC 20314-1000

Under Office of Naval Research Contracts N00014-90-J-1464,
N00014-92-J-1546, and N00014-88-J-1028
Upgrading of Discrete Spectral Hindcasting Models Work Unit 32523



US Army Corps
of Engineers
Waterways Experiment
Station



Waterways Experiment Station Cataloging-in-Publication Data

Observations and modelling of winds and waves during the surface wave dynamics experiment. Report 1, Intensive observation period
IOP-1 : 20-31 October 1990 / by Michael J. Caruso ... [et al.], Coastal Engineering Research Center ; prepared for U.S. Army Corps of Engineers.

206 p. : ill. ; 28 cm. — (Technical report ; CERC-93-6)

Includes bibliographical references.

1. Ocean waves — Atlantic Ocean. 2. Ocean-atmosphere interaction — Atlantic Ocean. 3. Oceanographic buoys. 4. Winds — Atlantic Ocean. I. Caruso, Michael J. II. United States. Army. Corps of Engineers. III. Coastal Engineering Research Center (U.S.) IV. U.S. Army Engineer Waterways Experiment Station. V. Series: Technical report (U.S. Army Engineer Waterways Experiment Station) ; CERC-93-6.

TA7 W34 no.CERC-93-6

Contents

Preface	v
1 Introduction	1
2 Buoy Measurements	2
SWADE buoys	2
Meteorological buoys	7
3 Ocean Wave Modeling	13
4 Model Domain and Grids	14
Atlantic Basin Model	14
Western North Atlantic Model	14
SWADE Model	14
5 Wind Fields	18
FNOC	18
ECMWF	18
NMC/GSFC	19
OW/AES	19
UKMO	20
6 Surface Currents	21
7 The SWADE Storm	22
8 Summary	26
References	27
Appendix A: Time Series from SWADE and NDBC Buoys	A1
Appendix B: Directional Wave Spectra from SWADE Buoys	B1
B.1 Discus Buoy "North"	B3
B.2 Discus Buoy "East"	B11
B.3 Discus Buoy "CERC"	B25
Appendix C: Time Series from MiniMet Buoys	C1
Appendix D: Custer Diagrams of Wind Fields and Wave Hindcasts	D1
D.1 Oceanweather/Atmospheric Environment Service (OW/AES)	D3
D.2 Fleet Numerical Oceanographic Center (FNOC)	D23
D.3 European Centre for Medium-Range Weather Forecasts (ECMWF)	D37
D.4 National Meteorological Center (NMC)	D51

D.4	National Meteorological Center (NMC)	D51
D.5	NASA Goddard Space Flight Facility (GSFC)	D65
D.6	United Kingdom Meteorological Office (UKMO)	D79
Appendix E: Custer Diagrams of Surface Current Fields		E1

List of Figures

1	A modified SWADE/NDBC 3-m discus buoy.	3
2	A modified SWADE/MiniMet buoy.	4
3	A WAVESCAN directional wave buoy.	5
4	The Brookhaven spar buoy.	6
5	Geographic location of the <i>SWADE</i> program and the positions of the buoys.	8
6	Geographic location of the <i>SWADE</i> buoys embedded within the network of buoys and C-MAN stations maintained by the National Data Buoy Center.	9
7	Drift track of MET-1 from September 1990 to April 1991.	11
8	Drift track of MET-2 from September 1990 to December 1990.	12
9	Drift track of MET-4 from September 1990 to May 1991.	12
10	Atlantic Ocean basin-scale model grid.	15
11	Western North Atlantic regional model grid.	16
12	Fine Mesh <i>SWADE</i> model grid.	17
13	Surface analysis of 26 October 1990 at 18:00 UTC (from Cardone et al. (1993))	23
14	Storm track of central pressure position of "SWADE Storm" (from Morris (1991)).	24

List of Tables

1	Deployment positions and logistics for <i>SWADE</i> buoys.	2
2	Measurement characteristics of meteorological variables on NDBC 3-m discus buoys (after Steele et al. 1992).	7

Preface

The authors gratefully acknowledge funding support by the Small-Scale Physics Program (Code 1122SS) at the Office of Naval Research (ONR) under Grant Nos. N00014-90-J-1464, N00014-92-J-1546, and N00014-88-J-1028. Support for shiptime of the R/V *Oceanus* was pooled and provided by Codes 1122SS and 1125OA at ONR.

This study was authorized by Headquarters, U.S. Army Corps of Engineers (HQUSACE), under Civil Works Research Work Unit 32523, Upgrading of Discrete Spectral Hindcasting Models, Coastal Flooding Program. Messrs. John H. Lockhart, Jr., John G. Housley, Barry W. Holliday, and David A. Roellig were HQUSACE Technical Monitors. This report was prepared by Mr. Michael J. Caruso, Woods Hole Oceanographic Institution (WHOI), Dr. Hans C. Graber, Rosenstiel School of Marine and Atmospheric Science (RSMAS), University of Miami, Dr. Robert E. Jensen, U.S. Army Engineer Waterways Experiment Station (WES) Coastal Engineering Research Center (CERC), and Dr. Mark A. Donelan, National Water Research Institute, Canada Centre for Inland Waters (CCIW). Dr. Jensen's work was carried out under the program management of Dr. C. Linwood Vincent and Ms. Carolyn Holmes, CERC, and under the direct supervision of Dr. M. C. Miller, Chief, Coastal Oceanography Branch, and Mr. H. Lee Butler, Chief, Research Division; and under the general supervision of Dr. James R. Houston and Mr. Charles C. Calhoun, Jr., Director and Assistant Director, CERC, respectively. This report was edited by Ms. Janean Shirley, Information Technology Laboratory, WES.

John Kemp and John Bouthillette, WHOI, and the entire crew of the R/V *Oceanus* are thanked for superb work during the deployment and recovery phases as well as during several repair/maintenance trips. The authors are grateful to the Command of the International Ice Patrol, Groton, CT, and the crew of the USGS *Bittersweet* who came through in the last minute to recover one of the adrift MET buoys. Peter Cornillon, University of Rhode Island, kindly provided the data set on the position of the Gulf Stream. The personnel of the National Data Buoy Center, especially Kenneth Steele, Ed Michelena, Lloyd Ladner, Bill Beacht, Jim Patterson, David Wittdorf, and Capt. Ted Colburn, now at the U.S. Coast Guard in Groton, CT, provided around the clock support during all phases of the field experiment. Joe Gabriele, Roland Desrosiers, and Harry Savile, CCIW, worked tirelessly to keep all systems going and were always available to lend a hand.

The authors extend special thanks to the following: Models Division of the Fleet Numerical Oceanography Center, National Meteorological Center of the National Weather Service (Dr. W.H. Gemmill), the Global Modeling and Simulation Branch, Goddard Space Flight Center/National Aeronautics and Space Administration (Dr. D. Duffy), the European Center for Medium Range Weather Forecasts, the United Kingdom Meteorological Office, and the Atmospheric Environment Service of Environment Canada, funding work conducted by Dr. V.J. Cardone, Oceanweather, Inc. The authors are also grateful to Ram Vakkayil and Louis Chemi, RSMAS, for producing the numerous plots.

Finally, continuous support and helpful advice provided by Dr. Melbourne G. Briscoe, now at NOAA, Dr. Alan Brandt, ONR, and Dr. C. Linwood Vincent, CERC, were always welcomed and appreciated.

1 Introduction

The primary scientific goals of the Surface Wave Dynamics Experiment (*SWADE*) are to understand the dynamics of the evolution of the directional wind-wave spectrum and the effect of waves on fluxes of momentum, heat and mass at the air-sea interface. A detailed discussion of the scientific and experimental objectives as well as a description of the measurement systems and sensors can be found in Weller *et al.* (1991). The experiment began on October 1, 1990 and lasted for a six-month period in the waters off the DelMarVa Peninsula. During three intensive observation periods (IOPs) the in-situ measurements from buoys were complemented by radar and remote sensing observations from aircraft and a ship.

An improved understanding of the evolution of the directional wave spectrum under a variety of spatially and temporally inhomogeneous wind fields will make it possible to determine and develop better parameterizations of the source term physics in numerical wind-wave models. Unlike previous field experiments (e.g. JONSWAP, ARSLOE) *SWADE* will provide wind data from a spatially dense array of buoys, which were deployed between Cape Hatteras and Cape Cod. The wind forcing field still remains the largest source of error in our capability to predict the directional wave field and hence the sea state. An improved specification of the wind field will be suitable for examining the physics of the source functions for wind energy input, nonlinear wave-wave interactions and dissipation by breaking.

Buoy measurements are summarized in Chapter 2. A brief description of the third-generation wave model (WAM) model is given in Chapter 3; the model domains used during *SWADE* are discussed in Chapter 4; the six wind fields are briefly described in Chapter 5; the model currents are described in Chapter 6; and finally some details of the first Intense Observation Period (IOP-1) are presented in Chapter 7. The appendices will present time series of meteorological and wave parameters, plots of directional wave spectra, maps of wind vector fields and the associated wave hindcasts, and maps of the modelled surface current fields.

2 Buoy Measurements

SWADE buoys

In addition to the existing operational network of buoys maintained by the National Data Buoy Center (NDBC), SWADE deployed two 3-m discus buoys with several modifications to their measuring capability (Figure 1), four MiniMet meteorological buoys (Figure 2), and one WAVESCAN directional wave buoy provided by SEATEX, Norway (Figure 3). The modified Mills-cross array was designed to provide spatial estimates of the variation in wave, wind, and flux data. At its center was the Brookhaven Spar buoy (Figure 4) which was instrumented with a centered pentagon wave gage array to measure high resolution directional wave spectra. Unfortunately, the Spar buoy sank after the peak of the October Storm on October 26, 1990. The Spar buoy was replaced by another 3-m discus buoy provided by NDBC and by the SWATH (Small Water Plane Area - Twin Hull) ship, *Frederick G. Creed*, from the Canadian Department of Fisheries and Oceans. The SWATH was used as a mobile research platform and with its special equipment could perform almost all tasks expected of the Spar (Donelan *et al.* 1992). The U.S. Army Engineer Waterways Experiment Station Coastal Engineering Research Center (CERC) and the Woods Hole Oceanographic Institution (WHOI) also contributed to SWADE, each providing a 3-m discus buoy. Figure 5 shows the locations of the SWADE experimental measurement array. Table 1 summarizes the deployment logistics for these buoys. Most buoys were deployed by the end of September from R/V *Oceanus*.

Table 1
Deployment positions and logistics for SWADE buoys.

Station	WMO Code	Latitude	Longitude	Depth	Comments
Spar		37° 30.1' N	74° 21.5' W	200 m	Sank on 10-26-90 Recovered in June 1992
D-East	44015	37° 06.8' N	73° 36.9' W	2,790 m	Adrift on 1-19-91
		37° 29.0' N	73° 23.9' W	2,469 m	Reset on 1-24-91
D-North	44001	38° 22.1' N	73° 33.5' W	115 m	
D-Central	44023	37° 32.1' N	74° 23.5' W	102 m	Replaced Spar
MET-1	41012	35° 15.0' N	70° 00.0' W	4,572 m	Adrift on 10-3-90
	41014				Recovered 4-5-91
MET-2	44018	37° 41.3' N	74° 43.2' W	49 m	Adrift on 10-27-90
	44022				ARGOS lost on 11-12-90
MET-3	44018	37° 59.9' N	72° 54.7' W	2,617 m	Equipped with Wotan
	44020				
MET-4	44017	40° 06.1' N	72° 14.3' W	77 m	Adrift on 11-19-90
	44021				Recovered 5-28-91
CERC	44014	36° 35.0' N	74° 50.0' W	48 m	
WAVESCAN		38° 56.8' N	73° 10.8' W	79 m	GOES stops on 1-29-91
IMET		37° 25.0' N	73° 48.0' W	2,101 m	Damaged on 10-26-90

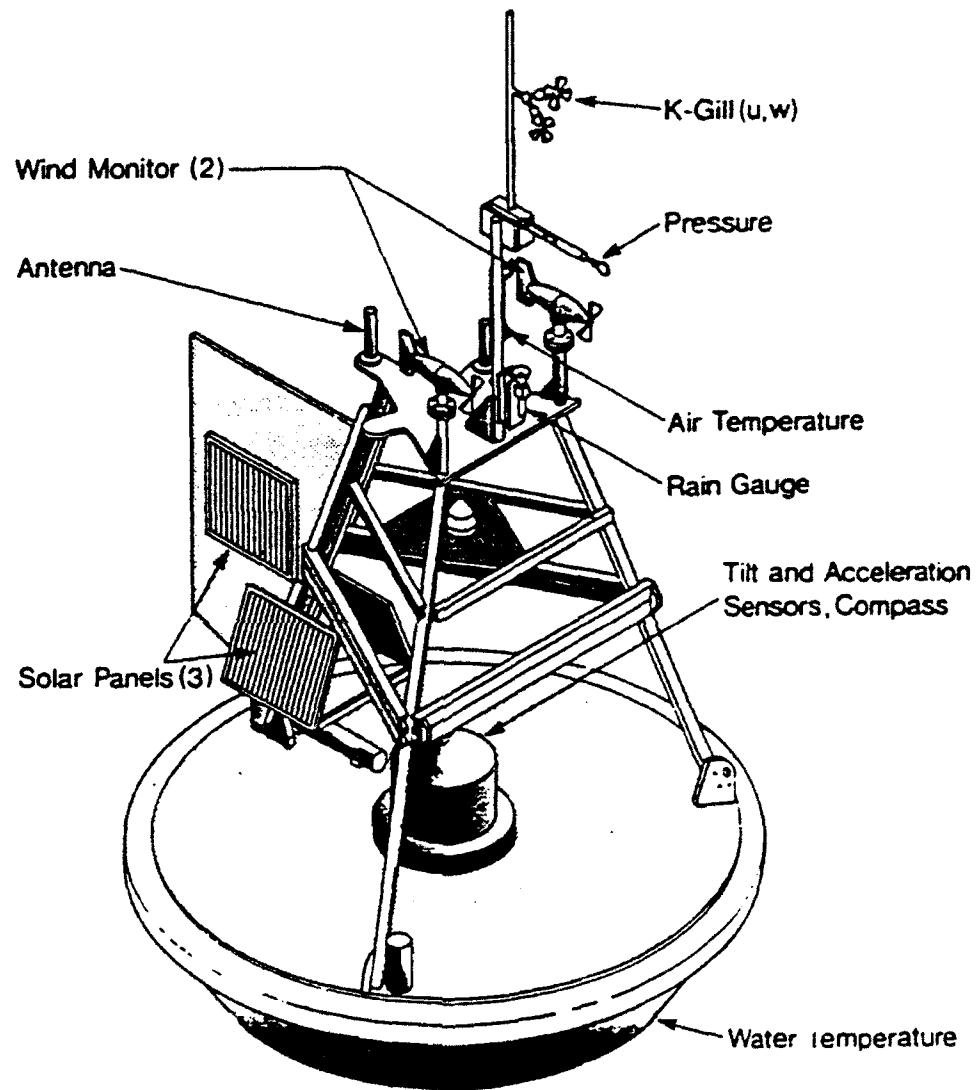


Figure 1: A modified SWADE/NDBC 3-m discus buoy.

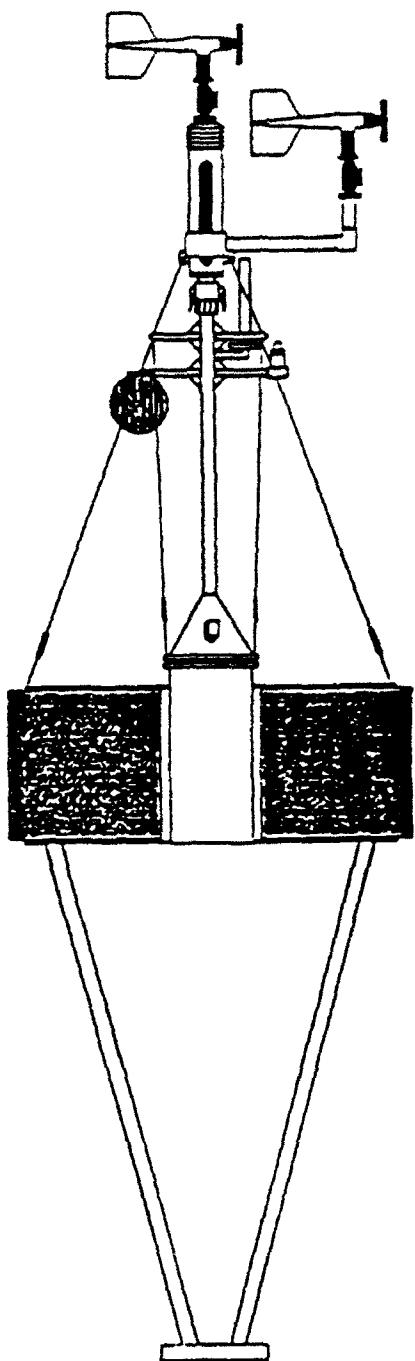


Figure 2: A modified SWADE/MiniMet buoy.

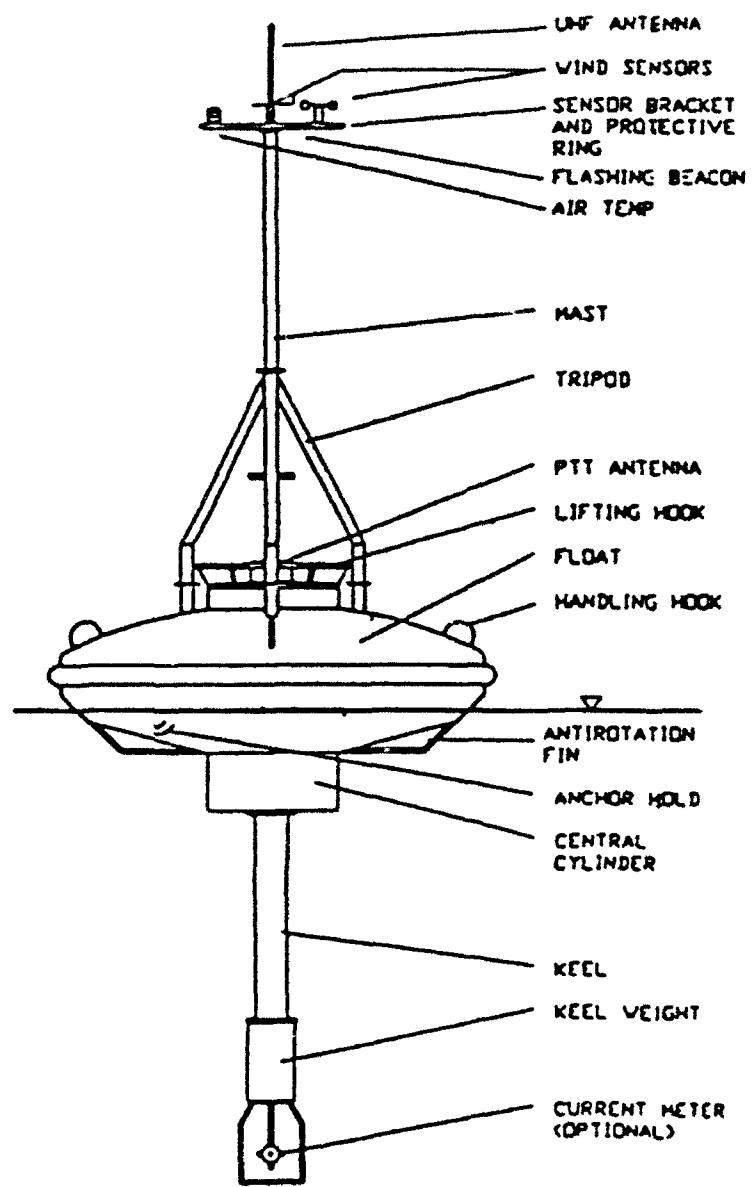


Figure 3: A WAVESCAN directional wave buoy.

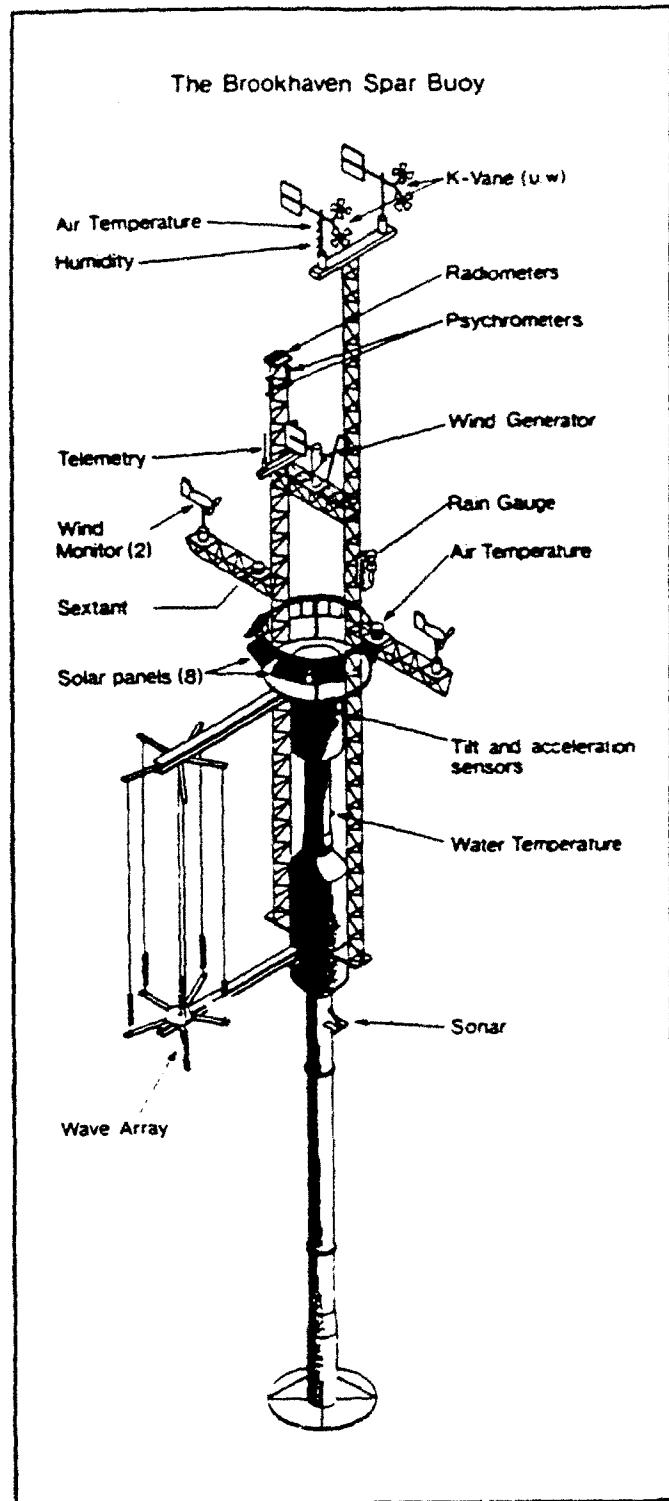


Figure 4: The length of the spar measures 30 m from the K-vane anemometers to the bottom drag plates. The K-vanes are installed at a height of 10 m and the wind anemometers are at 6 m. The wire wave gauges measure 6 m in length.

Data from the buoys listed above as well as all NDBC buoys and C-MAN stations along the East Coast (Figure 6) are available for the entire *SWADE* experimental period and have been archived at the National Aero. autics and Space Administration (NASA)/Wallops Data Archive Center (Oberholtzer and Donelan 1993). The NDBC portion of the buoy instrumentation transmits hourly values of wind speed and direction (two sensors), atmospheric pressure, air and water temperature, significant wave height, average and dominant wave period. In addition, the covariance spectra for directional wave data as a function of frequency are also transmitted. The Canada Centre for Inland Waters (CCIW) motion sensor packages and K-Gill anemometers sampled data continuously at 1 Hz and stored the data internally on five 120-Mbyte laser disks. A summary of the sampling interval, recording period and system accuracy is presented in Table 2. For details on the buoy sensors and calibration procedures, the reader is referred to Steele, Teng, and Wang (1992).

In Appendix A, time history plots of wind speed and direction, significant wave height, peak wave period, atmospheric pressure, air and sea temperature are presented for IOP-1 from *SWADE* buoys D-East and D-North and CERC (44014). In addition, time series of these variables are also shown for buoys 41001, 44004, 44008, 44009, 44011, 44012 and the C-MAN stations DSLN7, CHLV2 and BUZM3.

In Appendix B, plots of the directional wave spectra and the associated one-dimensional frequency spectra are presented for buoys D-East, D-North and CERC (44014) every 3 hr from 24 October 1990, 03:00 GMT to 29 October 1990, 00:00 GMT during IOP-1. The directional wave spectra were computed with a maximum-likelihood technique described in Drennan, Gruber, and Donelan (1993). Note there are several data gaps for buoy D-North.

Table 2
Measurement characteristics of meteorological variables
on NDBC 3-m discus buoys (after Steele et al. 1992).

Parameter	Range	Resolution	Sample interval	Sample period	Total system accuracy
Wind speed	0-80 ms^{-1}	0.1 ms^{-1}	1 sec	8 min	$\pm 1 \text{ ms}^{-1}$ or 10%
Wind direction	0-360°	1°	1 sec	8 min	$\pm 10^\circ$
Wind gust*	0-80 ms^{-1}	0.1 ms^{-1}	1 sec	5 sec	$\pm 1 \text{ ms}^{-1}$ or 10%
Air temperature	-40 to 50 °C	0.5 °C	90 sec	90 sec	$\pm 1^\circ\text{C}$
Sea surface temperature	-15 to 50 °C	0.5 °C	1 sec	1 sec	$\pm 1^\circ\text{C}$
Barometric pressure	900-1100 hPa (mb)	0.1 hPa (mb)	4 sec	8 min	$\pm 1\text{hPa}$ (mb)

* Highest 5-sec window average

Meteorological buoys

Four modified MiniMet buoys were deployed to improve the capability to measure the spatial mesoscale variability in the wind field. These buoys were placed along the axes of the modified Mills-cross to increase the number of spatial lags for the wind measurements both along west-east and south-north directions. Unfortunately, the environmental harshness

SWADE MEASUREMENT ARRAY

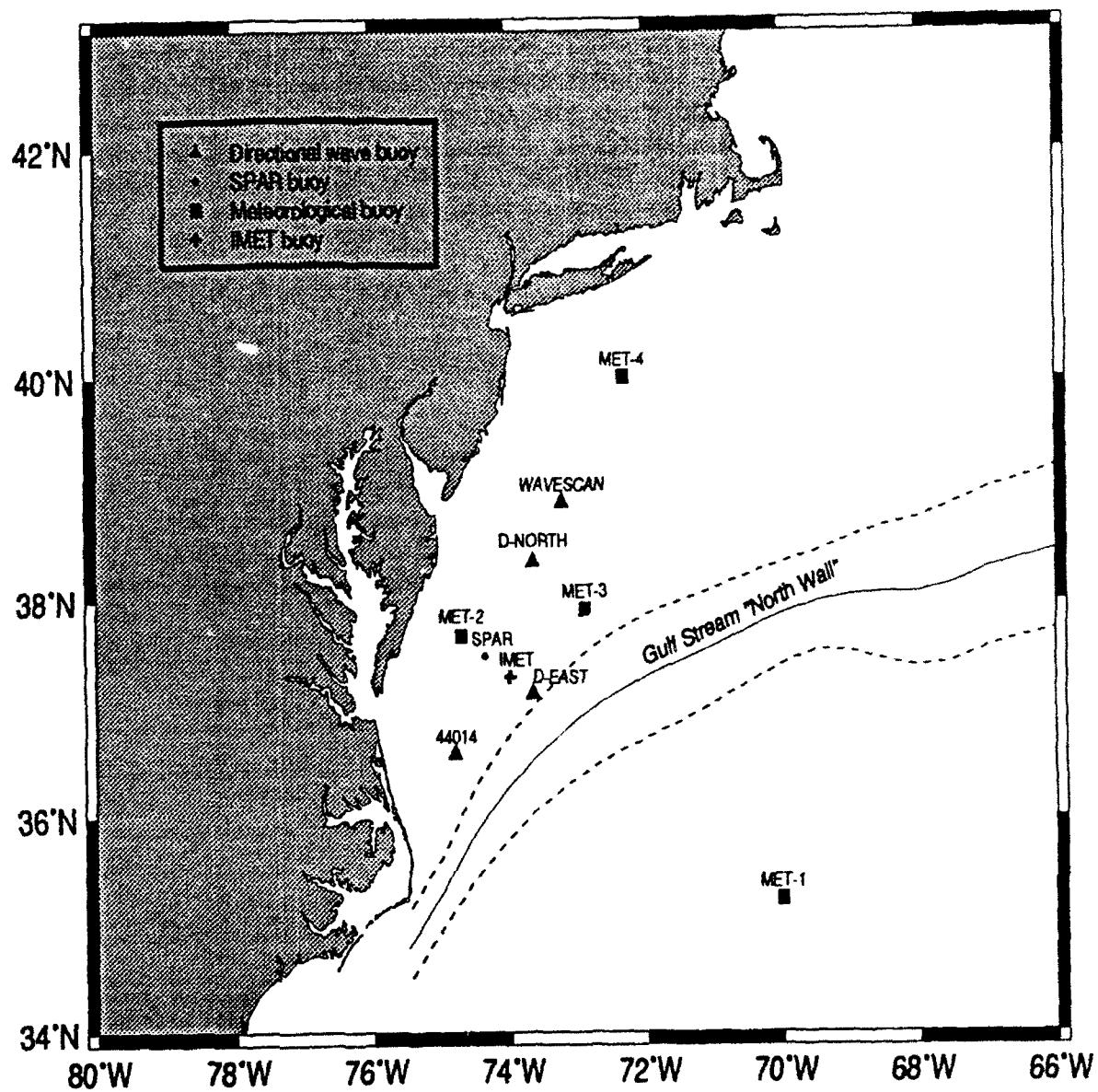


Figure 5: Geographic location of the SWADE program and the positions of the buoys during IOP-1. The mean (solid) and one standard deviation (dashed) positions of the "North Wall" of the Gulf Stream are also shown.

NDBC AND SWADE BUOY LOCATIONS

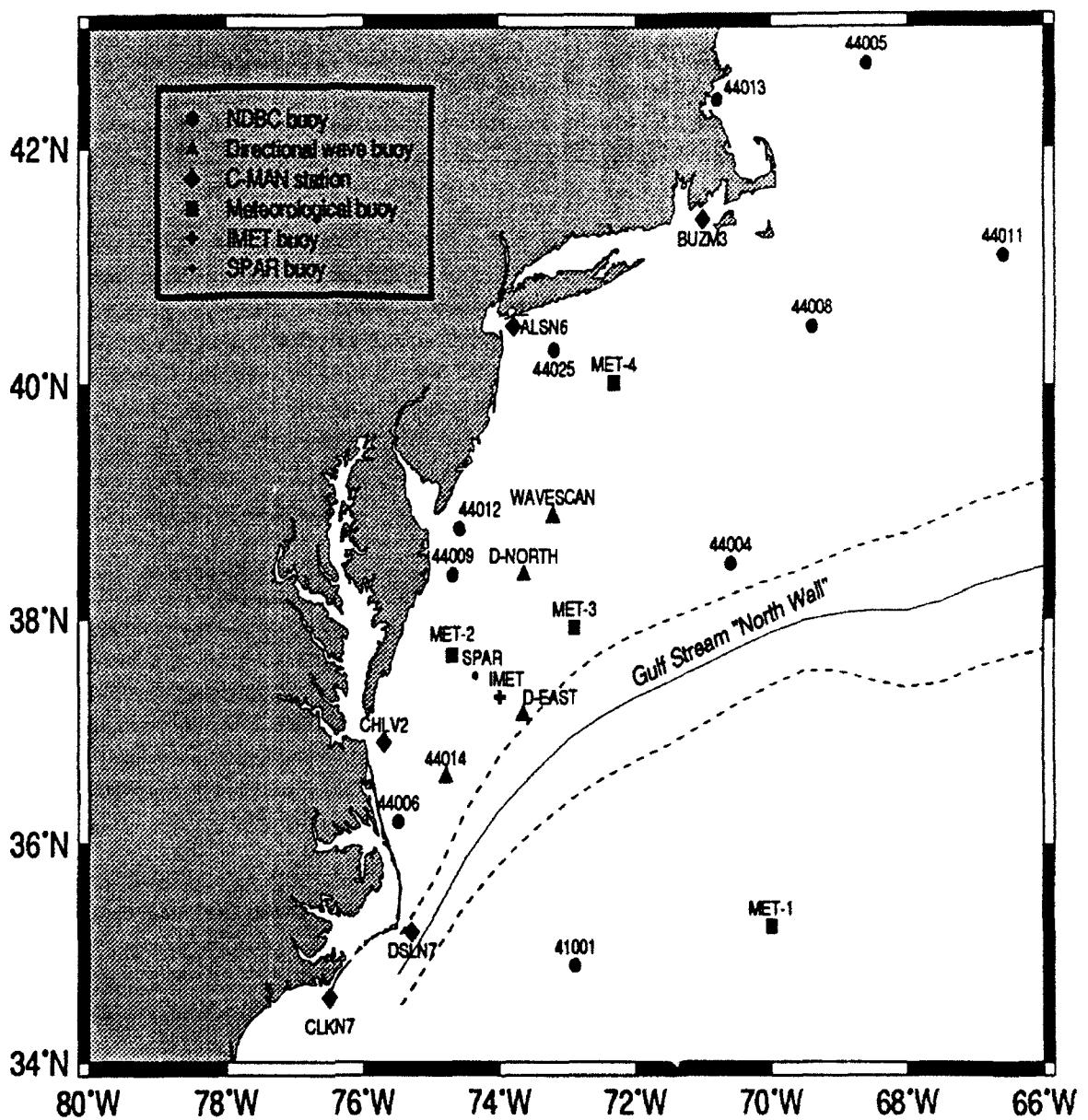


Figure 6: Geographic location of the SWADE buoys embedded within the network of buoys and C-MAN stations maintained by the NDBC. The mean (solid) and one standard deviation (dashed) positions of the "North Wall" of the Gulf Stream are also shown.

during the fall and winter months forced three of these buoys to move and remain adrift. MET-3 was the only buoy to remain stationary for the entire experiment.

Shortly after its deployment MET-1 began to move as a result of an eddy. The buoy drifted southwestward from its original position and reanchored itself at around $33^{\circ} 56' N$ and $72^{\circ} 14' W$. Around the middle of January the buoy began to drift again initially in a southeasterly direction, but later changed course and turned back towards the southwest. According to Advanced Very High Resolution Radiometer (AVHRR) imagery, a cold core ring located in this region appeared to influence the buoy. It reattached itself to the bottom around $32^{\circ} 38' N$ and $73^{\circ} 57' W$. In the beginning of April 1991 the buoy was successfully recovered by the R/V *Cape Henlopen*. Figure 7 shows the track of the buoy from deployment to recovery.

MET-2 was located in shallow water just offshore from Wallops Island. Both wind anemometers were damaged shortly after deployment, but spare sensors were installed during a second deployment cruise. During the SWADE October storm the buoy was set in motion due to intense wind and wave forcing. The initial course was south towards the CERC buoy 44014. At this time the Gulf Stream was in close proximity to Cape Hatteras and finally engulfed the buoy and quickly transported it northeastward. ARGOS contact was lost on November 12, 1990. Although several more signals were received at later dates, their sparsity made it impossible to determine the buoy's position uniquely. At this time SWADE researchers assume that the buoy has been lost. Figure 8 depicts the buoy's course until ARGOS transmission ceased.

MET-4 was located southeast off Long Island. It is not yet apparent what set the buoy in motion around November 19, 1990. There was an intense storm (cold-air outbreak) passing over the region, but winds and waves were not intense enough to shift the buoy from its anchored location. With the southward flowing coastal current the buoy drifted towards Cape Hatteras where it was caught by the Gulf Stream. Figure 9 shows the curious and sometimes erratic path of the buoy. There is evidence from AVHRR imagery that this track resembles some of the dynamics of the Gulf Stream. The buoy was recovered from the icy waters of the Labrador Sea by the USCG *Bittersweet* on May 28, 1991.

In Appendix C, time history plots of wind speed and direction, air and sea temperature and atmospheric pressure are shown for all four MET buoys. Note that the measurement height of the wind sensors on the MiniMet buoys were about 2.7 m above the mean sea surface.

MET-1 PATH

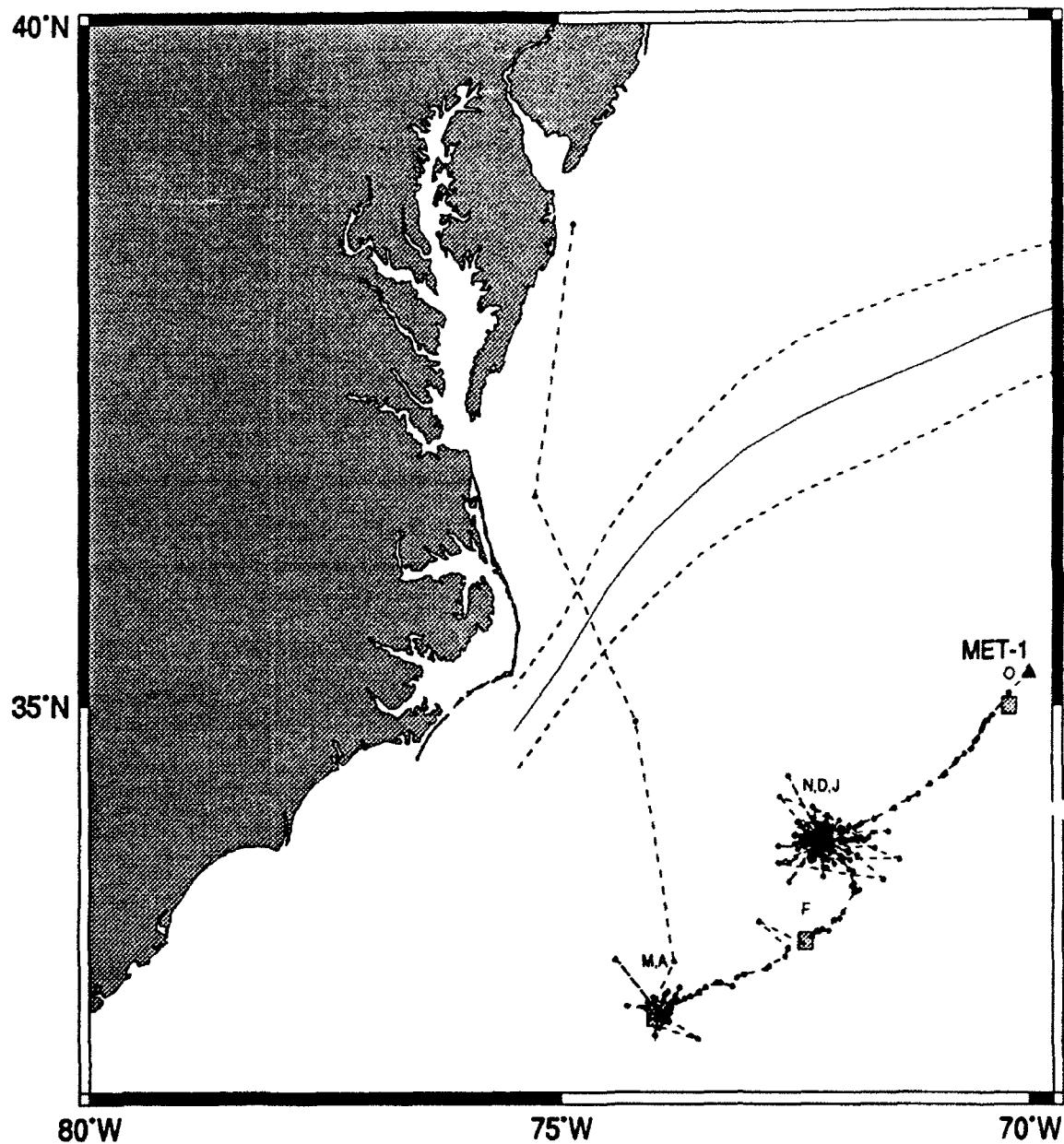


Figure 7: Drift track of MET-1 from September 1990 to April 1991. Each dot corresponds approximately to a daily position transmitted via ARGOS. The mean (solid) and one standard deviation (dashed) positions of the "North Wall" of the Gulf Stream are also shown. Note, shaded squares mark the position at the beginning of each month identified by letters (O = OCT, N = NOV, D = DEC, J = JAN, F = FEB, M = MAR and A = APR).

MET-2 PATH

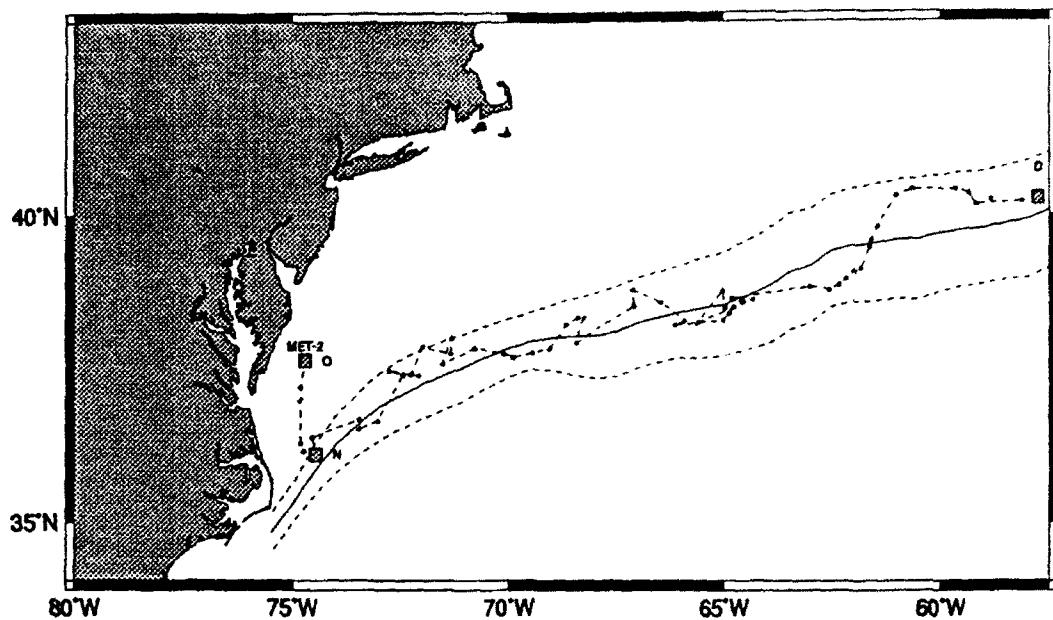


Figure 8: Drift track of MET-2 from September 1990 to December 1990 when contact was lost. (See caption in Figure 7 for meanings of letters).

MET-4 PATH

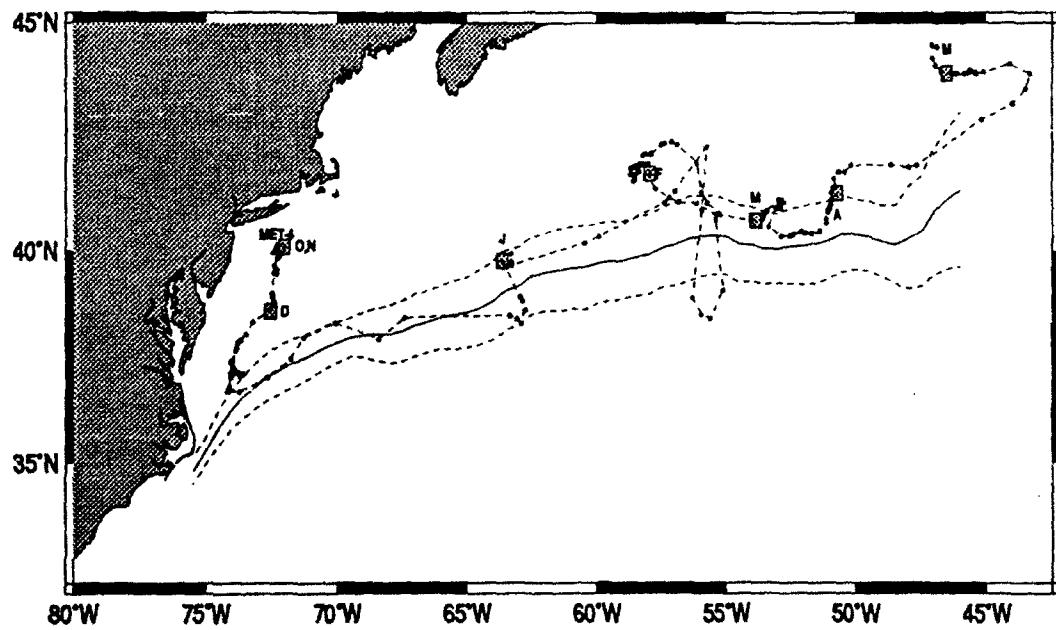


Figure 9: Drift track of MET-4 from September 1990 to May 1991. (See caption in Figure 7 for meanings of letters).

3 Ocean Wave Modeling

Numerical modelling plays a complementary role in achieving the goals of *SWADE*. In particular, the objectives are to examine the usefulness of a wave model as an analysis tool and in general validate wave models with the high quality wave data sets from *SWADE*. Furthermore, a comparison of measured and modelled source physics and the effect of incorporating wave-current interaction will provide additional evidence for refinement of numerical models.

The principal ocean wave prediction model used for these simulations is the third-generation WAM model (WAMDIG, 1989), which computes the directional wave spectrum by integration of the energy transport equation without prior specification of the spectral shape. There are 25 frequency bands from 0.0418 to 0.4114 Hz in logarithmic equally-spaced increments and 24 directional bins at 15-deg intervals. The wind fields are internally interpolated onto the model grids and initially converted to friction velocities using the wind speed dependent drag coefficient described in Wu (1982). The growth and dissipation terms are computed based on a simple coupling of the air-sea dynamics following the wind-wave generation theory of Janssen (1989, 1991). The resulting growth rate depends on both the friction velocity and the roughness length produced by the waves themselves.

Several forecast (Jensen, Gruber, and Caruso 1991) and hindcast (Gruber, Caruso, and Jensen 1991) studies for the *SWADE* IOPs have been carried out with WAM *Cycles 2, 3, 3.5*, and most recently *4* (Günther, Hasselmann, and Janssen 1991), where the later versions include options for nested grids to specify proper boundary conditions as would arise in situations when swell is propagating into the model domain, and for time and spatially varying currents to study wave-current interactions. More detailed studies are presently under way by the *SWADE* modelling team to investigate (1) sources of errors attributed to wind field specification; (2) differences in source term physics and grid nesting; and (3) the inclusion of depth-dependent wave physics and the influence of wave-current interaction. Model output fields include maps of significant wave height, mean wave period, mean wave direction, swell wave height, swell period and swell direction. In addition, two-dimensional wave spectra are produced at selected output points near buoy stations within the *SWADE* experimental area.

4 Model Domain and Grids

A hierarchy of model grids was designed for *SWADE* to examine the wave physics at different spatial and temporal scales, and the usefulness of a nested system. Each grid is supposed to fulfill a specific function and provide results that can be used to accomplish the goals of the experiment. The WAM model has been implemented in spherical coordinates on three grids described previously (Weller *et al.* 1991):

1. Basin-scale North and South Atlantic model
2. Regional-scale Western North Atlantic model
3. Fine Mesh *SWADE* Array model

Atlantic Basin Model

The basin scale grid covers the entire North and South Atlantic Oceans and extends from 63° S to 72° N and from 100° W to 34° E in 1-deg increments in both latitude and longitude (Figure 10). The primary purpose of this grid is to accurately simulate northward propagating swell originating in the southern ocean and provide boundary conditions for the regional scale model. Also, wave height maps provide some overview of storm activities in both Atlantic basins. The output results will show the quality of the synoptic scale forecast and provide some indication of subscale variability.

Western North Atlantic Model

This medium-resolution grid covers the Western North Atlantic from 24° N to 48° N and from 82° W to 52° W in 0.25-deg increments in both latitude and longitude (Figure 11). The purpose of this model grid is to provide high quality wind and wave analyses for evaluation of *SWADE* scientific objectives and for assessing sources and magnitudes of errors in the wind field specification.

SWADE Model

This high-resolution grid was designed to simulate the small scale wave physics and to improve and verify the source term physics. The grid extends from 35° N to 42° N and from land to 70° W in 0.083-deg increments in both latitude and longitude (Figure 12). The measured meteorology and different interpolation and assimilation schemes will be used to provide winds for these simulations.

Atlantic Ocean Basin Scale Model

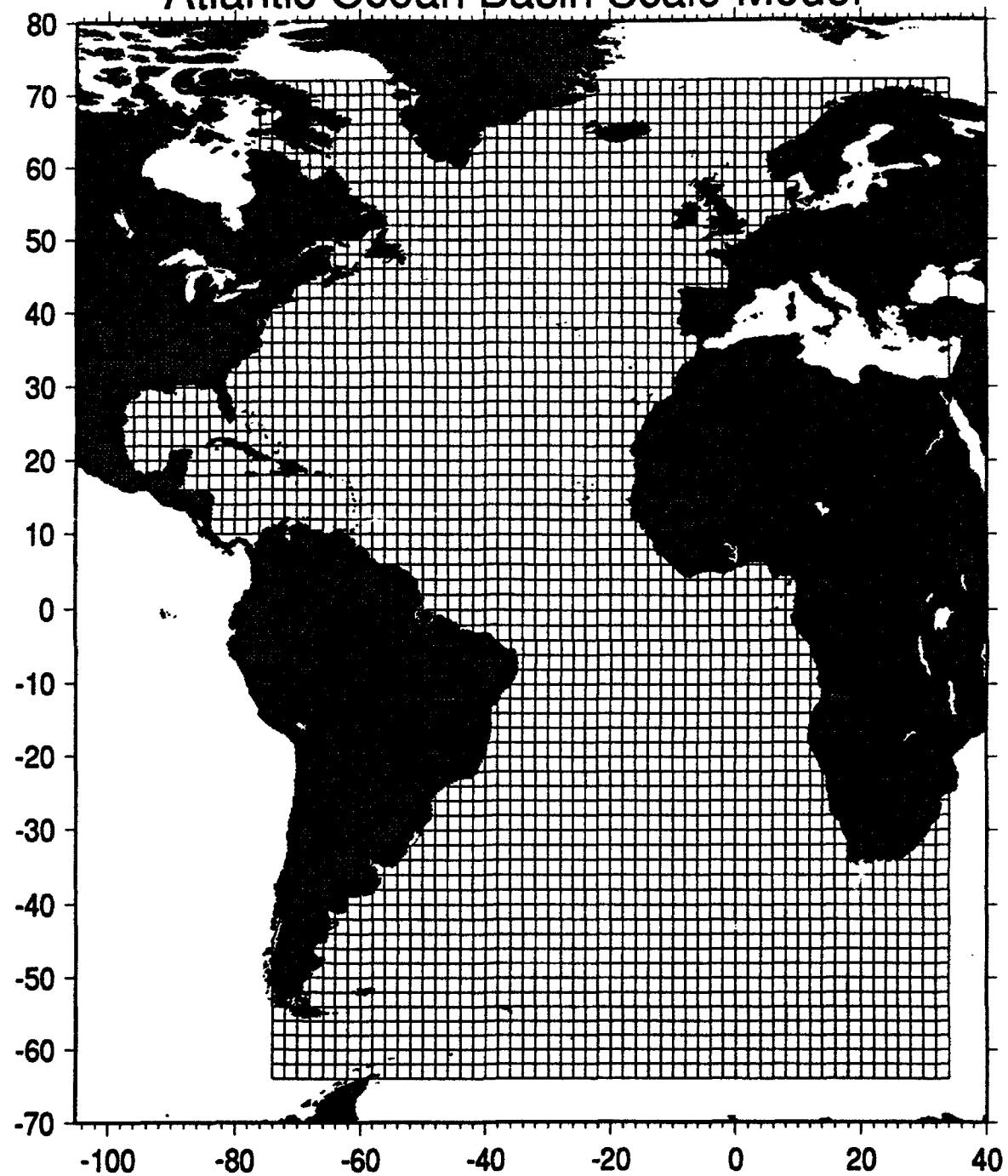


Figure 10: Atlantic Ocean basin-scale model grid.

Western North Atlantic Regional Model

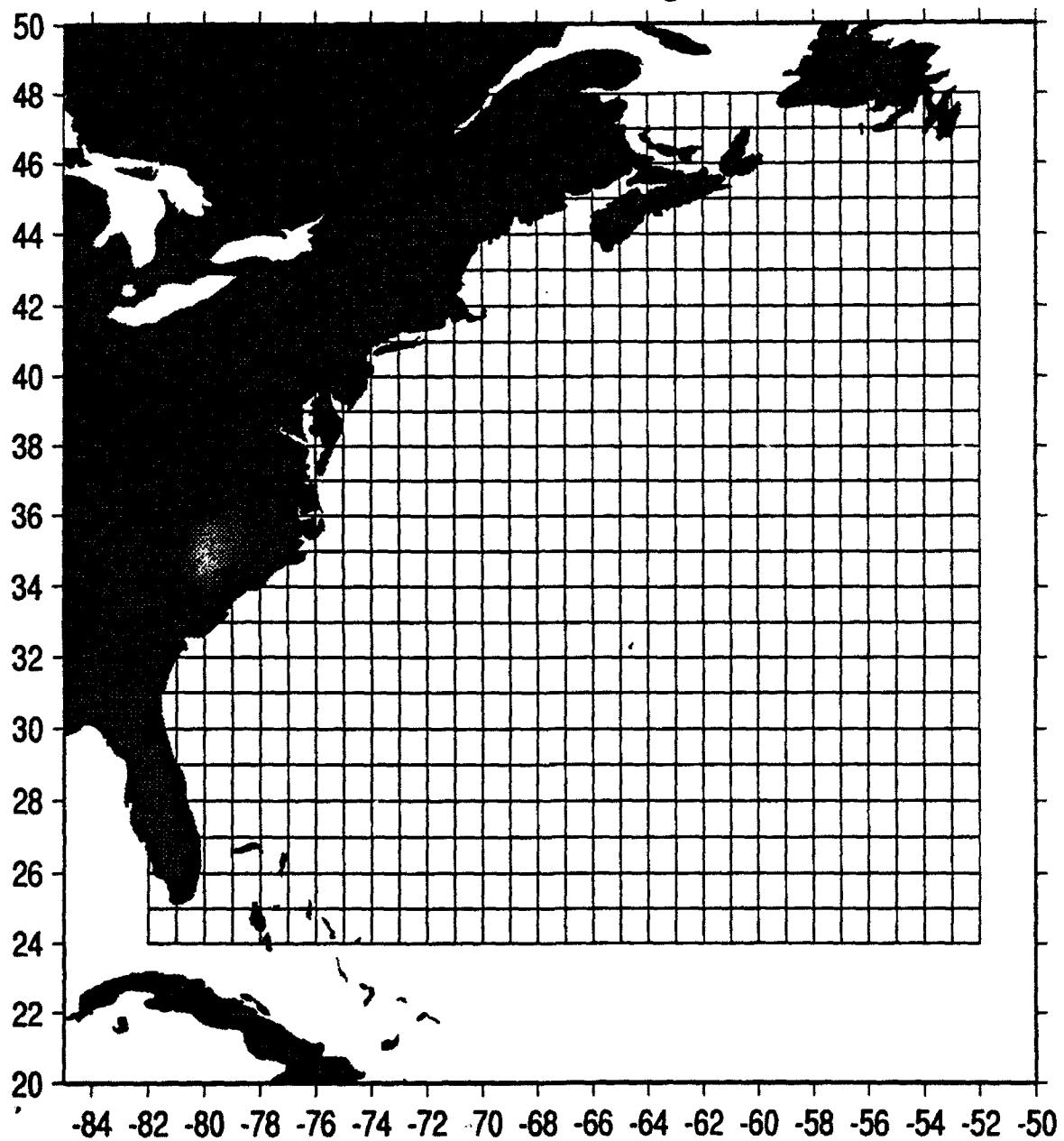


Figure 11: Western North Atlantic regional model grid.

Fine Mesh SWADE Model

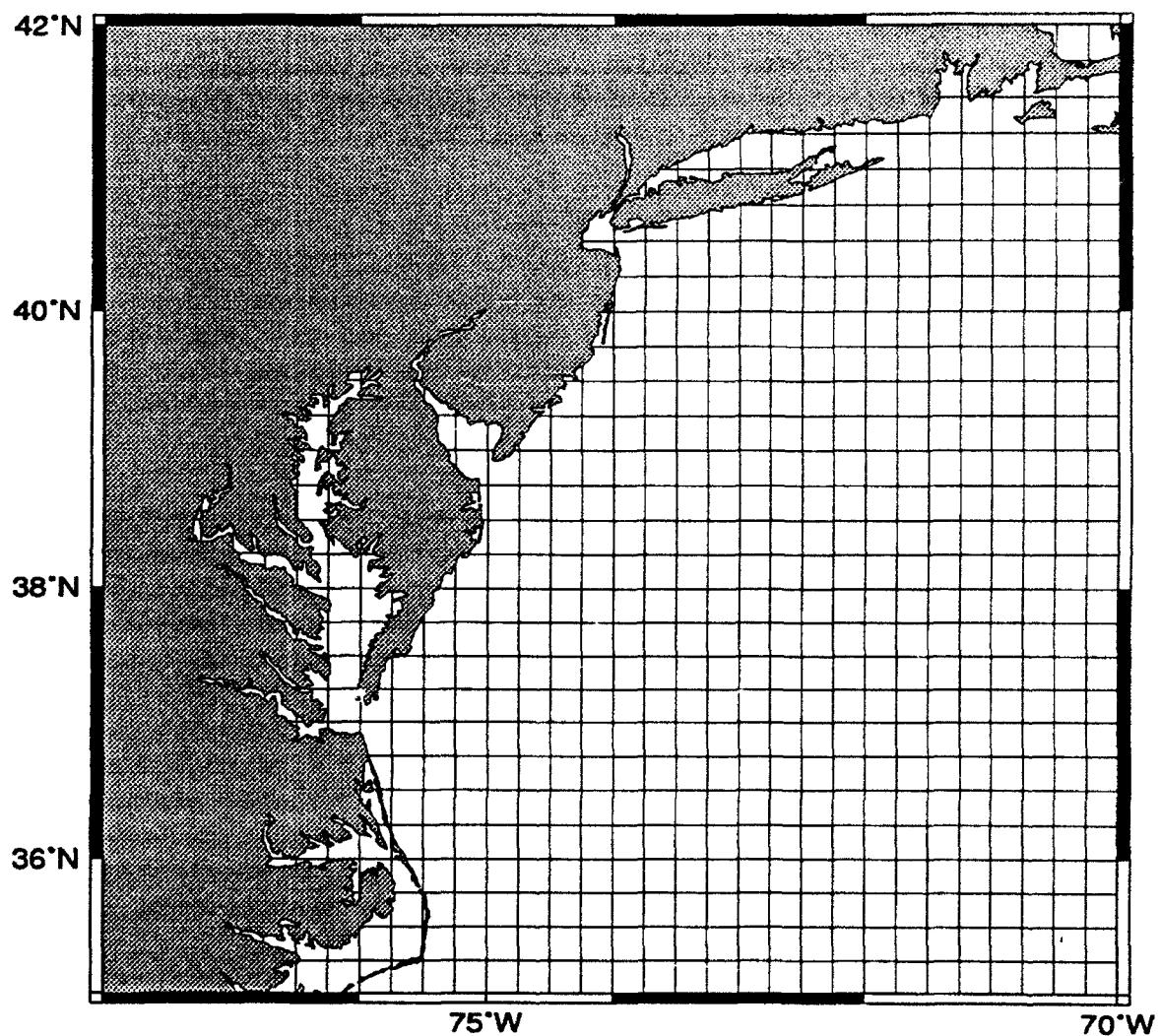


Figure 12: Fine Mesh SWADE model grid.

5 Wind Fields

Six different wind field representations are available for this particular time period. Some preliminary results using a subset of these wind fields have been briefly discussed in Graber, Caruso, and Jensen (1991), and they indicate considerable differences in the representations of the atmospheric conditions. The set of wind fields includes analyses from operational numerical weather prediction models such as Fleet Numerical Oceanography Center (FNOC), European Centre for Medium-Range Weather Forecasts (ECMWF), and United Kingdom Meteorological Office (UKMO), objectively interpolating model results from National Meteorological Center (NMC) and NASA/Goddard Space Flight Center (GSFC) and a manual kinematic analysis from Oceanweather/Atmospheric Environment Service (OW/AES). A brief description of each of the wind fields is given below.

Appendix D includes two maps per day of wind vectors and the corresponding contours of significant wave height for the OW/AES model simulations on the regional grid for the entire IOP-1. For the time period from 24 October 1990, 12:00 GMT to 28 October 1990, 12:00 GMT the wind vector fields and corresponding wave hindcasts from the other wind field models are also presented. Note that the frequency of maps is every 3 hr from 26-28 October, which covers the major storm period.

FNOC

The FNOC has provided analyzed and forecast wind stress and 19.5-m neutrally stable wind fields derived from the Navy Operational Global Atmospheric Prediction System (NOGAPS) spectral forecast model (Hogan and Rosmond 1991). The predicted winds are computed with the (T80) model system, which uses 80 Fourier coefficients and 18 vertical layers from the surface to a pressure level at 10 mb. The fields are spectrally interpolated in the horizontal to 1.5 deg. The NOGAPS uses a planetary boundary-layer (PBL) model similar to that of the ECMWF (Louis, Tiedtke, and Geleyn 1982), but with a major modification for the computation of surface fluxes when the PBL is conditionally unstable. The 19.5-m neutrally stable winds are directly computed from the wind stress fields at each local grid point taking into account atmospheric stability effects. A final, linear interpolation is done onto a spherical grid with a spatial resolution of 1.25 deg in latitude and longitude. The time interval of wind and wind stress fields is every 6 hr starting at 00:00.

ECMWF

Analyzed 10-m wind fields from the ECMWF generated by their operational atmospheric general circulation model are available for the entire SWADE period. These analyzed winds are from the ECMWF/TOGA (Tropical Ocean-Global Atmosphere) advanced operational analysis surface and diagnostic fields data set. The geometrical coverage is specified on a (N80) Gaussian grid with a spatial resolution of 1.125 deg in latitude and longitude. The time interval of wind fields is every 6 hr beginning at 00:00. Analyzed surface pressure fields and surface temperature fields are also available with the same spatial and temporal

resolution.

NMC/GSFC

Two additional wind field products are available from the NMC and NASA/GSFC. Both wind fields were derived from the first guess fields of NMC's coarse ($2.5^\circ \times 2.5^\circ$) large-scale analysis. In each case the observed data are reinserted into a high-resolution grid where grid points with data remain unaltered, whereas non-data points are computed using a "conditional" relaxation procedure.

The NMC model winds are generated with an *objective interpolation* scheme which corrects the nearest grid point according to the data value and relaxes all non-data points. The method includes a check on gross errors. The fidelity of the wind field is determined by withholding one piece of ship data at a time. This is repeated about 10 times. The resulting wind fields are regridded covering the regional model domain with a resolution of 0.3 deg in latitude and 0.5 deg in longitude. The time interval between wind fields is 6 hr.

The GSFC model winds are determined with the *successive correction method* which uses seven sweeps over the model domain and successively reduces the area of influence in each pass from 500 km to 120 km. Consistency checks and error minimization are only performed at buoy locations. No additional quality checks are made by withholding individual buoy measurements. The final output is a spatially high-resolution wind field on a 0.25- by 0.25-deg grid. The time interval between successive wind fields is every 3 hr.

Both methods make a final check of the wind fields for consistency and the goodness of these winds is evaluated with root mean square error statistics.

OW/AES

High-resolution wind fields were developed by OW/AES over a limited domain, coinciding approximately with the fine-mesh *SWADE* grid. These wind fields were produced with a manual kinematic analysis, originally described in Cardone et al. (1980), from pressure fields, air and sea surface temperature fields, ship and buoy data. All data are carefully screened for inconsistencies and measured winds are adjusted in height and corrected with a stability-dependent surface layer model to effective neutral 20-m height hourly averages. Hourly averages of wind speed and direction are computed from three consecutive hourly buoy observations with weights of 0.25, 0.5 and 0.25, respectively. The detailed hand analysis of the pressure and temperature fields carefully preserves temporal and spatial continuity of low pressure centers and frontal boundaries. Outside of the limited domain, the effective neutral winds are calculated with the marine boundary layer model of Cardone (1969). Time histories of measured and modelled and standard statistical measures of difference are used to evaluate the quality of the final wind fields.

The resulting high-resolution winds are gridded onto a 0.5- by 0.5-deg grid over the regional model domain and are available hourly to simulate accurately the temporal evolution

of the storm centers and frontal systems passing over the SWADE domain.

UKMO

These wind fields are computed from the coarse-mesh, 11-layer general atmospheric circulation model in operational use at the UKMO (Bell and Dickinson 1986). Global coverage is implemented on a mesh with grid lengths of 1.5-deg in latitude and 1.875-deg in longitude. A 6-hr data assimilation cycle is employed, and physical and subgrid-scale processes are also included in the model (Gilchrist and White 1982). Analyzed winds at the 19.5-m height are available every 2 hr beginning at 00:00.

Winds from the limited-area fine-mesh model are also available at hourly intervals. While the resolution of the fine-mesh model is twice that of the coarse mesh model (*i.e.*, $\Delta\phi = 0.75 - \text{deg}$ and $\Delta\lambda = 0.9375 - \text{deg}$), its North Atlantic coverage extends only as far south as 30° N, which is not sufficient for the Western North Atlantic regional model grid domain.

6 Surface Currents

A special data set of surface currents was generated from the quasi-geostrophic Harvard open ocean model (Robinson and Walstad 1987). The currents were generated using the Harvard GULFCAST "feature model" for the Gulf Stream with embedded rings from the nowcast locations (Glenn, Porter, and Robinson 1991). Input data of the location of the Gulf Stream North Wall and warm and cold core rings were provided by the Naval Oceanographic Office. Daily maps of surface velocity fields consisting of nowcast and forecast fields are available from October 20 to 31, 1990. The spatial resolution of the current vectors is 15 km. The average accuracy of the Gulf Stream position within the GULFCAST model domain is estimated to be about ± 30 km based on the assumption that the input data from digital infrared imagery, AVHRR, and GEOSAT altimetry is accurate to about ± 15 km and the Oceanographic Analysis Charts to within ± 30 km (Glenn, Porter, and Robinson 1991).

The cartesian grid of the GULFCAST model is projected onto an f-plane at $\phi_o = 38.4^\circ$ N and $\lambda_o = 61.4^\circ$ W. The grid domain is rotated by $\theta = 22^\circ$ counterclockwise from east and is approximately parallel to the coastline between Cape Hatteras and Nova Scotia, but covers only the northern model domain of the Western North Atlantic grid. The relationship between a point (X, Y) in a cartesian coordinate system with principal axes along east-west and north-south directions and a point (x, y) in the GULFCAST model domain is given by

$$\begin{aligned} X &= x \cos \theta - y \sin \theta \\ Y &= x \sin \theta + y \cos \theta \end{aligned}$$

The equivalent longitude and latitude specification of a point (X, Y) in a spherical earth coordinate system is determined by

$$\begin{aligned} \lambda &= \lambda_o - \frac{X}{a \cos \phi_o} \\ \phi &= \phi_o + \frac{Y}{a} \end{aligned}$$

where $a = 111.12$ km.

Daily maps of the surface currents within the fine-mesh SWADE model grid for IOP-1 are shown in Appendix E from 20 October 1990, 00:00 GMT to 31 October 1990, 00:00 GMT.

7 The SWADE Storm

The original IOP-1 or "shake-down" period took place from November 5 to 9, 1990. During this time the weather was uncooperative in the sense of being uneventful for winds and waves, most aircraft were not available and several other measurement components were still being prepared or serviced due to an intense extra-tropical storm which swept over the *SWADE* experimental region on October 26. Therefore, the steering committee of *SWADE* decided to designate the time period from October 20 - 31, which included the now famous *SWADE Storm*, as IOP-1. The following paragraphs will briefly describe the meteorological and oceanic conditions leading up to, during, and after the *SWADE Storm*. An overview is given of the measurements collected during this storm period and some results are presented from the wind and wave model simulations for this severe event.

During IOP-1, three separate storm systems passed in rapid succession over the *SWADE* array, causing significant damage along the Atlantic seaboard and reaching hurricane force gusts from Cape Hatteras to Cape Cod. The middle storm turned out to be the most severe one of them all.

On October 24 a newly formed surface low over coastal North Carolina became quickly energized from the unseasonably warm waters of the Gulf Stream and deepened at a much faster rate than predicted. This led to very steep pressure gradients along the North Carolina and Virginia coasts due to a number of small-scale cyclonic centers that formed an elongated shear zone extending all the way up to the Canadian maritime coast. This elongated structure resulted in a greatly "linearized" fetch and led to higher than expected winds in this region. As the storm proceeded in an east-northeastward direction, it reached a minimum pressure of 984 mb on October 26 just over the *SWADE* region. Figure 13 shows the surface analysis chart at the height of the storm. The very intense and tight circulation more commonly found in tropical cyclones was clearly evident in the drastic changes of atmospheric pressures observed by the *SWADE* buoys. Pressure drops of 12 mb within 6 hr and subsequent pressure rises of nearly 25 mb are often features of hurricanes. The storm proceeded along an east-northeast track and after occlusion (a warm front is overtaken by a cold front) the storm accelerated towards the open sea. Figure 14 shows the storm track over a 24-hr period for October 26.

Sea states associated with this storm were in excess of 5 m almost everywhere along the seaboard between Cape Hatteras and Cape Cod. Some buoys further offshore such as 41001 and 44015 recorded significant wave heights up to 9 and 8 m, respectively. It is very probable that individual waves attained heights twice the observed significant height values. It was also during this storm that the Spar buoy was sunk. According to the captain of the tanker M/S *Tropic Sun*, which passed by the Spar around 1600 EDT inbound to Delaware Bay, the buoy was floating upright and with all its sensors intact. This was approximately 4 hr after the peak of the storm as observed by the nearby buoy 44015. ARGOS transmission stopped around 2000 EDT (Dr. Charles Flagg, Brookhaven National Laboratory, 1992, personal communication). The Spar was located on the bottom by the R/V *Oceanus* on October 30. Data from an acoustic survey determined that the resting place of the Spar was

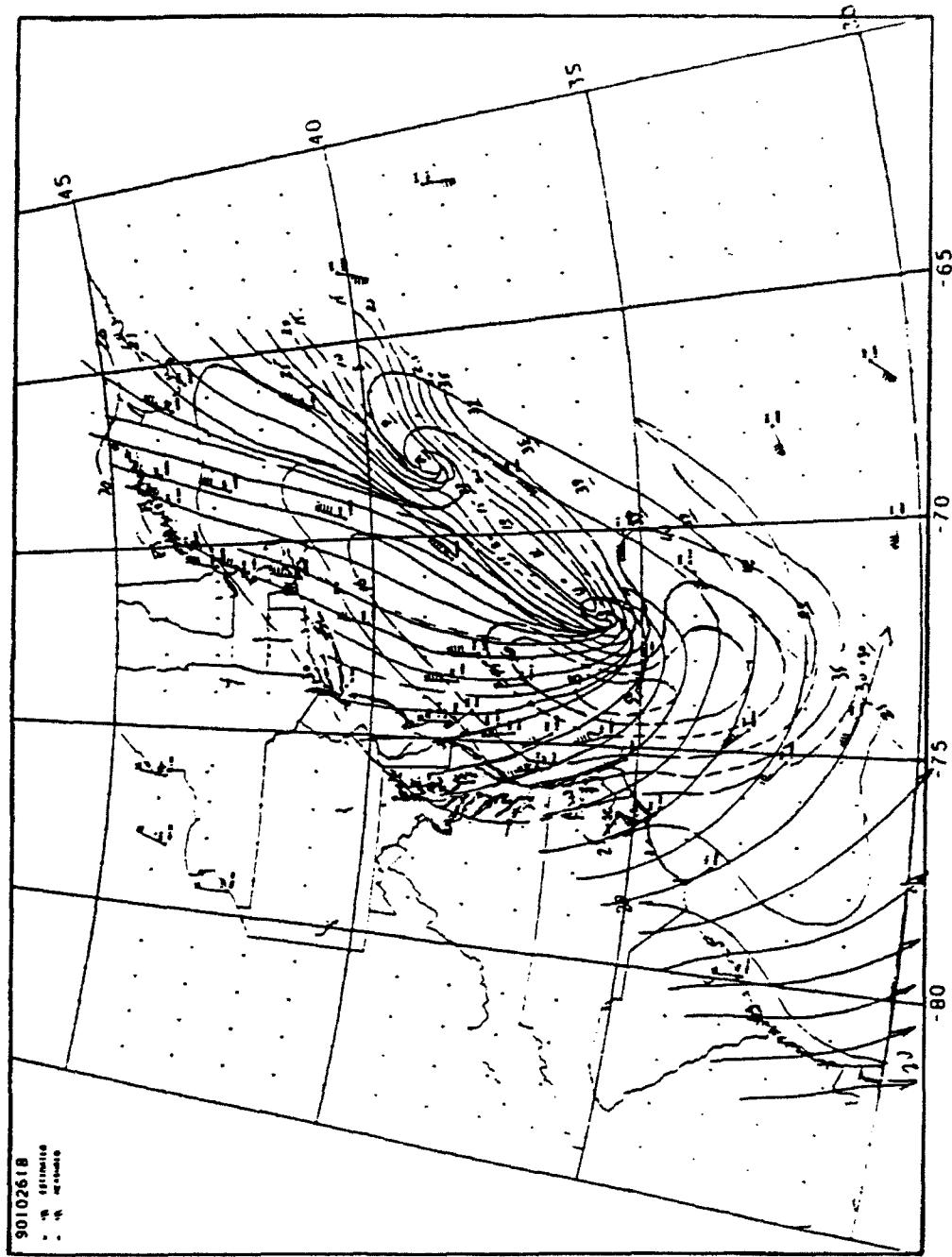


Figure 13: Surface analysis of 26 October 1990 at 18:00 UTC (from Cardone et al. (1993)).

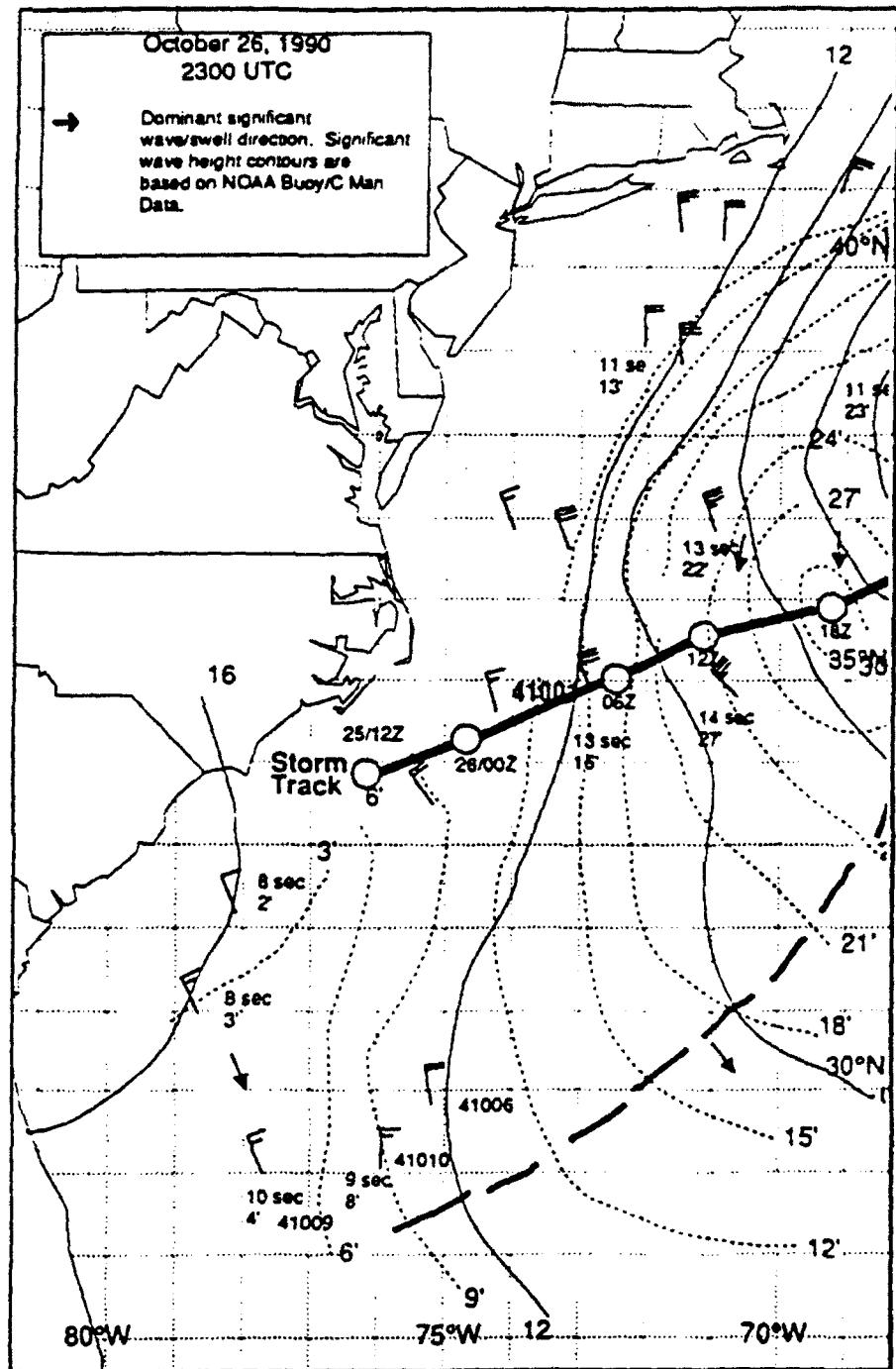


Figure 14: Storm track of central pressure position of "SWADE Storm" (from Morris (1991)).

in waters 301.9-m deep at $37^{\circ} 28.4' \text{ N}$, $74^{\circ} 22.6' \text{ W}$. This location is about 3 km southwest of the original deployment position, which was in 200-m water depth (Graber and Boutin 1991). In mid-June 1992 the USNS *GRASP* recovered the Spar and evaluations are under way to determine the cause of its failure.

8 Summary

This report provides a summary of wind, wave and meteorological measurements during the first intensive observation period (IOP-1) of the *SWADE*. The time series of wind, wave and meteorological parameters provide a guide to the availability of various observations during IOP-1 and a first look at the temporal and spatial variability of the dynamics during this extreme storm event. The hindcast results from the third-generation ocean wave model (WAM) with six different wind fields is intended to show the diverse representation of this storm event as well as a description of the larger scale meteorological and sea state conditions during IOP-1.

Two subsequent reports will describe the general observations of the meteorological and oceanographic conditions for IOP-2 and IOP-3.

References

Bell, R.S. and A. Dickinson, 1986: The Meteorological Office operational numerical weather prediction system. *Sci. Pap., Meteorol. Off.* No. 41, Her Majesty's Stationery Office, London, 61pp.

Cardone, V.J., 1969: Specification of the wind distribution in the marine boundary layer for wave forecasting. Report TR-69-01, Geophys. Sciences Lab., New York University, 137pp.

Cardone, V.J., A.J. Broccoli, C.V. Greenwood and J.A. Greenwood, 1980: Error characteristics of extratropical storm wind fields specified from historical data. *J. Petrol. Tech.*, **32**, 873-880.

Cardone, V., H.C. Graber, R. Jensen, S. Hasselmann, and M. Caruso, 1993: In search of the true surface wind field: Ocean wave modelling perspective. (In preparation).

Donelan, M.A., W.M. Drennan, N. Madsen, K.B. Katsaros, E.A. Terray, and C.N. Flagg, 1992: Directional spectra from the SWATH ship in SWADE. Report NWRI, CCIW, 51pp.

Drennan, W.M., H.C. Graber and M.A. Donelan, 1993: On the measurement of directional wave spectra from pitch-roll and acceleration buoys. (In preparation).

Gilchrist, A. and P.W. White, 1982: The development of the Meteorological Office new operational forecasting system. *Meteorol. Mag.*, **111**, 161-179.

Glenn, S.M., D.L. Porter, and A.R. Robinson, 1991: A synthetic geoid validation of Geosat mesoscale dynamic topography in the Gulf Stream region. *J. Geophys. Res.*, **96**, 7145-7166.

Graber, H.C. and P.R. Boutin, 1991: *SWADE* cruise report for voyages 224 and 226 on the R/V *Oceanus*. ONR Contract Report, 21 pp.

Graber, H.C., M.J. Caruso and R.E. Jensen, 1991: Surface wave simulations during the October storm in *SWADE*. *Proc. MTS '91 Conf.*, Marine Technology Society, New Orleans, LA, 159-164.

Günther, H., S. Hasselmann and P.A.E.M. Janssen, 1991: Wamodel Cycle 4. Tech. Rept. 4, Deutsches Klimarechenzentrum, Hamburg, 91pp.

Hogan, T.F. and T.E. Rosmond, 1991: The description of Navy operational global atmospheric prediction system's spectral forecast model. *Mon. Wea. Rev.*, **119**, 1786-1815.

Janssen, P.A.E.M., 1989: On the interaction of wind and waves. *Phil. Trans. R. Soc. Lond.*, **A 329**, 289-301.

Janssen, P.A.E.M., 1991: Quasi-linear theory for wind-wave generation applied to wave forecasting. *J. Phys. Oceanogr.*, **21**, 1631-1642.

Jensen, R.E., Graber, H.C., and M.J. Caruso, 1991: A Wind-Wave Forecast for the Surface Wave Dynamics Experiment. *Proc. MTS '91 Conf.*, Marine Technology Society, New Orleans, LA, 147-153.

Louis, J.F., M. Tiedtke and J.F. Geleyn, 1982: A short history of the operational PBL parametrization at ECMWF. *Workshop on Planetary Boundary Layer Parametrization*, ECMWF, Reading, Shinfield Park, England, 59-79.

Morris, V.F., 1991: The Bonner Bridge storm. *Mar. Wea. Log.*, **35**, No. 2, 4-9.

Oberholtzer, D. and M.A. Donelan, 1993: SWADE data guide. NASA Report, (In preparation).

Robinson, A.R. and L.J. Walstad, 1987: The Harvard open ocean model: Calibration and application to dynamical process forecasting and data assimilation studies. *J. Appl. Numer. Math.*, **3**, 89-131.

Steele, K.E., C.-C. Teng and D.W.C. Wang, 1992: Wave direction measurements using pitch-roll buoys. *Ocean Engng.*, **19** (4), 349-375.

The WAMDIG Group, 1988: The WAM model - a third generation ocean wave prediction model. *J. Phys. Oceanogr.*, **18**, 1775-1810.

Weller, R.A., M.A. Donelan, M.G. Briscoe and N.E. Huang, 1991: Riding the crest: A tale of two wave experiments. *Bull. Amer. Met. Soc.*, **72**, No. 2, 163-183.

Wu, J., 1982: Wind-stress coefficients over sea surface from breeze to hurricane. *J. Geophys. Res.*, **87**, 9704-9706.

Appendix A: Time Series from SWADE and NDBC Buoys

Time series plots of the observed data are presented in this appendix in the following sequence:

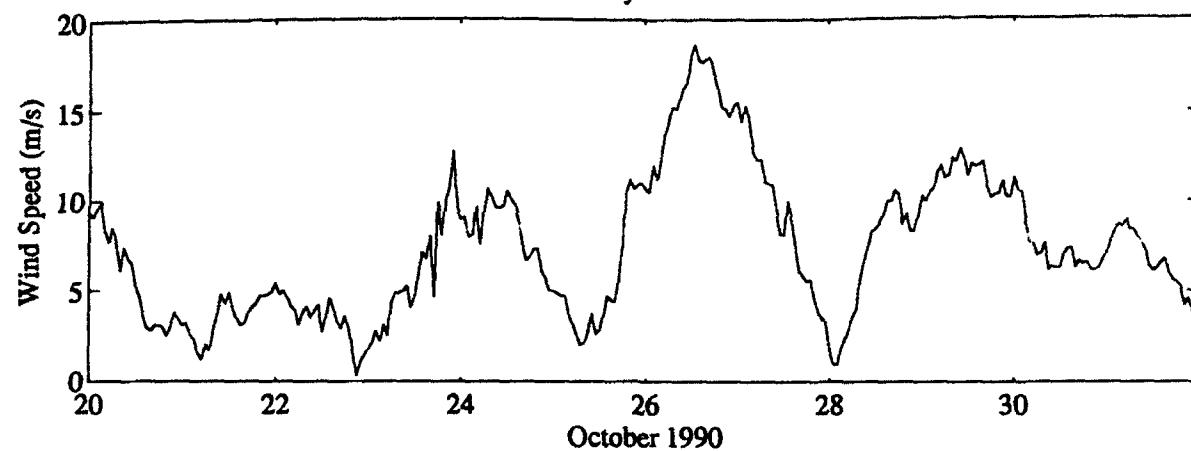
1. Directional Wave Buoys

- Discus Buoy "North" (44001)
- Discus Buoy "East" (44015)
- Discus Buoy "CERC" (44014)

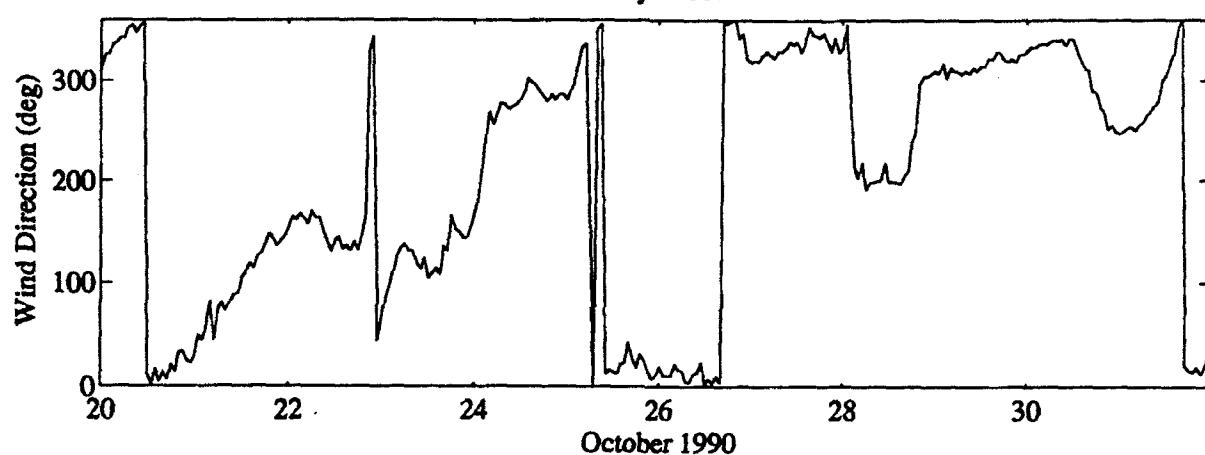
2. Non-directional Buoys and C-MAN Stations

- Buoy 41001
- Buoy 44004
- Buoy 44008
- Buoy 44009
- Buoy 44011
- Buoy 44012
- C-MAN Station DSLN7
- C-MAN Station CHLV2
- C-MAN Station BUZM3

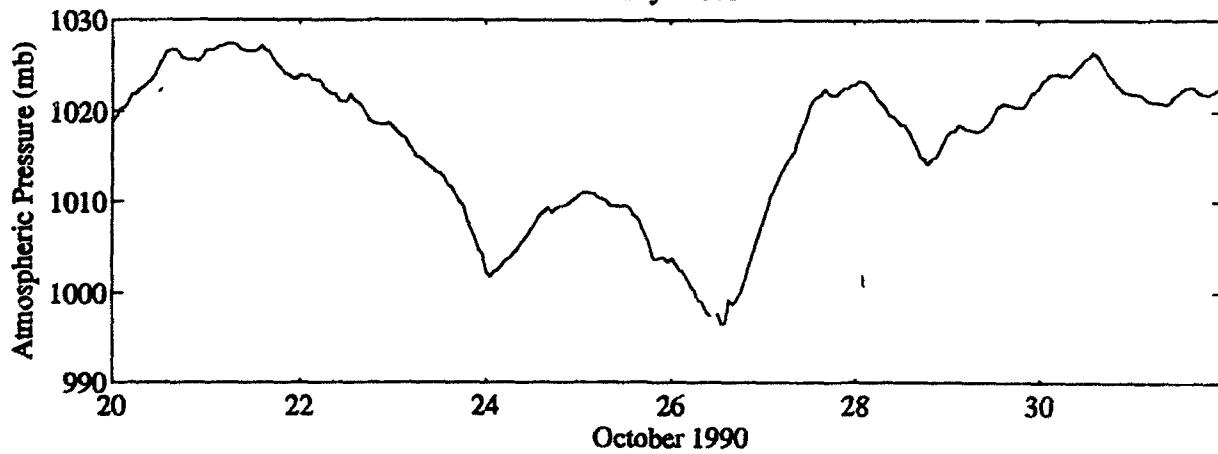
Buoy 44001



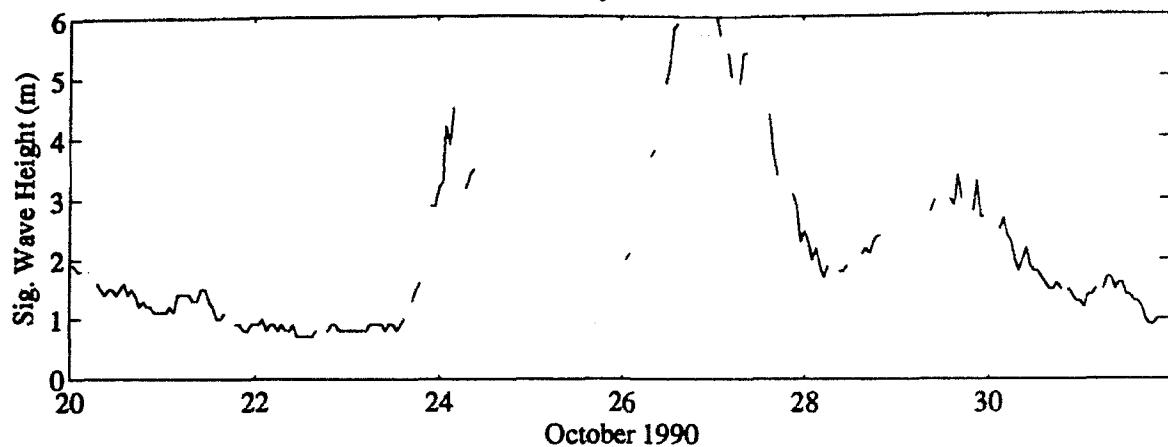
Buoy 44001



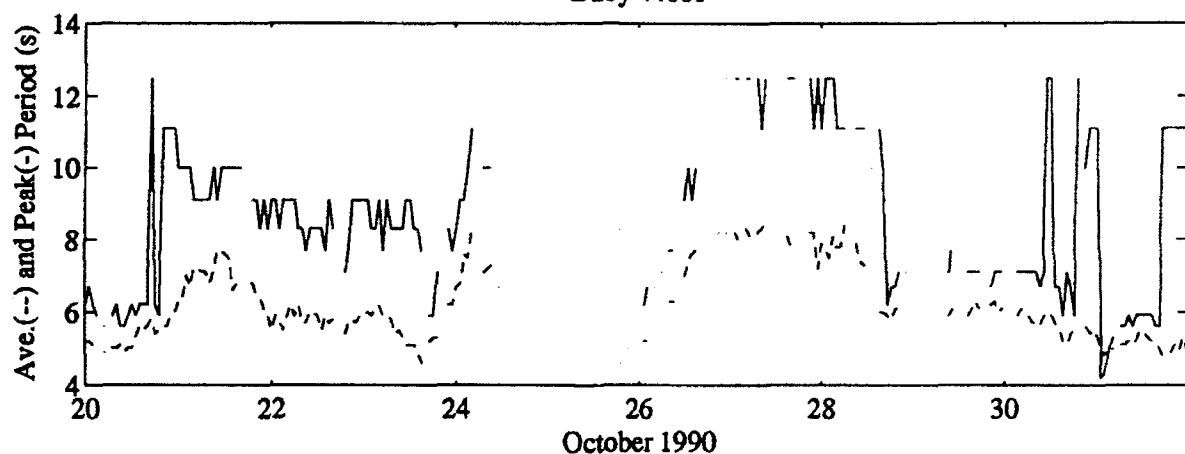
Buoy 44001



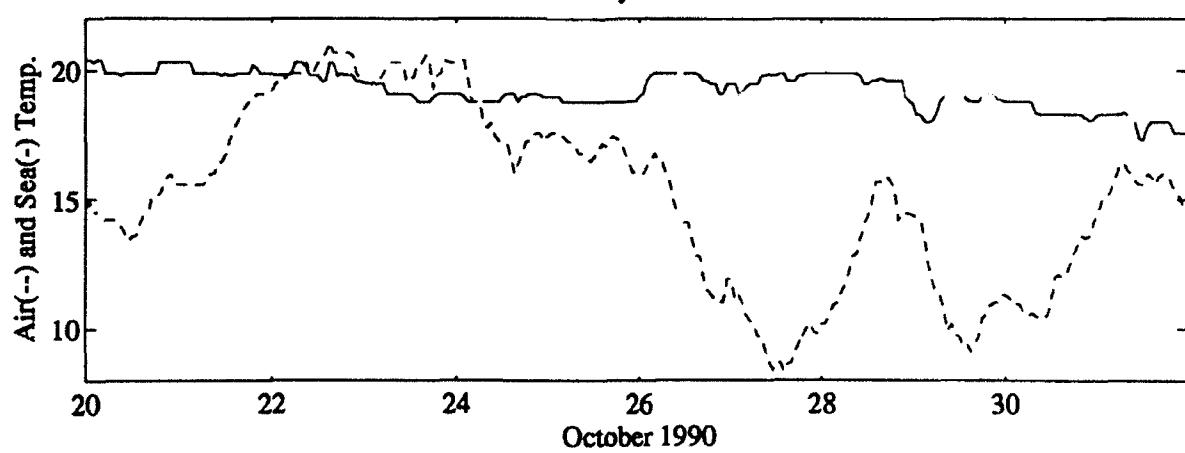
Buoy 44001



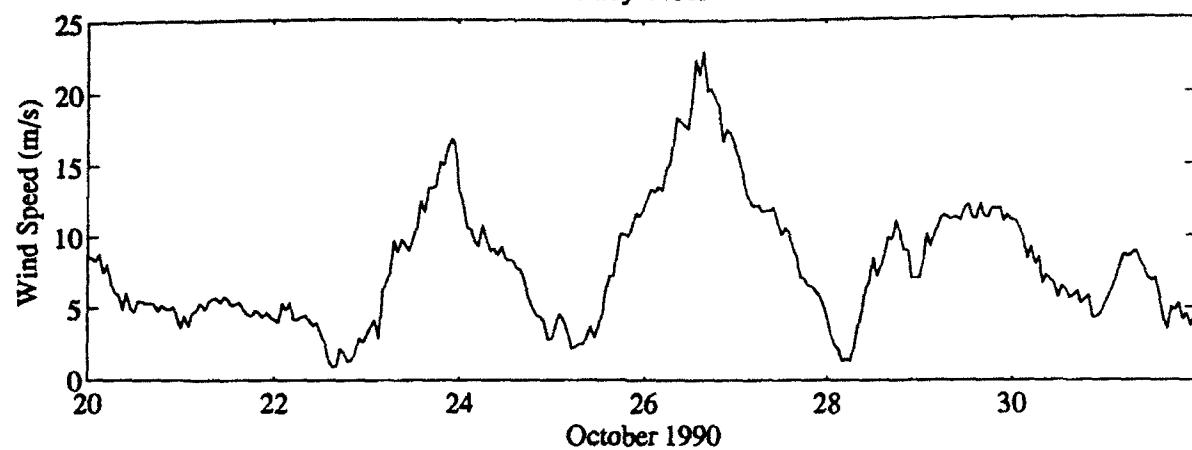
Buoy 44001



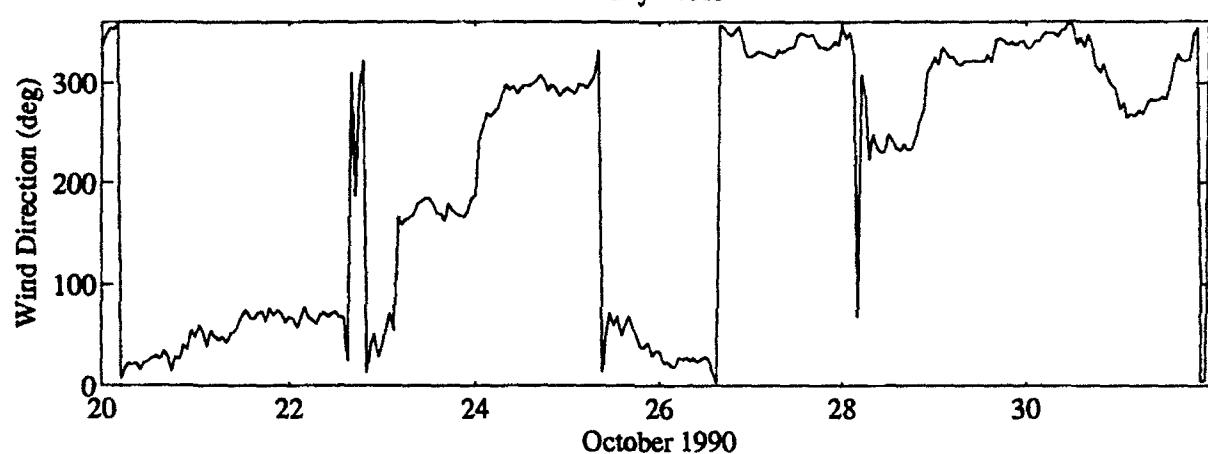
Buoy 44001



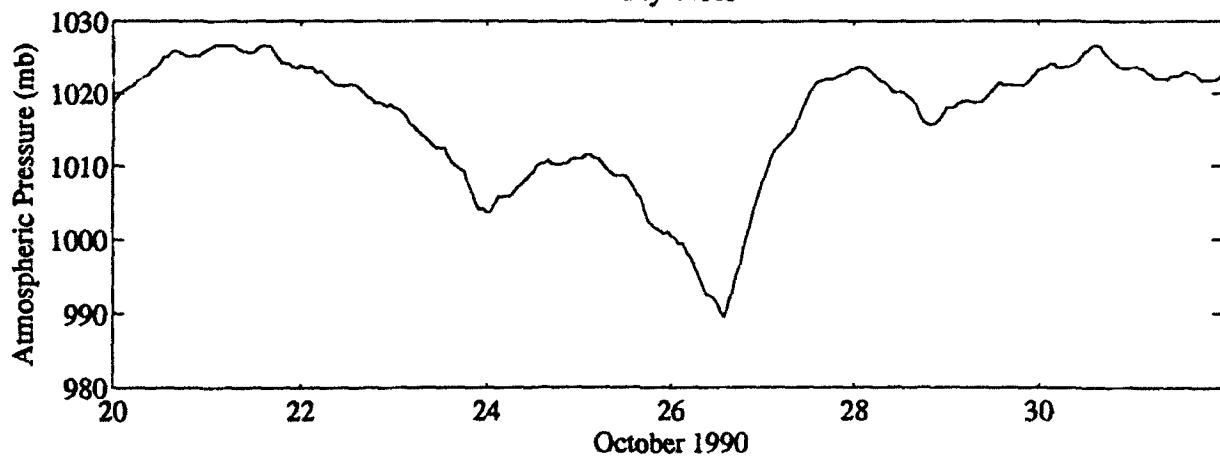
Buoy 44015



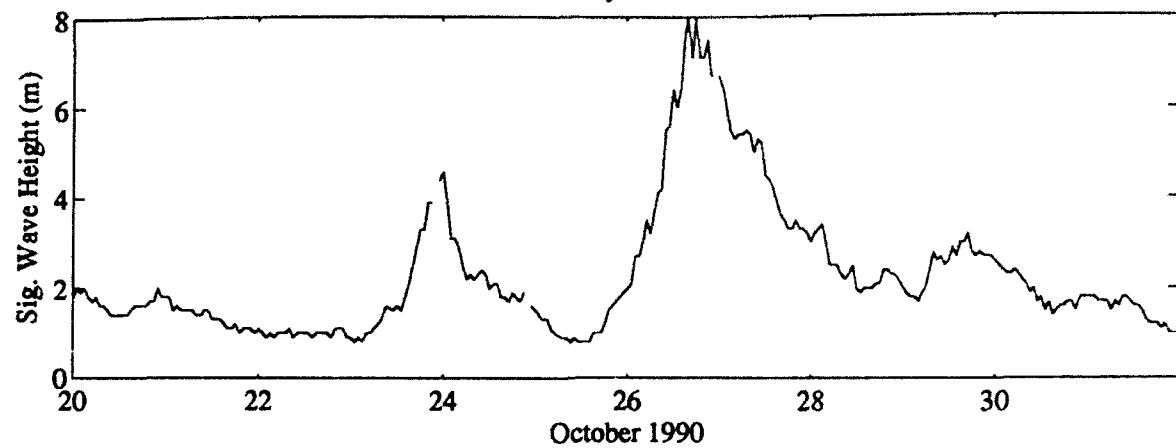
Buoy 44015



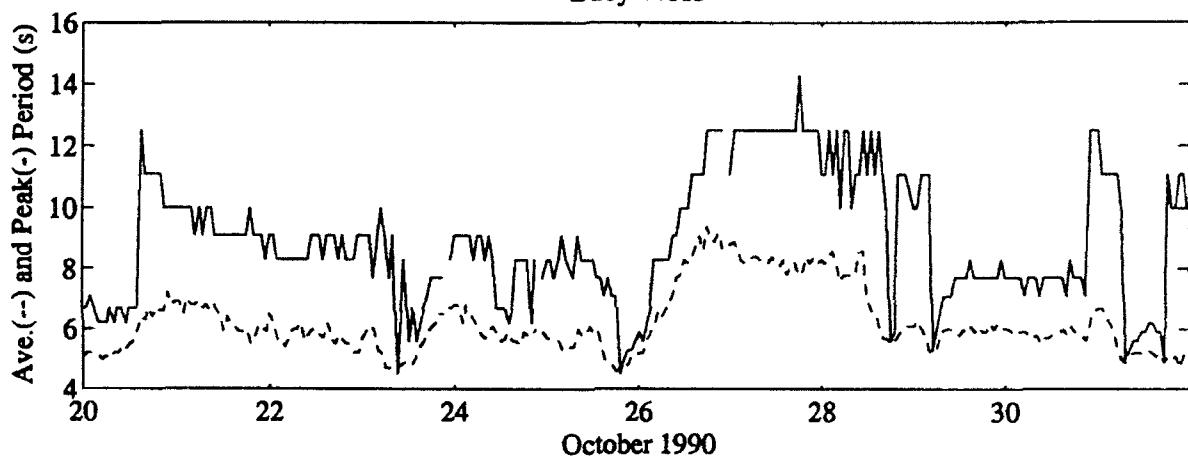
Buoy 44015



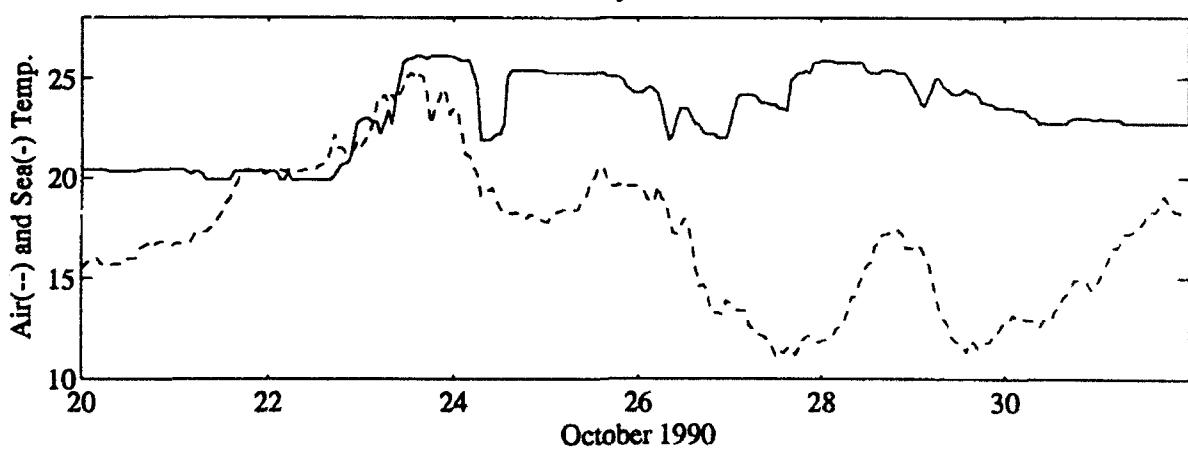
Buoy 44015



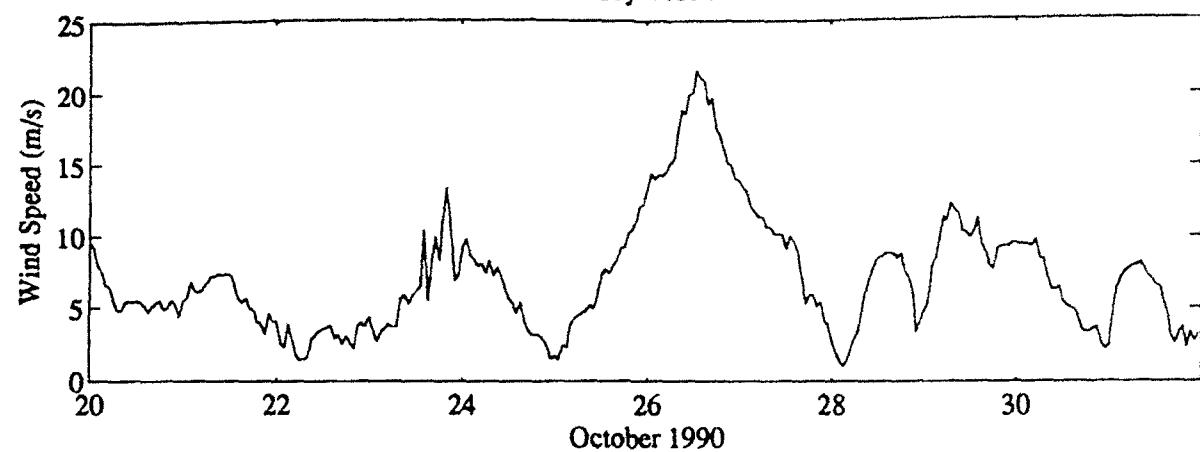
Buoy 44015



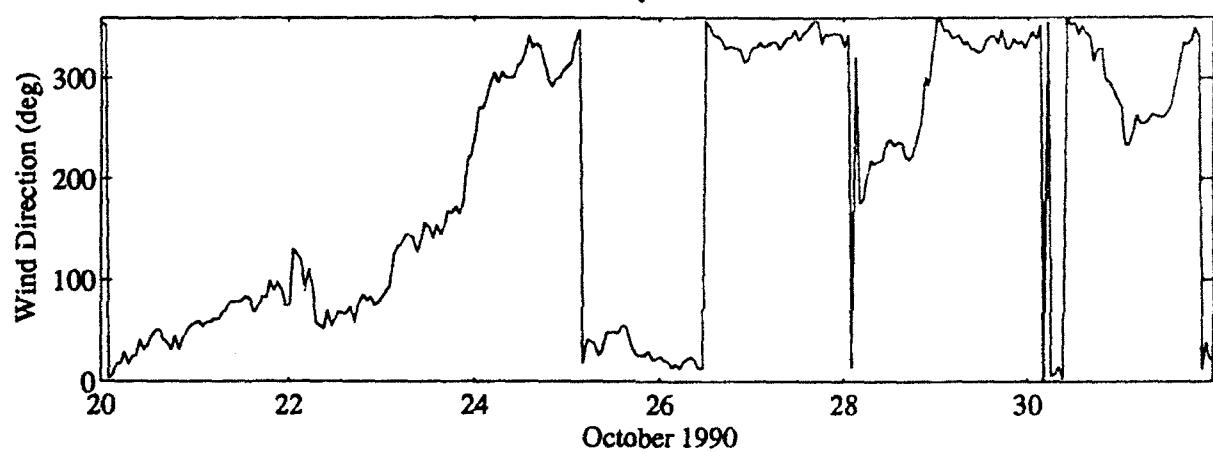
Buoy 44015



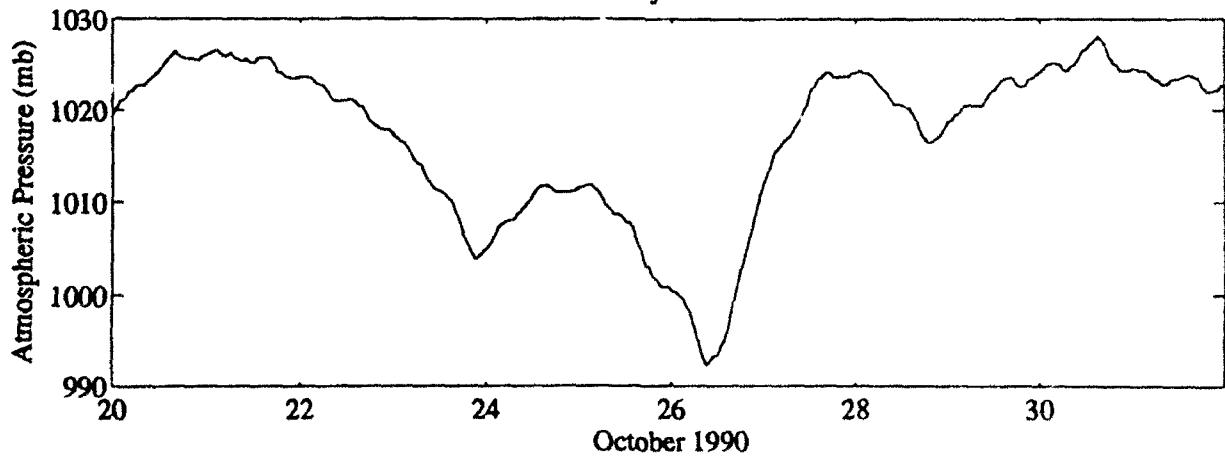
Buoy 44014



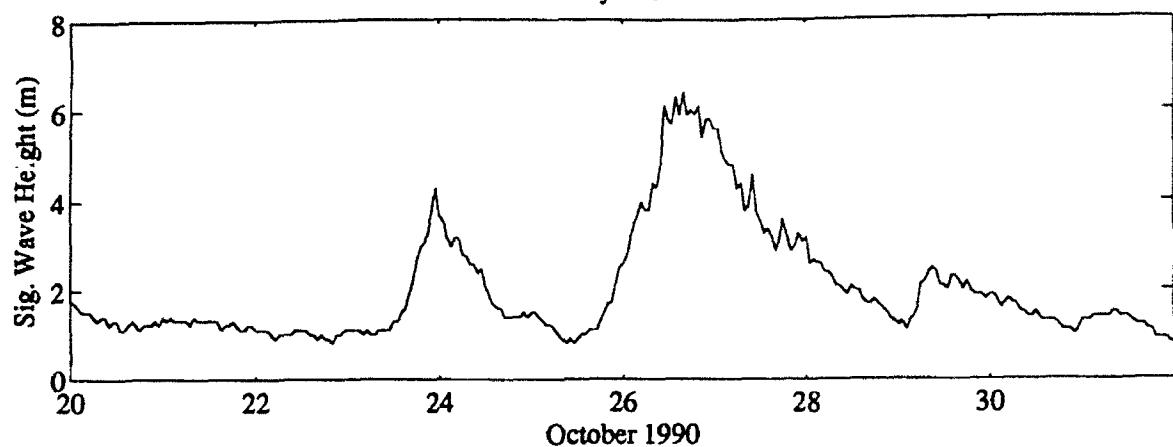
Buoy 44014



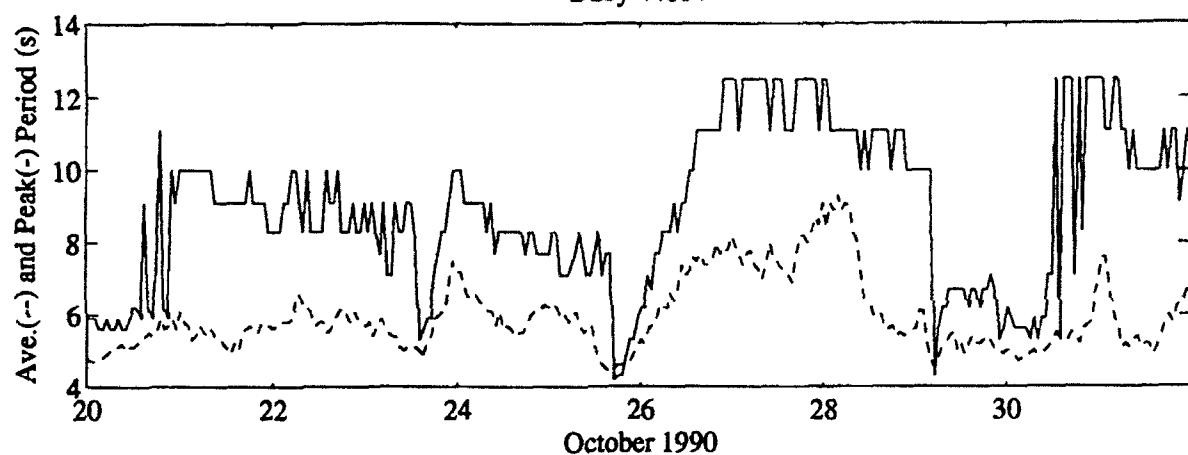
Buoy 44014



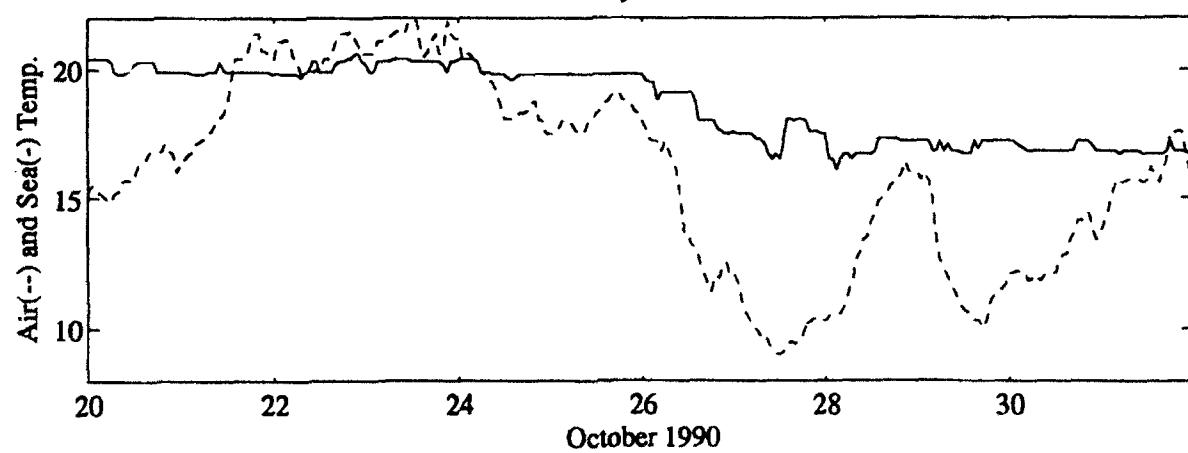
Buoy 44014



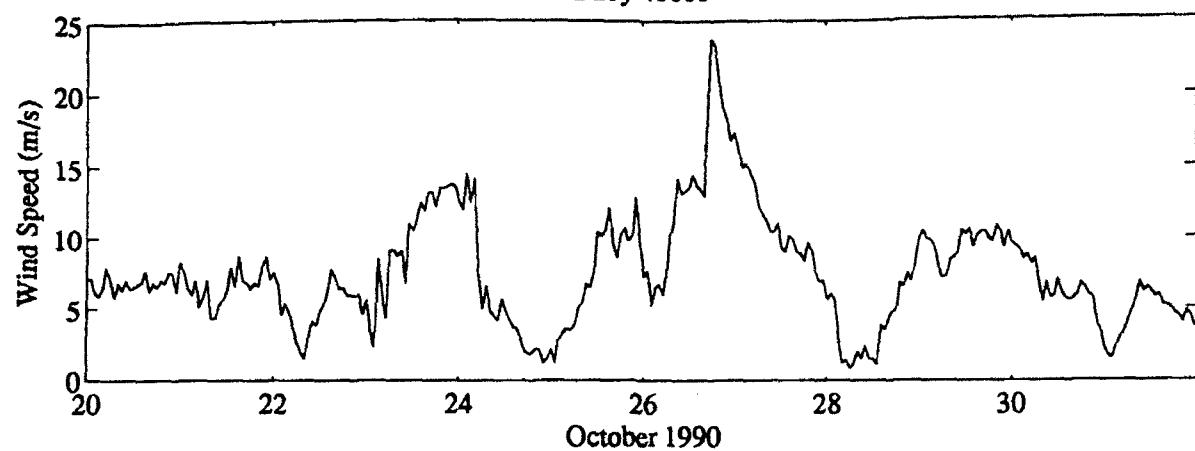
Buoy 44014



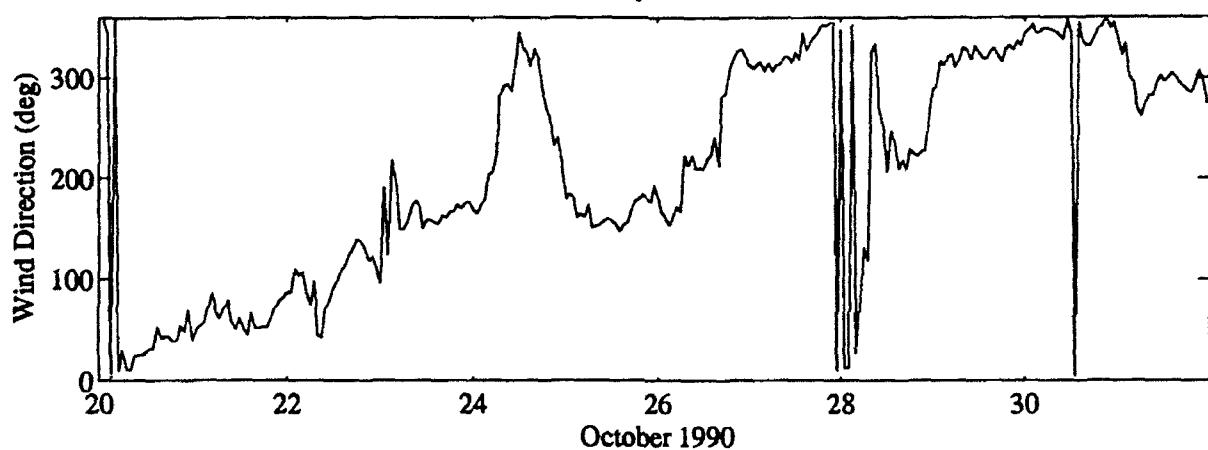
Buoy 44014



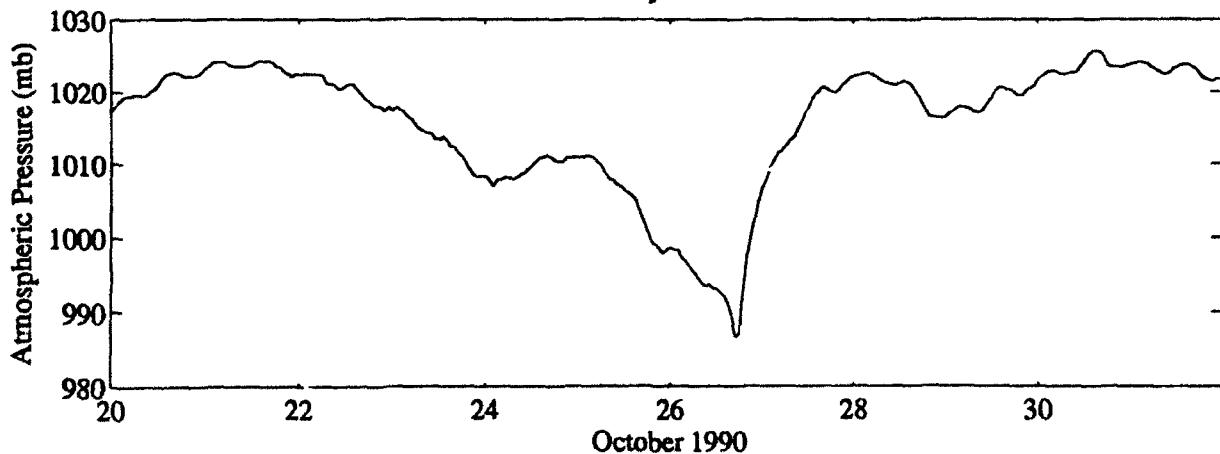
Buoy 41001



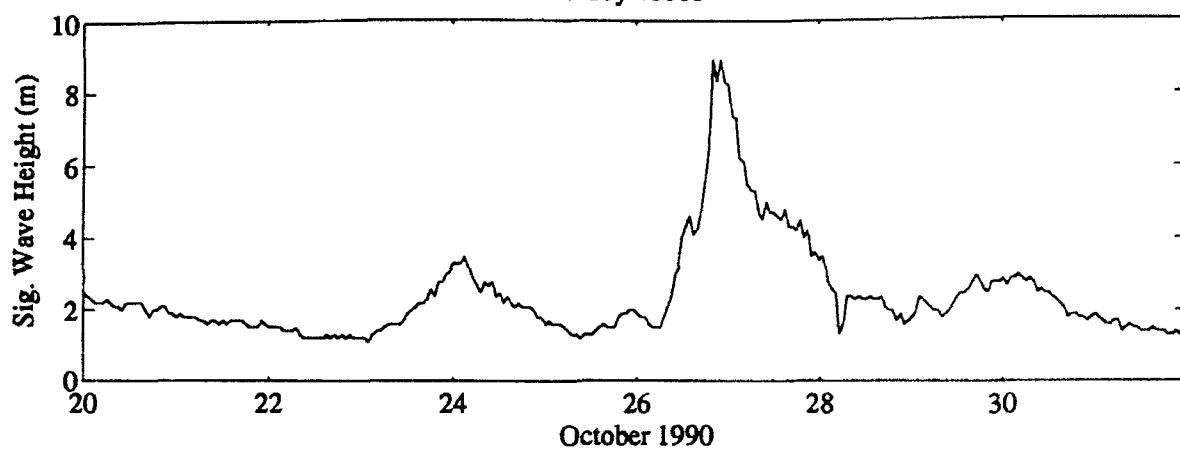
Buoy 41001



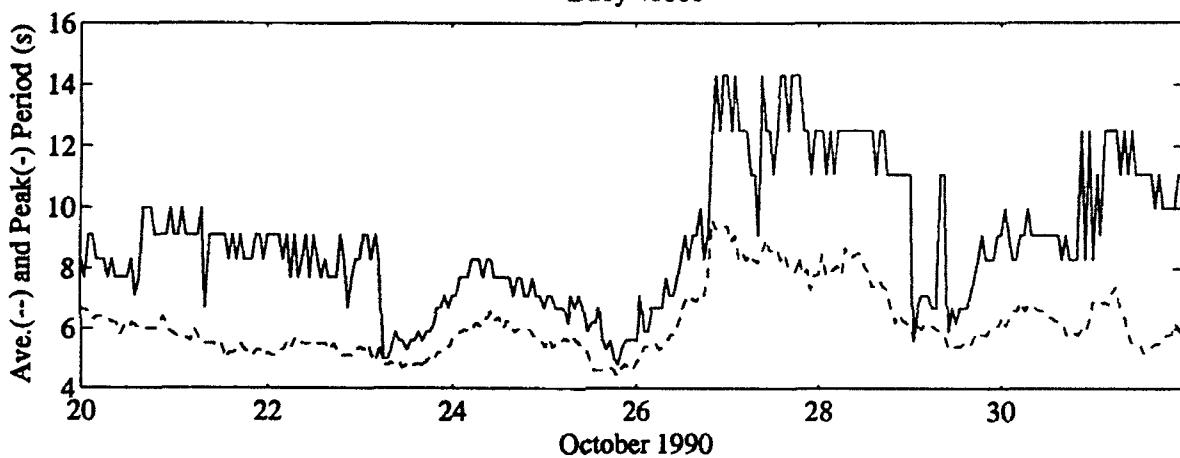
Buoy 41001



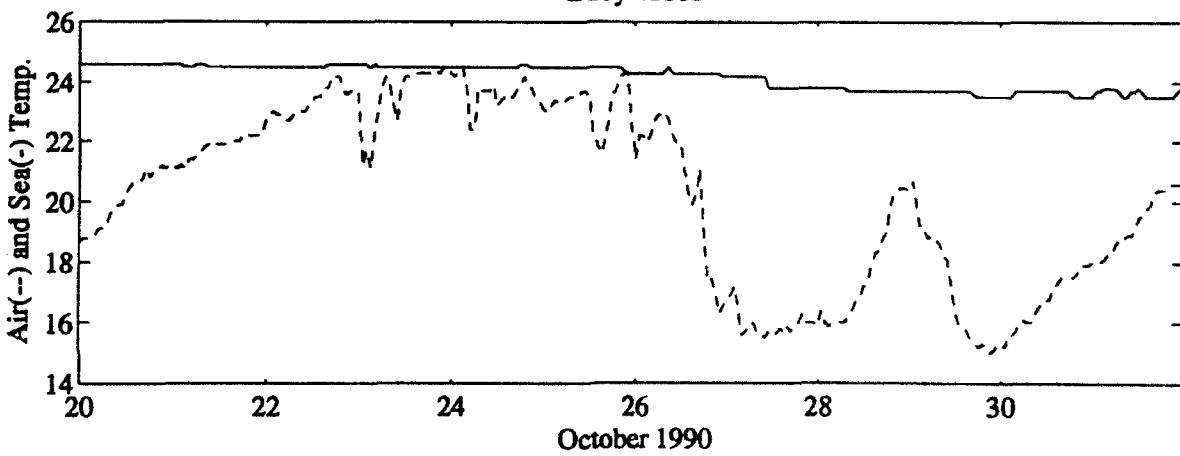
Buoy 41001



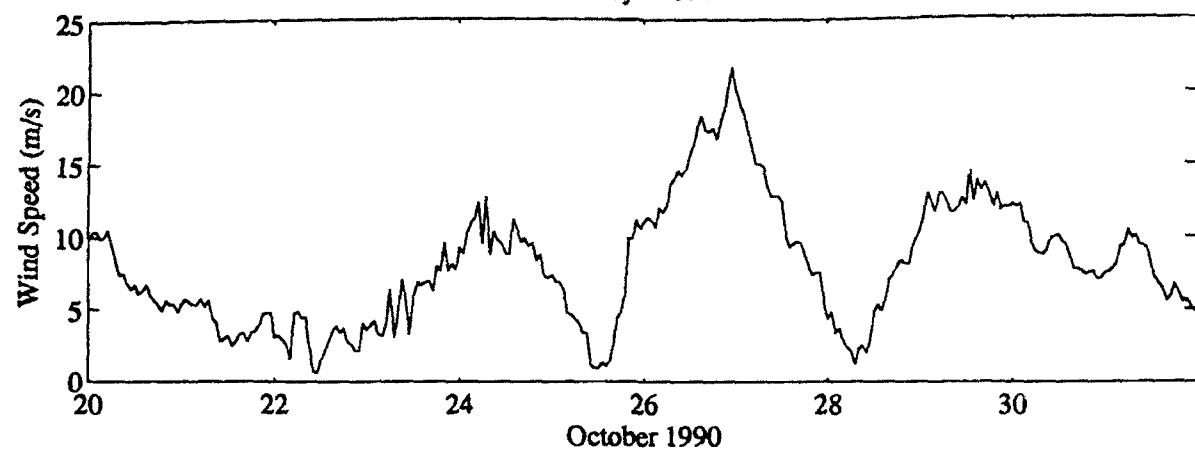
Buoy 41001



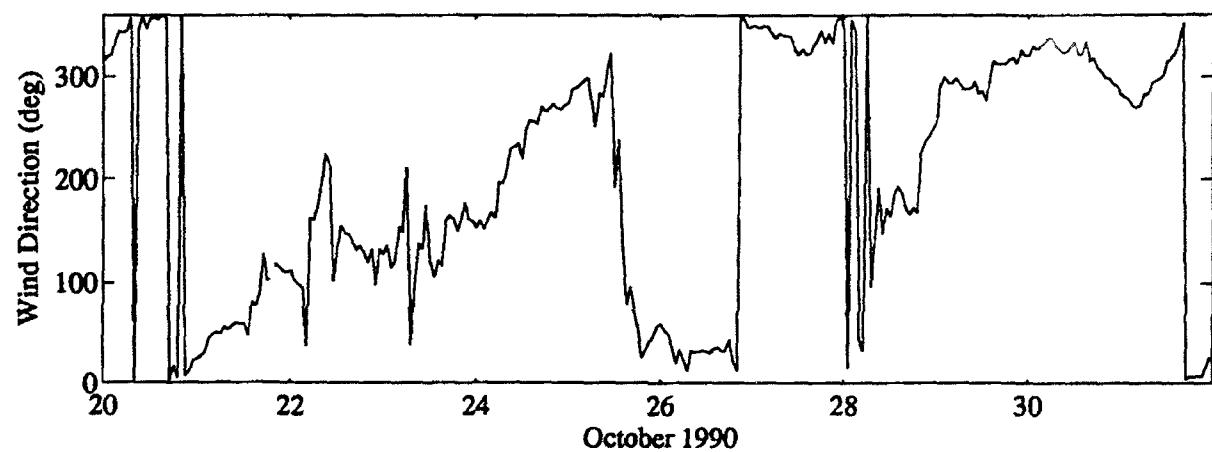
Buoy 41001



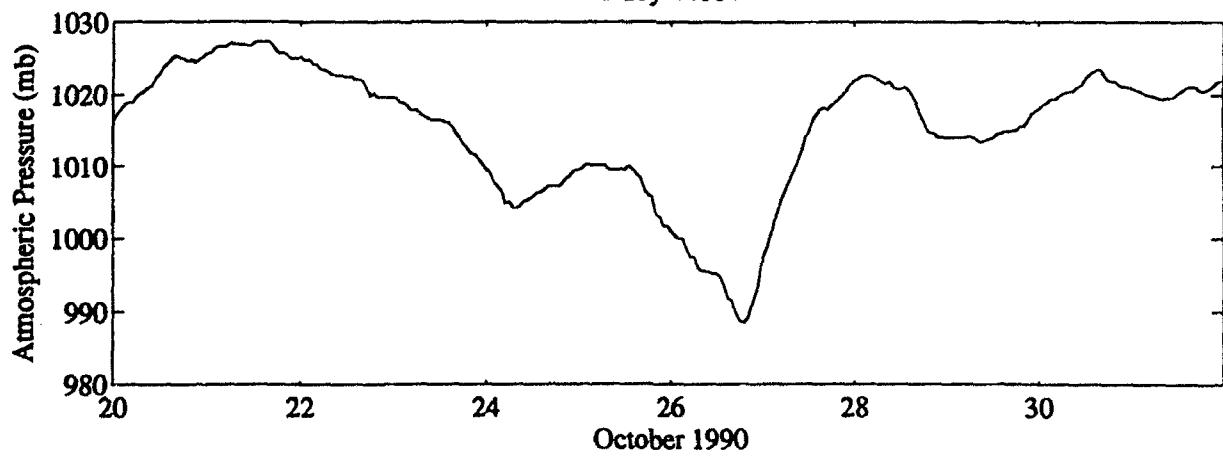
Buoy 44004



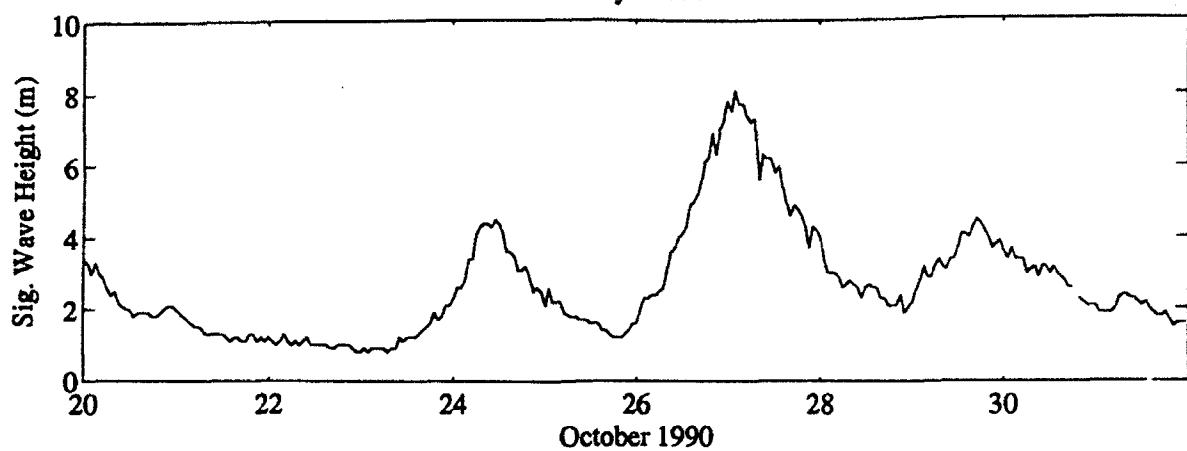
Buoy 44004



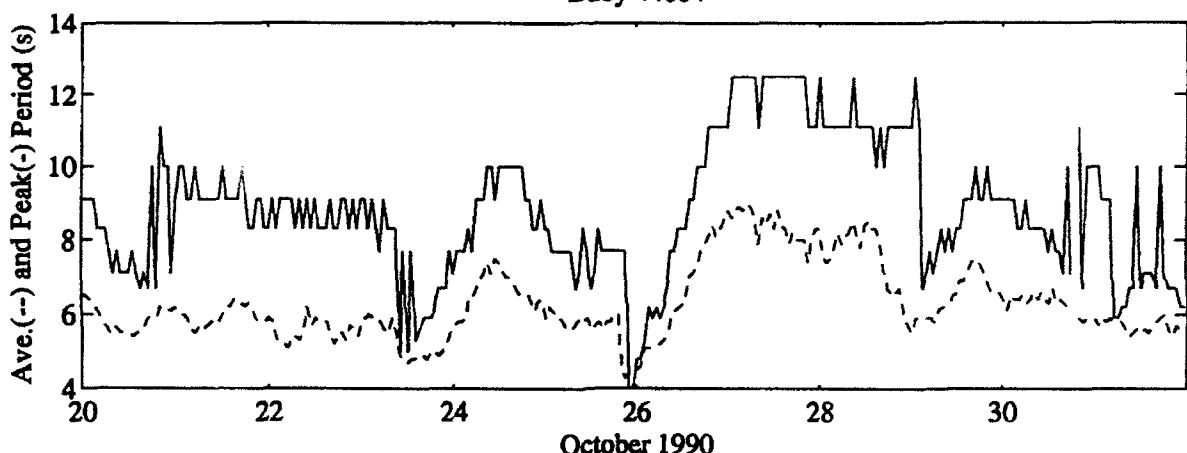
Buoy 44004



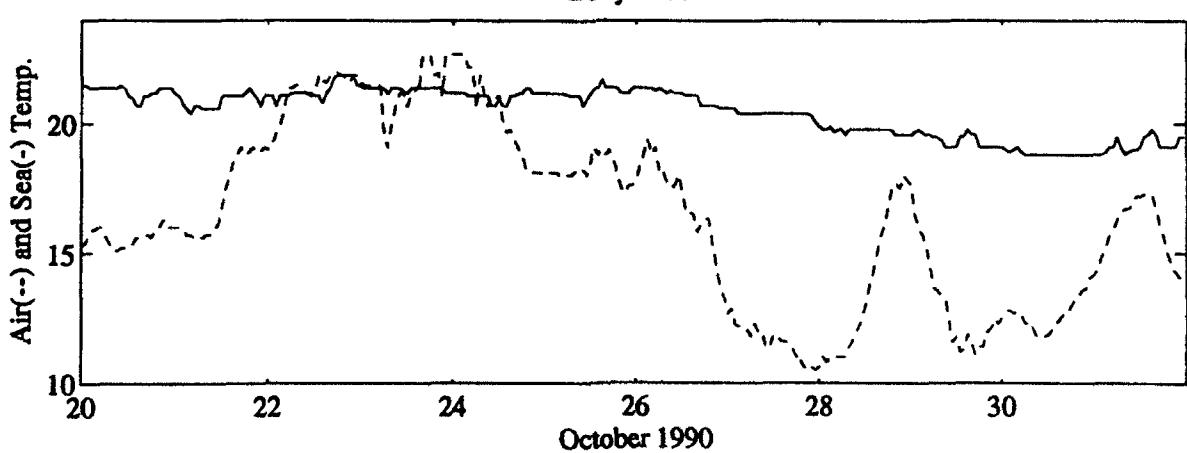
Buoy 44004



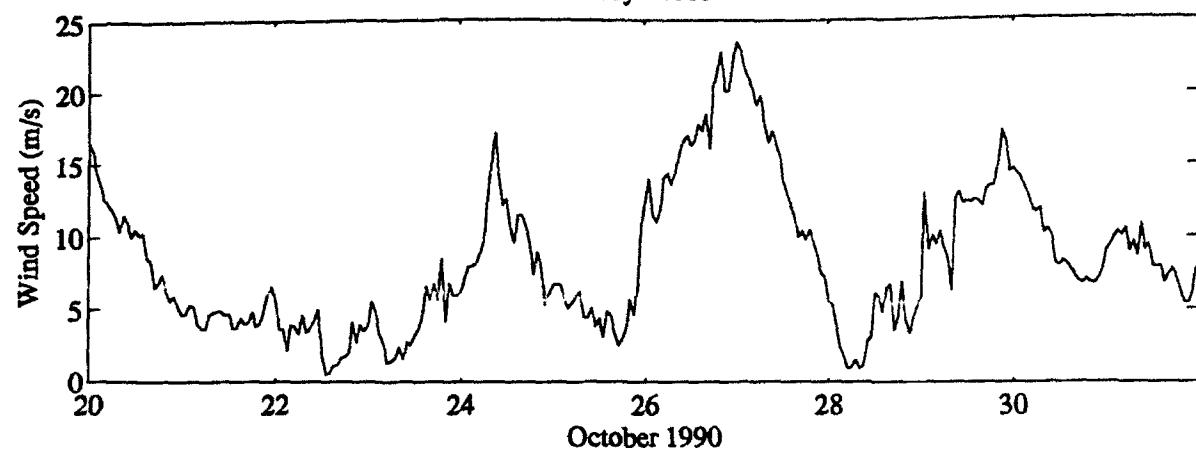
Buoy 44004



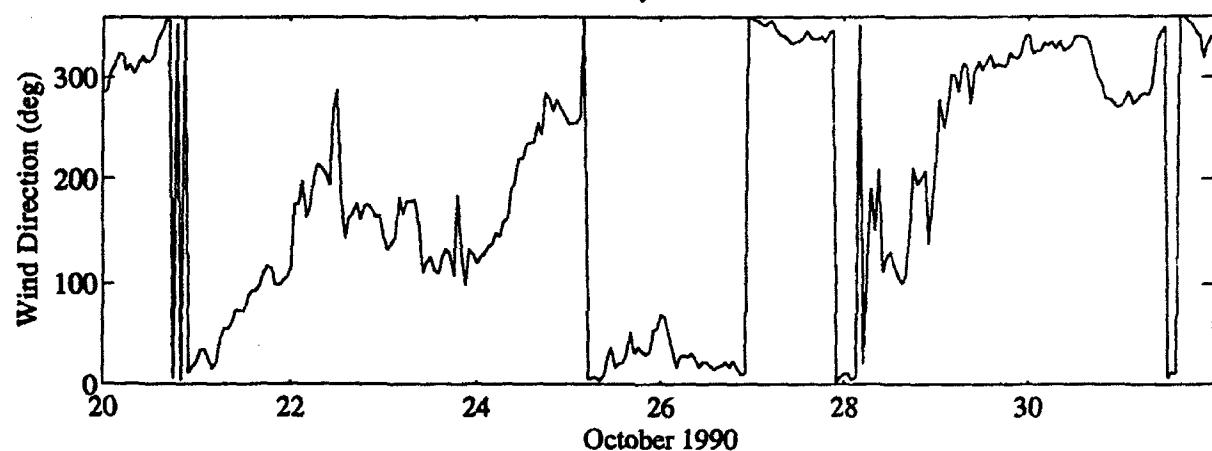
Buoy 44004



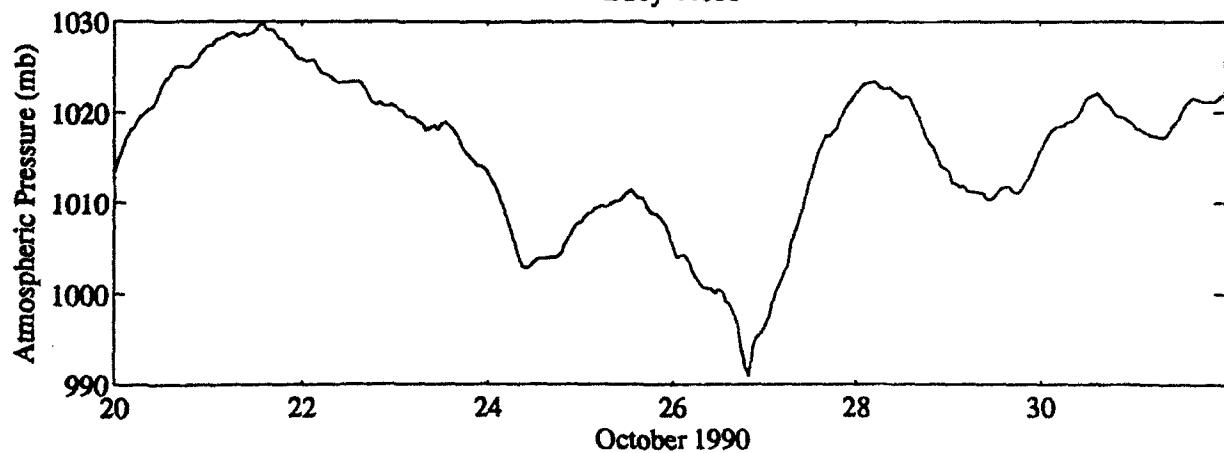
Buoy 44008



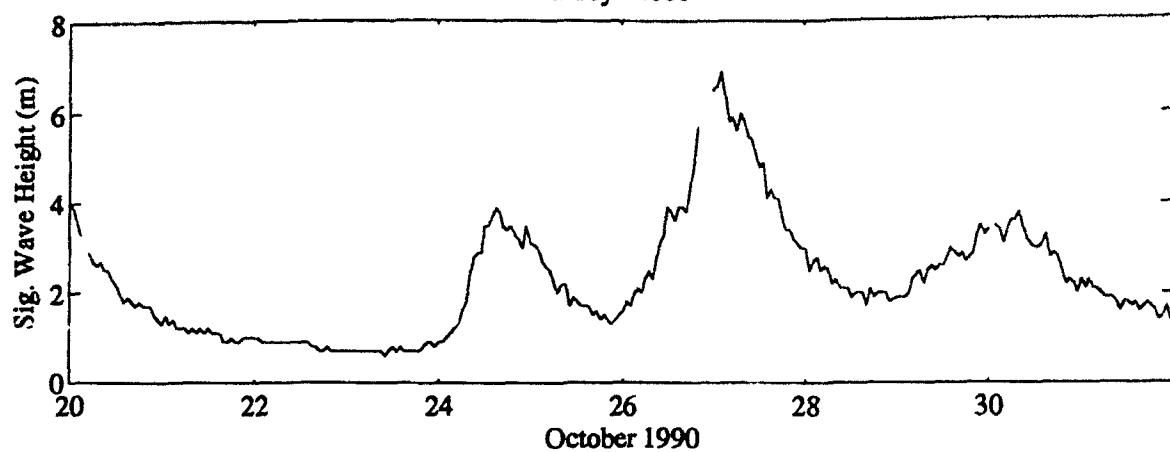
Buoy 44008



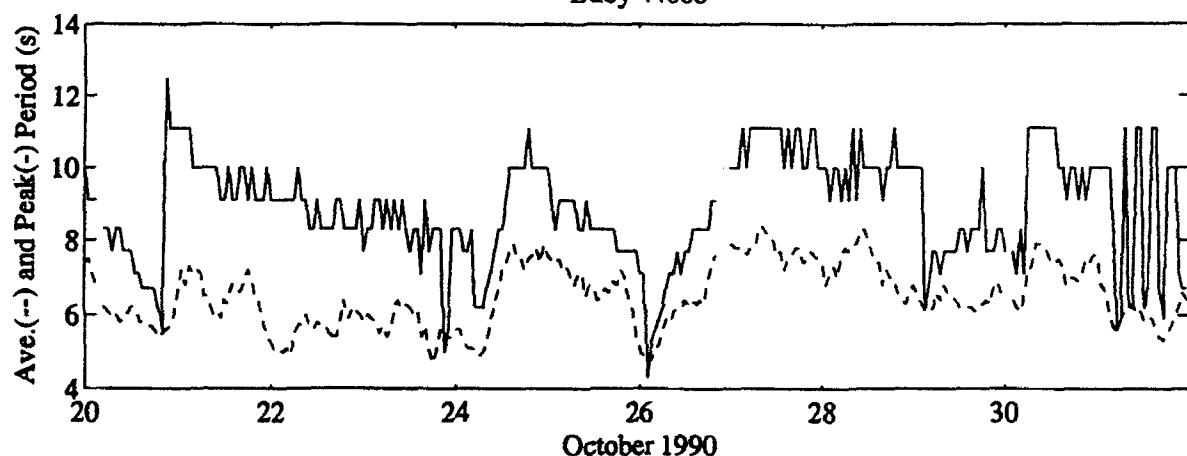
Buoy 44008



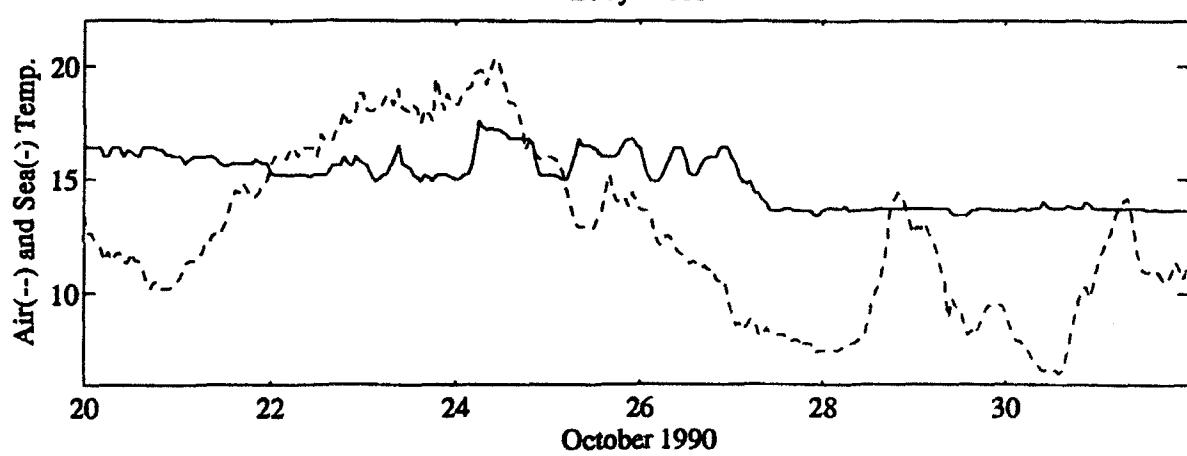
Buoy 44008



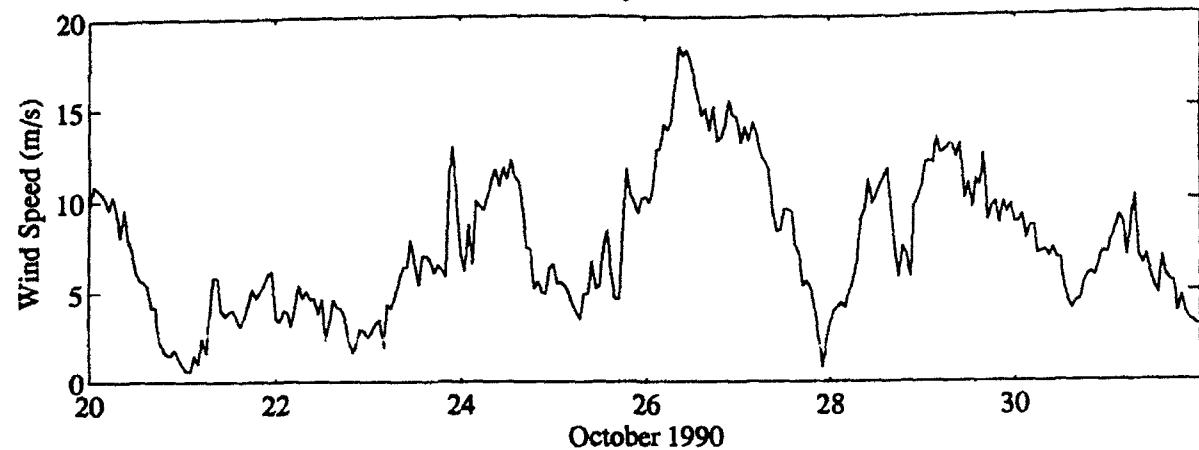
Buoy 44008



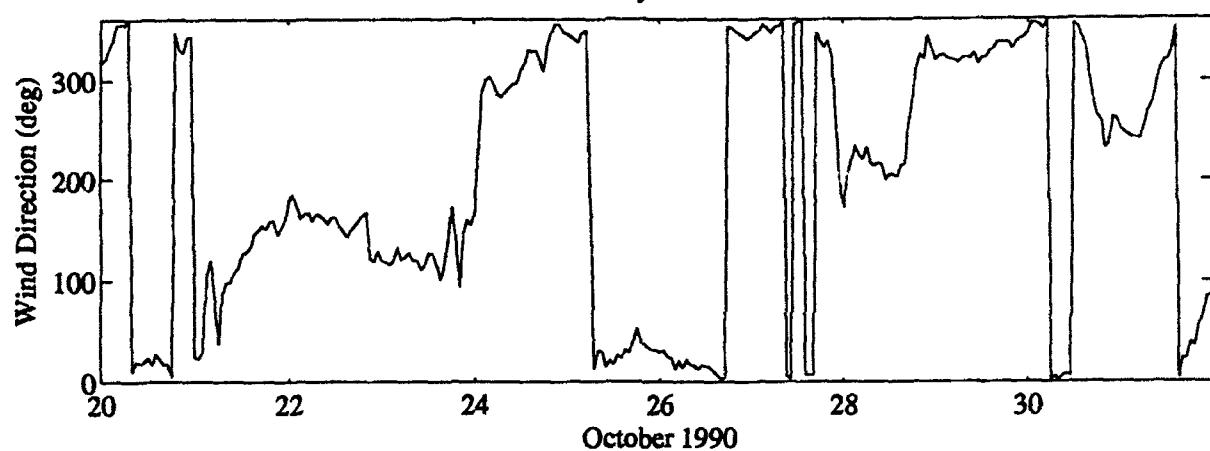
Buoy 44008



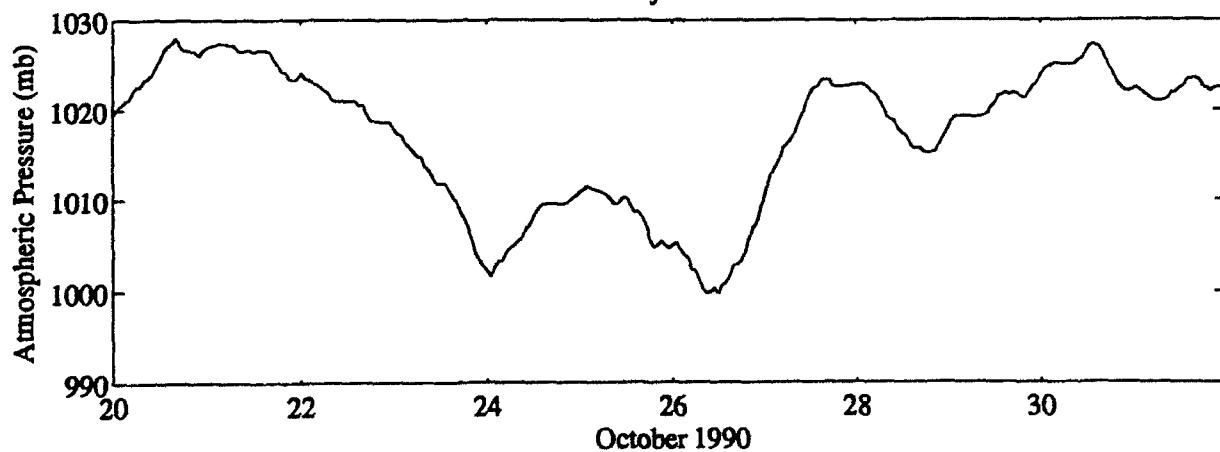
Buoy 44009



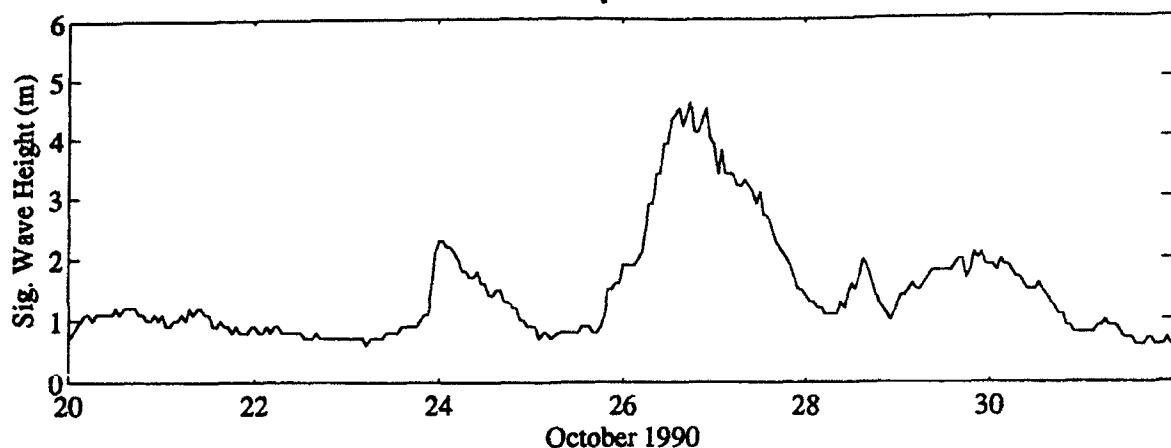
Buoy 44009



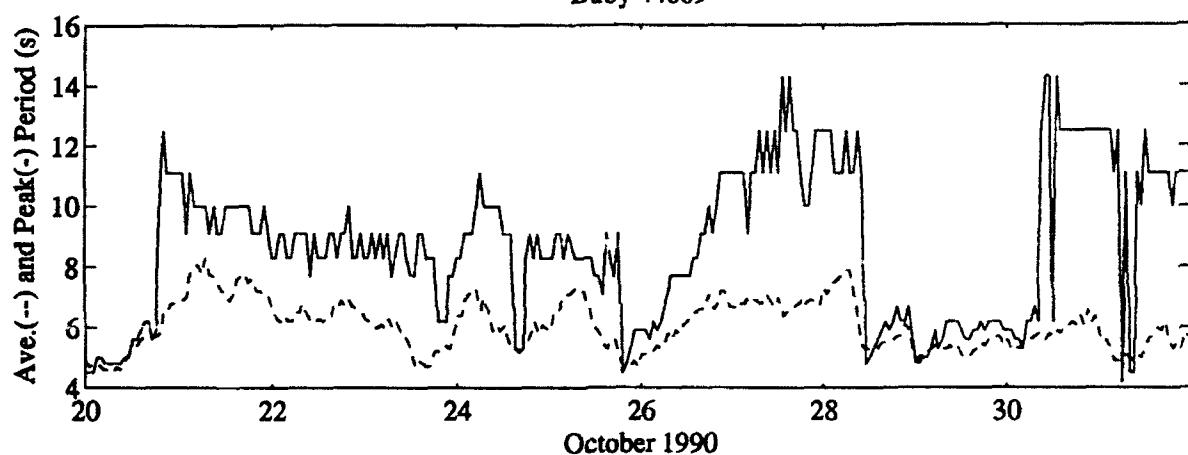
Buoy 44009



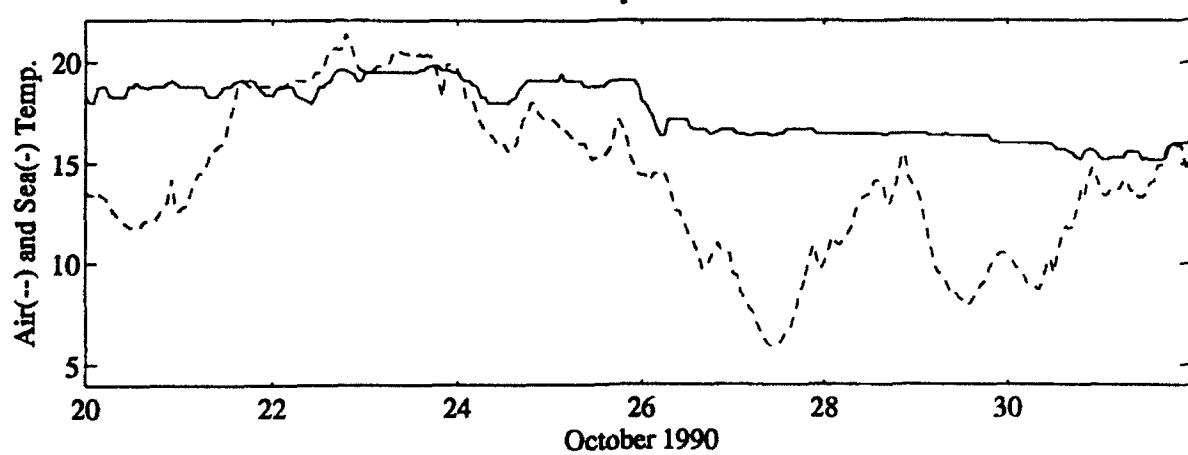
Buoy 44009



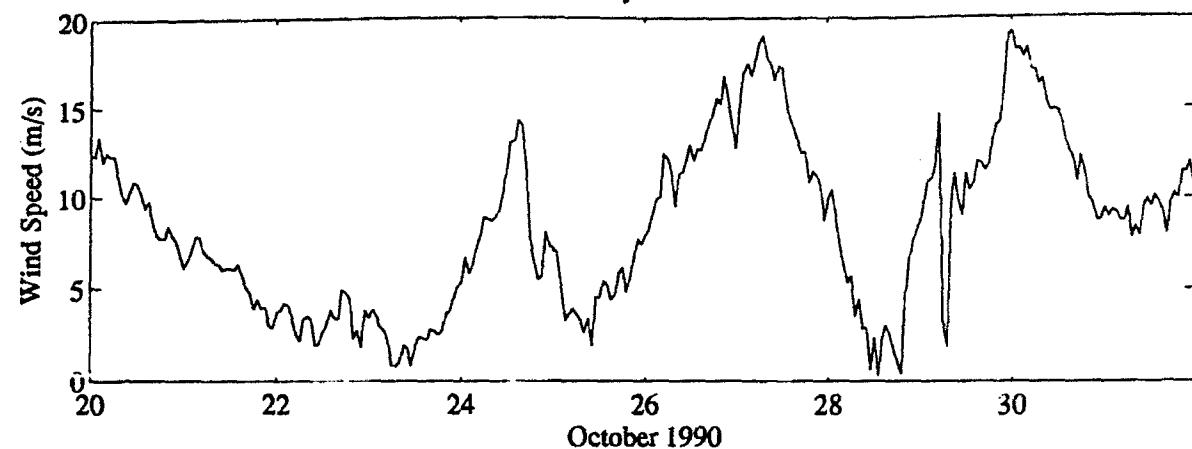
Buoy 44009



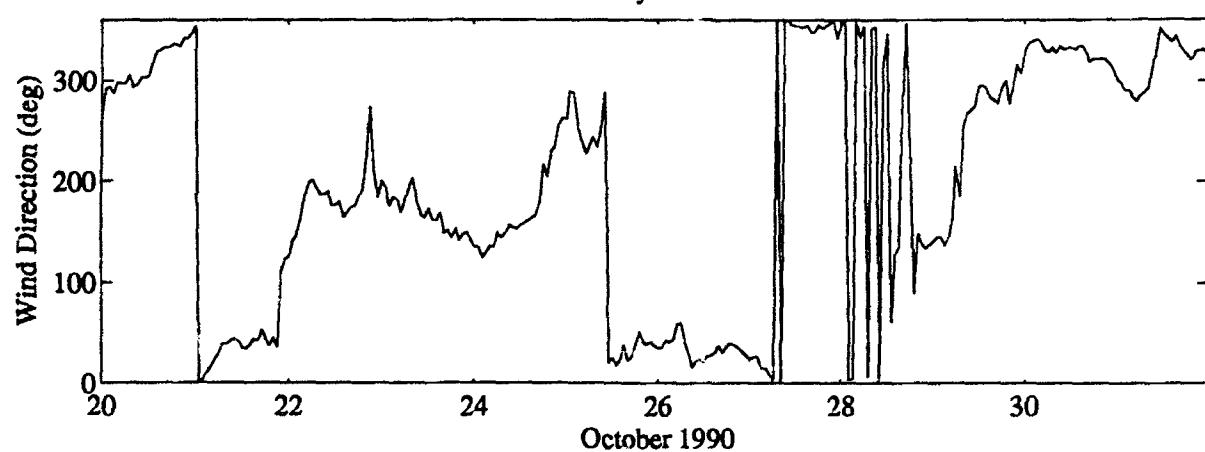
Buoy 44009



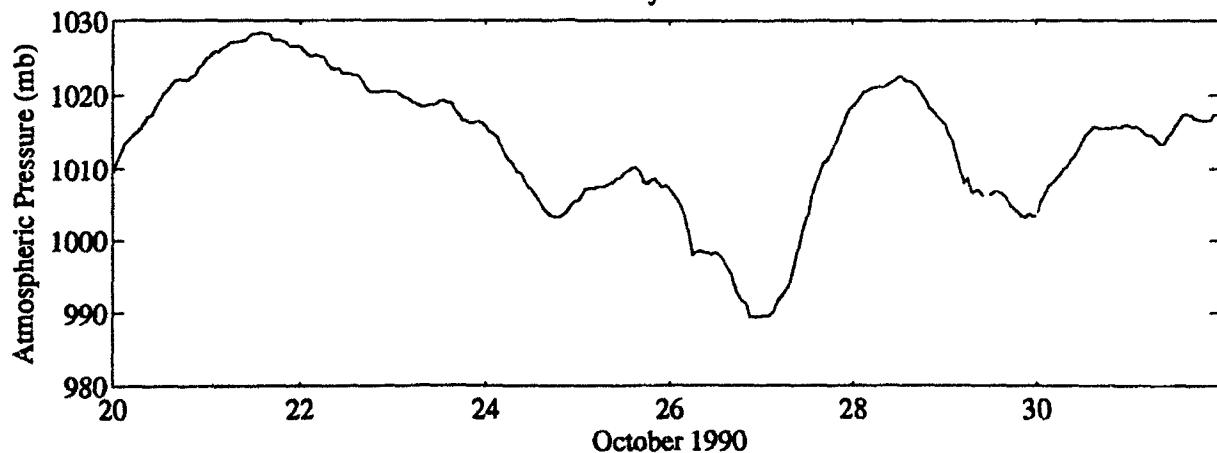
Buoy 44011



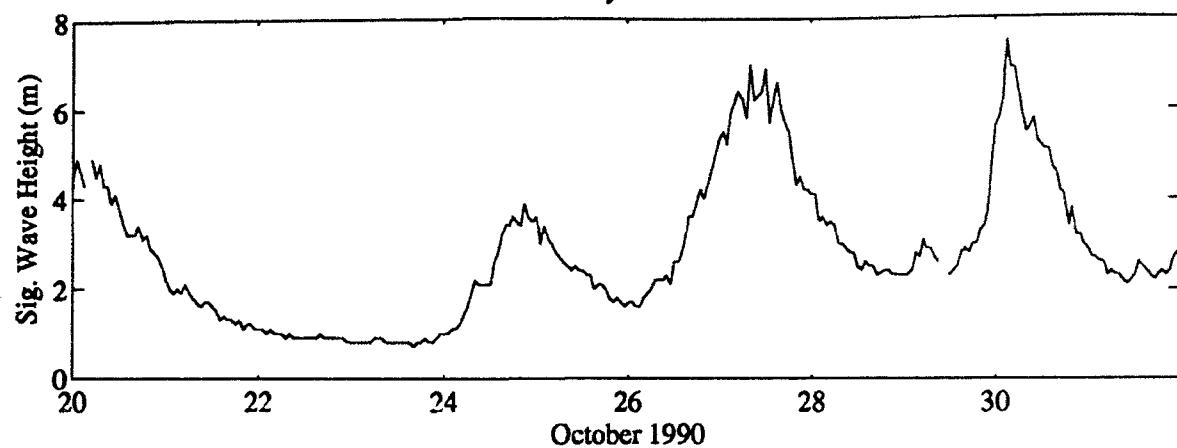
Buoy 44011



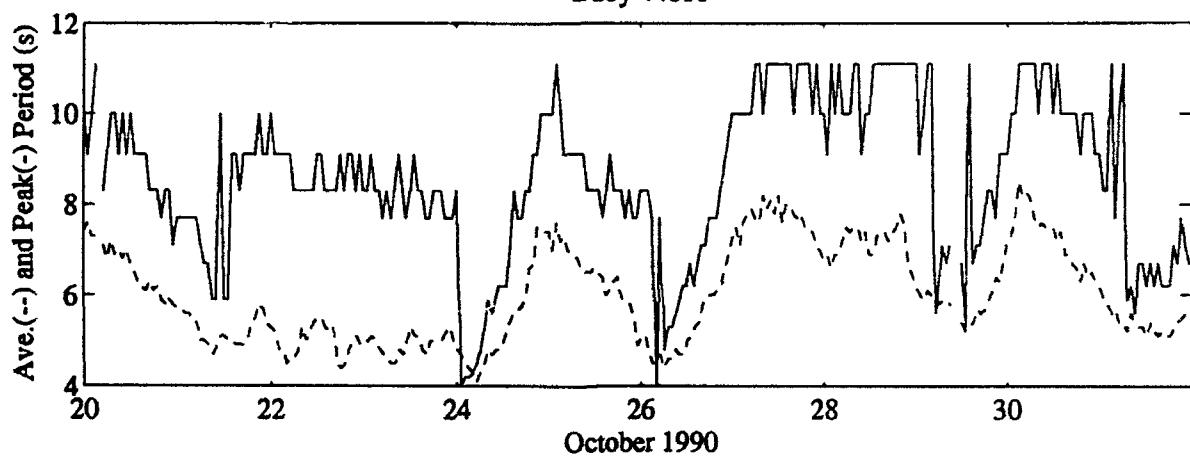
Buoy 44011



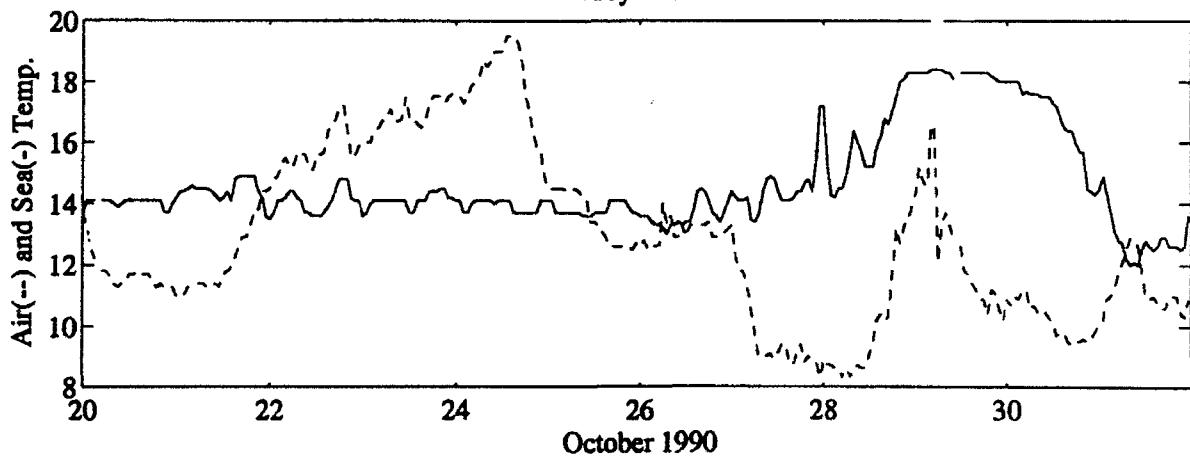
Buoy 44011



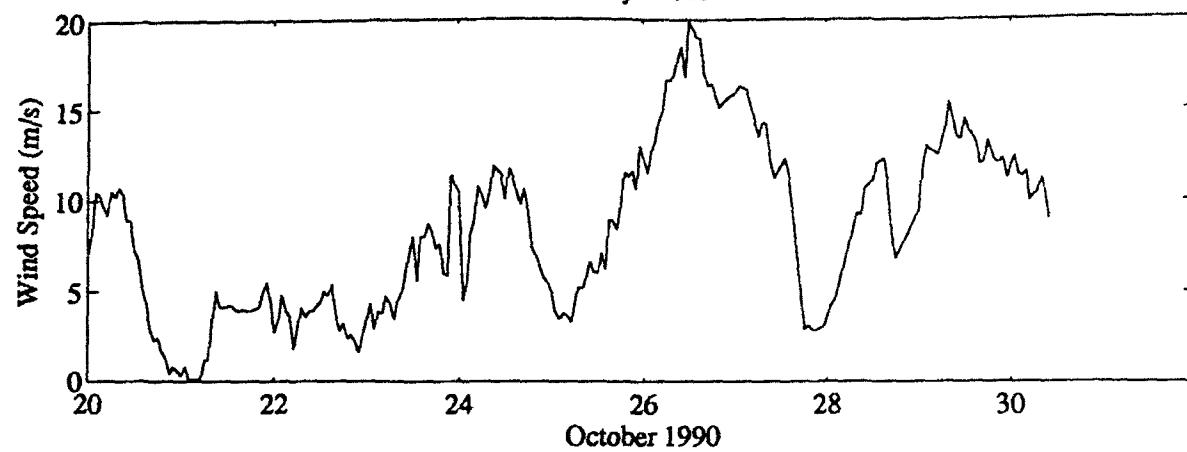
Buoy 44011



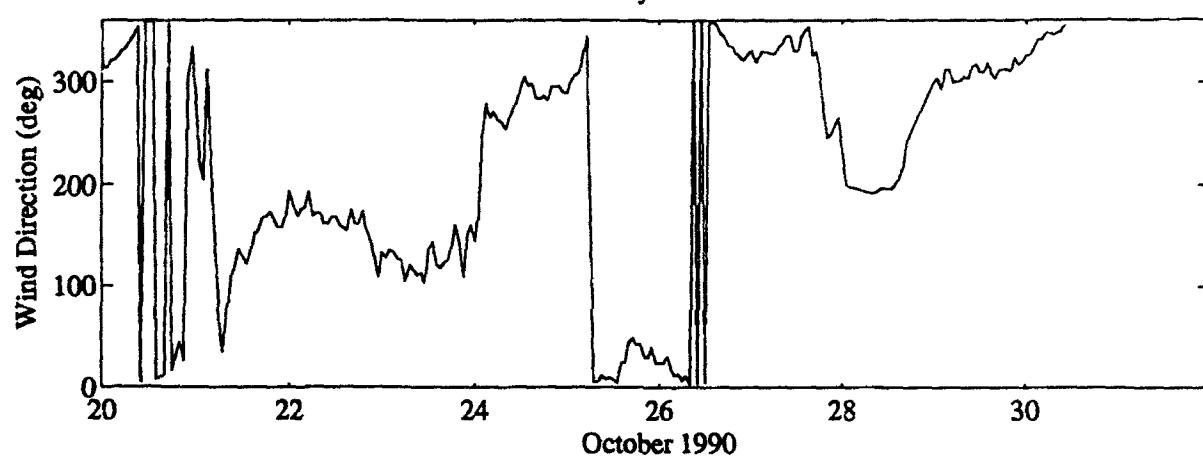
Buoy 44011



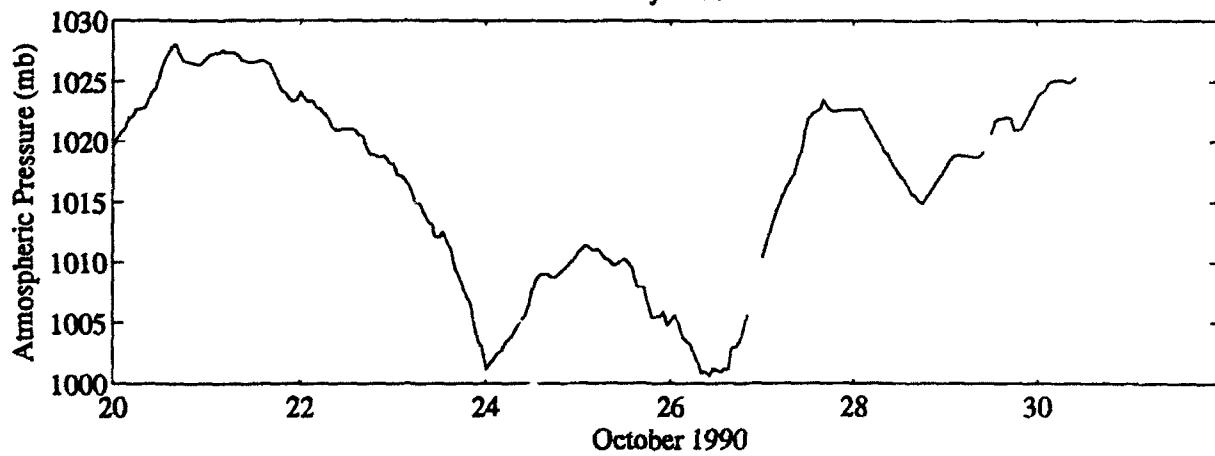
Buoy 44012



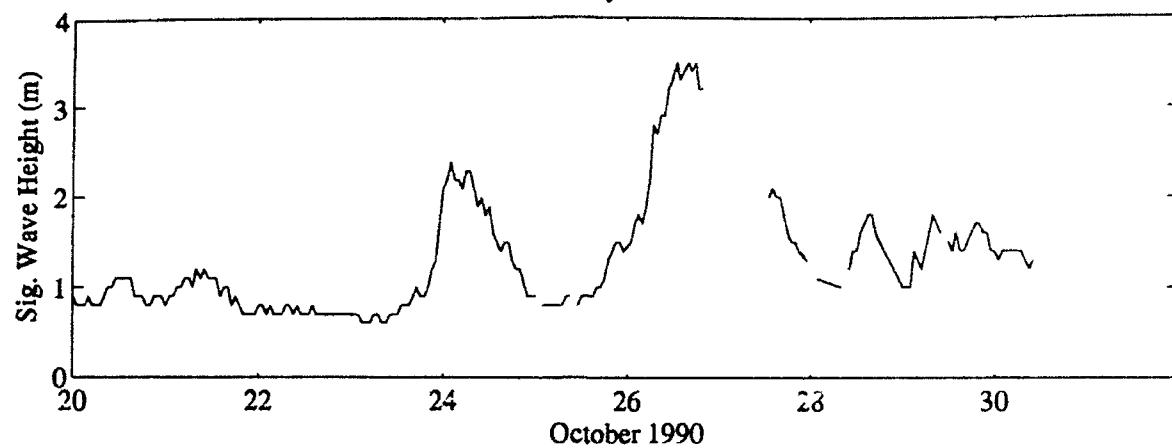
Buoy 44012



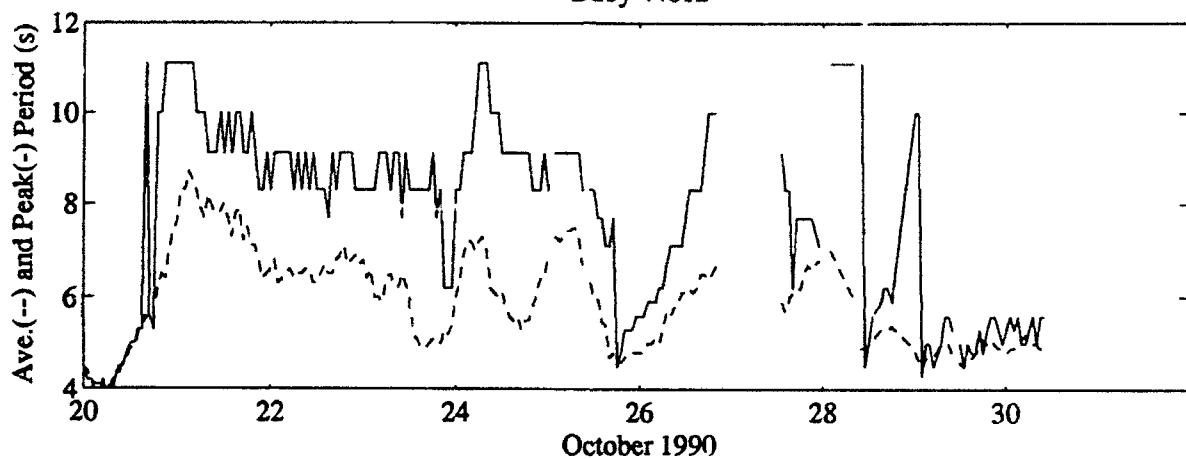
Buoy 44012



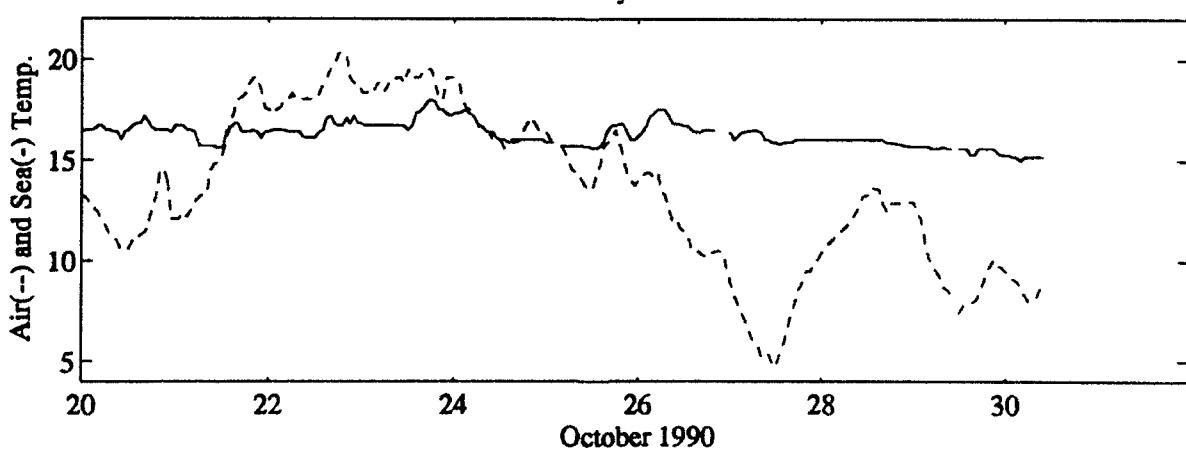
Buoy 44012



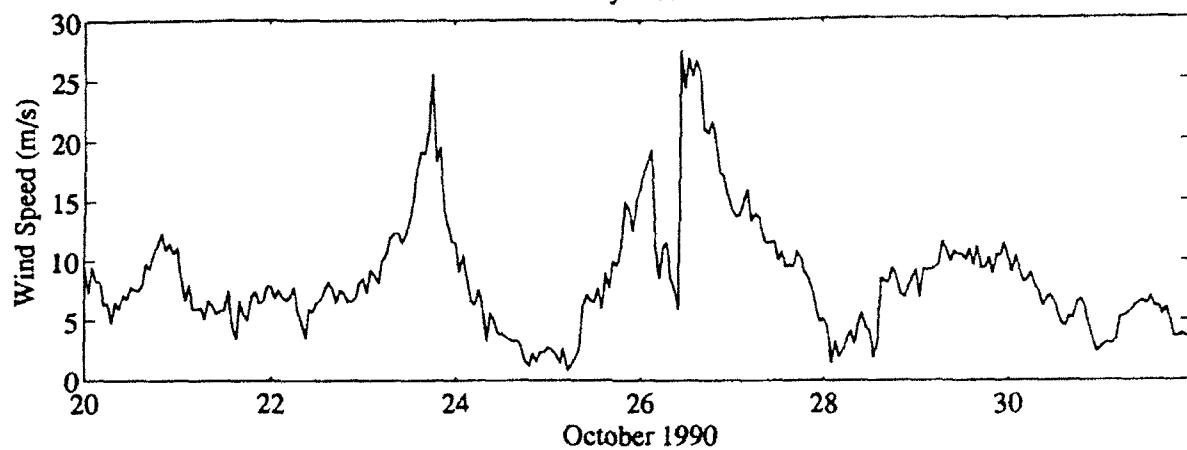
Buoy 44012



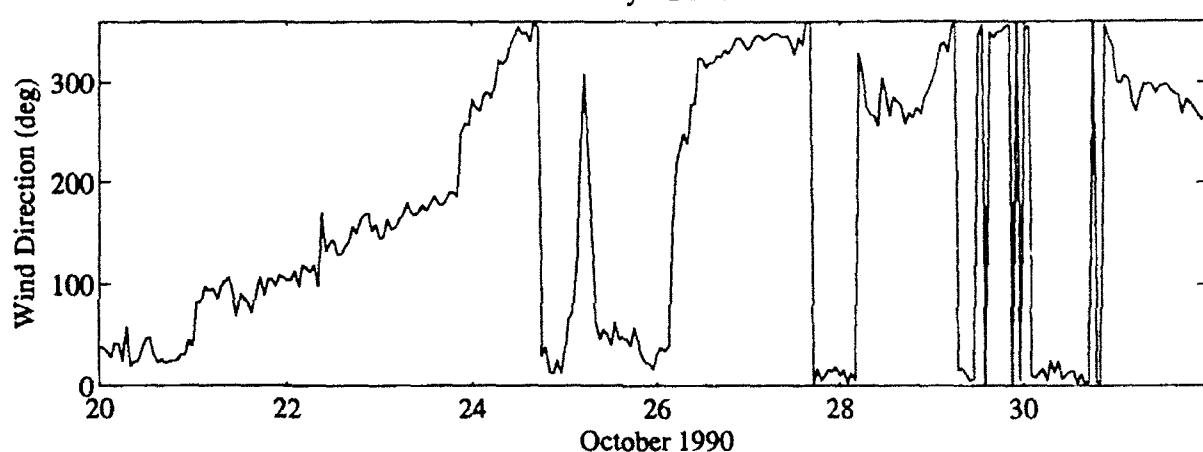
Buoy 44012



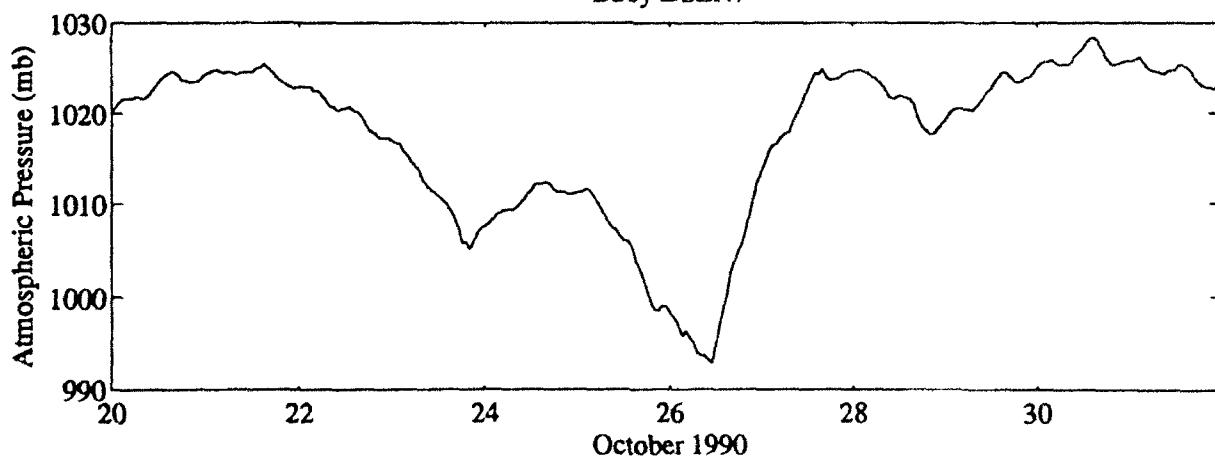
Buoy DSLN7



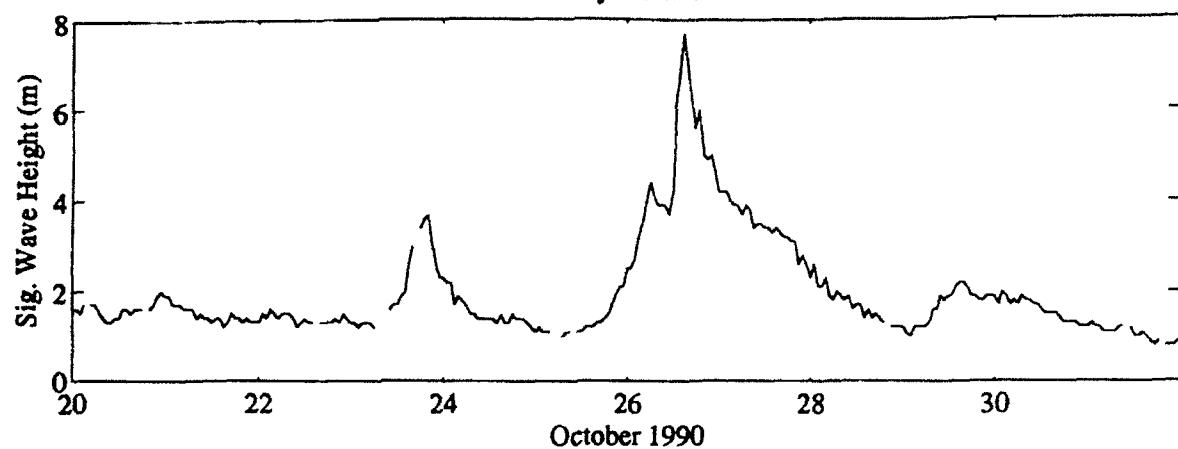
Buoy DSLN7



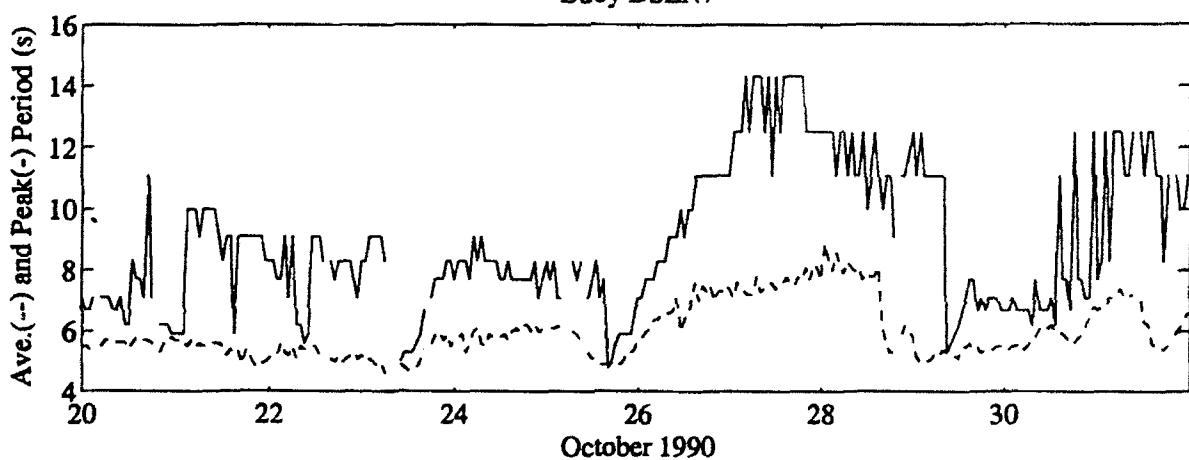
Buoy DSLN7



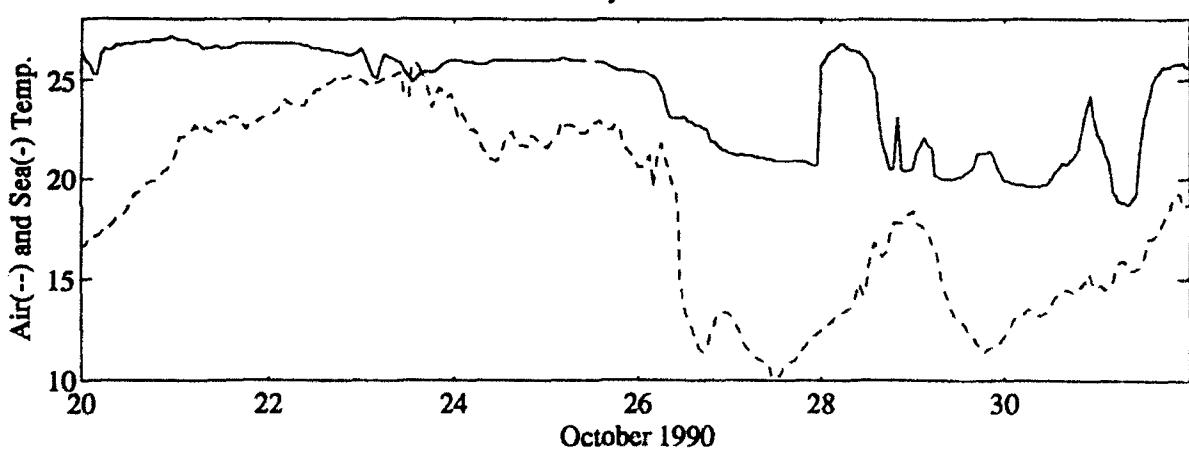
Buoy DSLN7



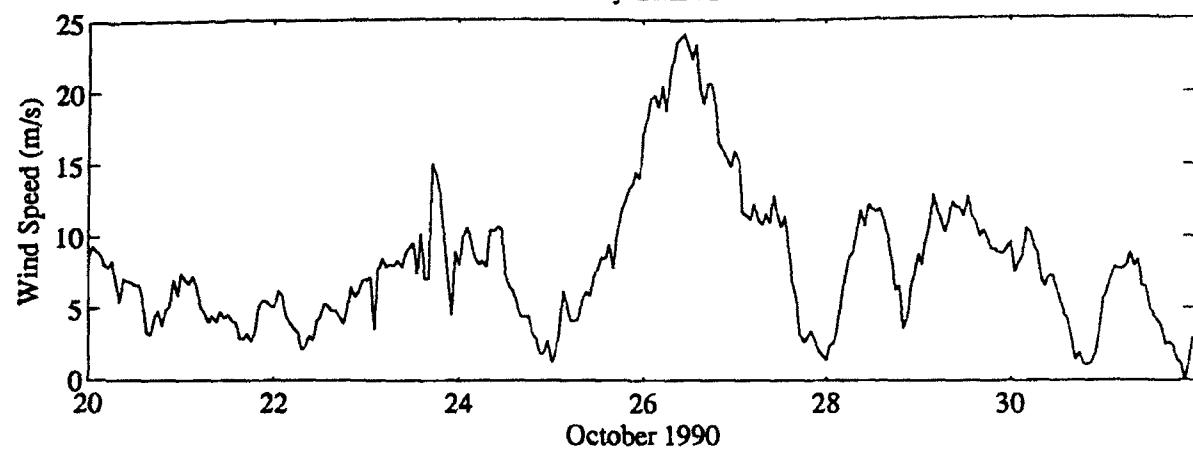
Buoy DSLN7



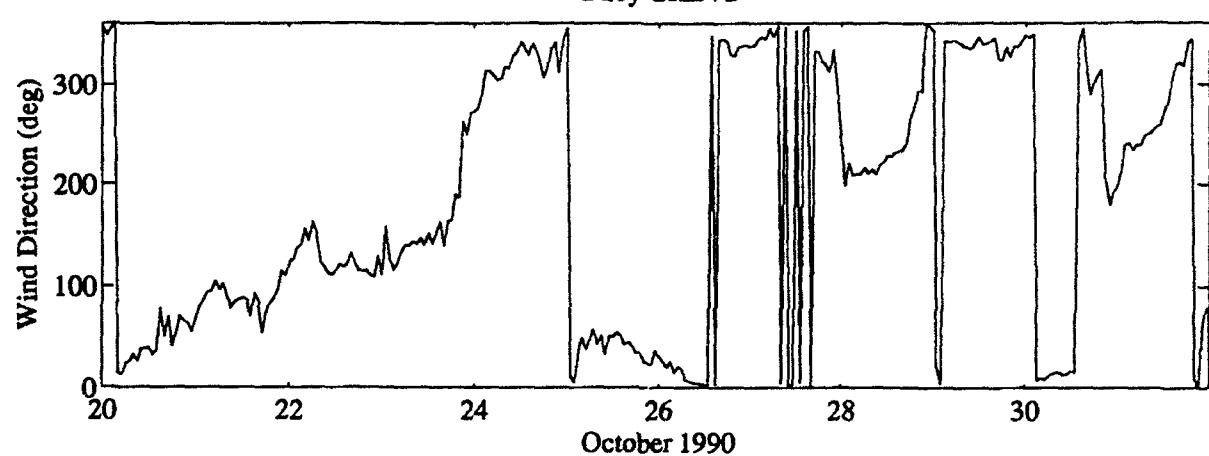
Buoy DSLN7



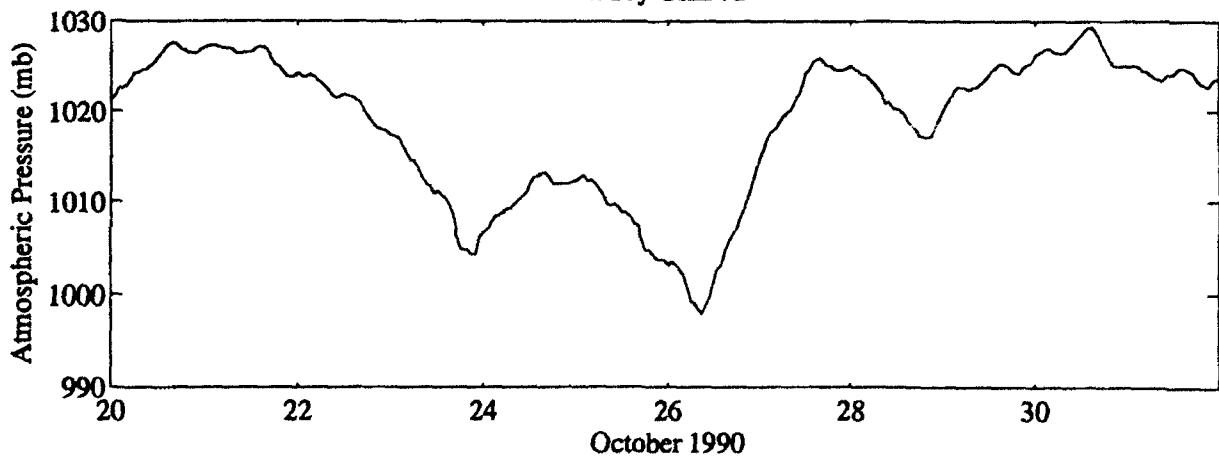
Buoy CHLV2



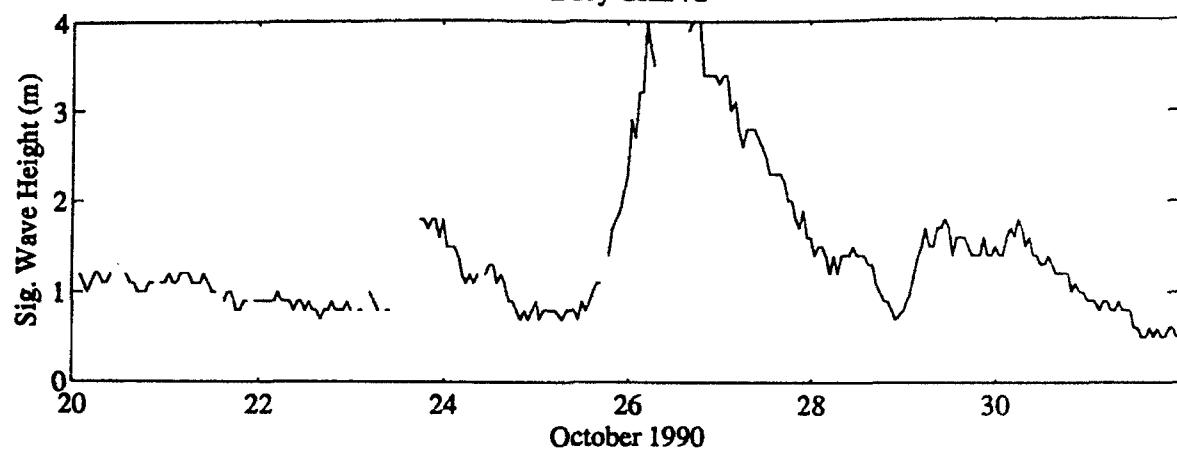
Buoy CHLV2



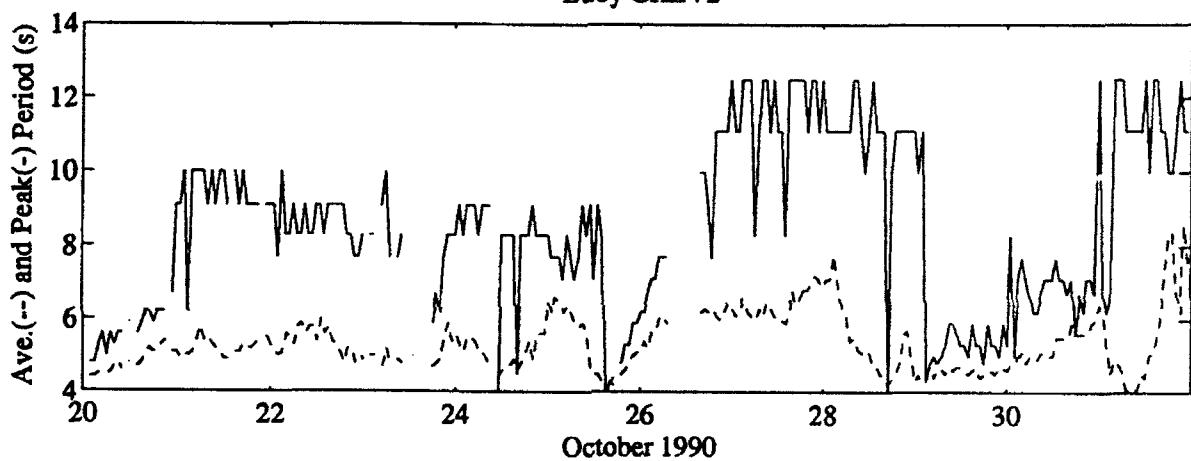
Buoy CHLV2



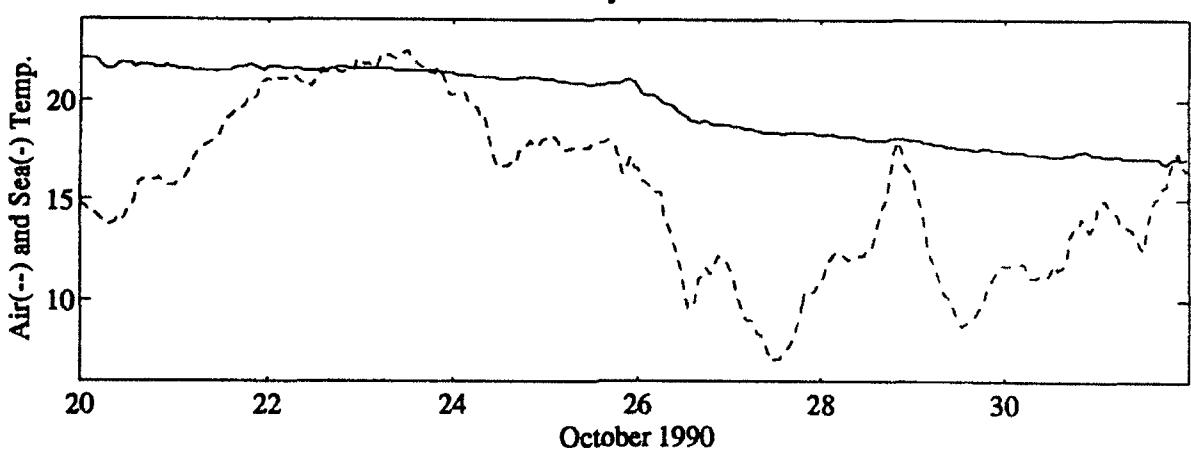
Buoy CHLV2



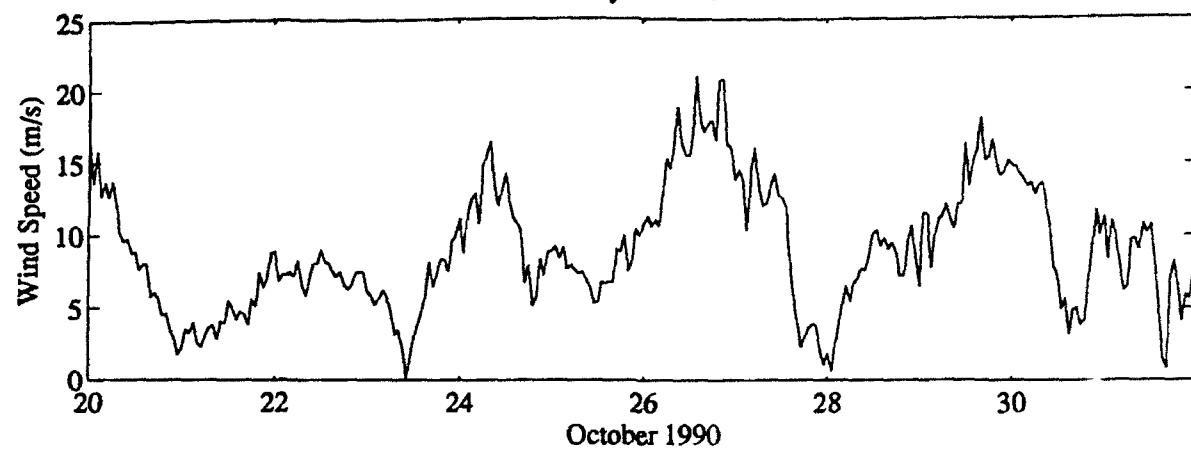
Buoy CHLV2



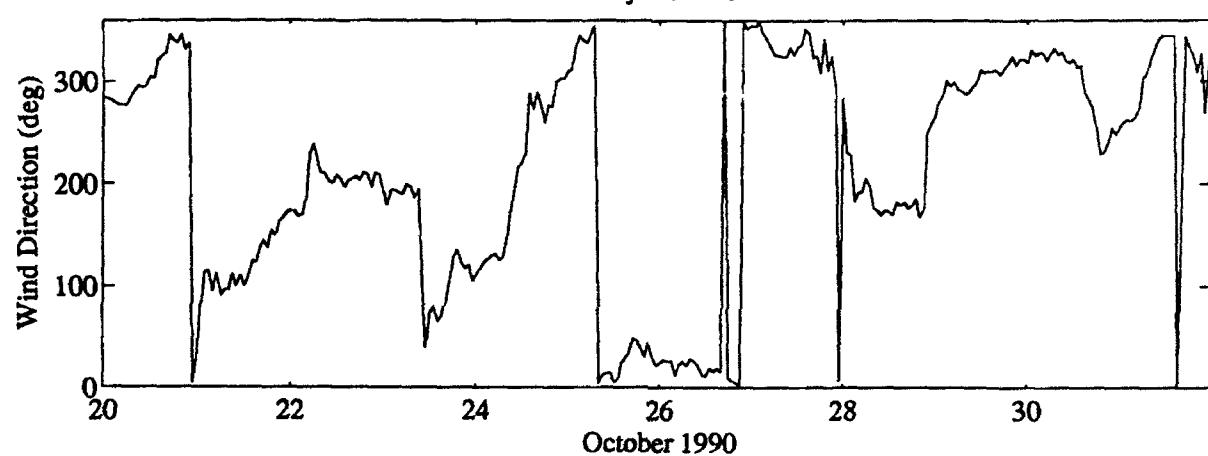
Buoy CHLV2



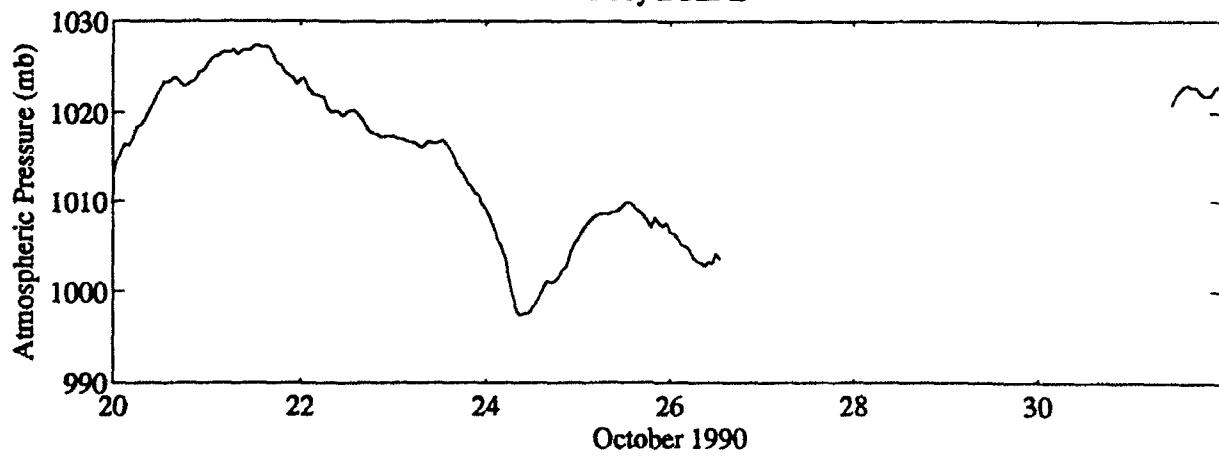
Buoy BUZM3



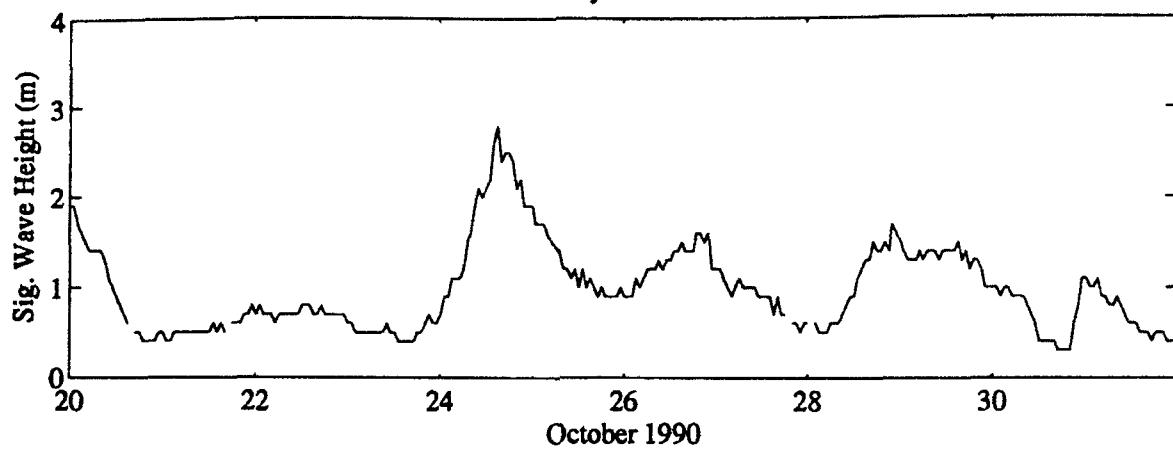
Buoy BUZM3



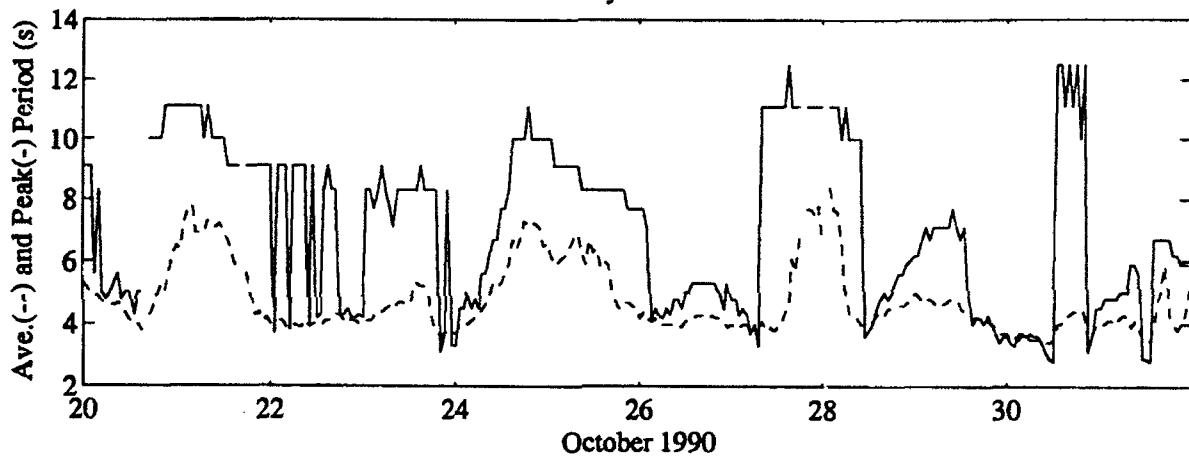
Buoy BUZM3



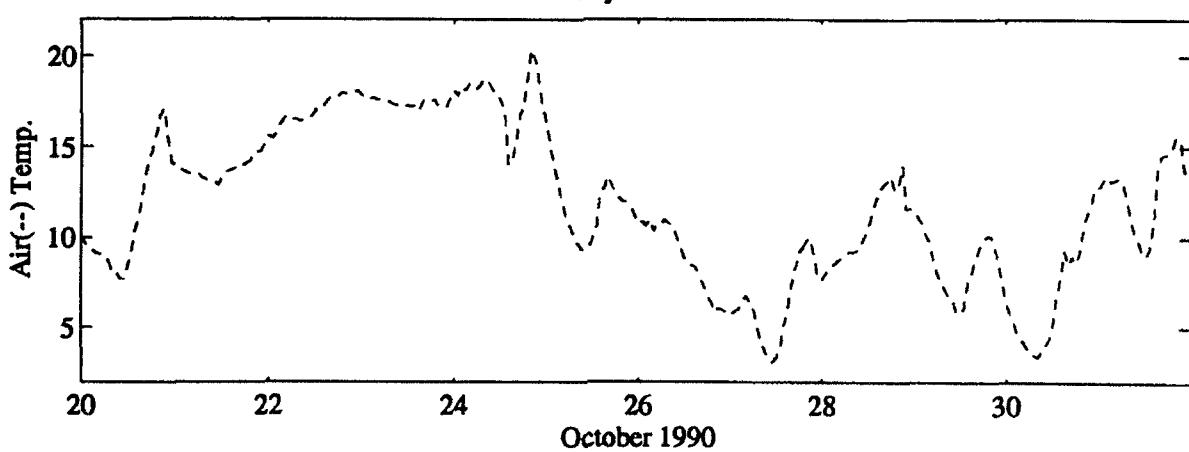
Buoy BUZM3



Buoy BUZM3



Buoy BUZM3

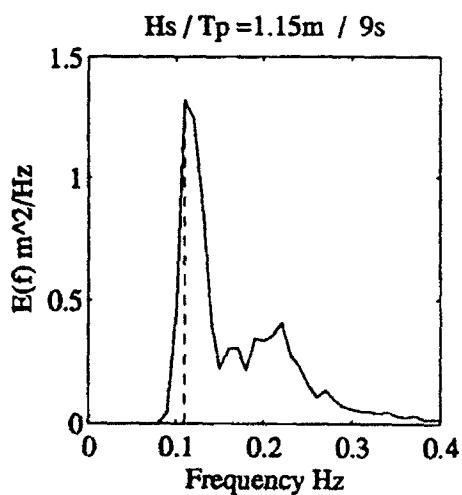
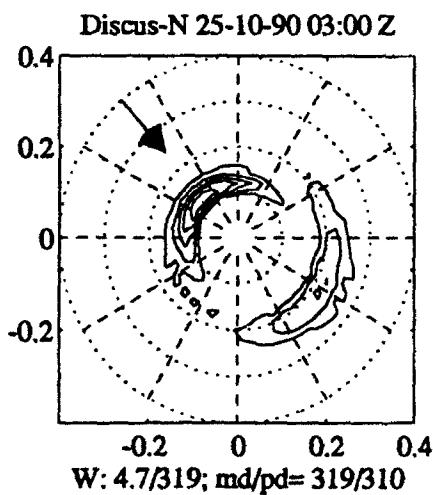
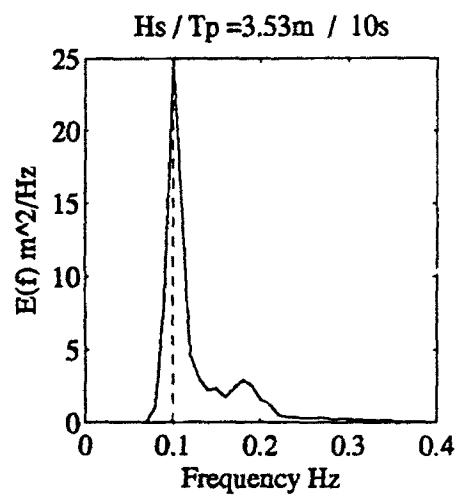
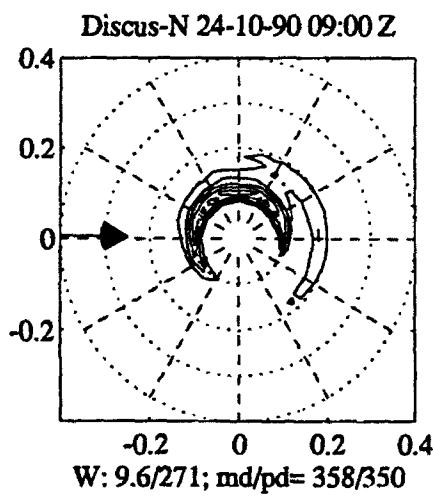
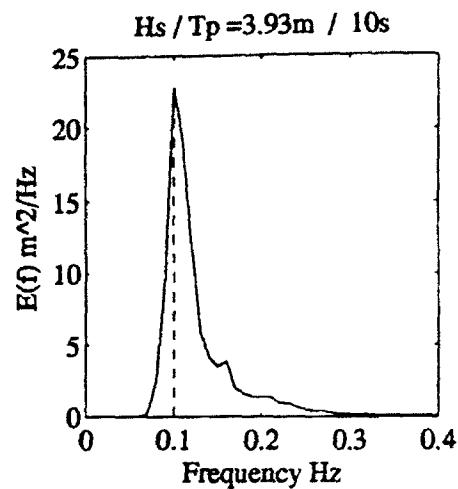
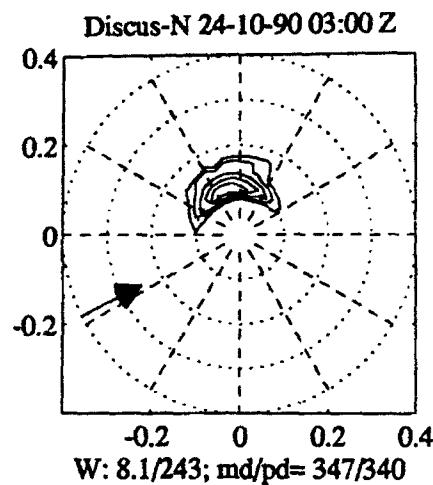


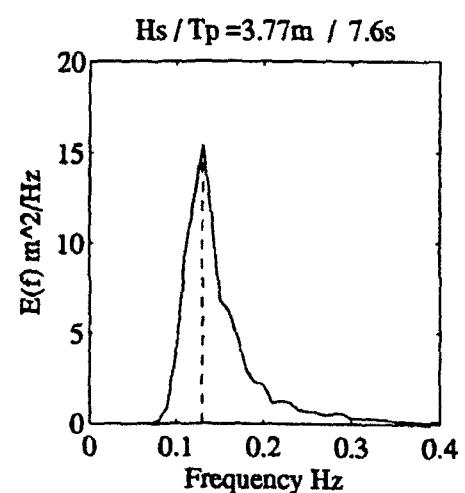
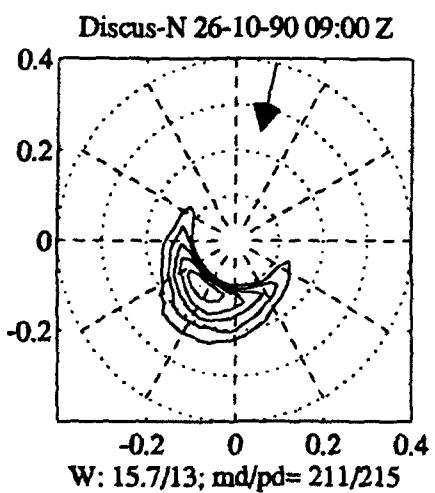
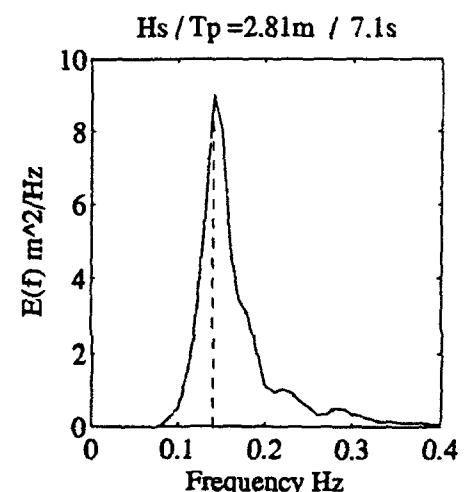
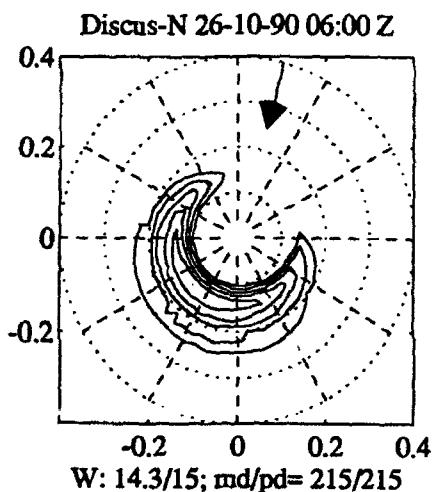
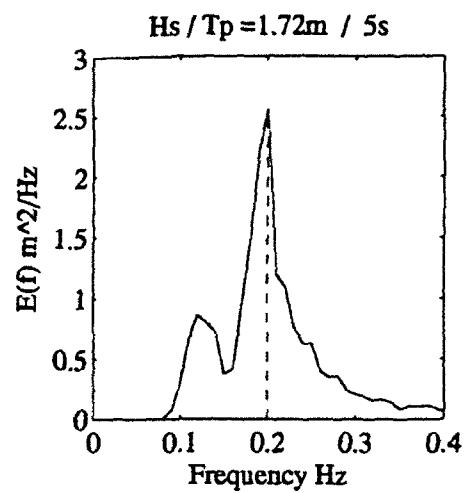
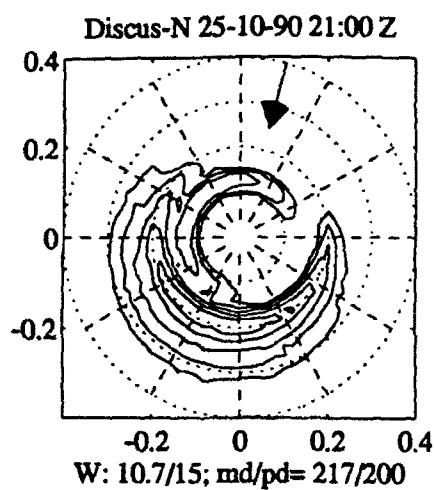
Appendix B: Directional Wave Spectra from SWADE Buoys

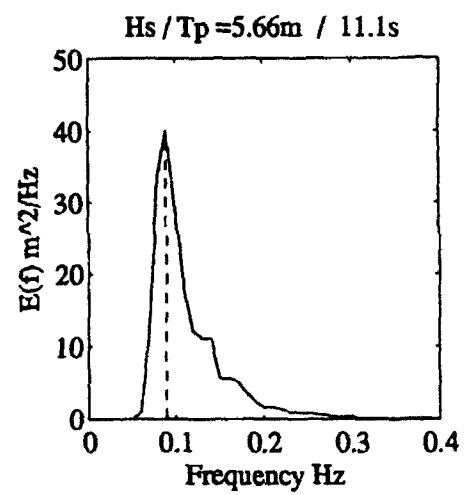
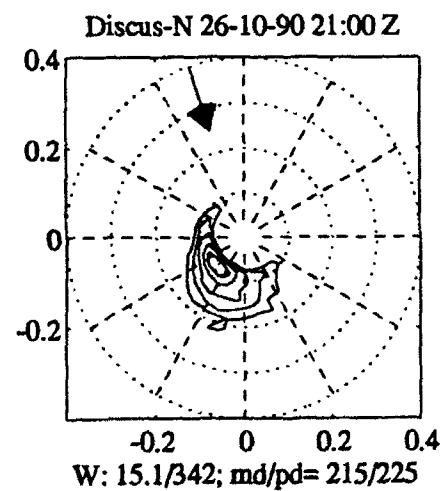
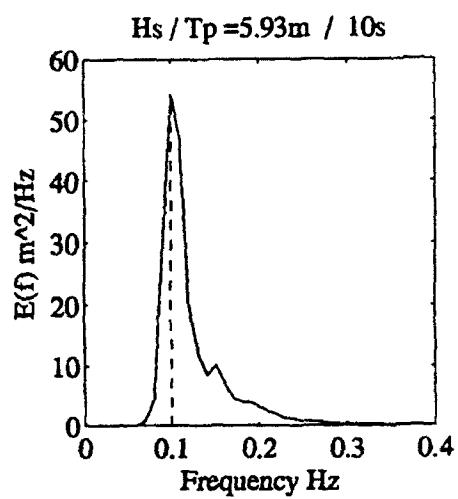
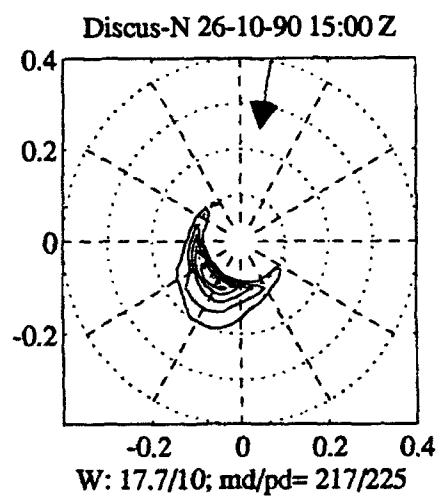
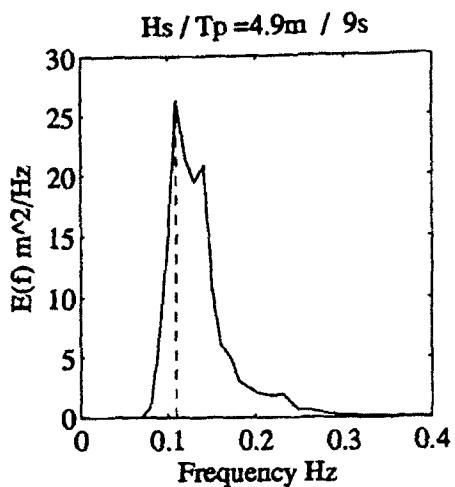
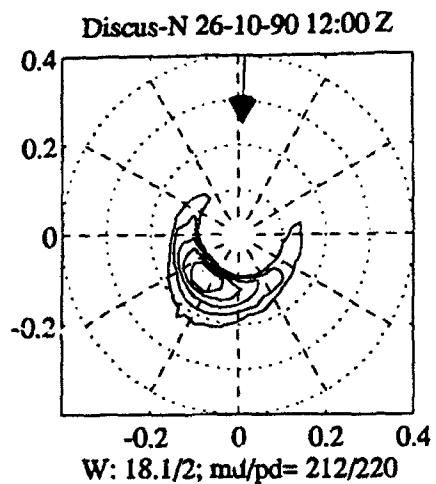
Plots of the directional wave spectra and the corresponding one-dimensional frequency spectra are presented in this appendix for buoys D-North, D-East and CERC (44014) every 3 hr from 24 October 1990, 03:00 GMT to 29 October 1990, 00:00 GMT.

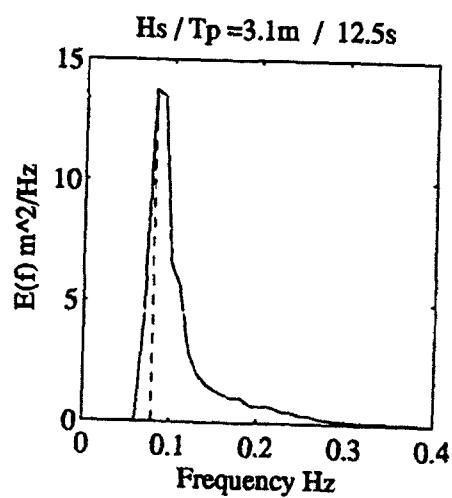
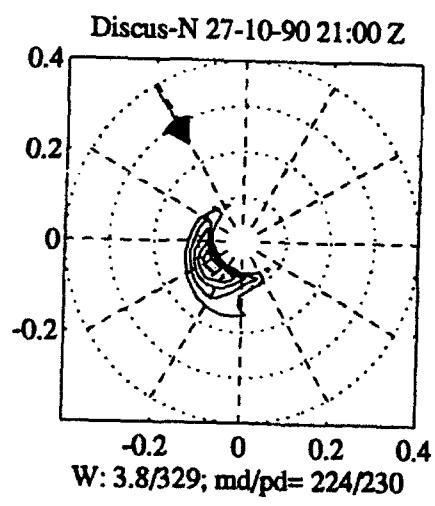
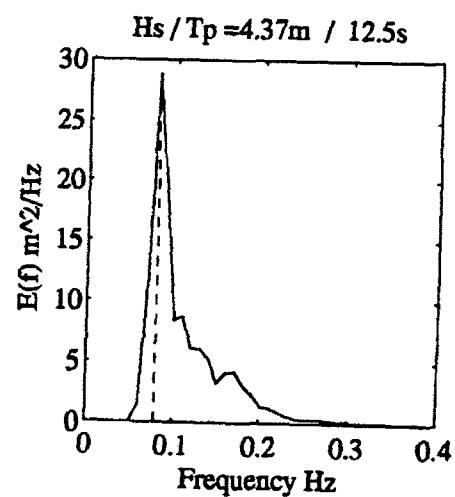
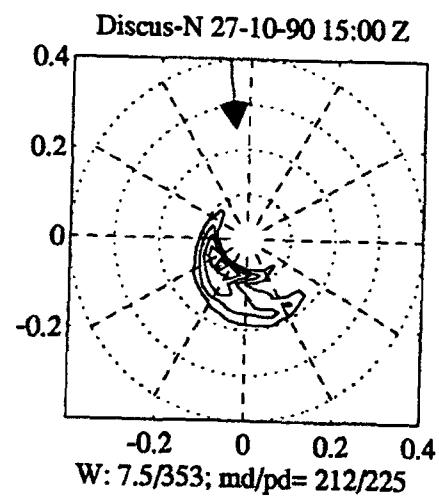
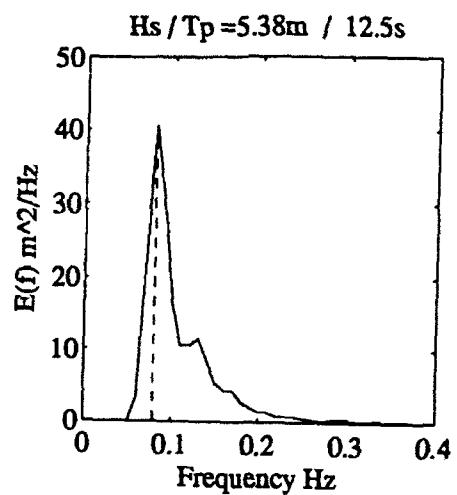
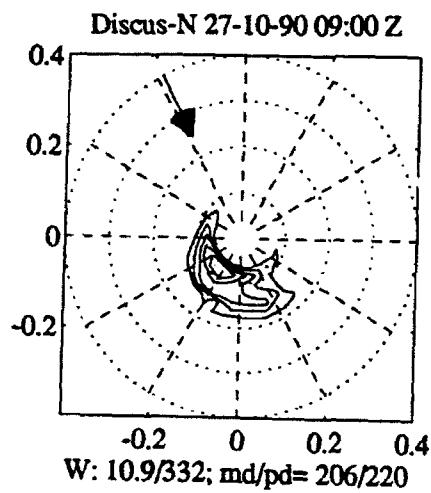
The two-dimensional wave spectra are plotted in polar coordinates with five equally spaced contours between the maximum of $\log[F(f, \theta)]$ and $\log[F(f, \theta)] = -1.25$. Each plot presents a directional wave spectrum, its corresponding one-dimensional frequency spectrum, $E(f) = \int F(f, \theta) d\theta$ and a vector of the prevailing wind direction. The frequency axis ranges from 0 to 0.4 Hz with concentric circles every 0.1 Hz. The top header of the directional wave spectral plot identifies the buoy station, date and time in GMT. The bottom header provides the wind speed and wind direction (from) measured clockwise from north, as well as the mean and peak wave directions (towards). The header of the frequency spectrum provides the significant wave height and the peak period, which is also marked (dashed line) on the plot.

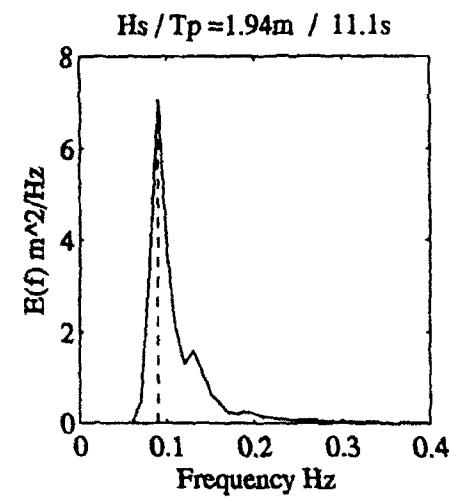
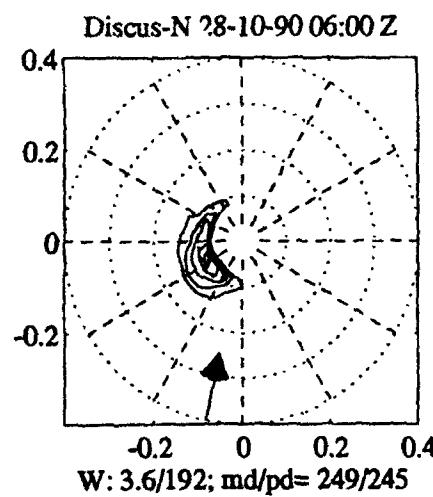
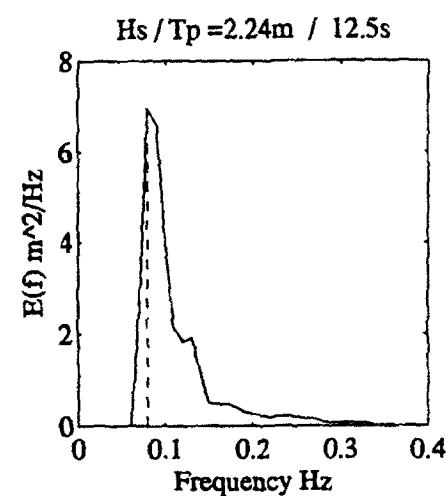
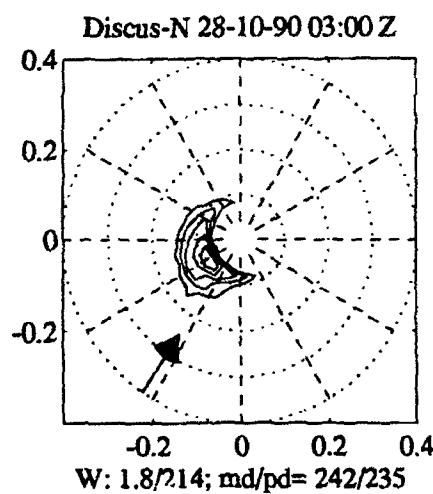
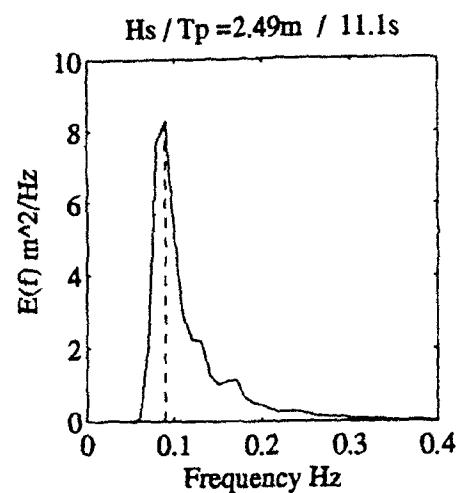
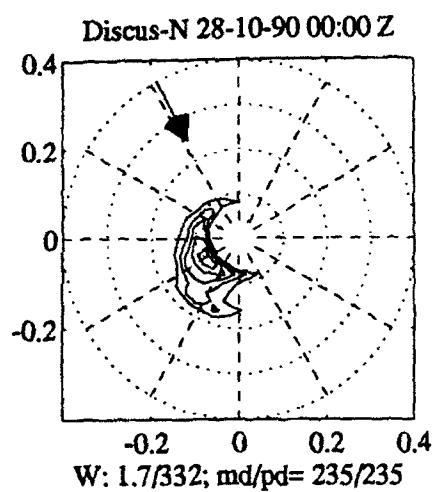
B.1: Discus Buoy “North”

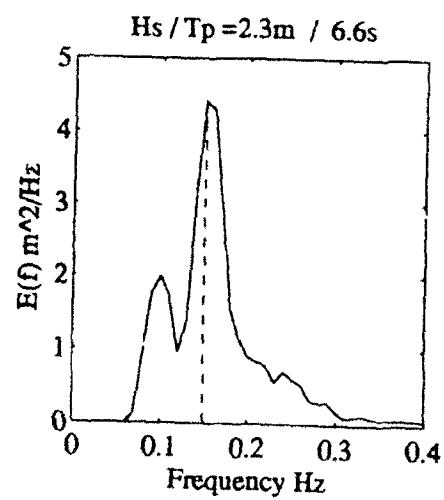
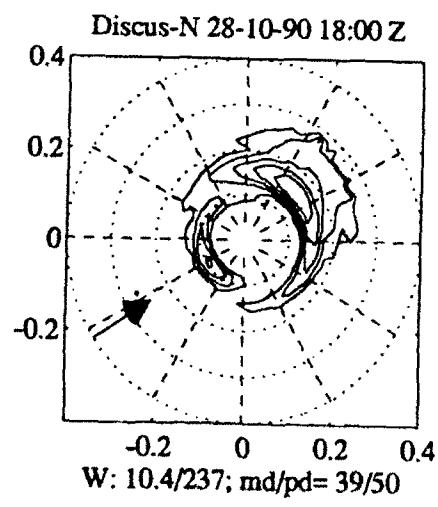
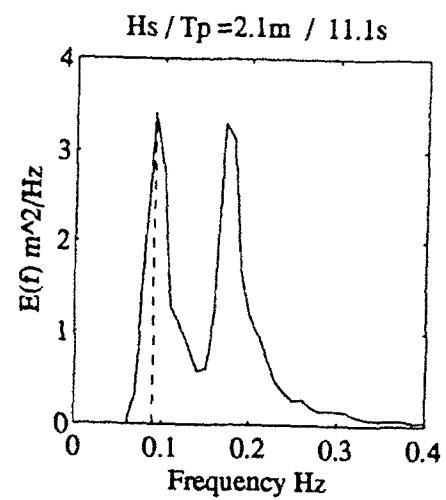
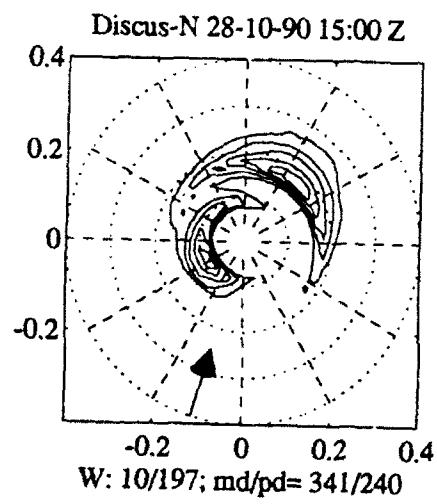
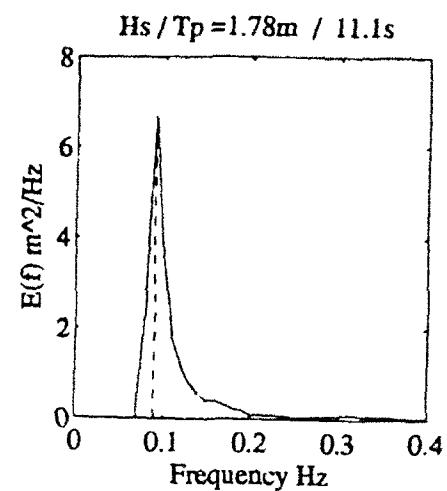
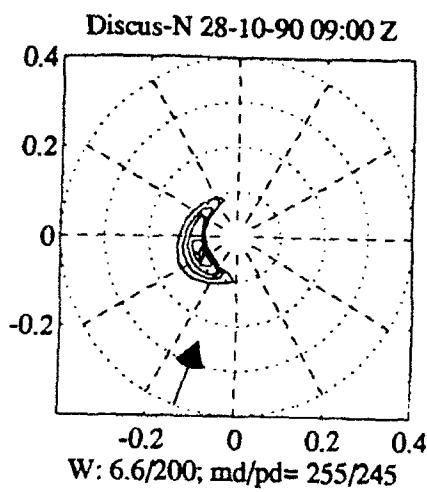




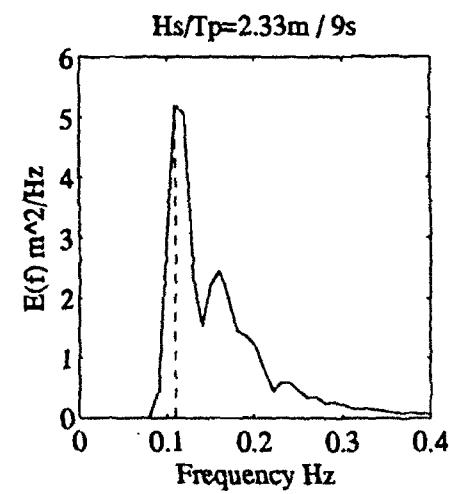
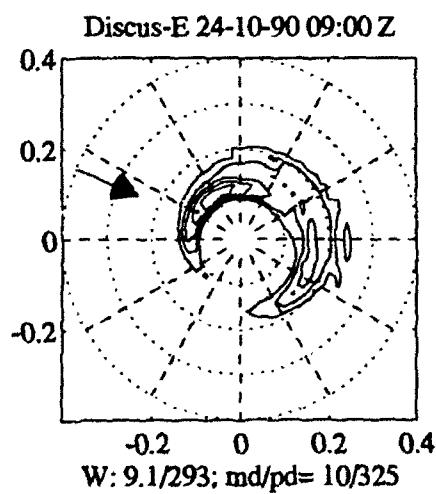
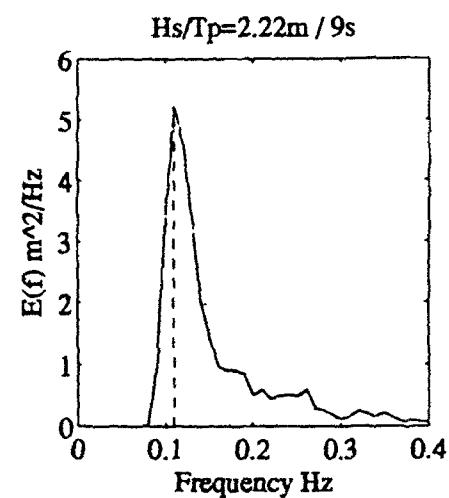
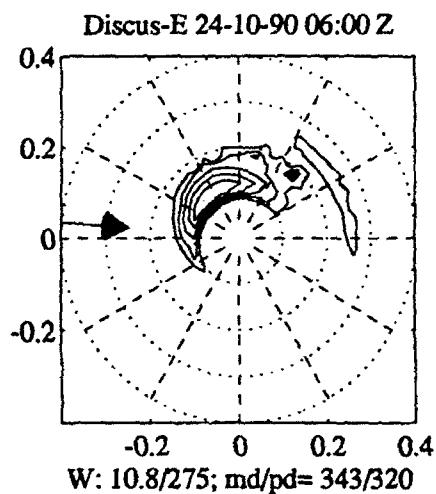
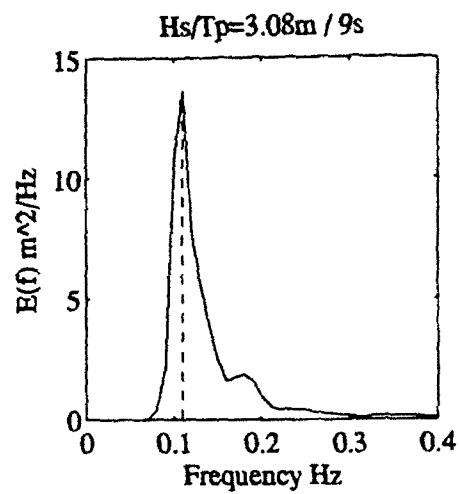
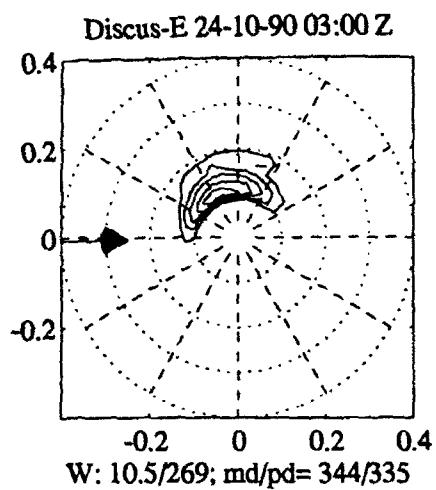


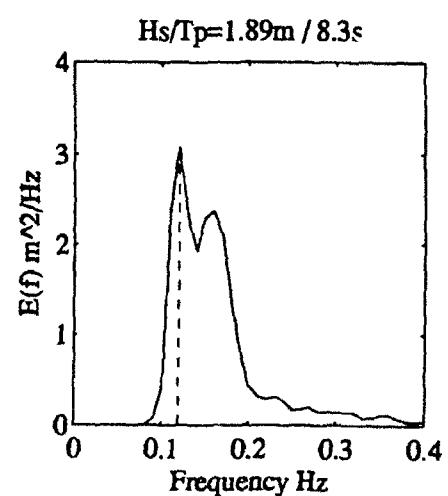
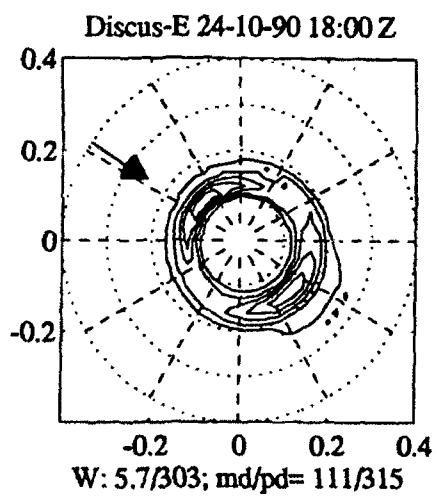
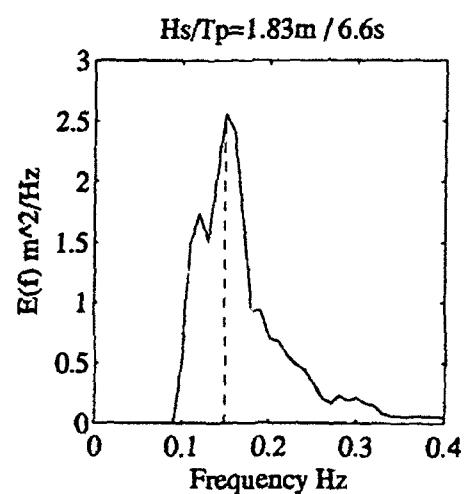
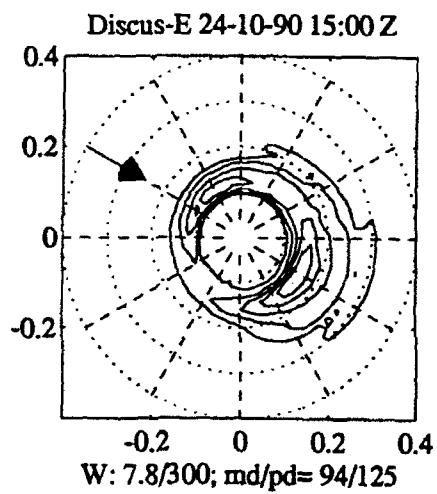
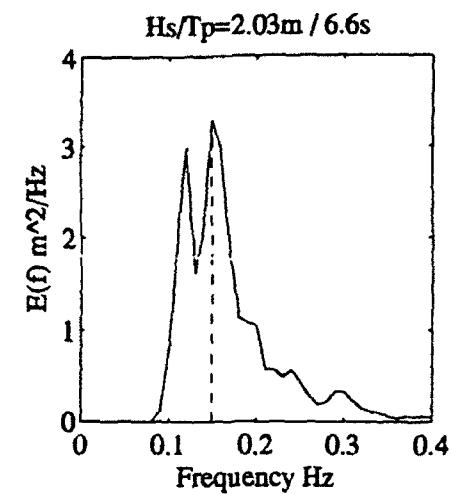
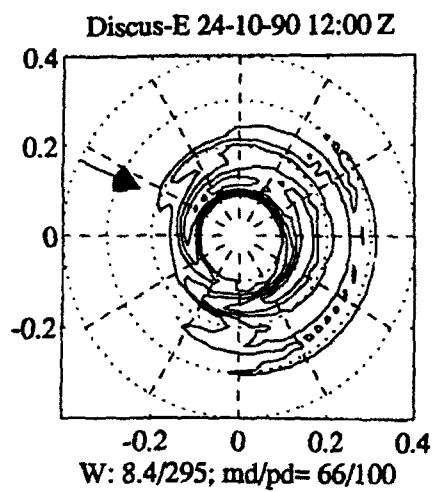


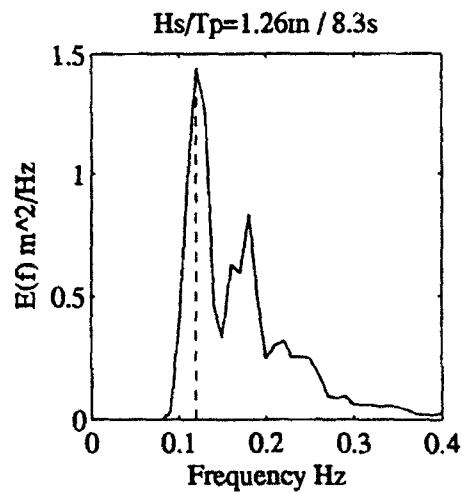
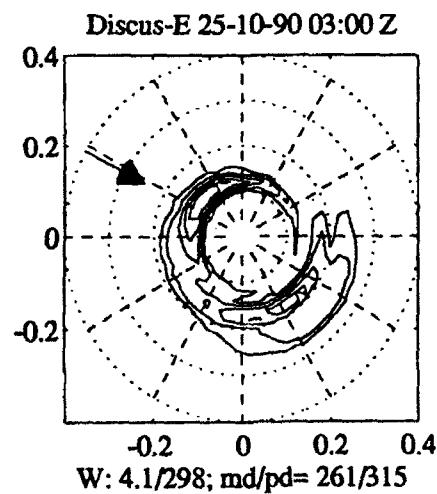
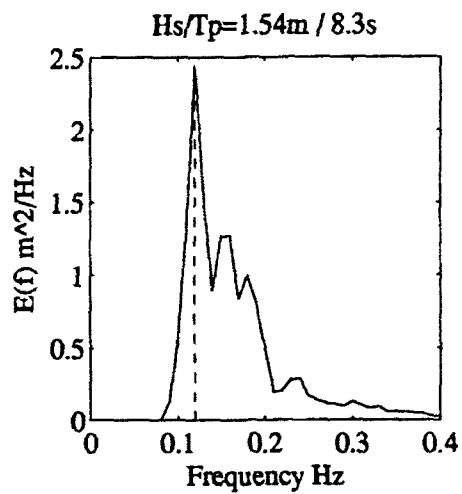
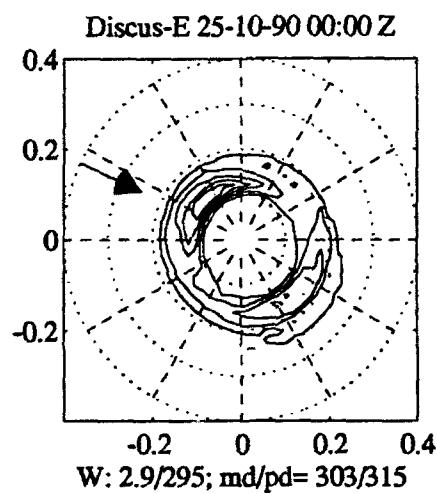
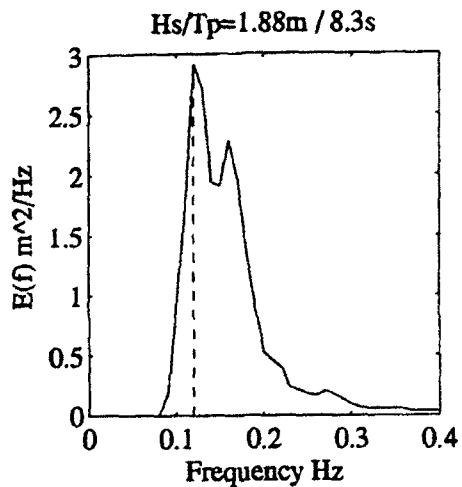
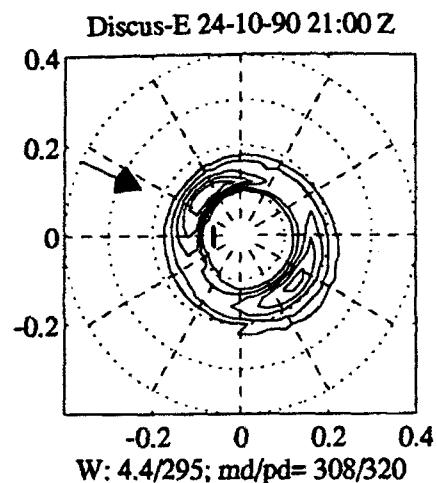


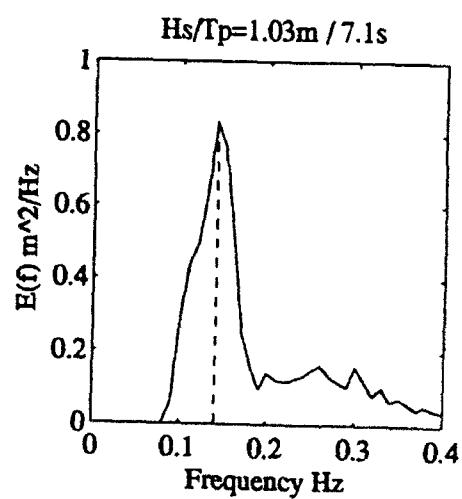
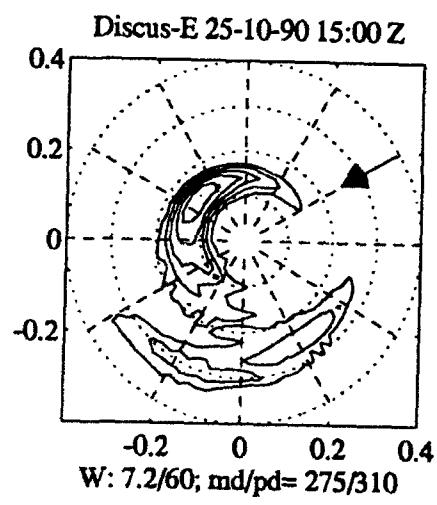
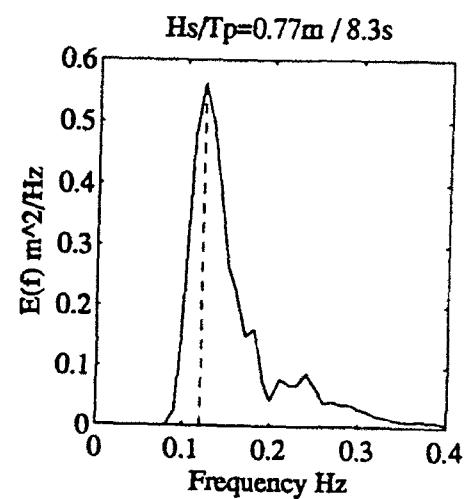
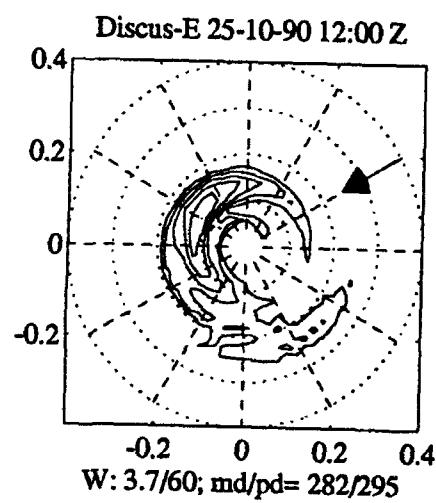
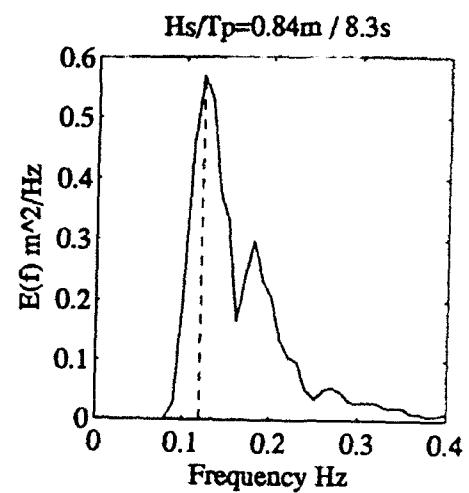
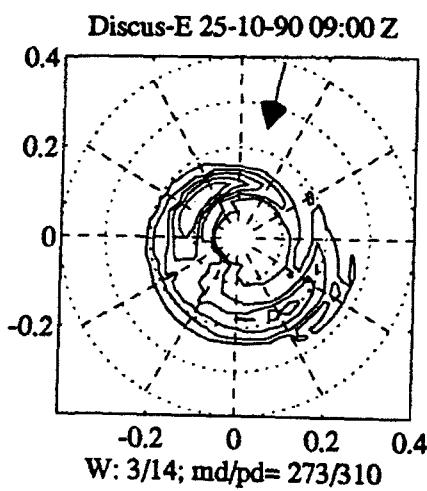


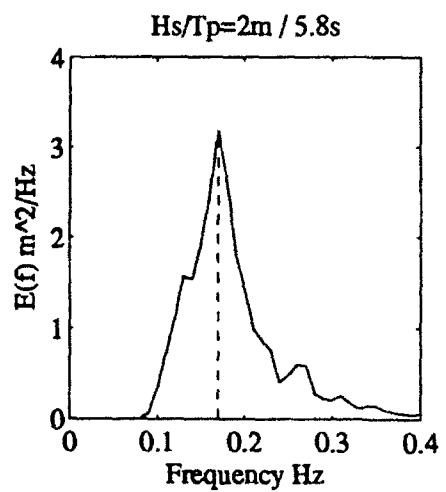
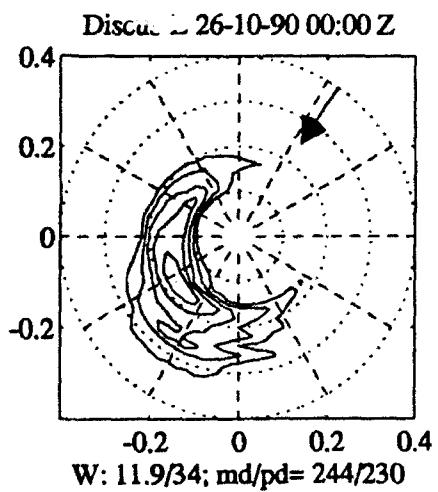
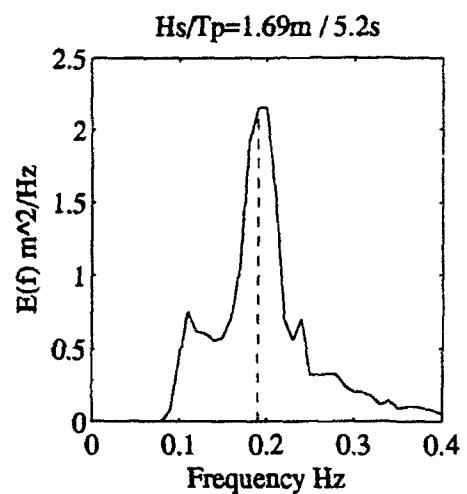
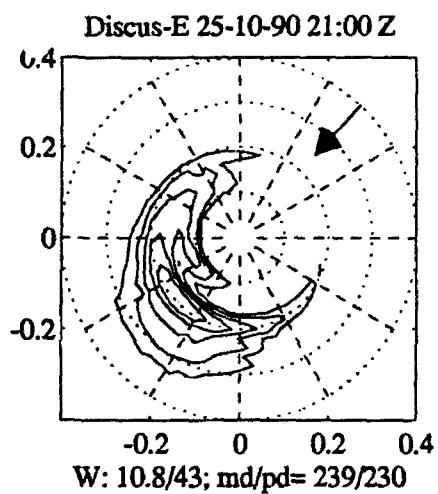
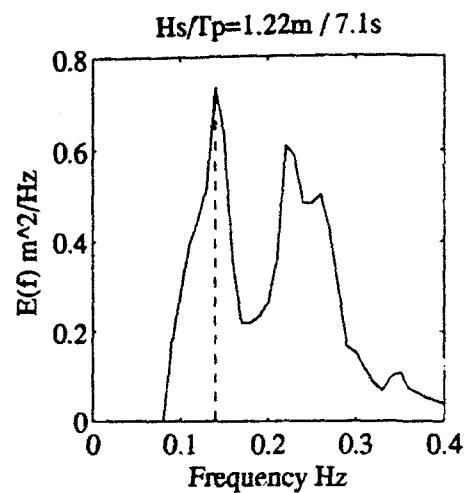
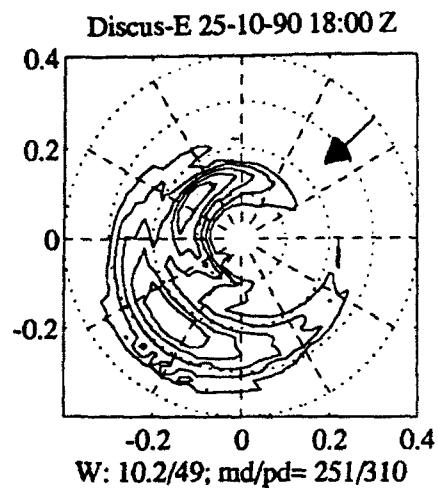
B.2: Discus Buoy “East”

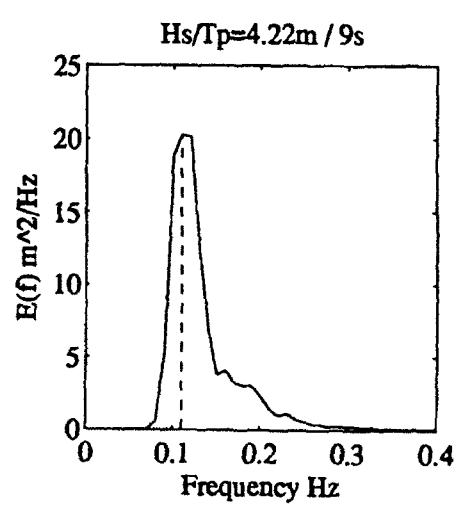
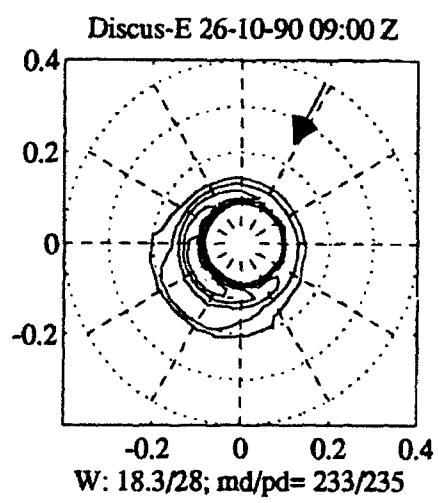
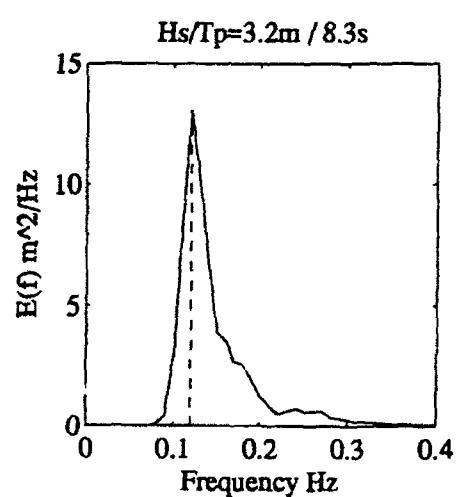
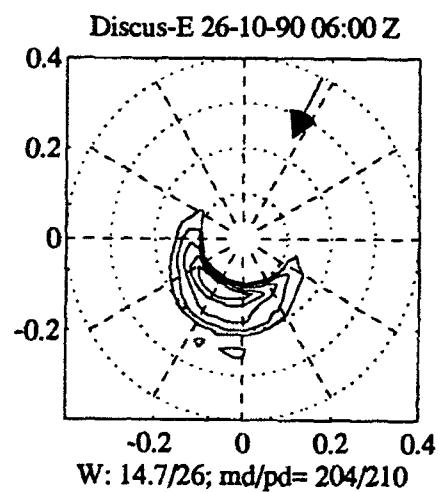
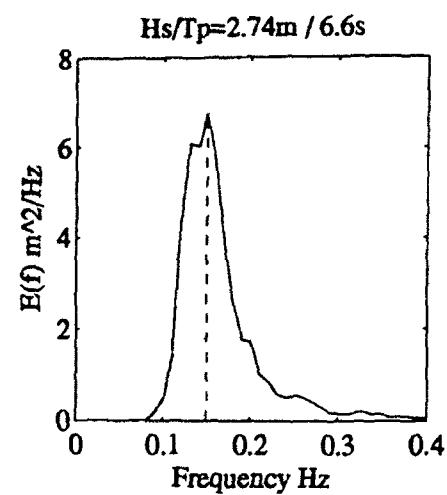
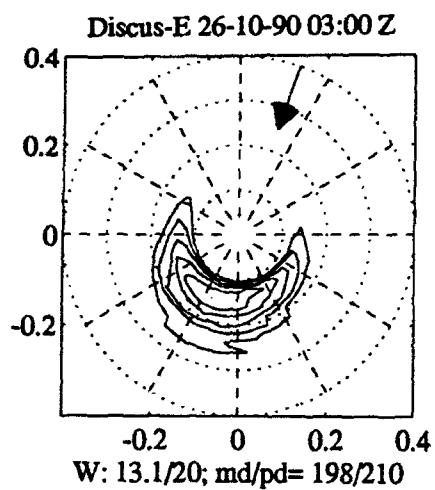


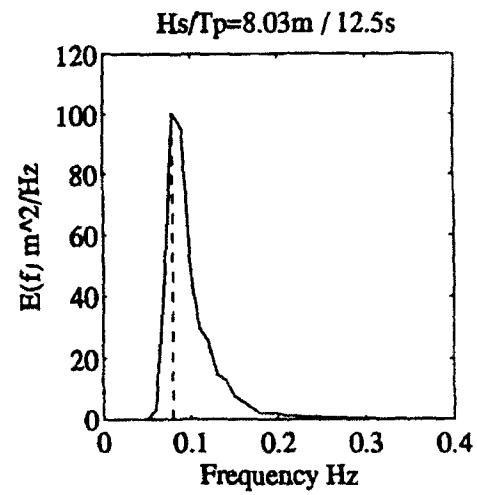
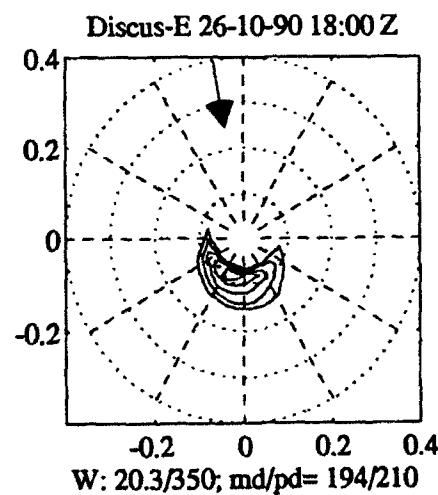
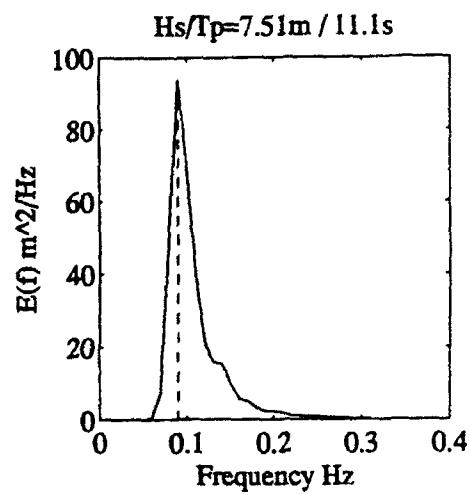
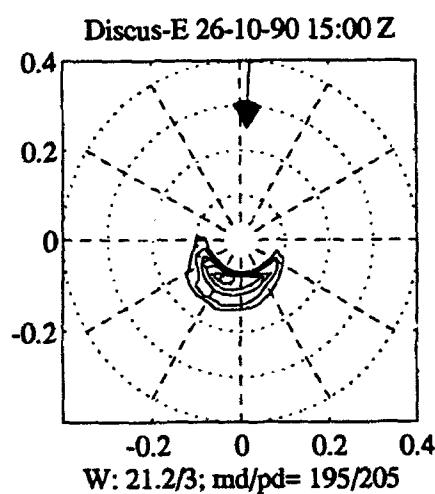
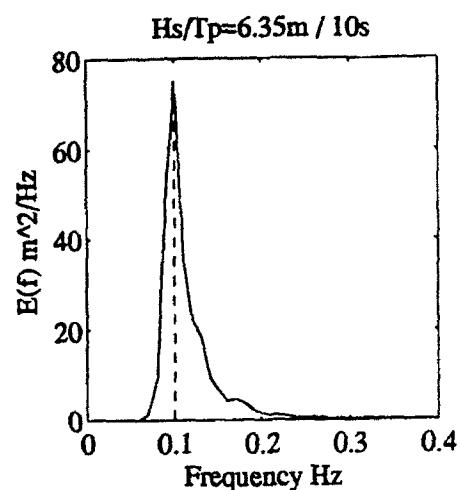
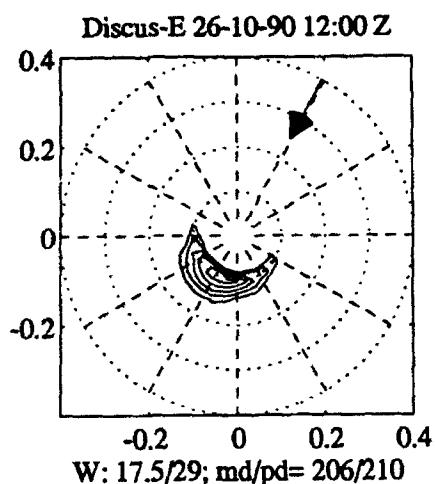


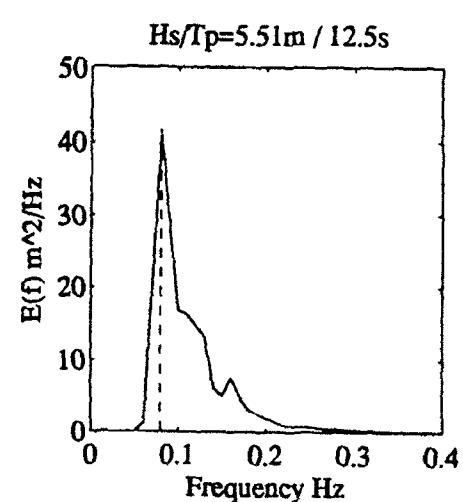
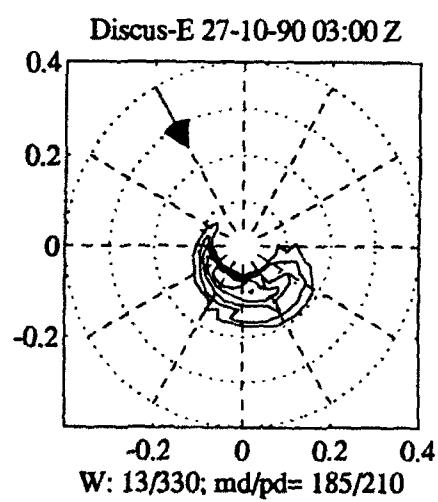
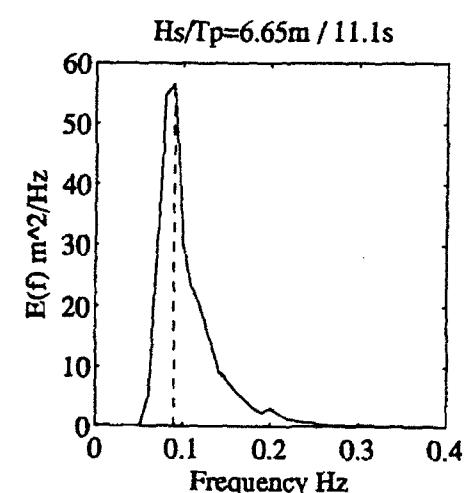
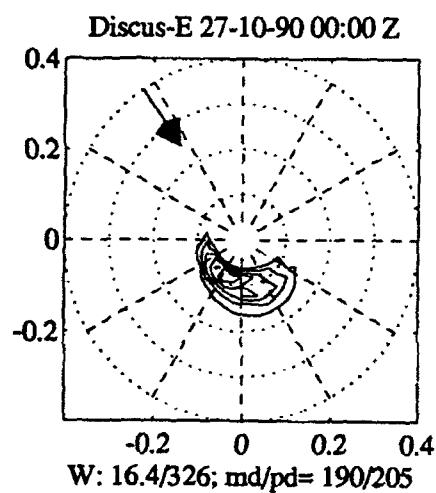
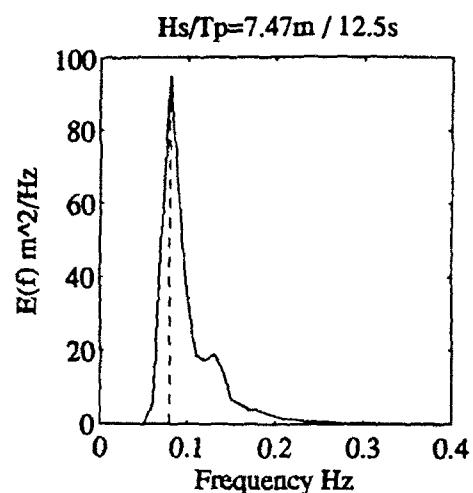
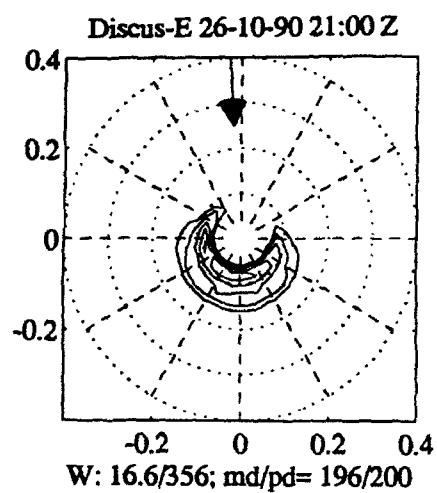


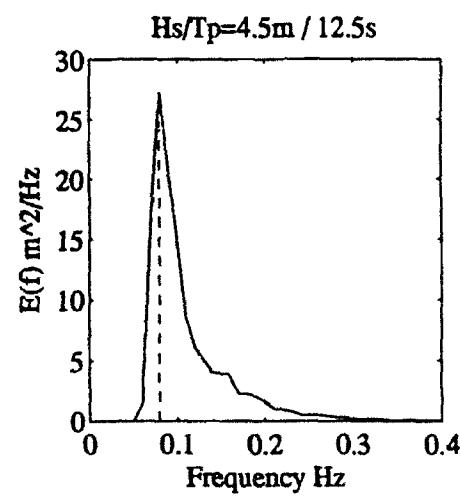
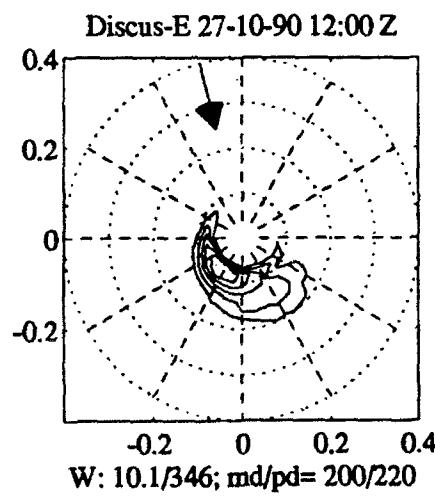
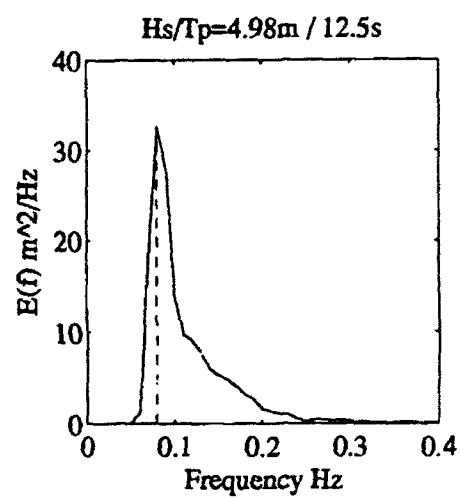
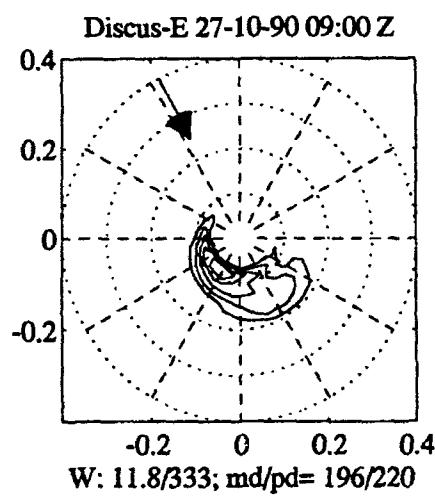
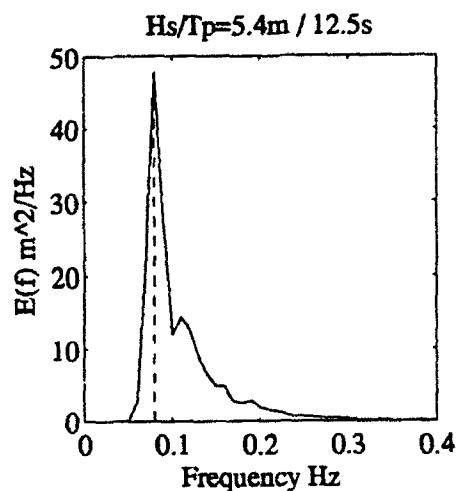
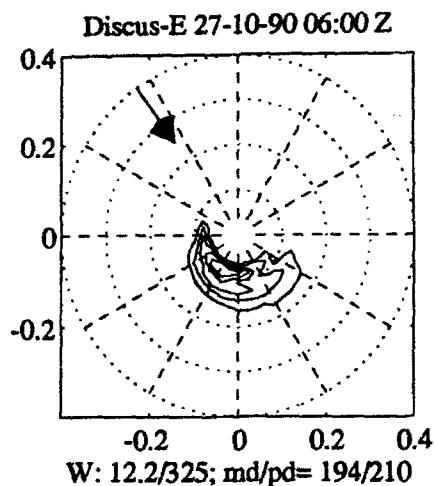


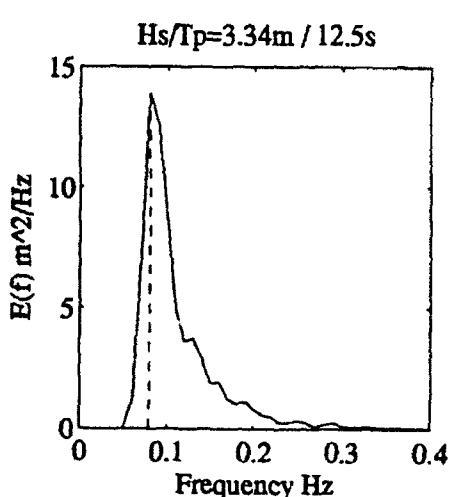
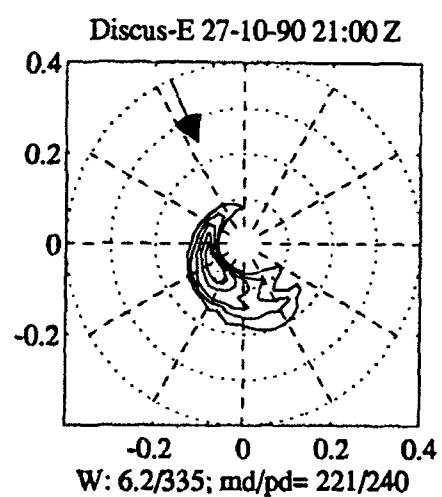
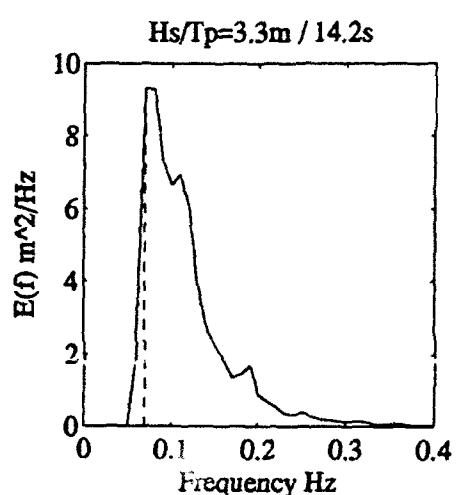
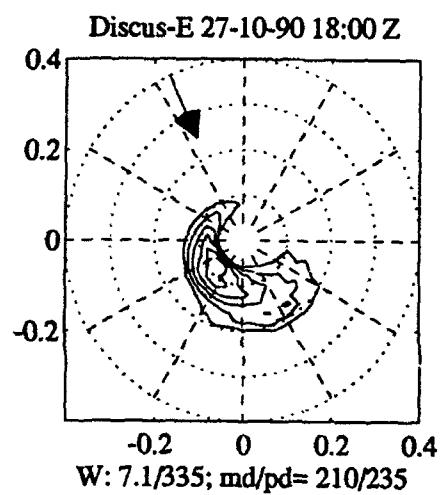
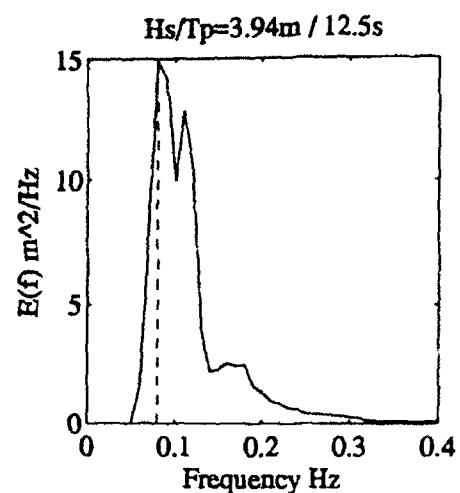
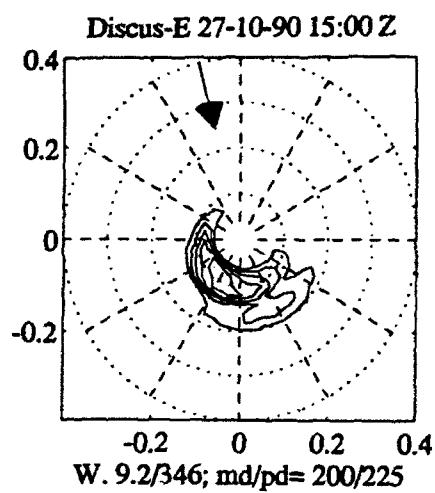


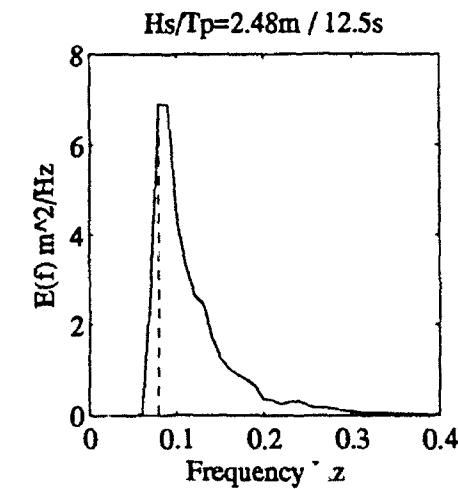
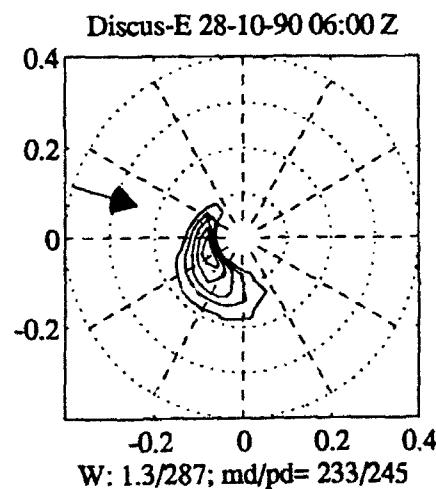
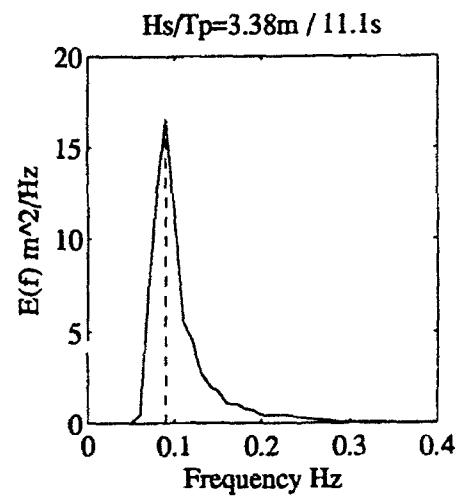
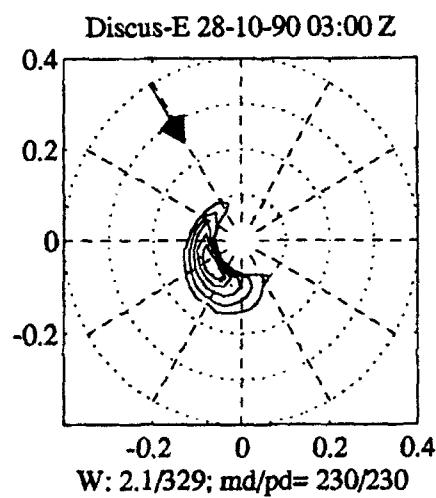
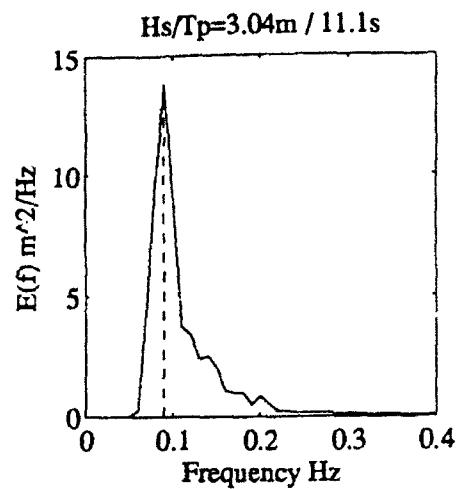
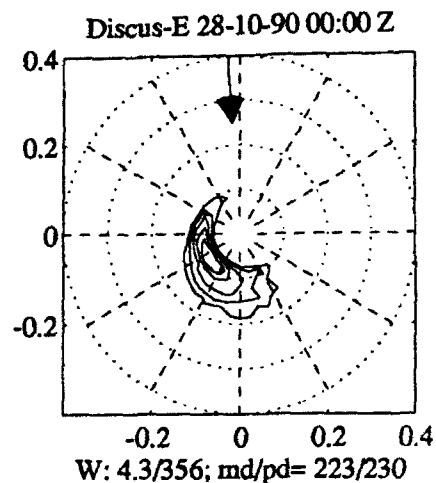


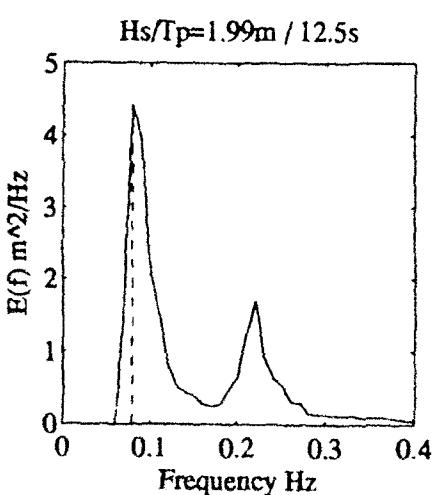
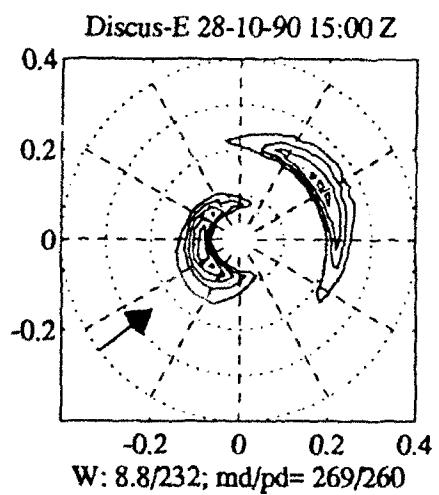
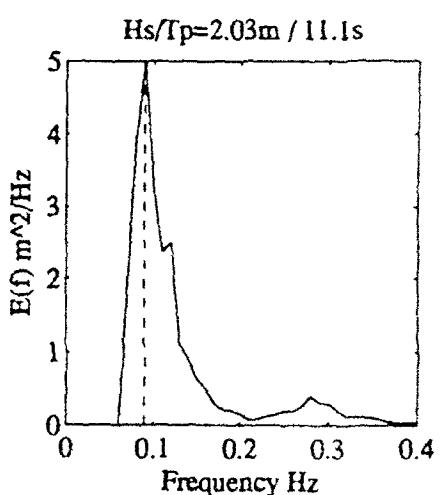
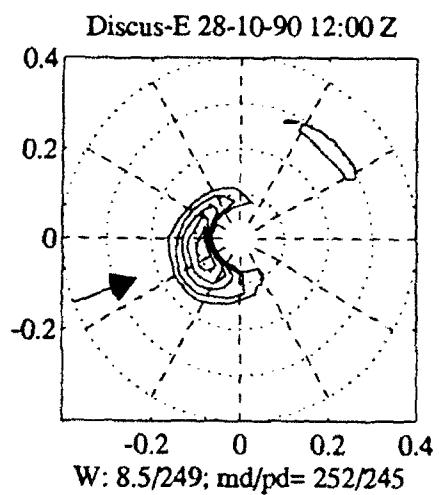
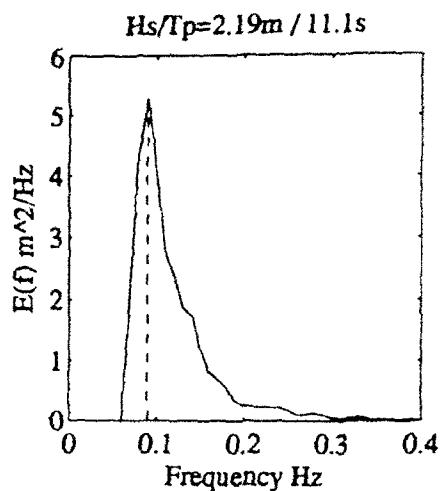
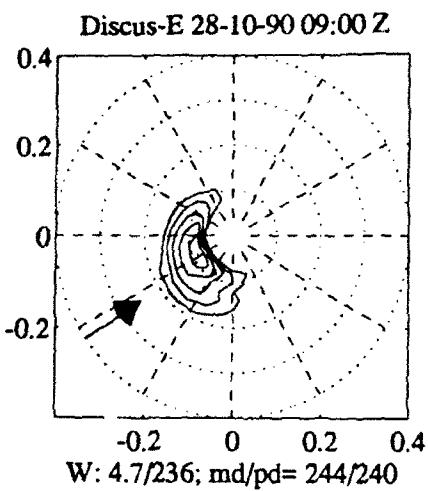


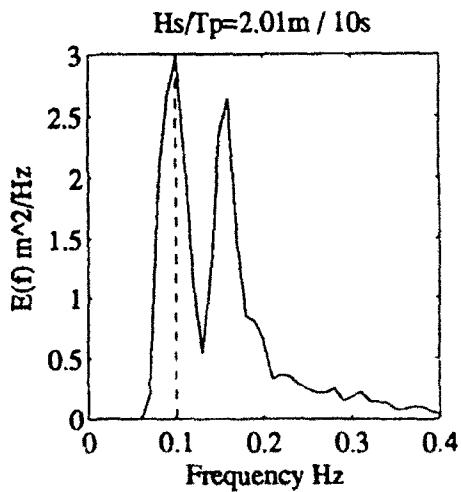
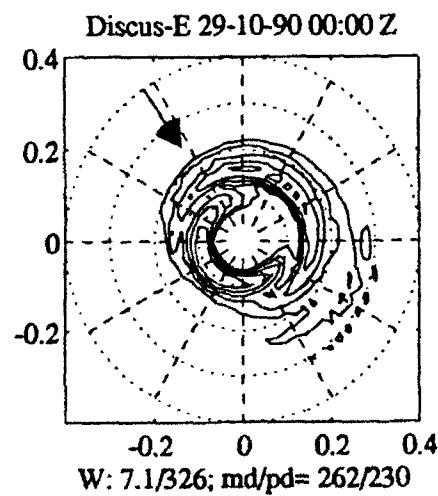
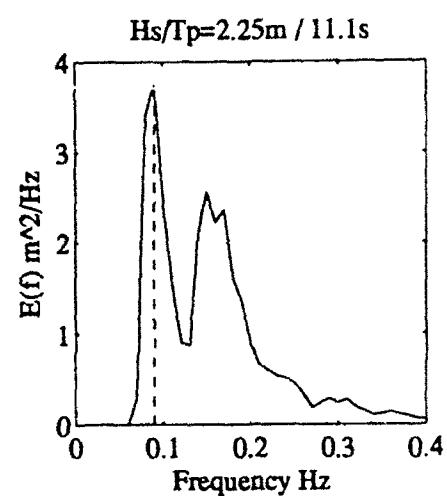
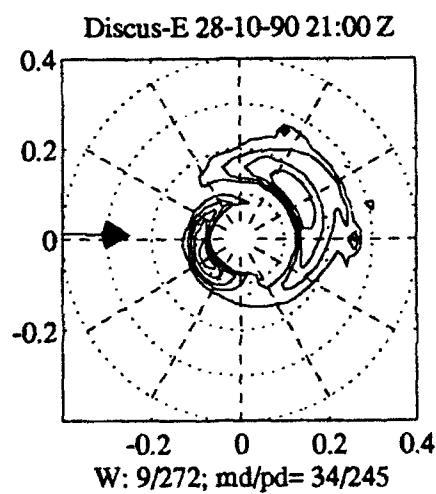
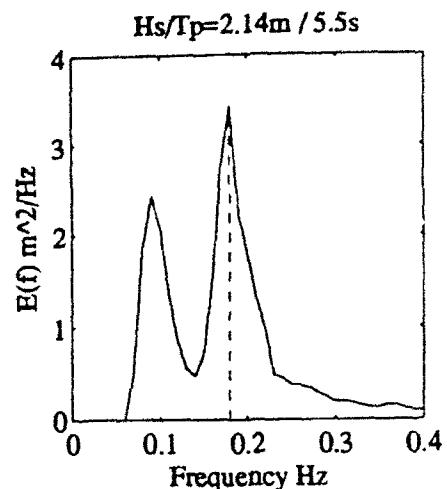
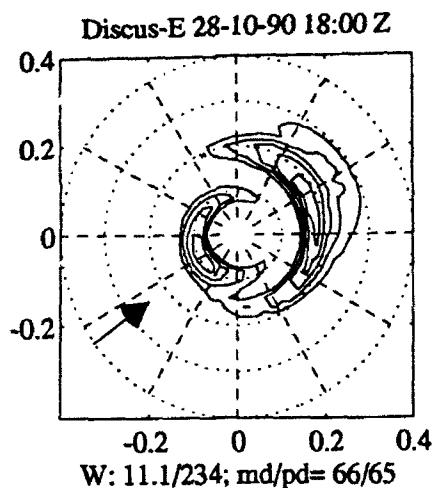




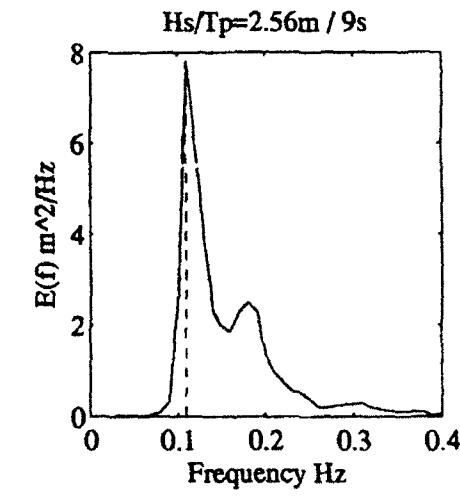
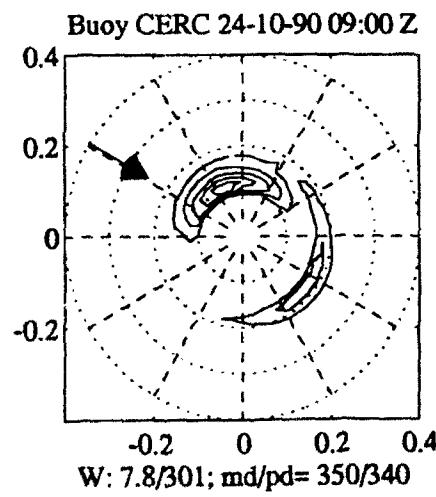
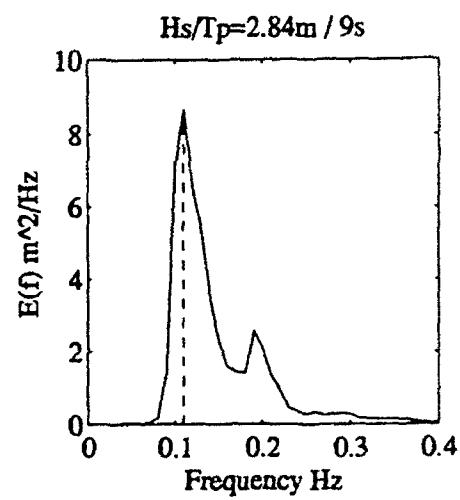
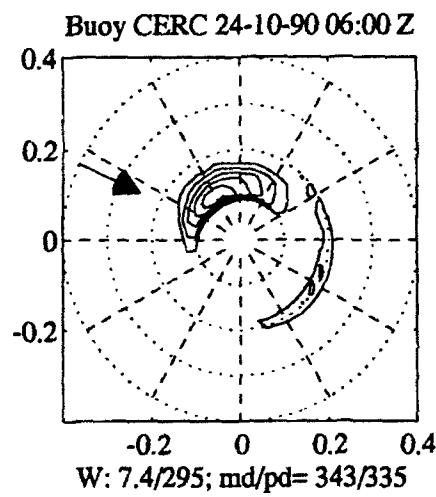
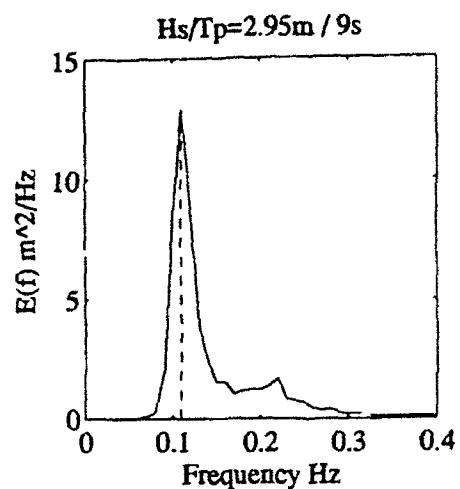
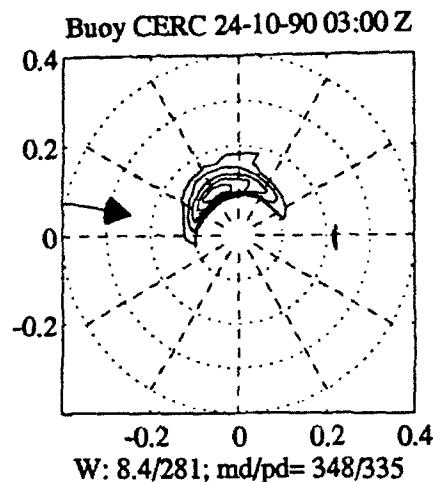


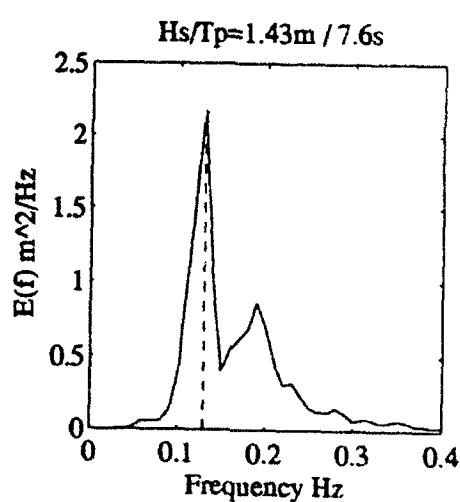
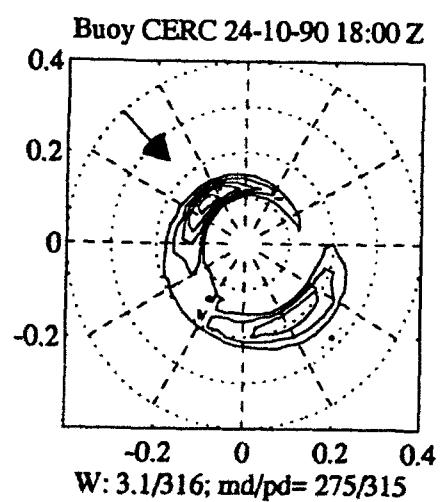
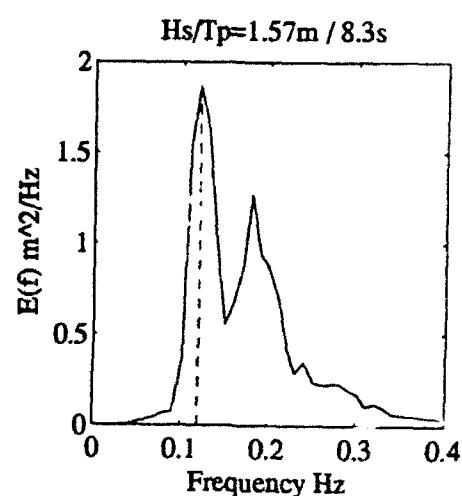
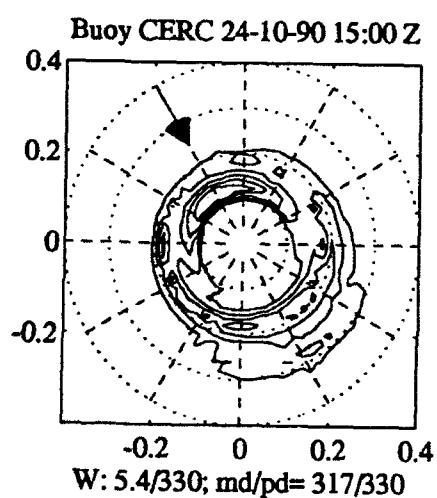
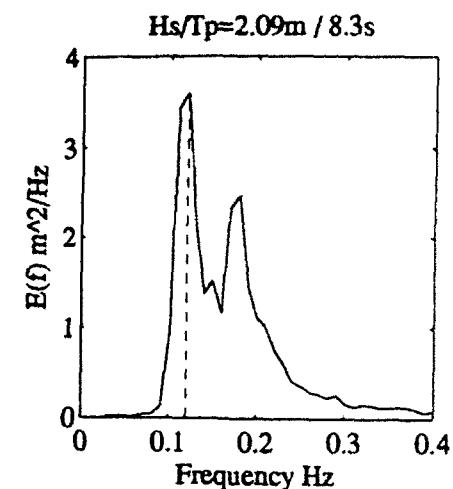
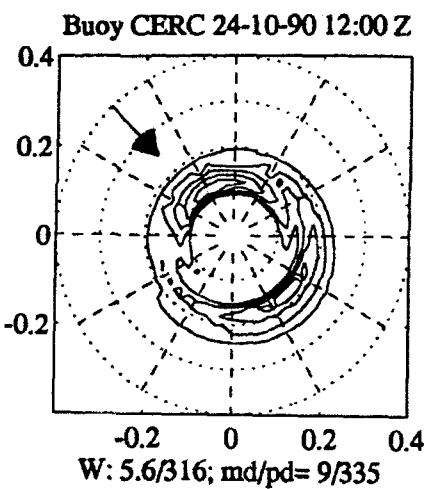


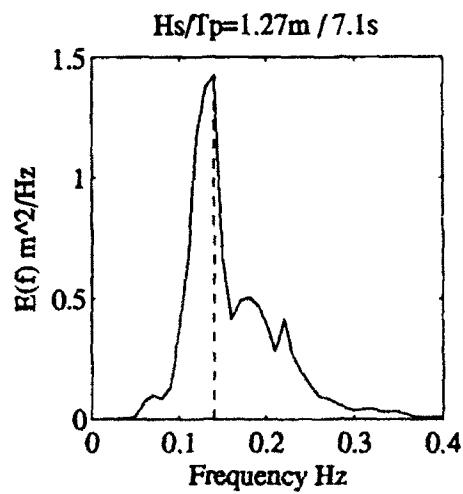
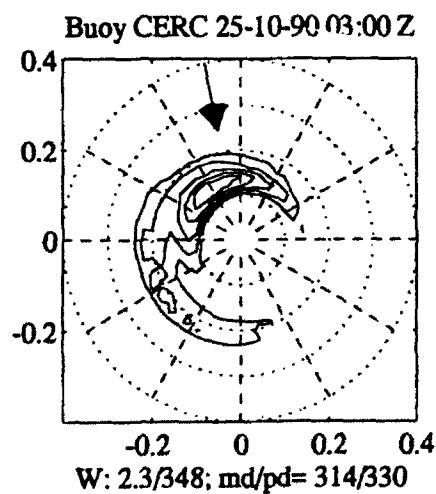
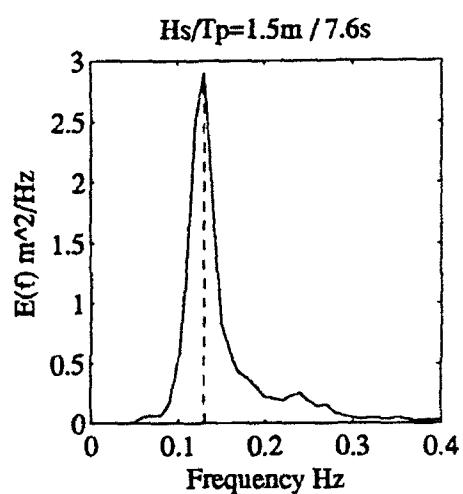
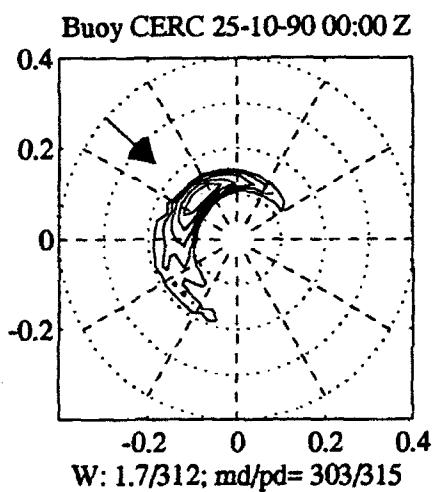
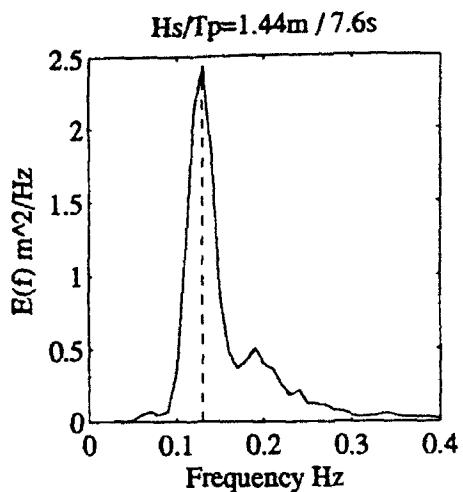
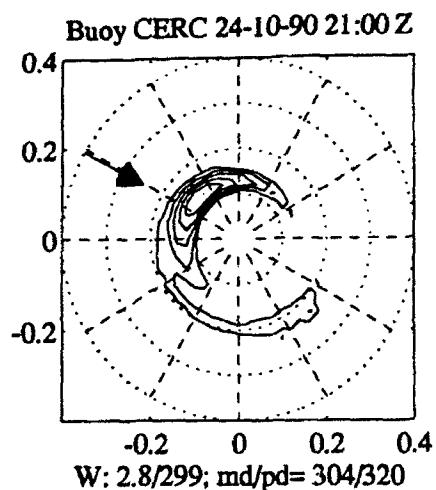


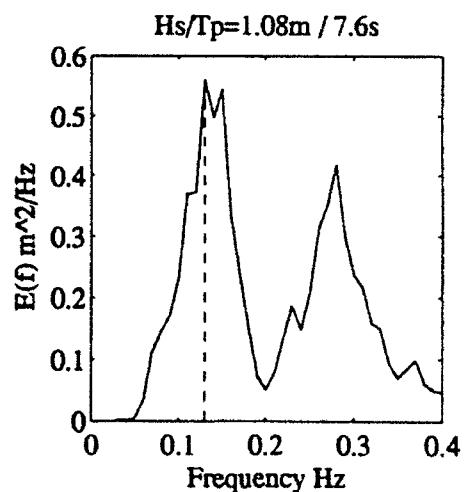
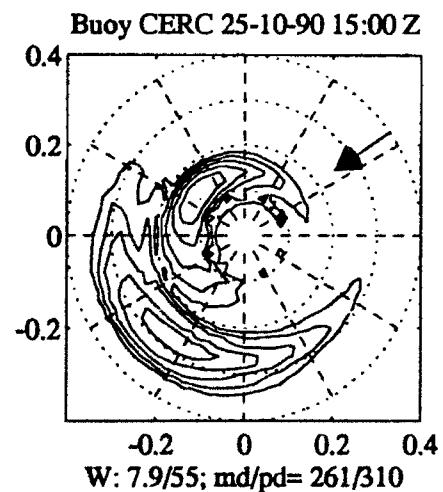
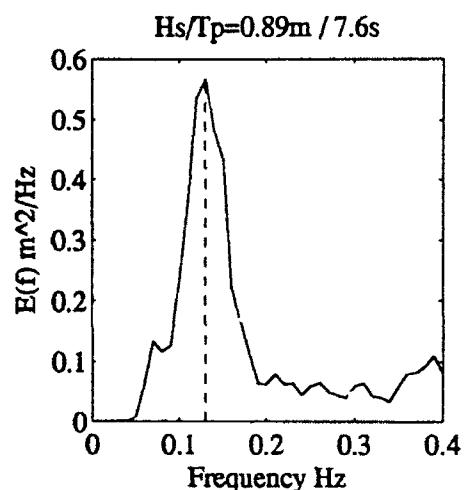
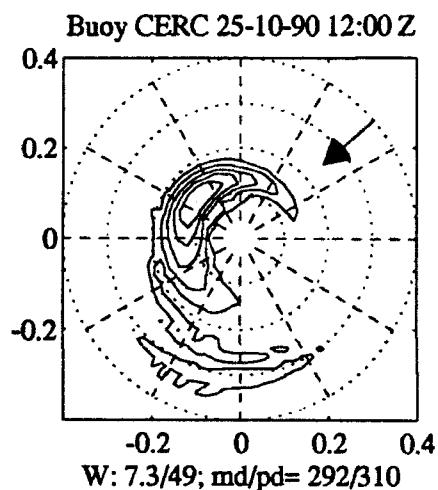
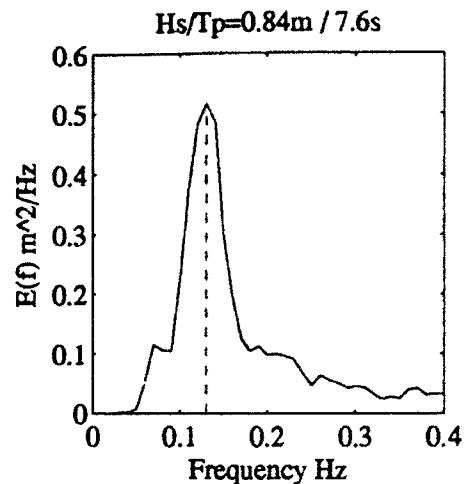
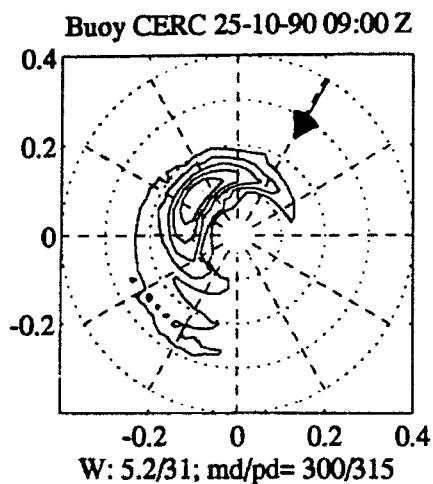


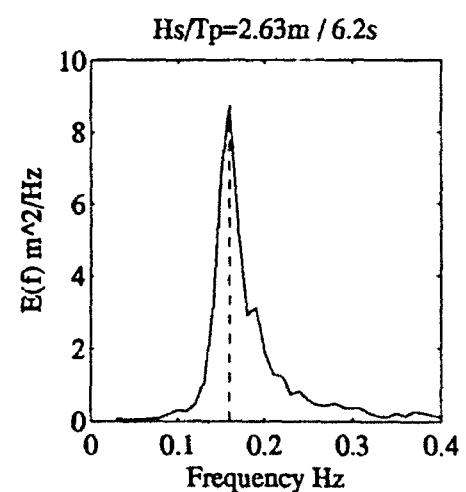
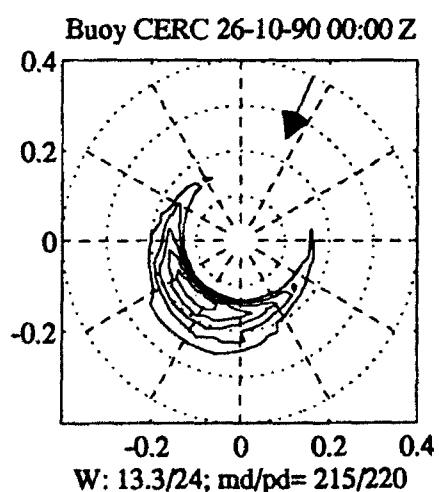
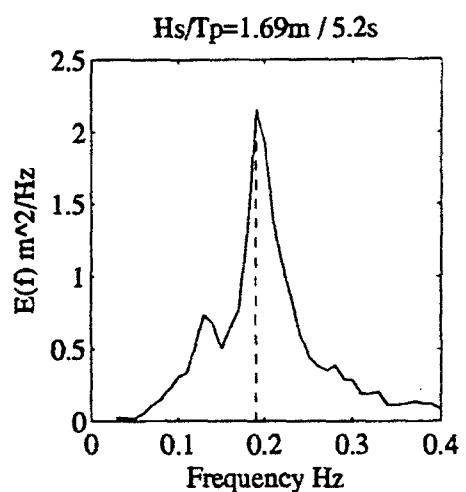
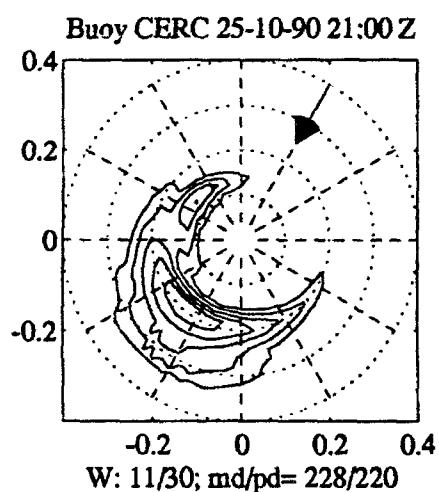
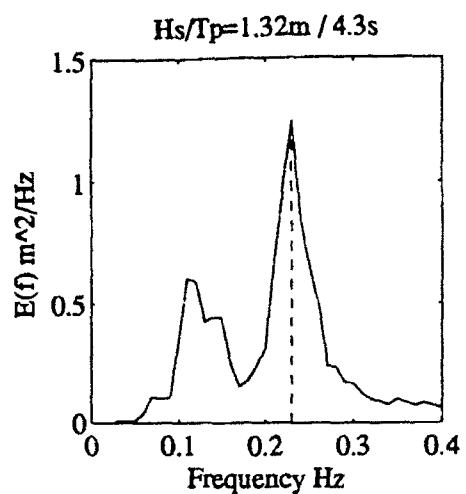
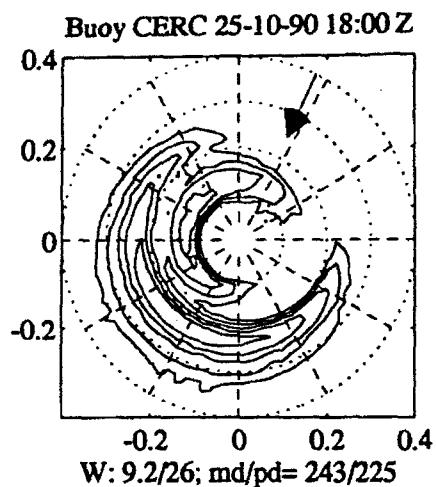
B.3: Discus Buoy "CERC"

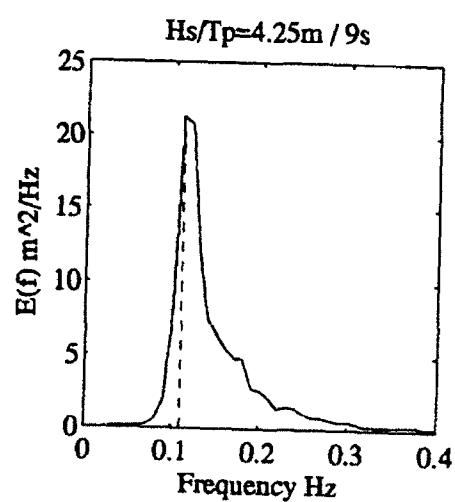
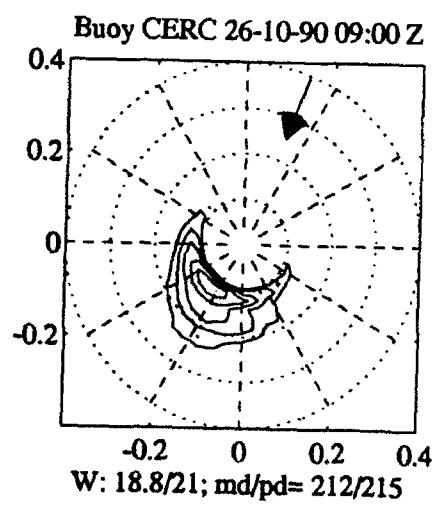
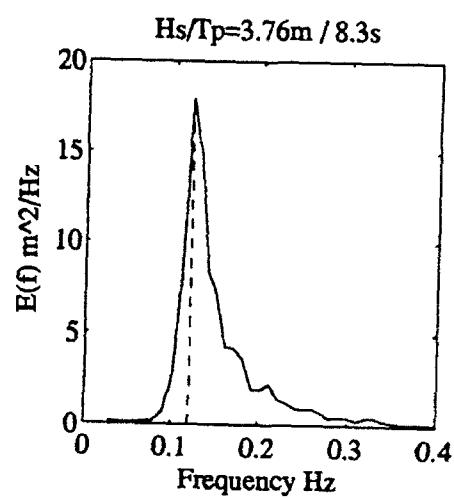
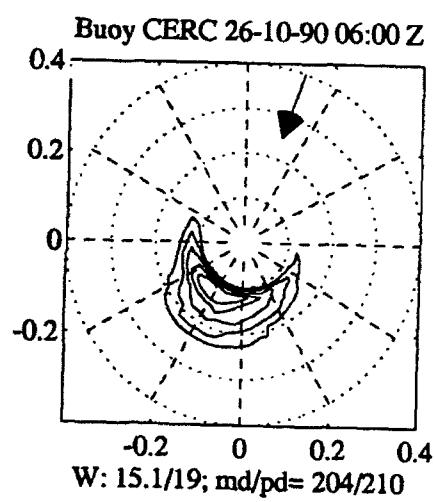
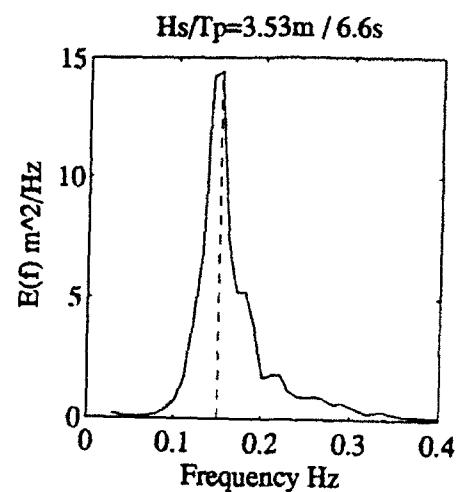
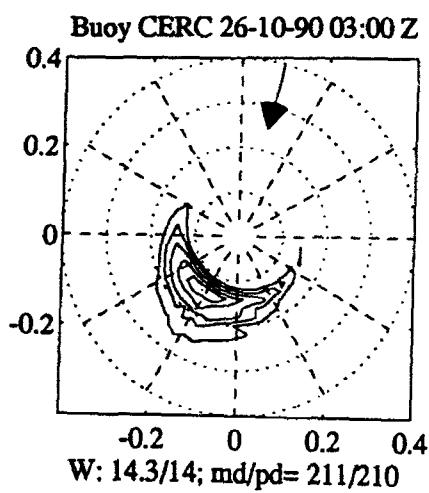


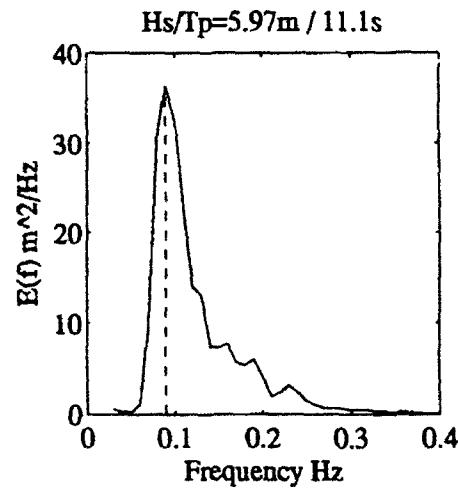
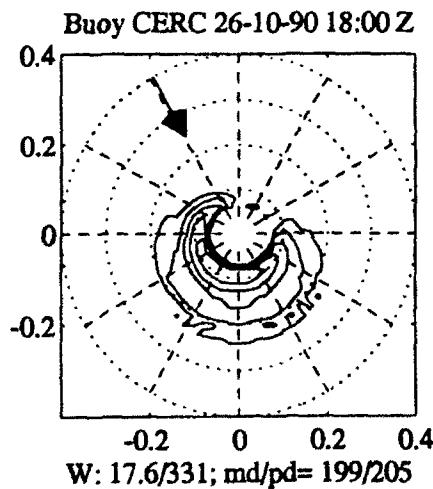
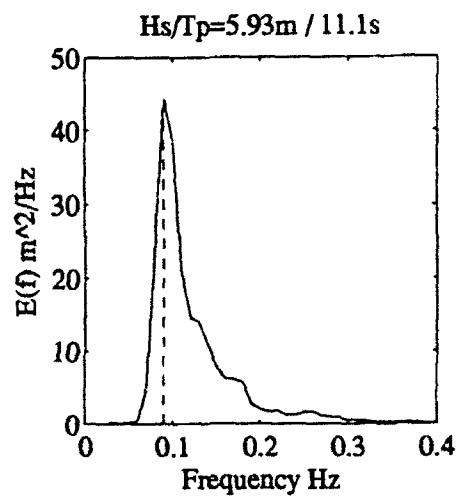
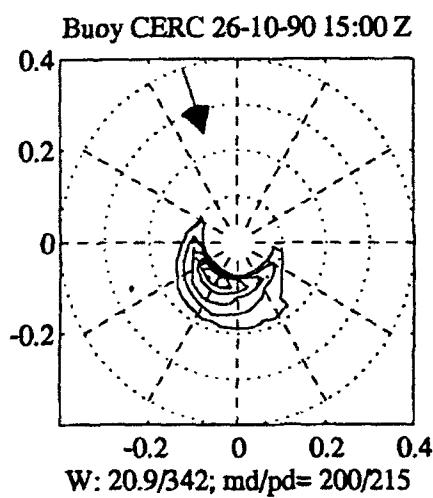
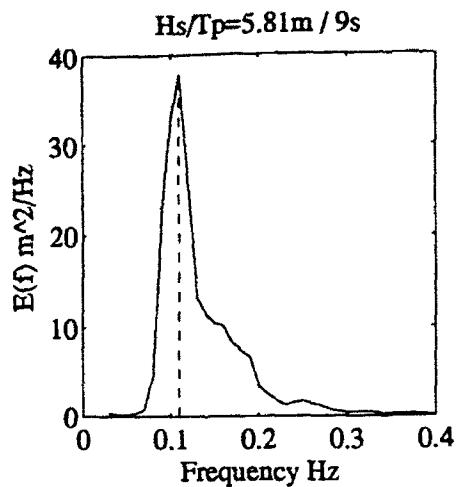
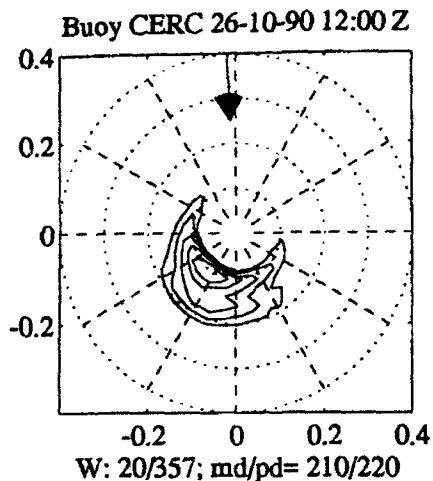


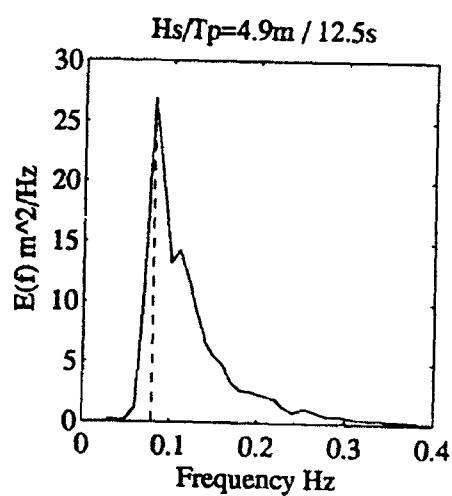
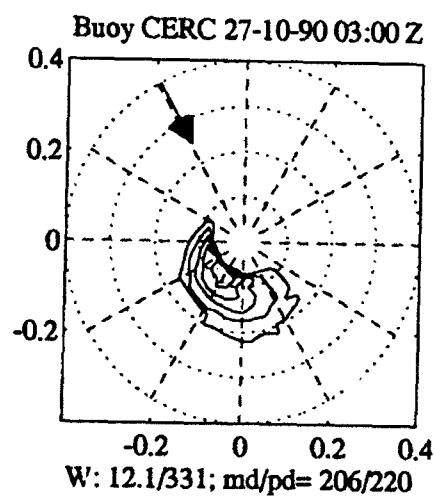
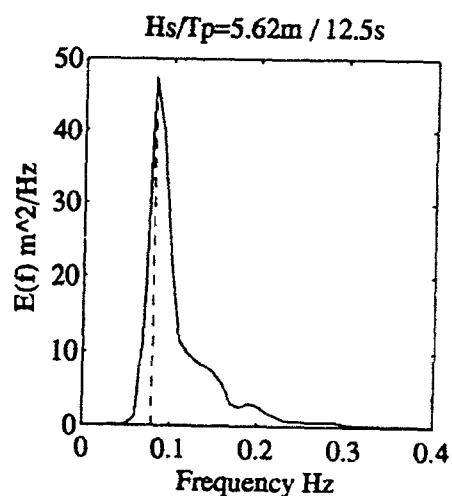
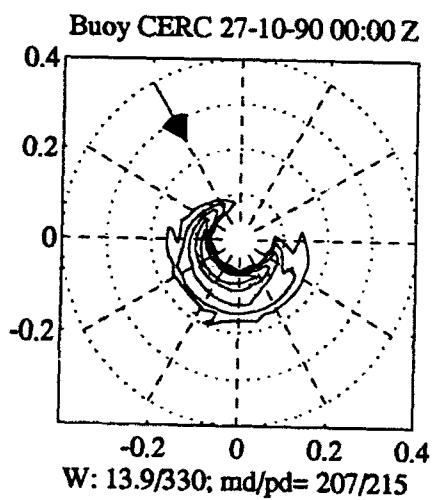
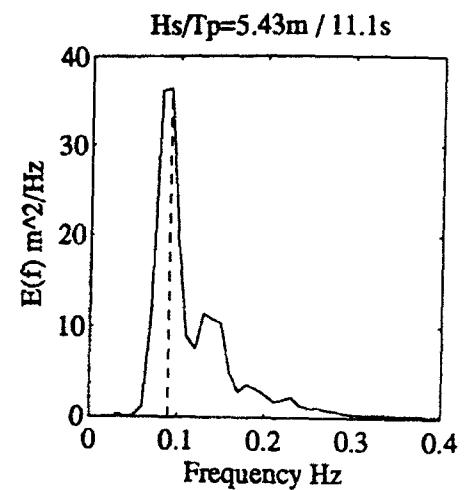
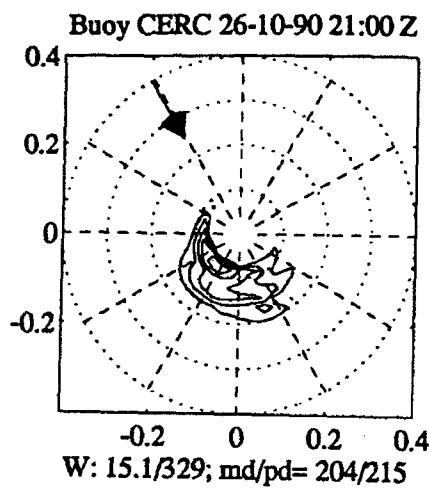


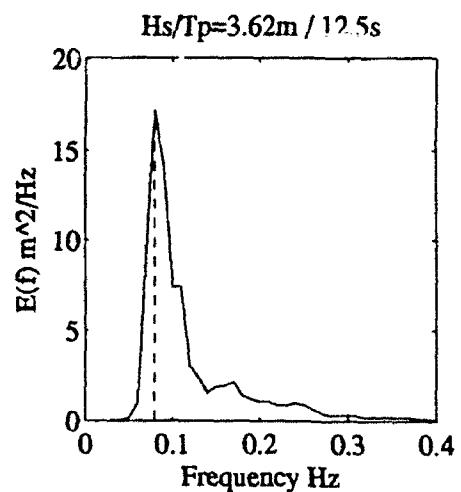
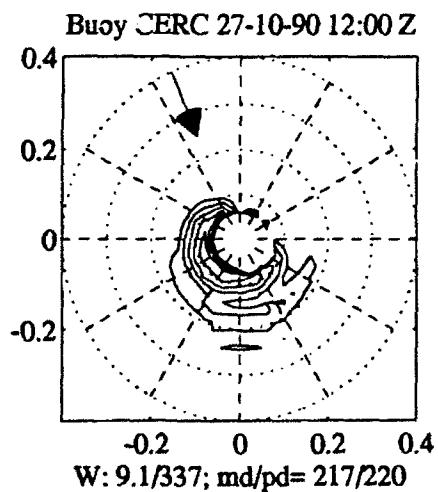
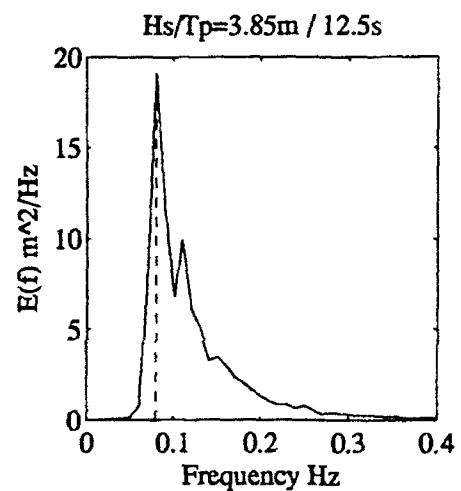
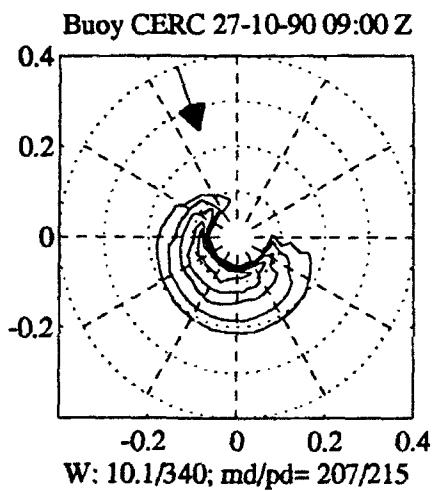
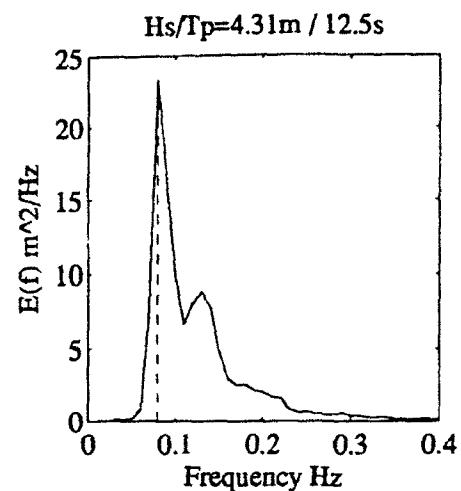
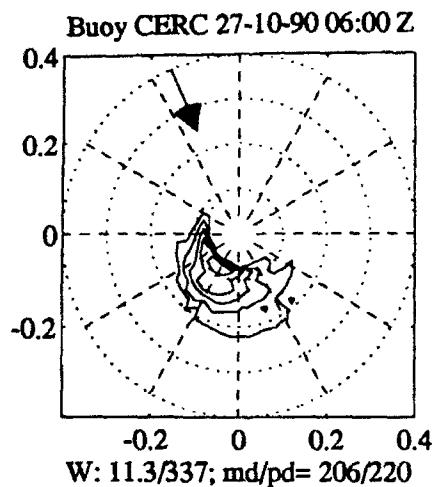


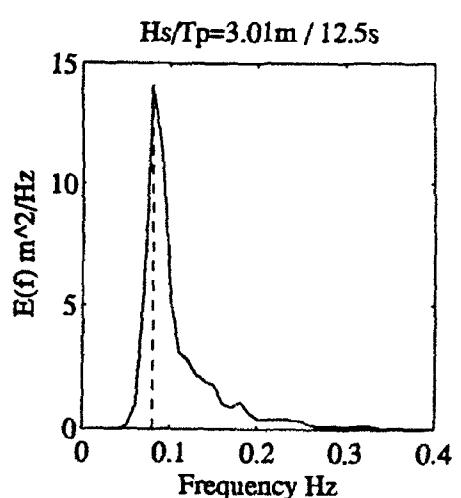
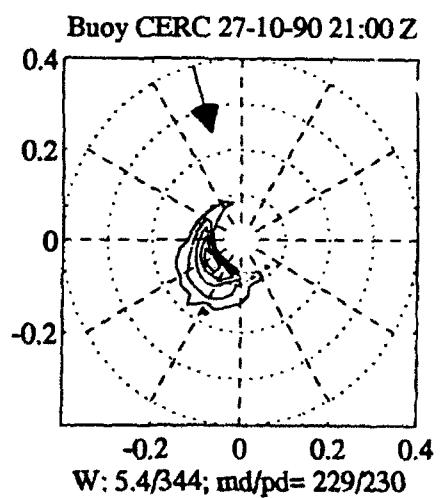
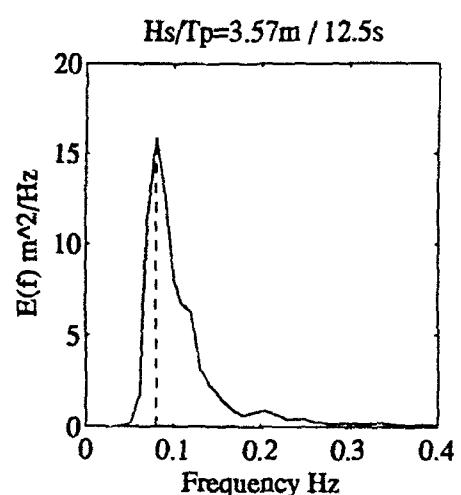
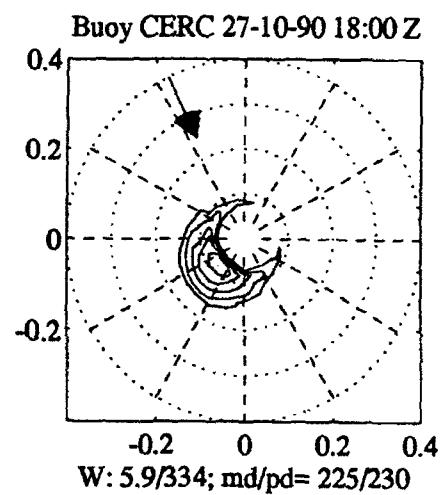
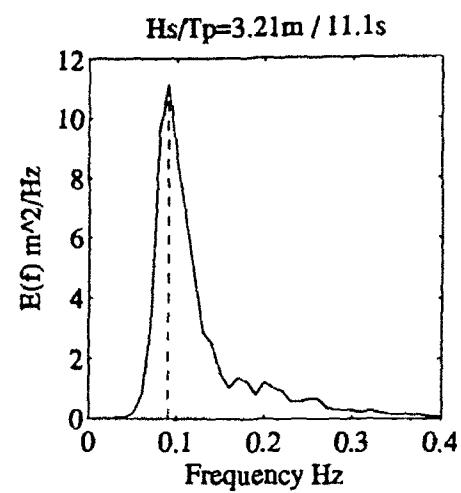
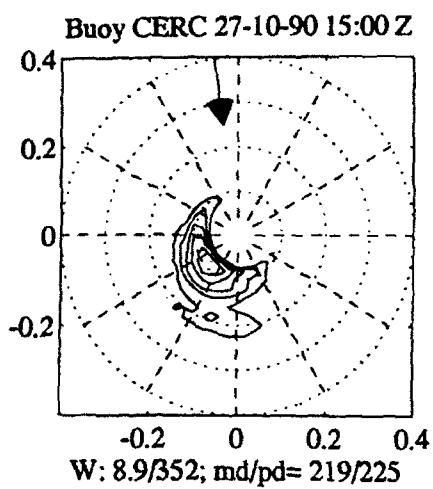


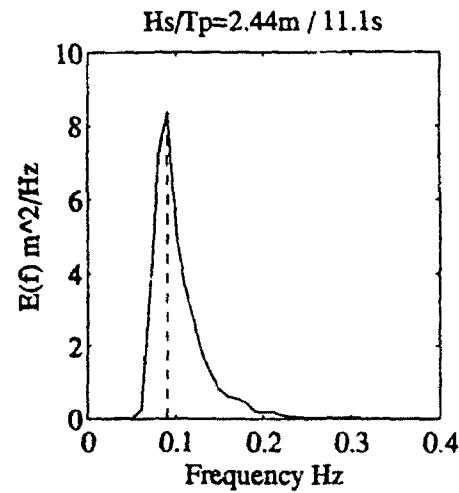
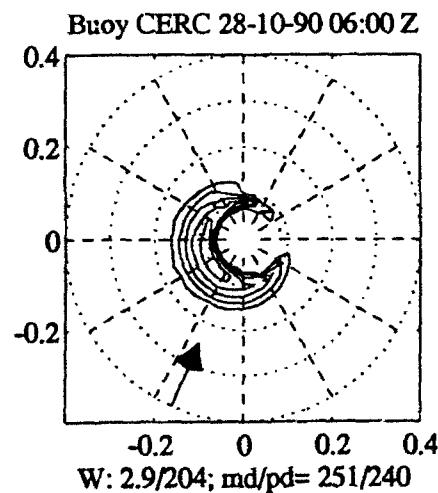
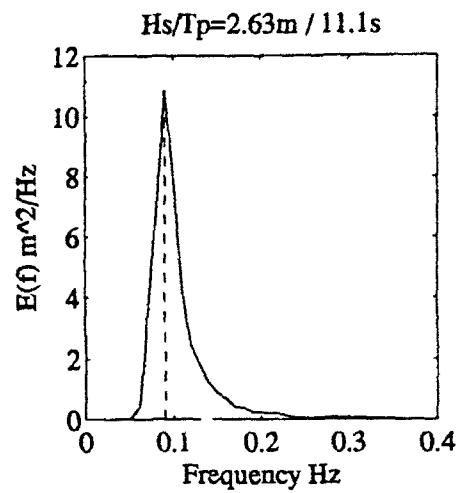
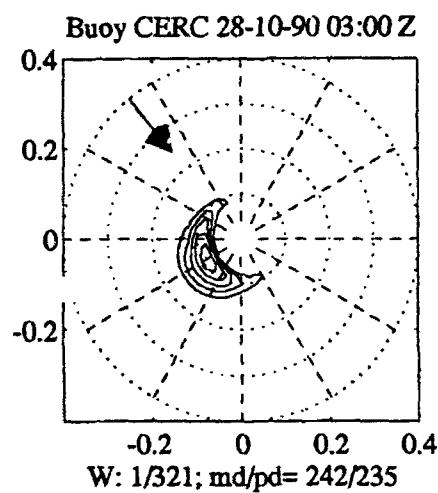
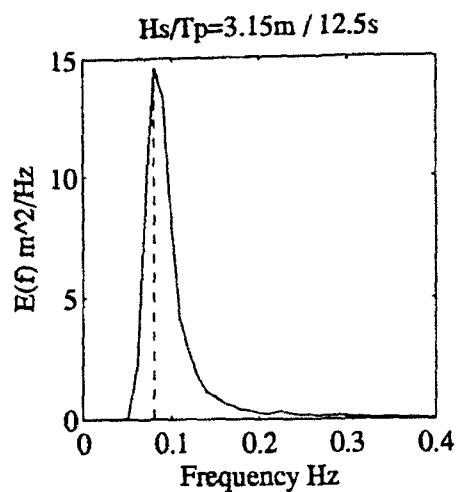
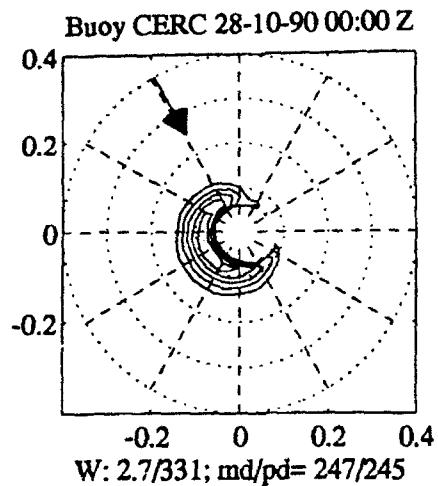


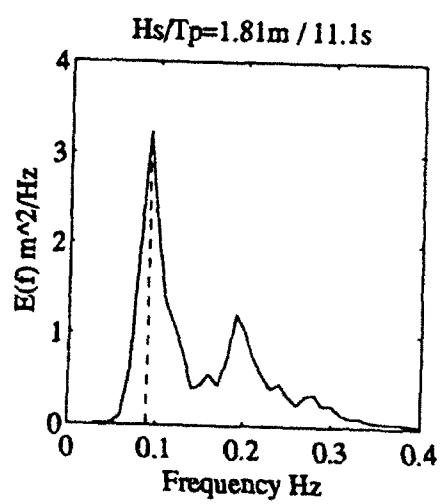
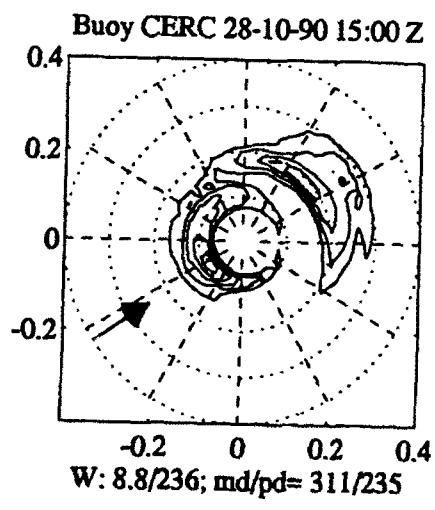
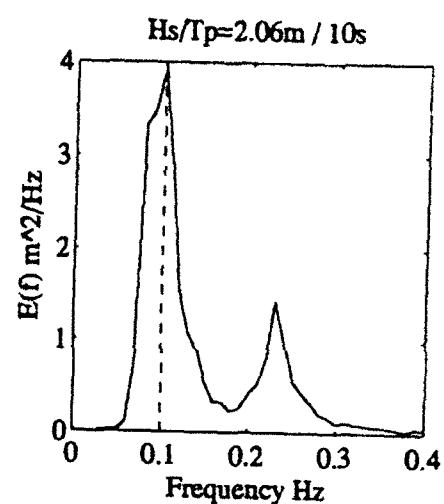
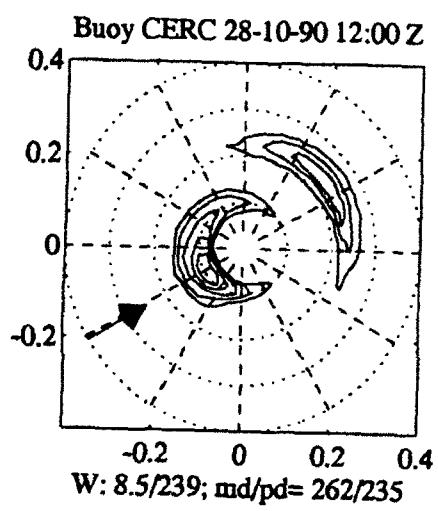
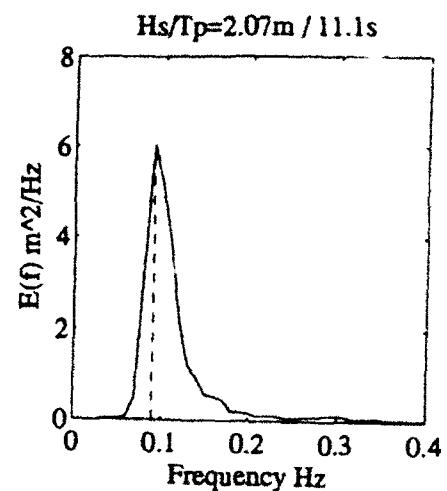
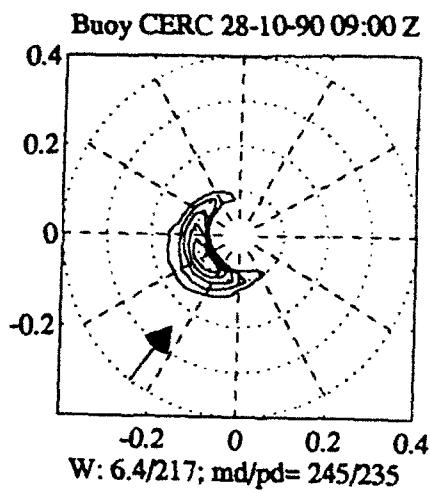


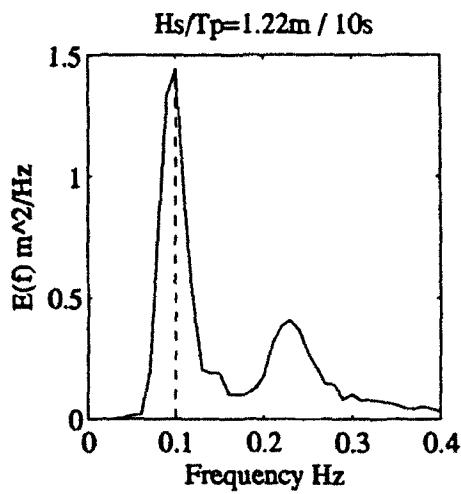
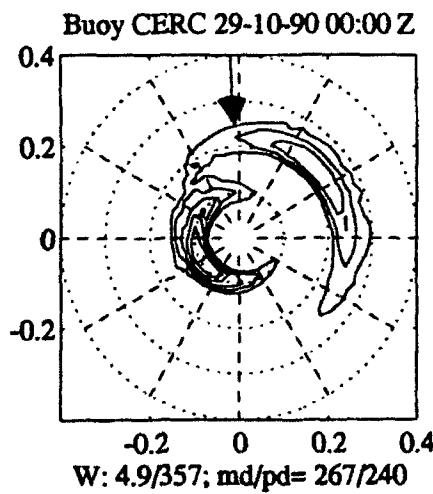
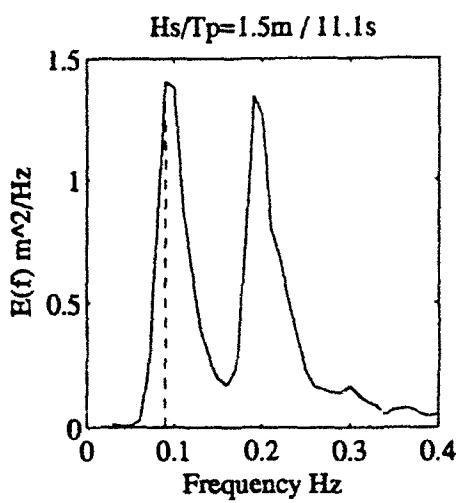
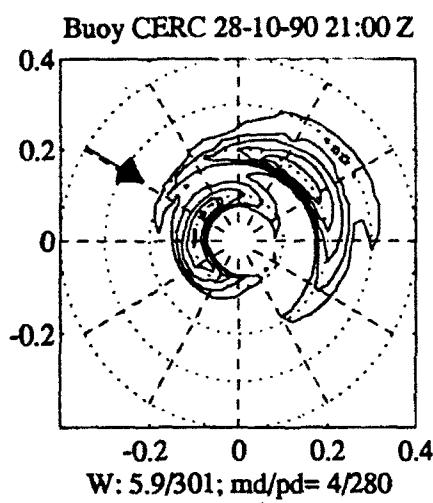
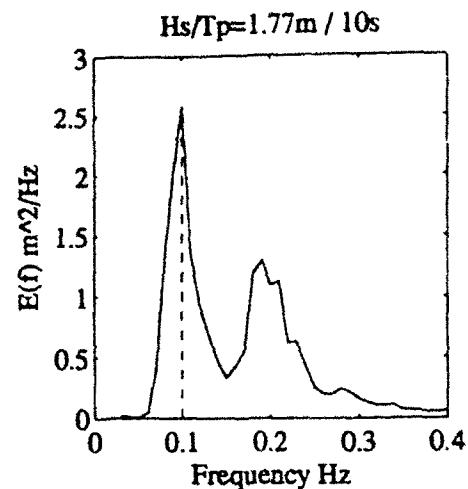
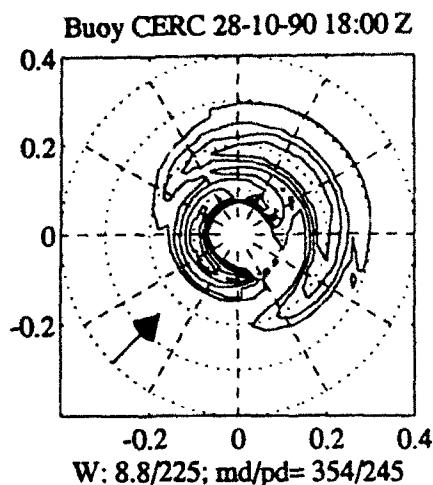








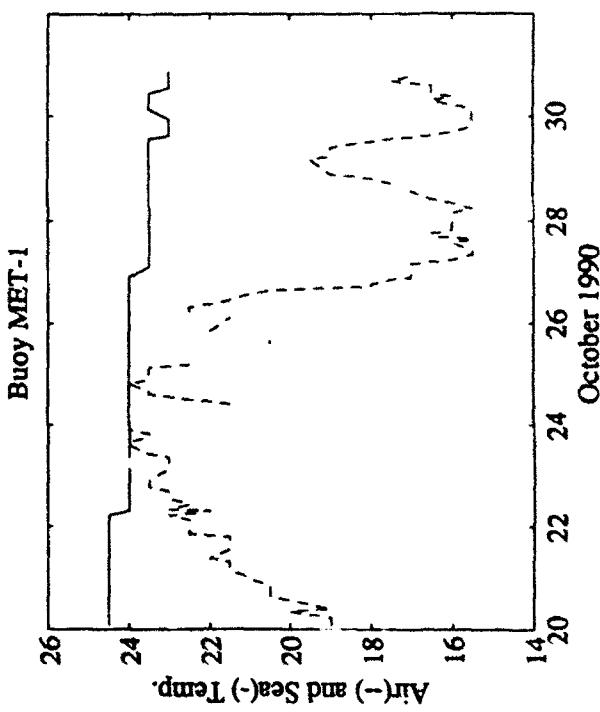
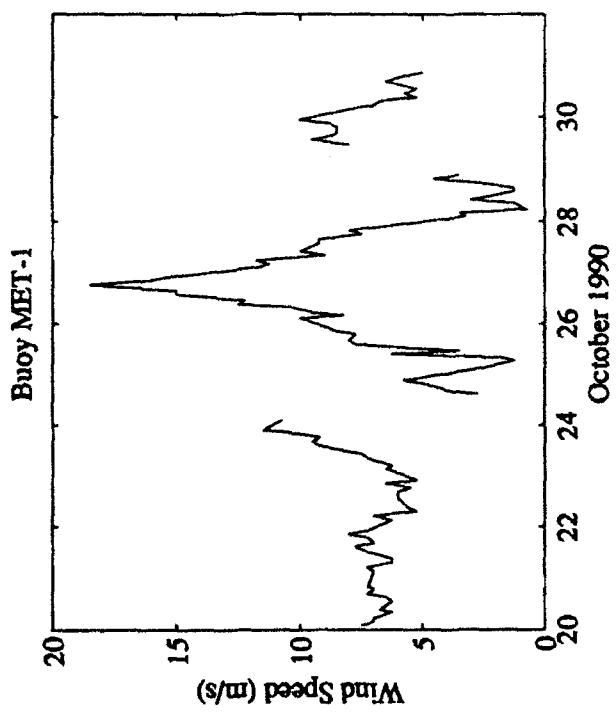
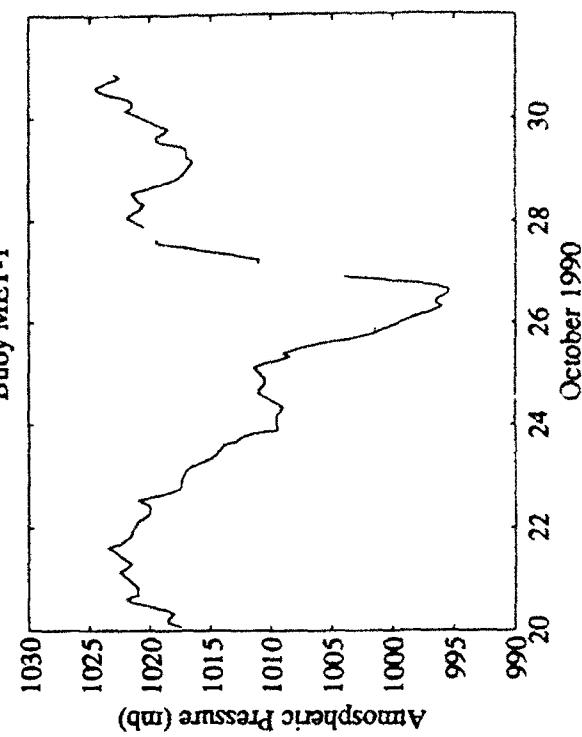
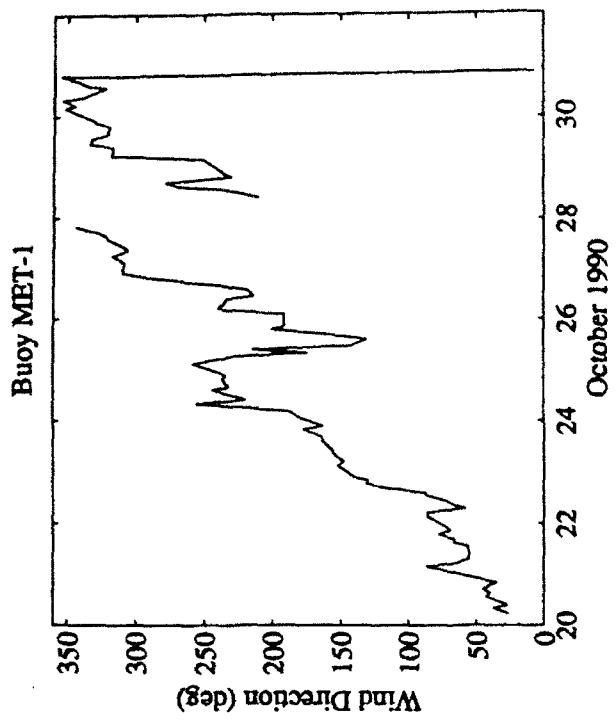




Appendix C: Time Series from MiniMet Buoys

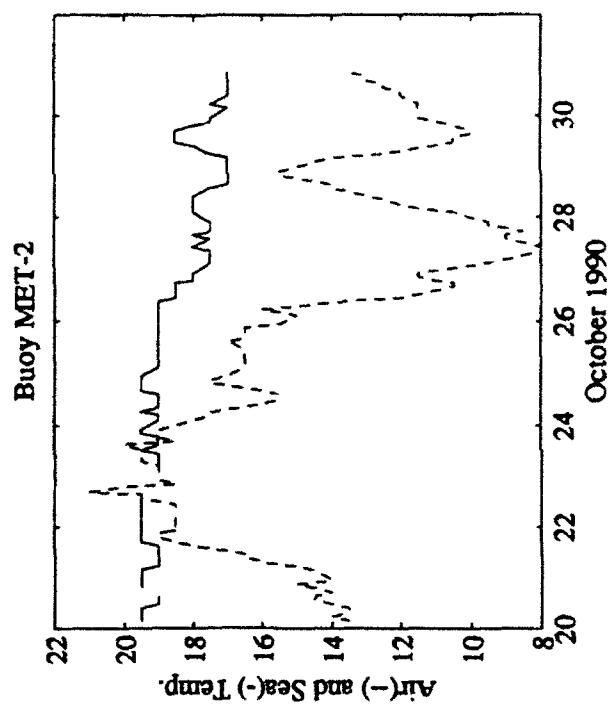
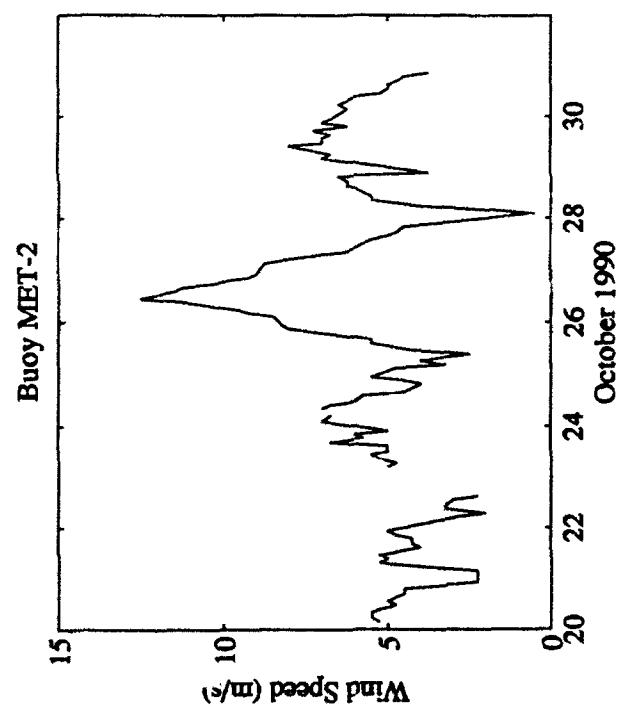
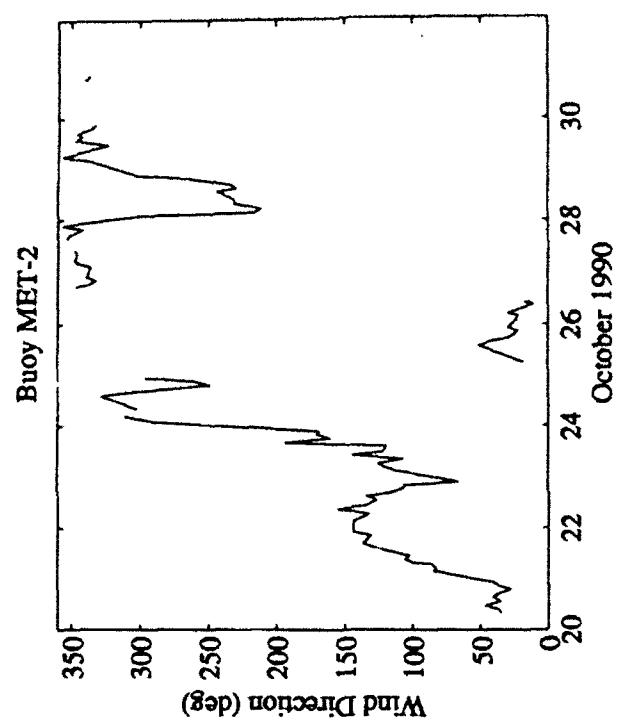
Time series plots of the observed data are presented in this appendix in the following sequence:

- MiniMet Buoy "MET-1" (41012, 41014)
- MiniMet Buoy "MET-2" (44018, 44022)
- MiniMet Buoy "MET-3" (44016, 44020)
- MiniMet Buoy "MET-4" (44017, 44021)

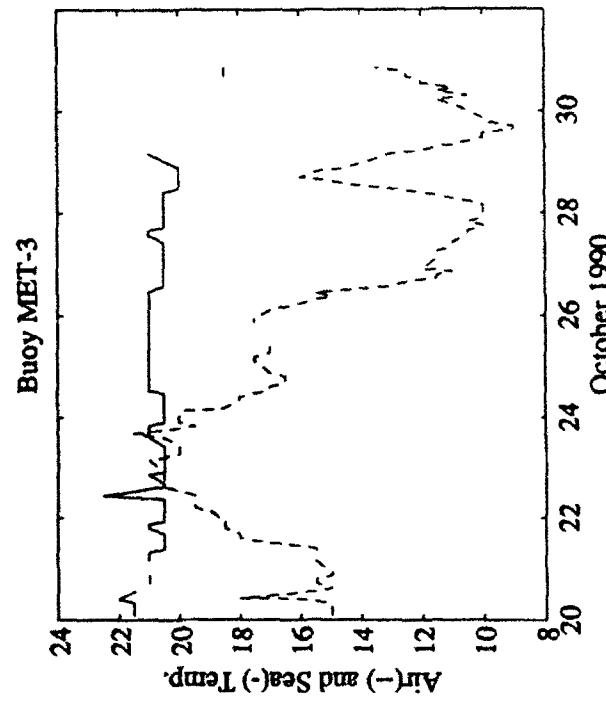
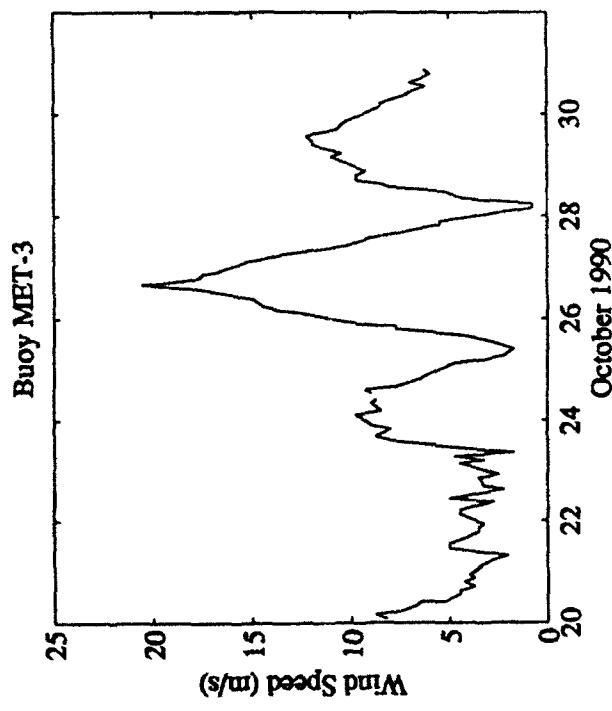
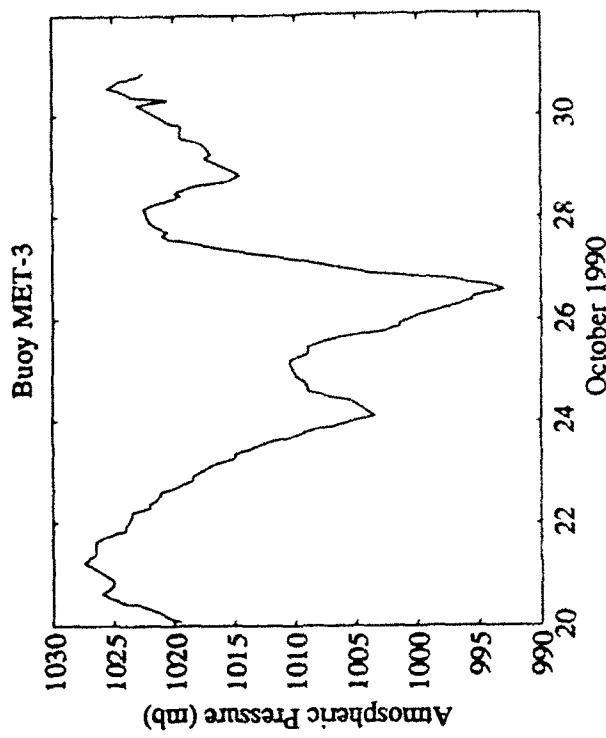
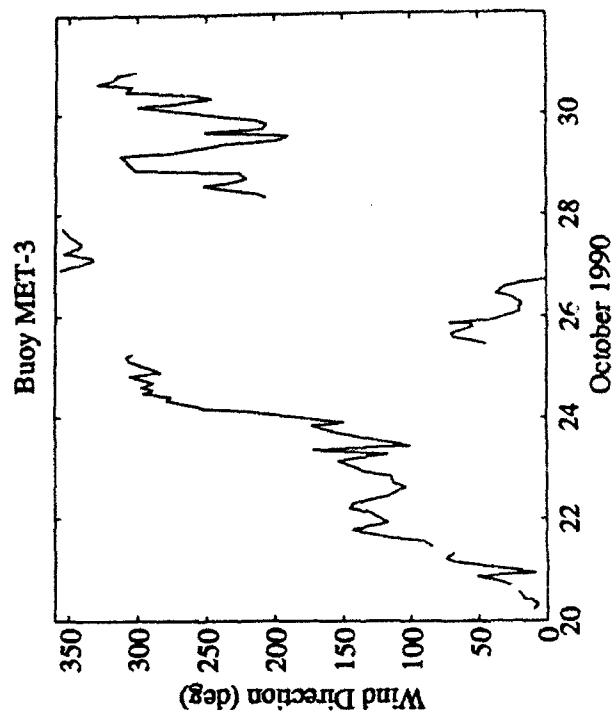


C2

Appendix C Time Series from MiniMet Buoys

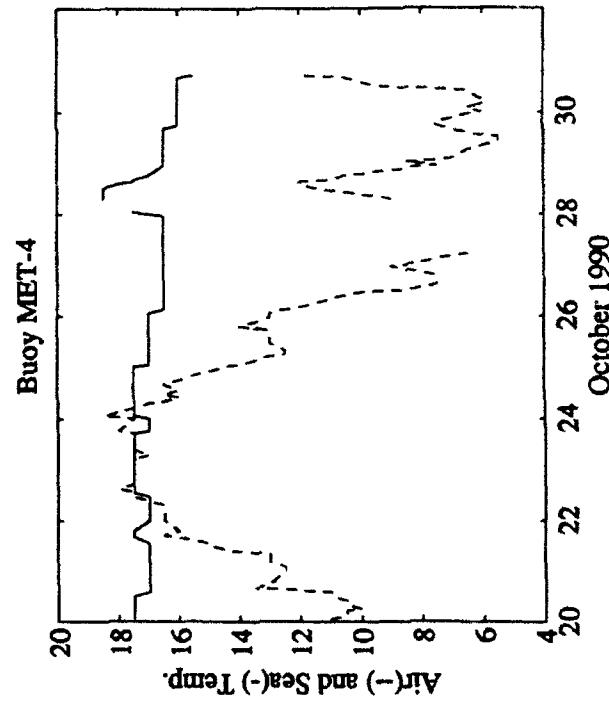
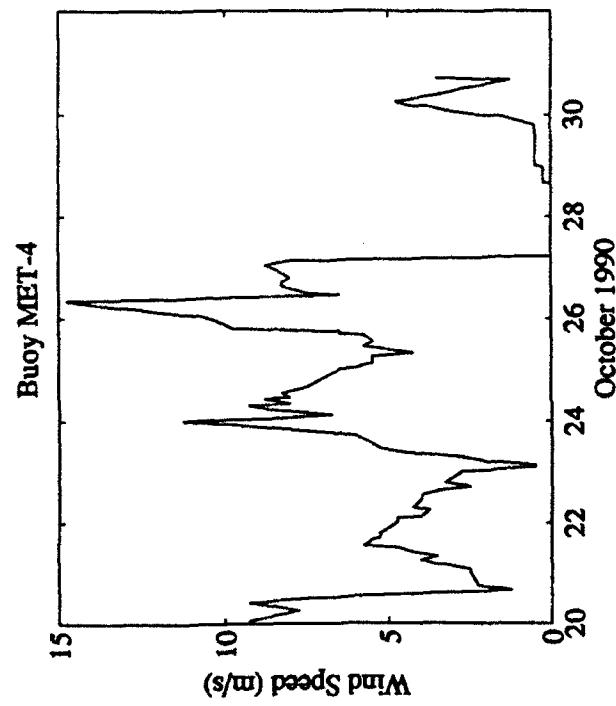
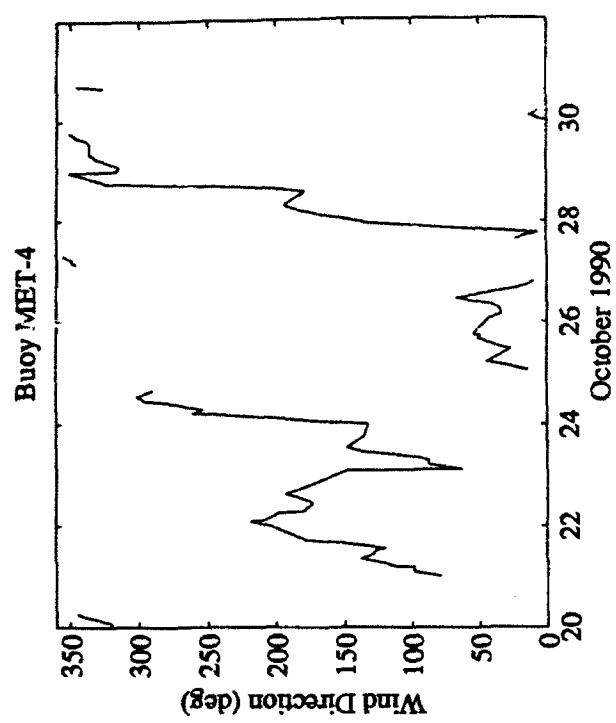


Appendix C Time Series from MiniMet Buoys



C4

Appendix C Time Series from MiniMet Buoys

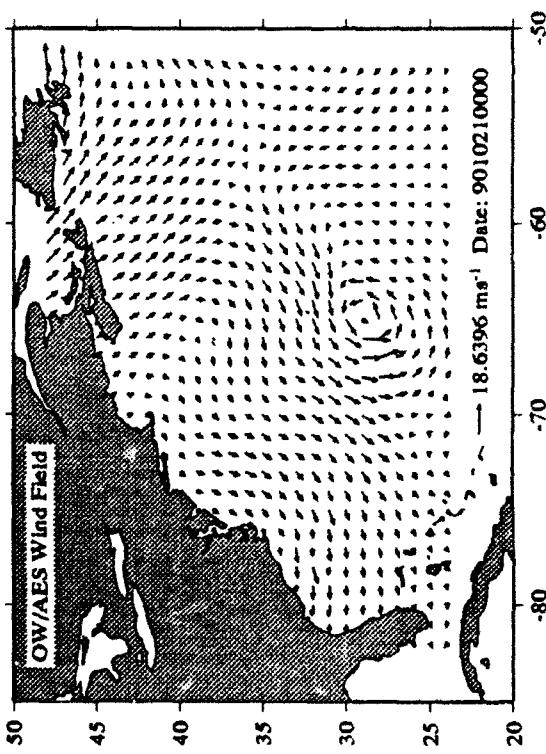
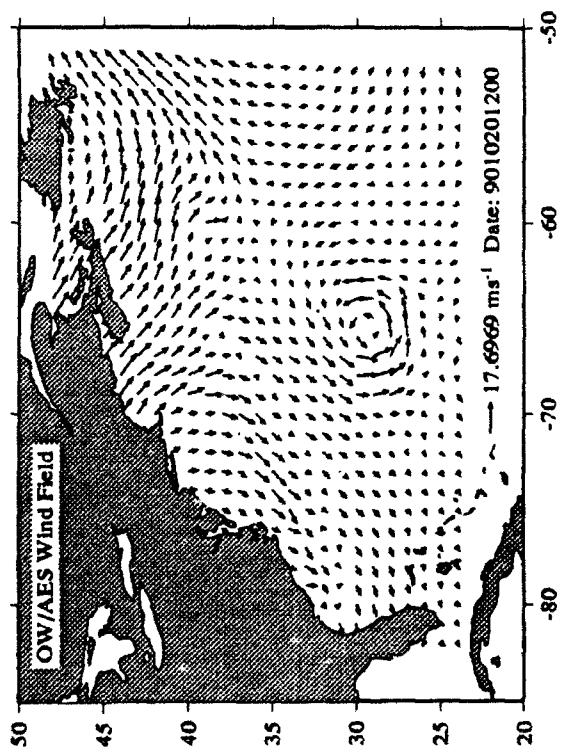
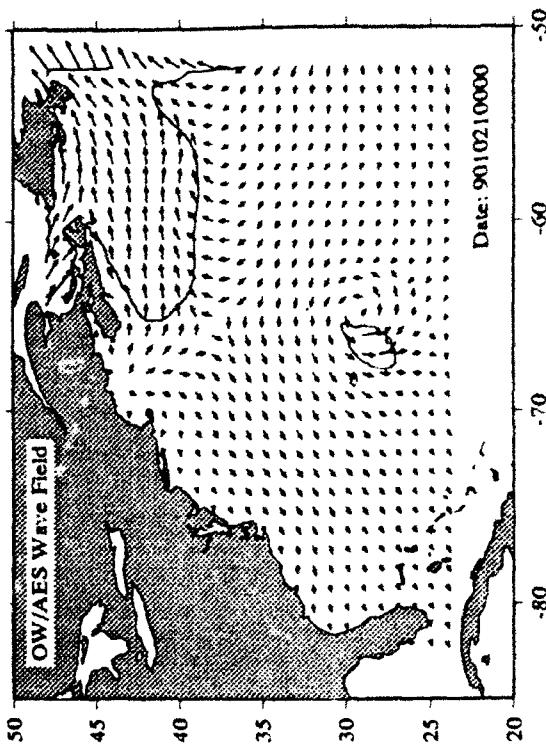
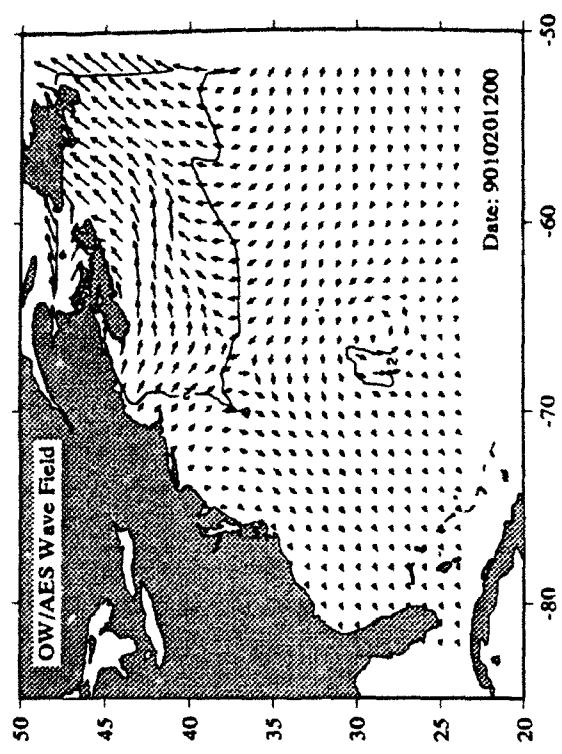


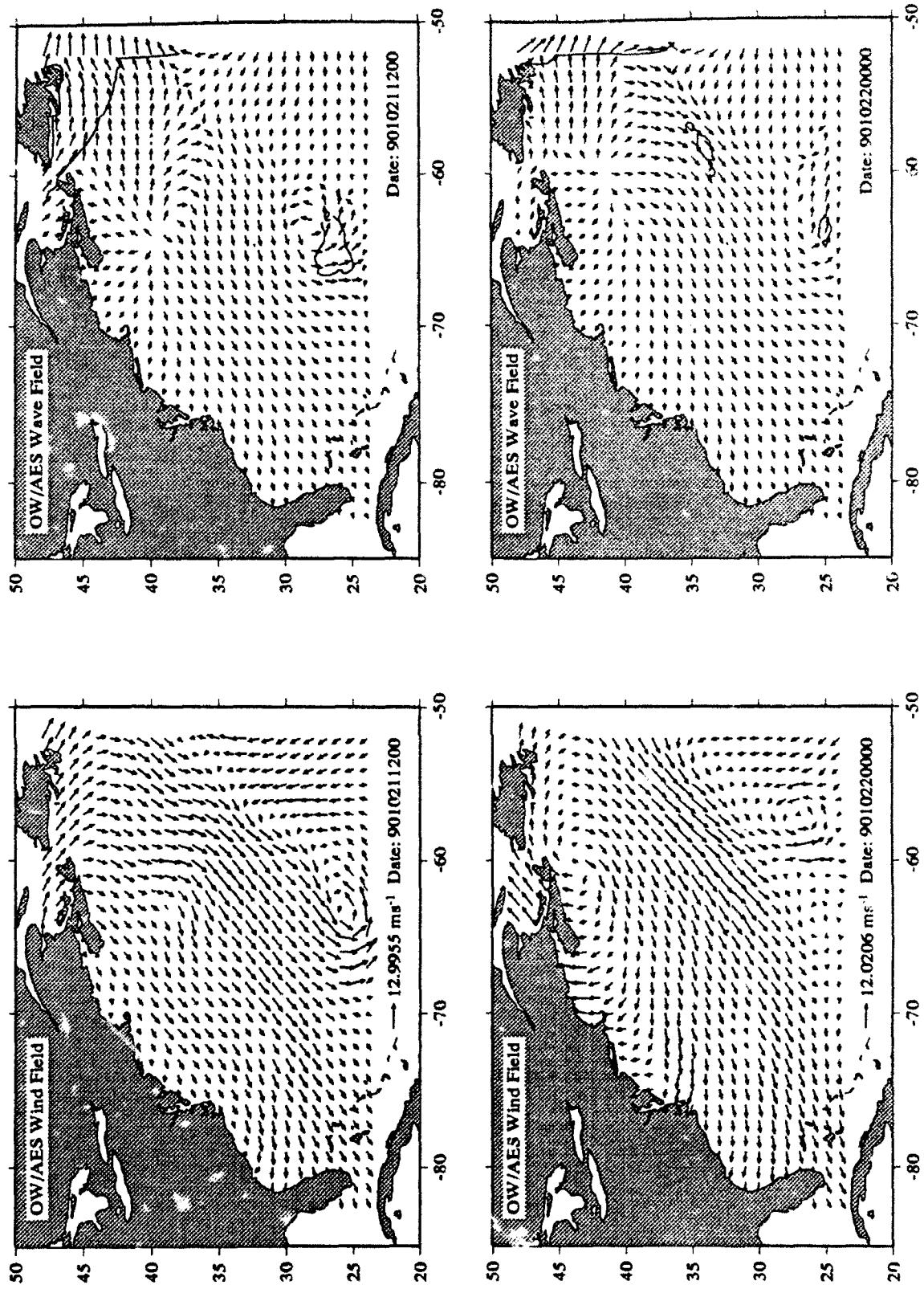
Appendix D: Custer Diagrams of Wind Fields and Wave Hindcasts

Maps of the wind vector fields (Custer diagrams) and corresponding wave height hindcasts with the ocean wave model "WAM" are presented in this appendix for six different wind field specifications. Each wind field Custer diagram presents the maximum wind speed for this time. The vectors of the wave height Custer diagram correspond to mean wave direction as computed by the WAM model. Contours of the wave heights are given in meters.

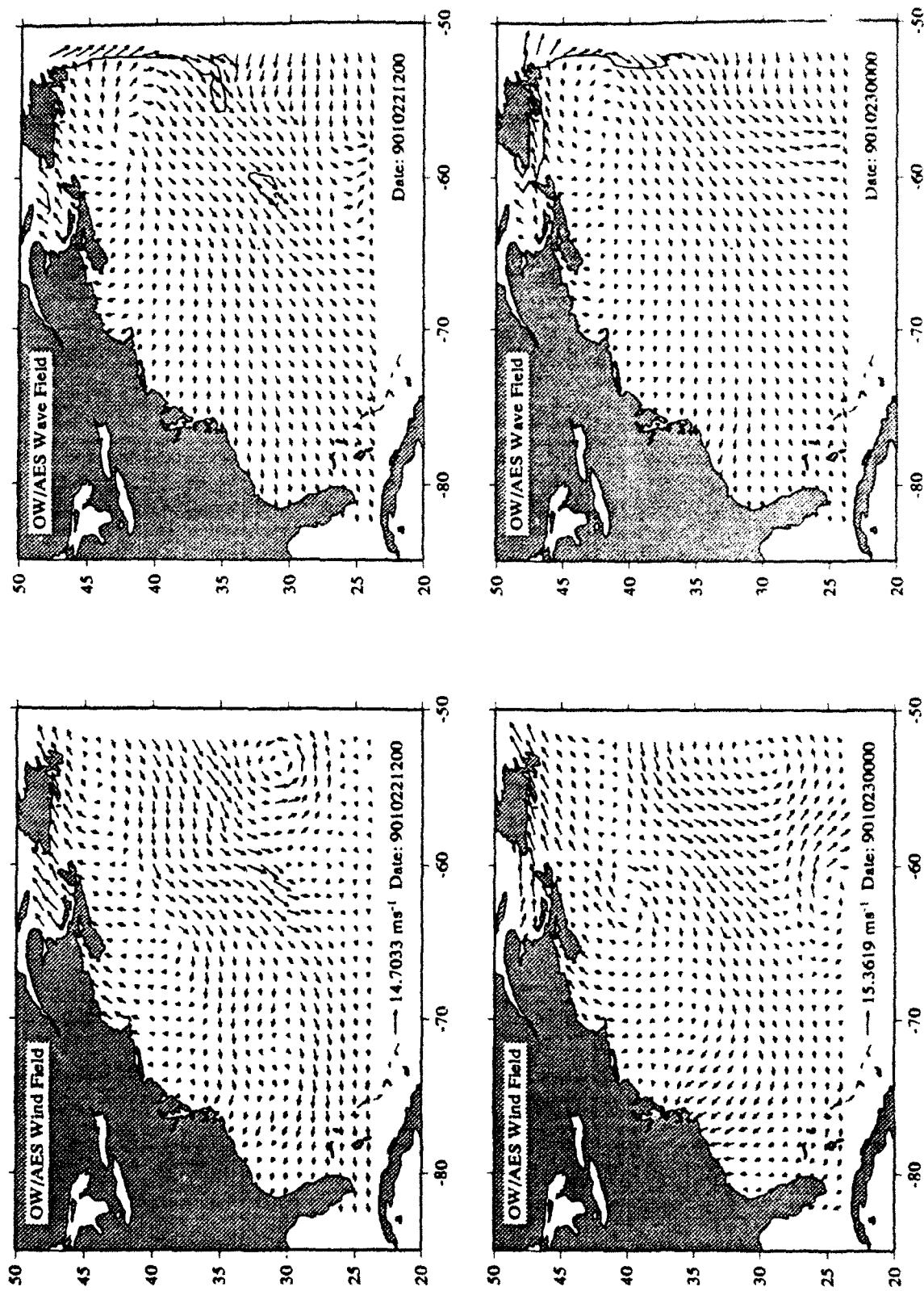
D.1: Oceanweather/Atmospheric Environment Service (OW/AES)

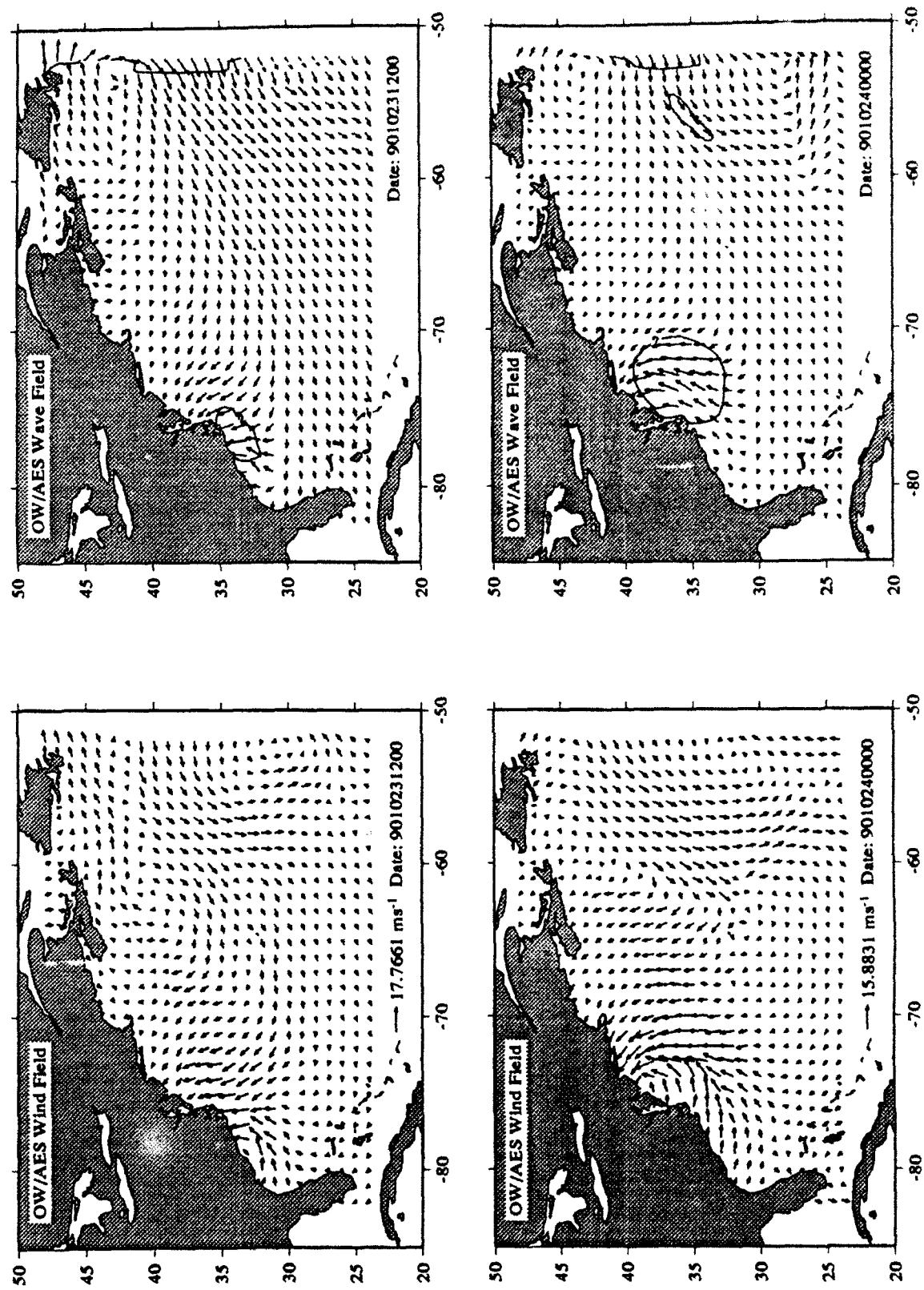
Custer diagrams are presented for the time period from 20 October 1990, 12:00 GMT to 31 October 1990, 12:00 GMT of the wind fields and corresponding wave hindcasts. Note that the frequency of maps is every 3 hr from 26-28 October, which covers the major storm period.



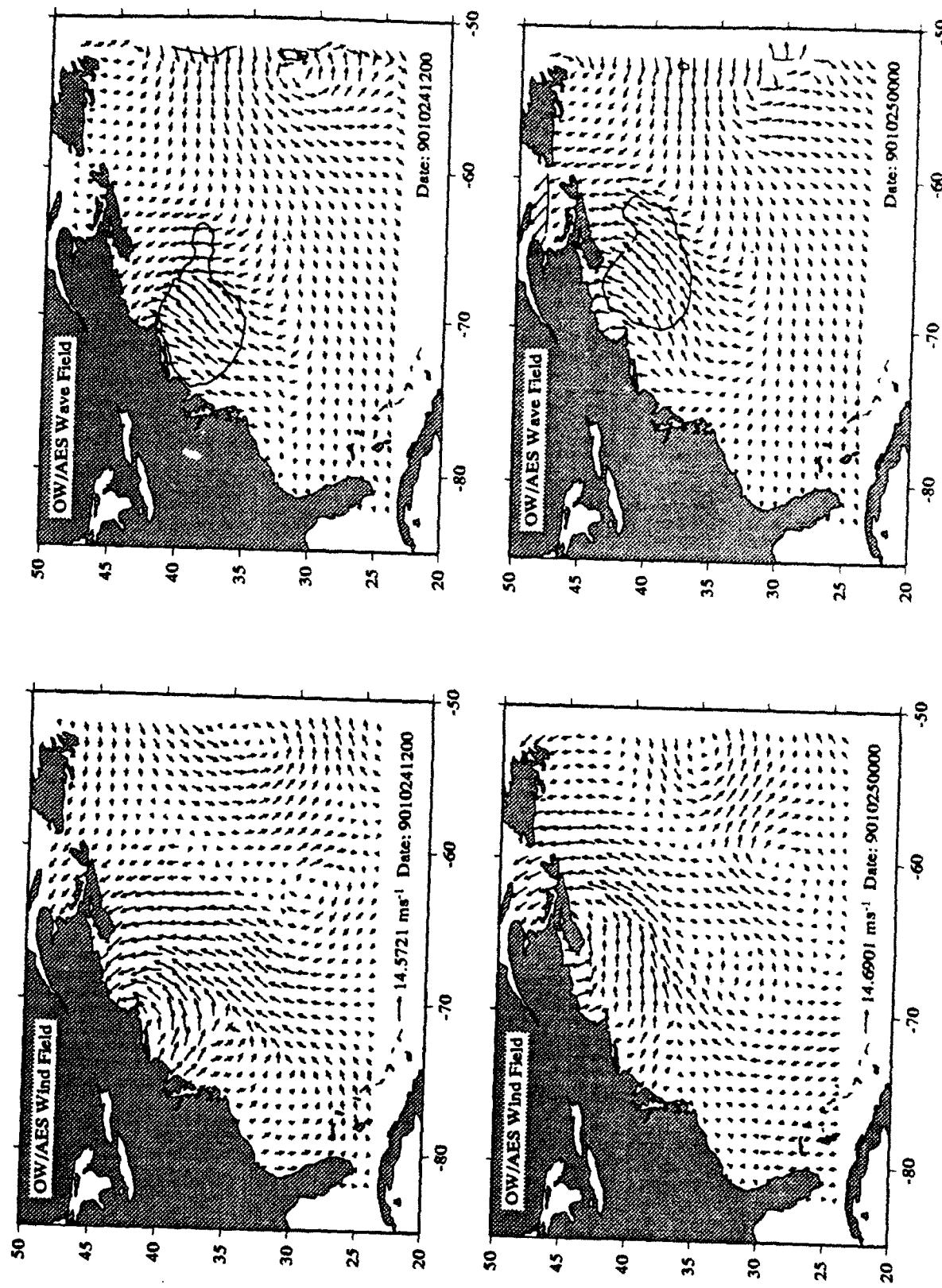


Appendix D Cluster Diagrams of Wind fields and Wave Hindcasts



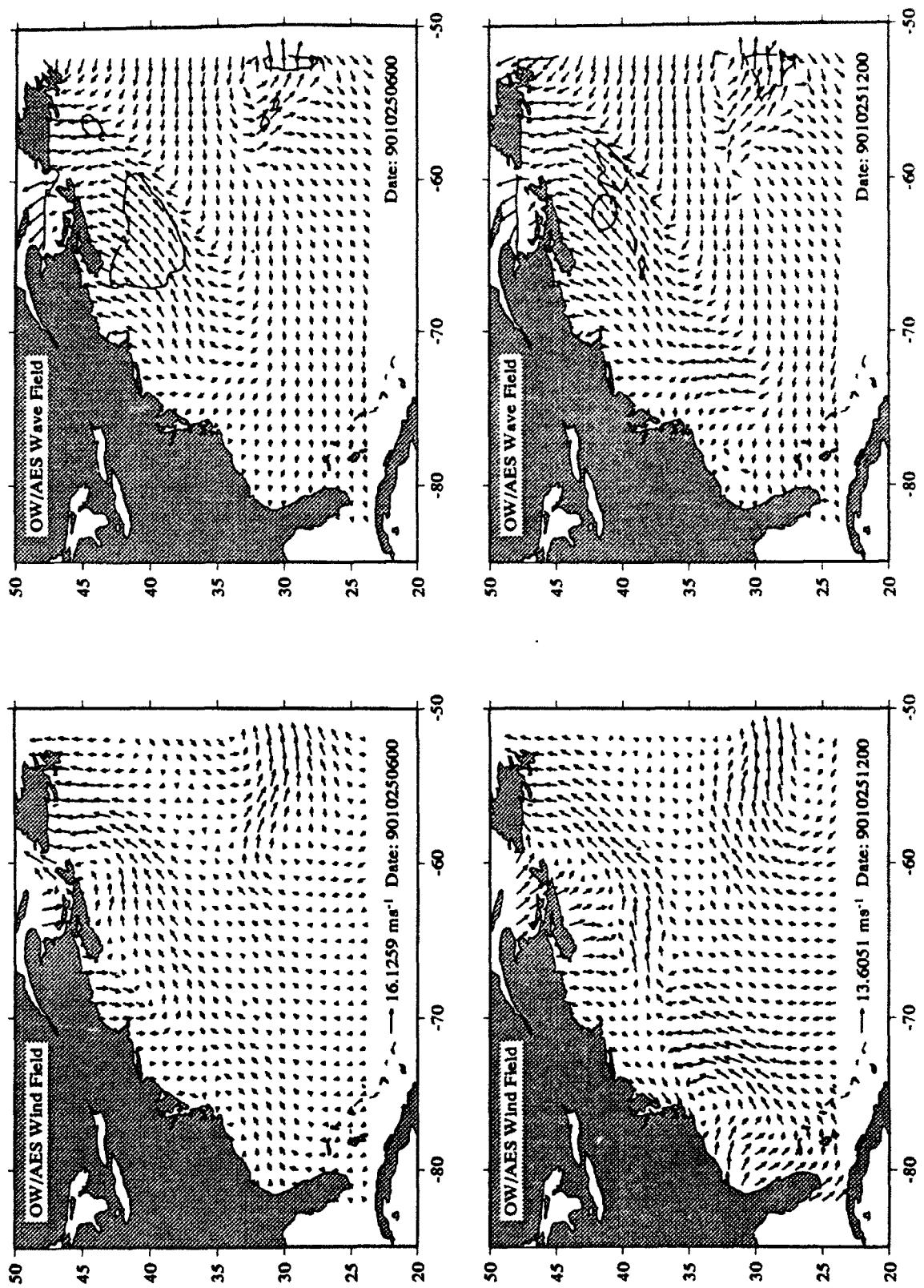


Appendix D Cluster Diagrams of Wind fields and Wave Hindcasts

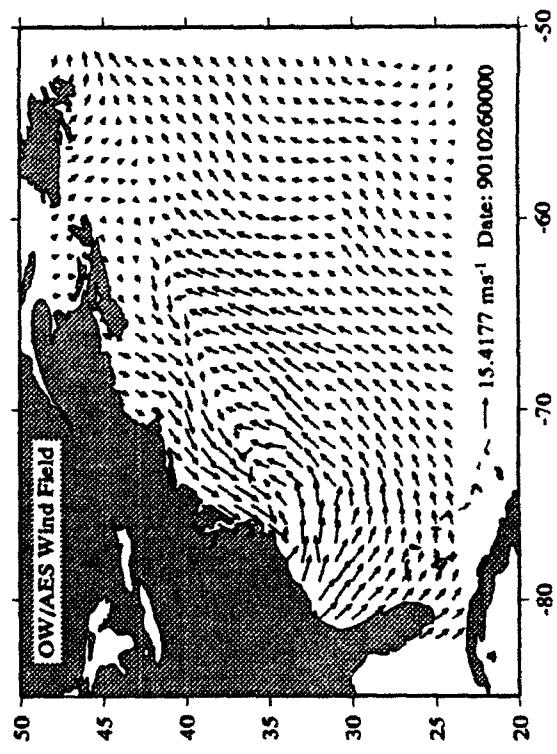
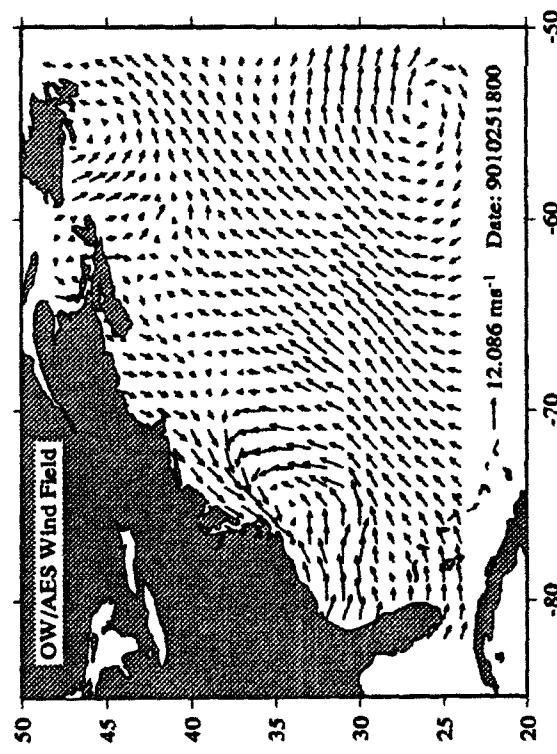
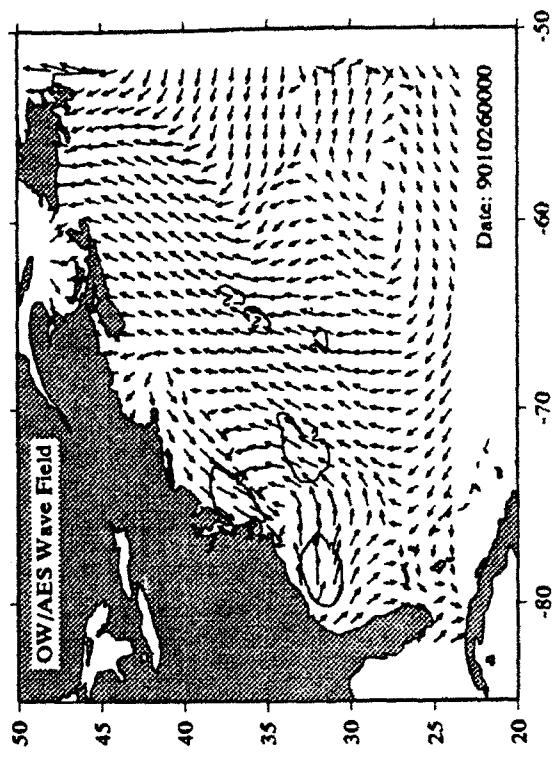
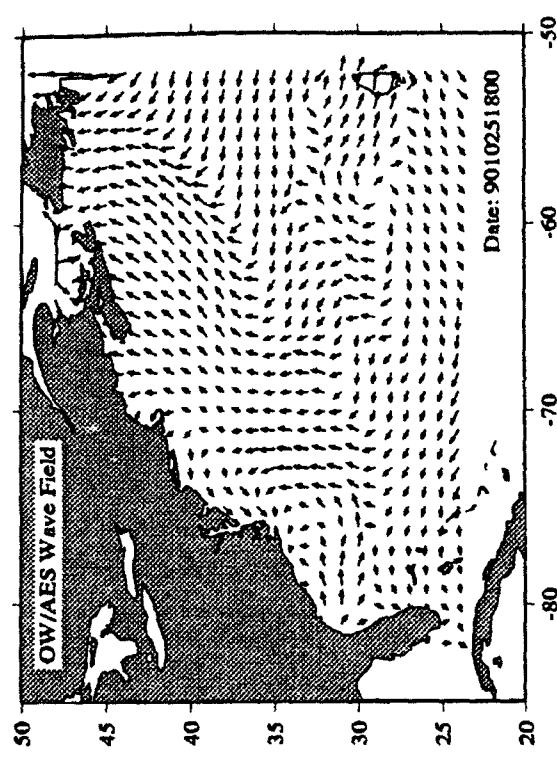


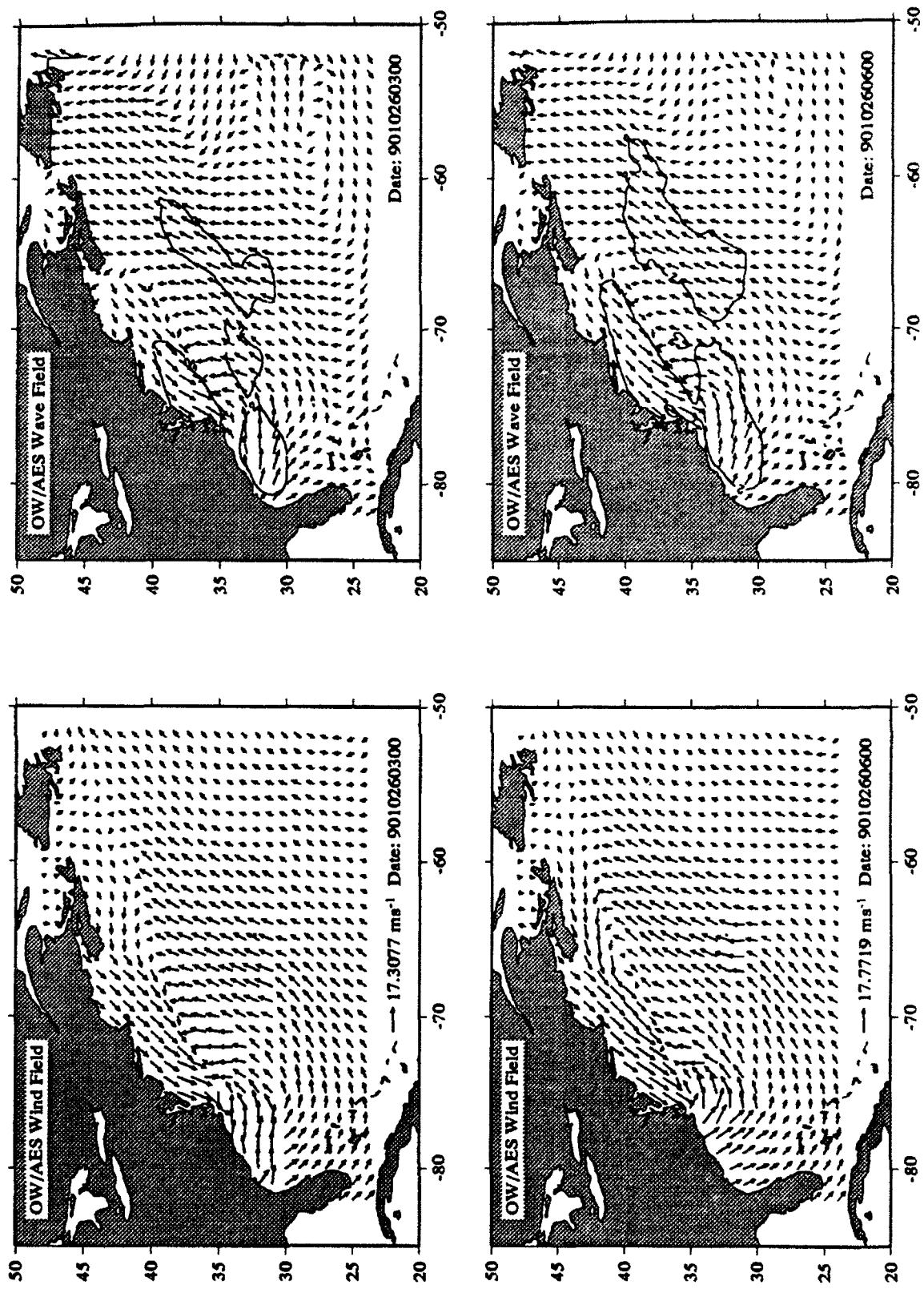
D8

Appendix D Cluster Diagrams of Wind fields and Wave Hindcasts

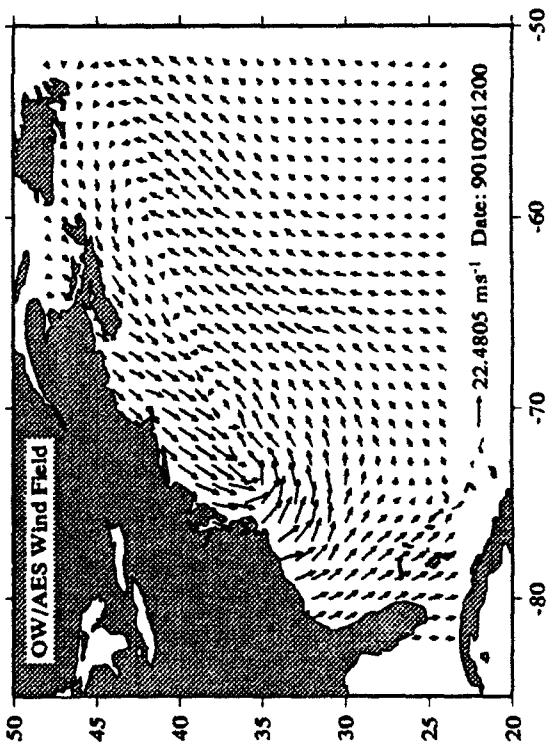
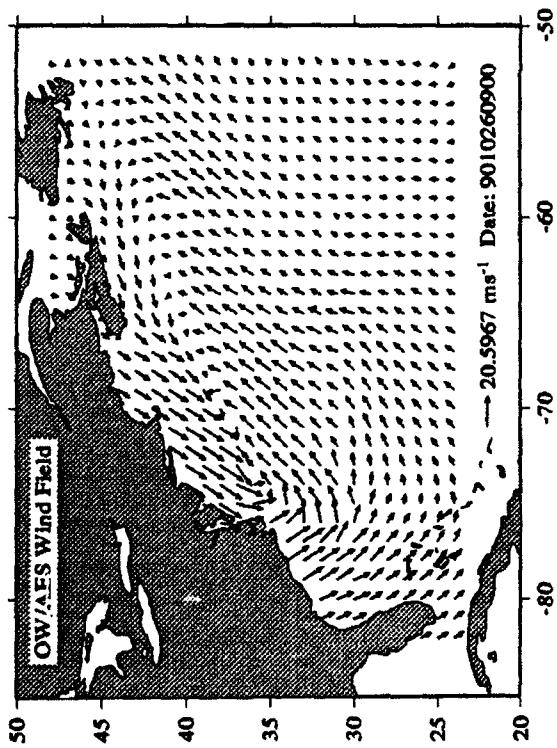
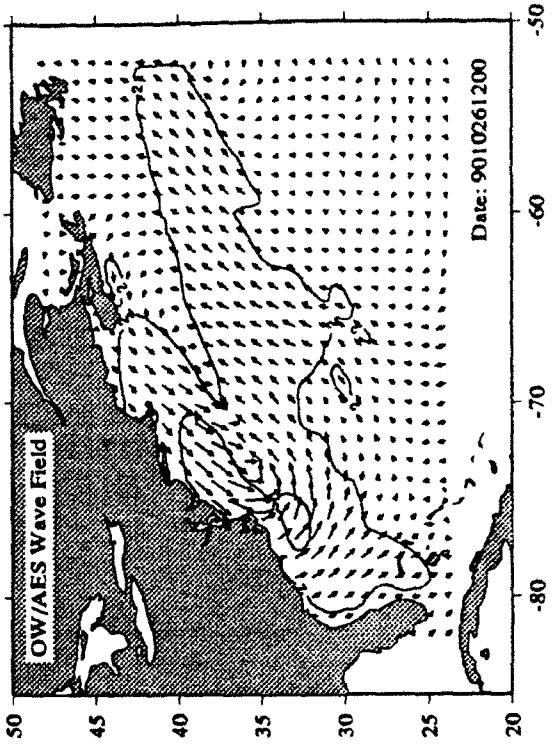
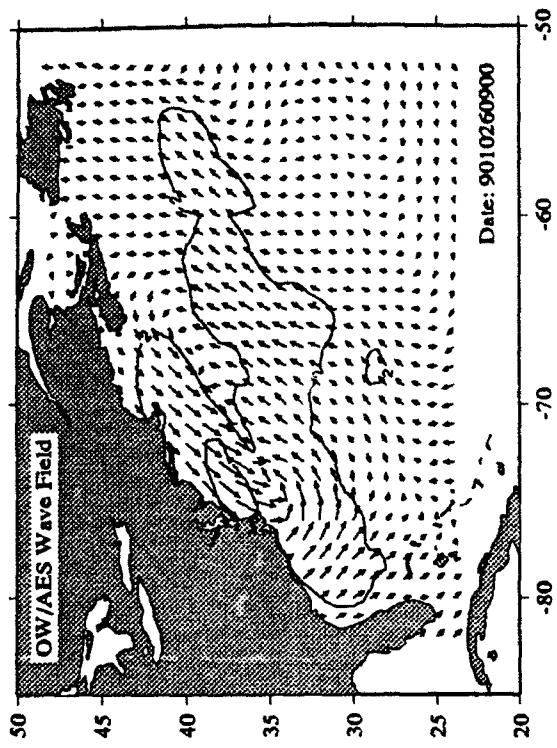


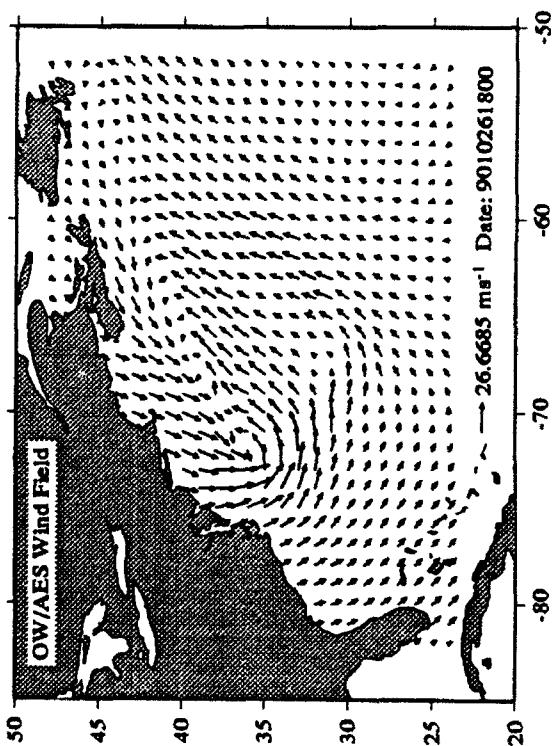
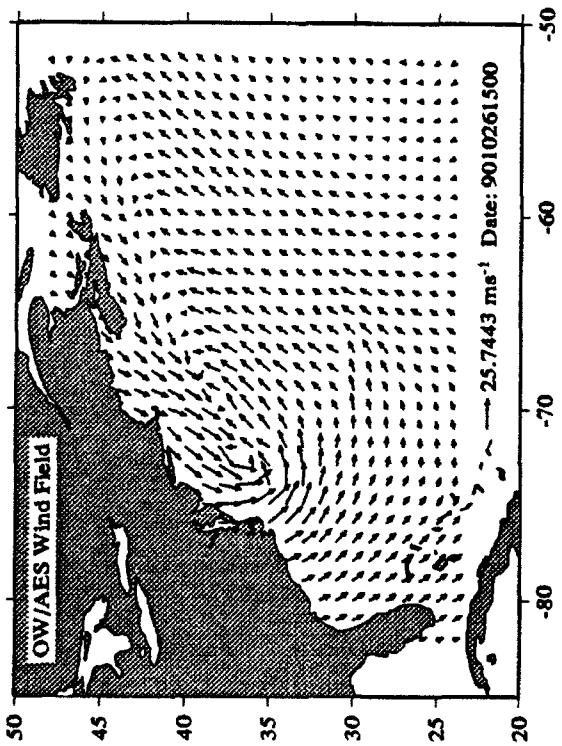
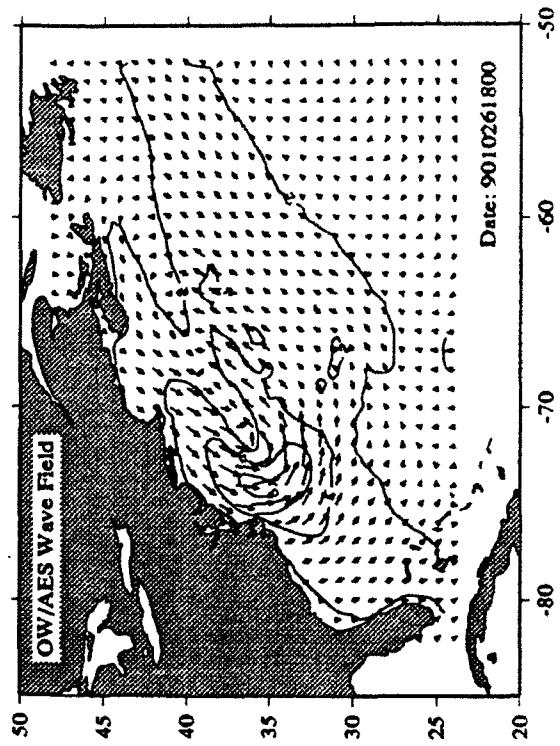
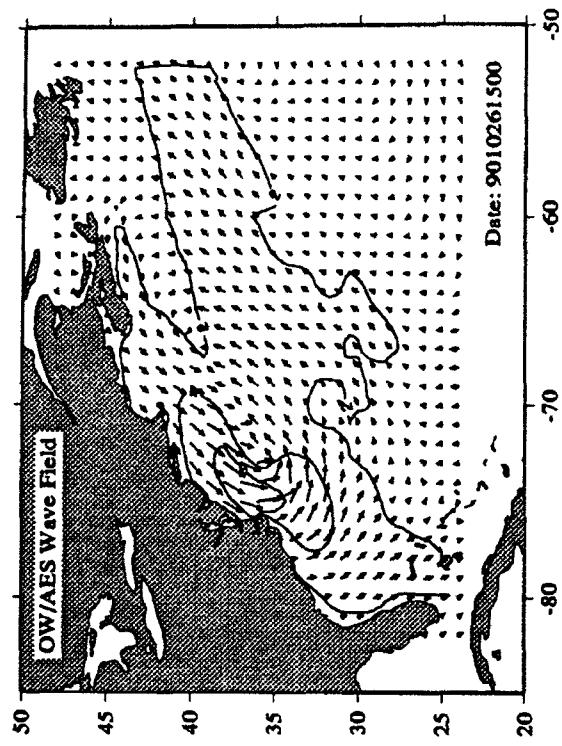
Appendix D Custer Diagrams of Wind fields and Wave Hindcasts

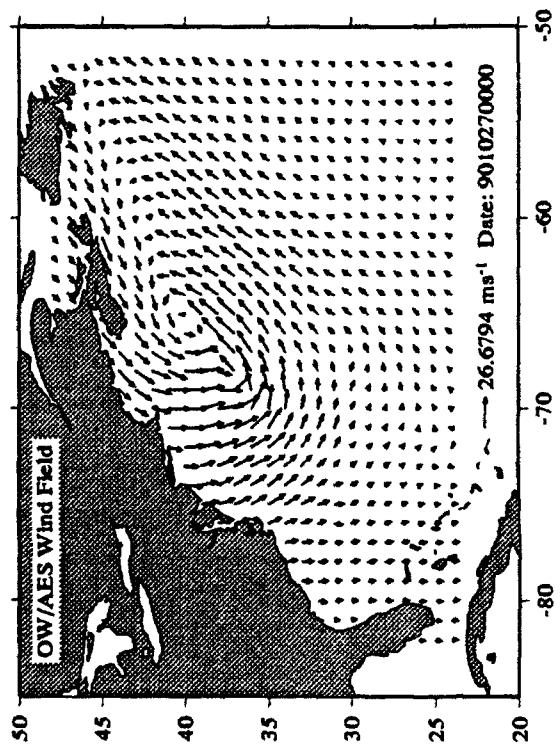
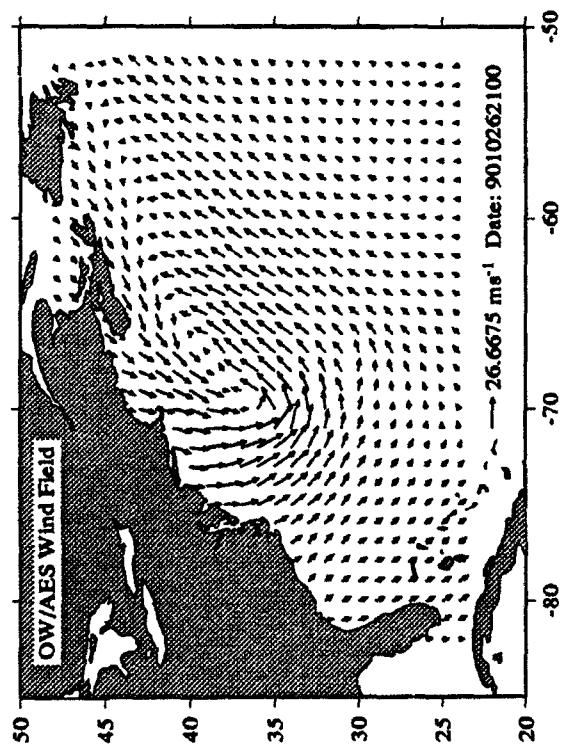
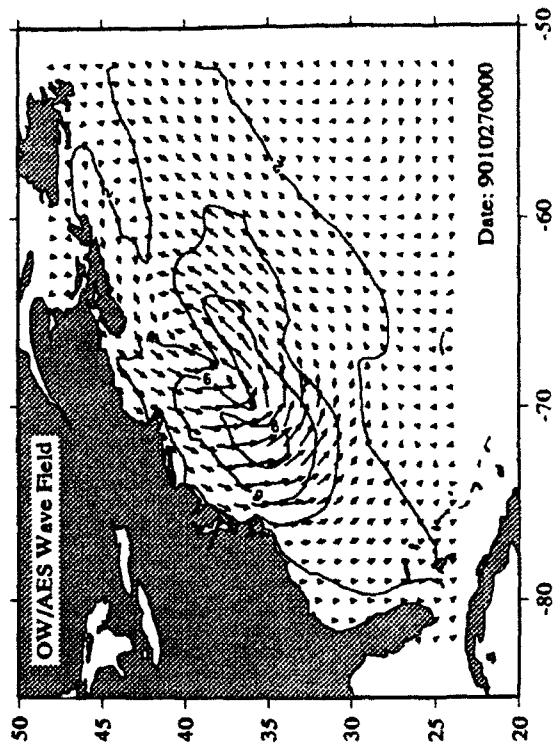
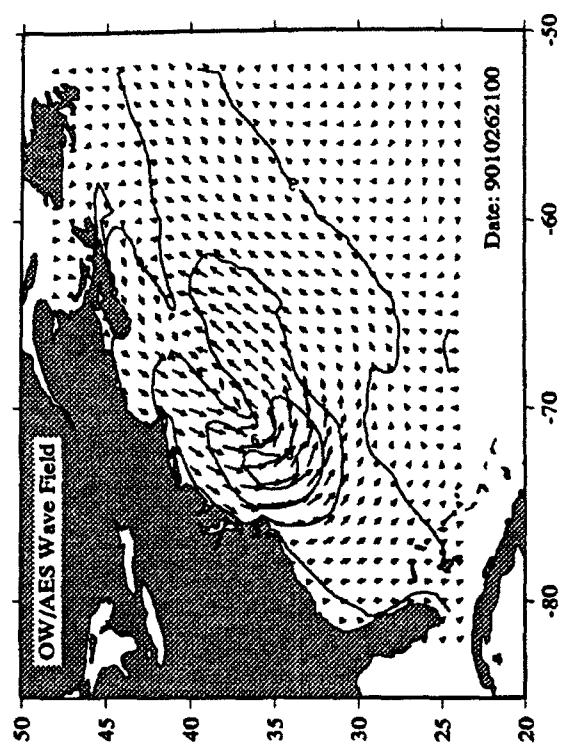


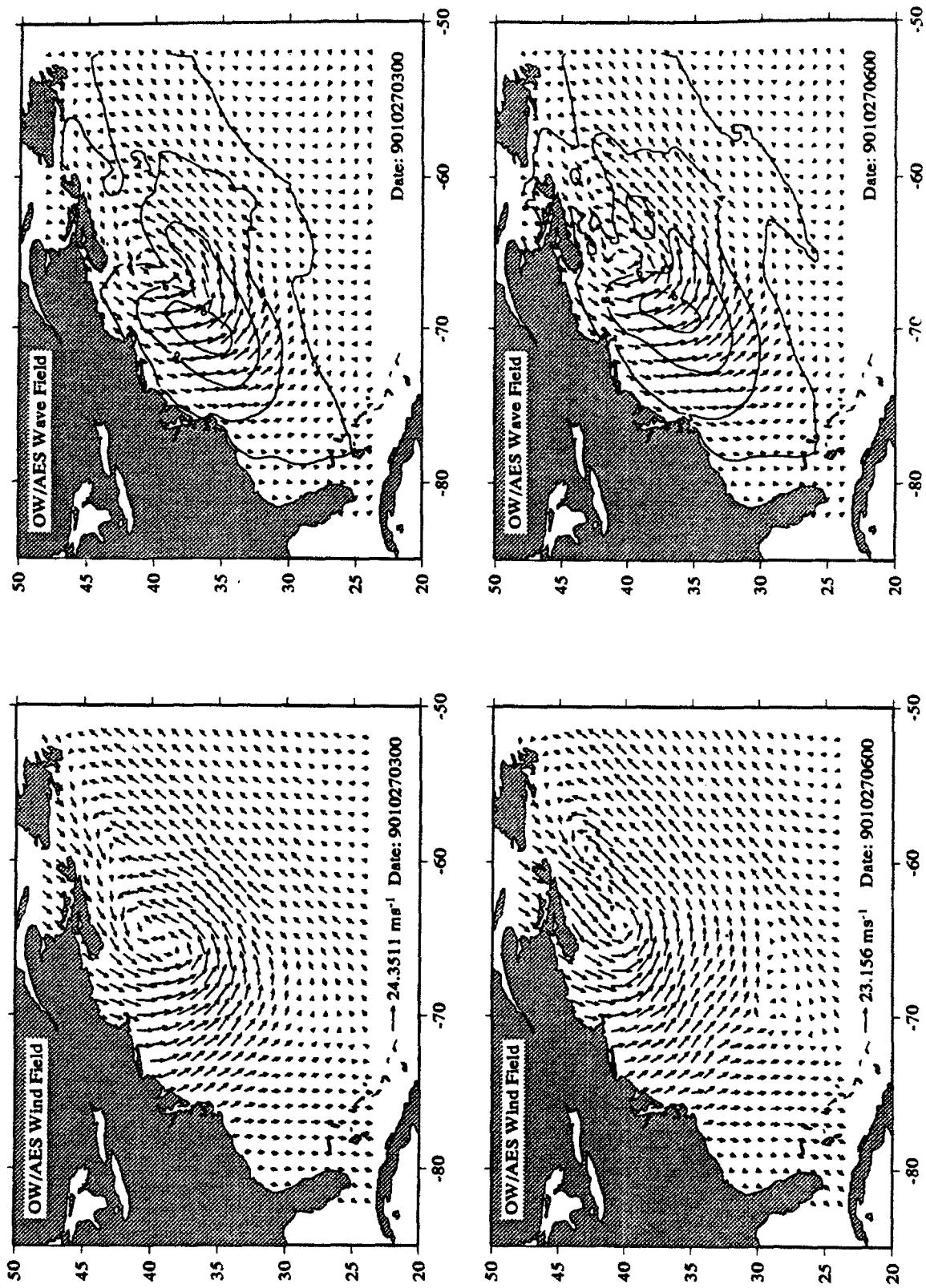


Appendix D Custer Diagrams of Wind fields and Wave Hindcasts

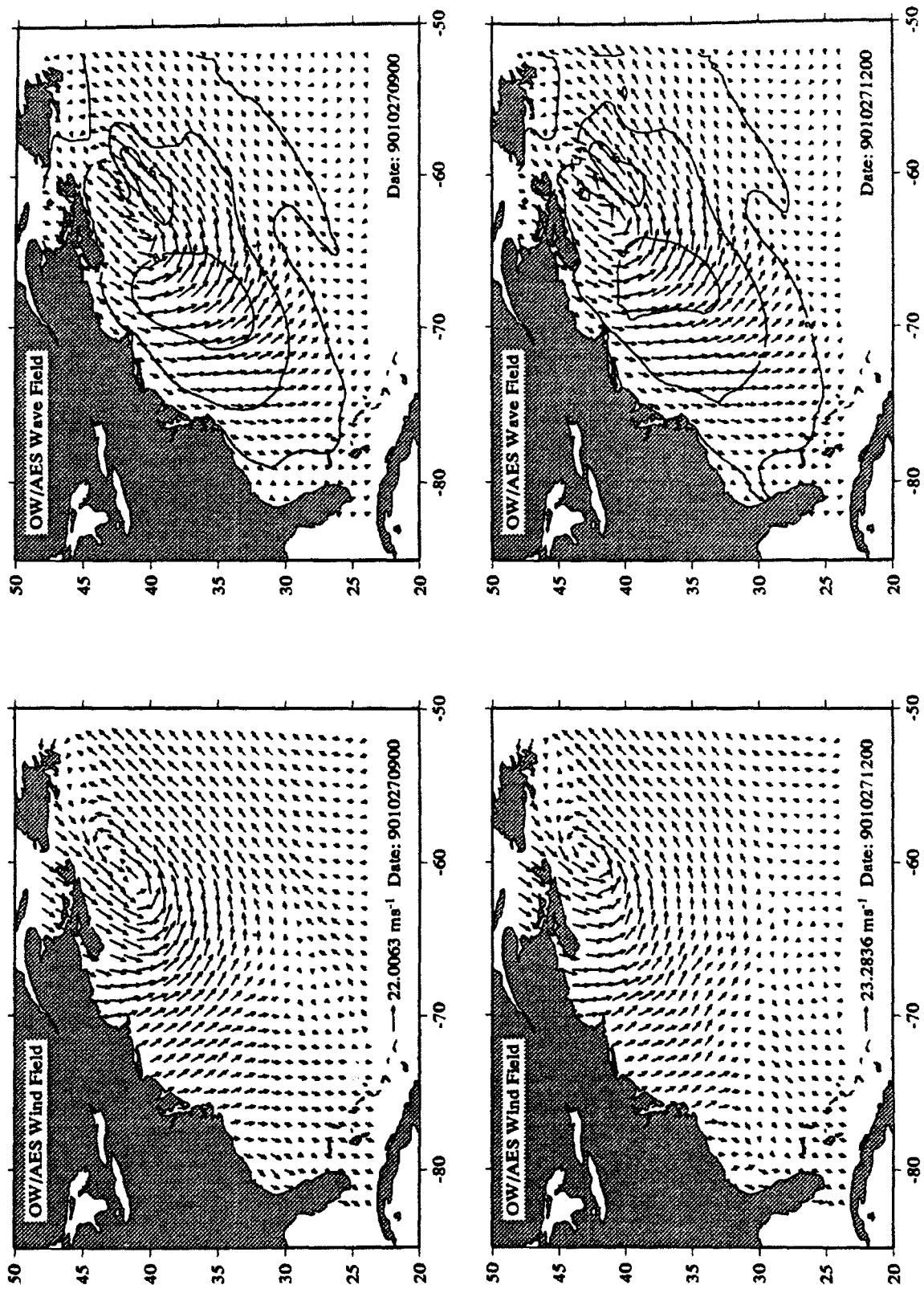


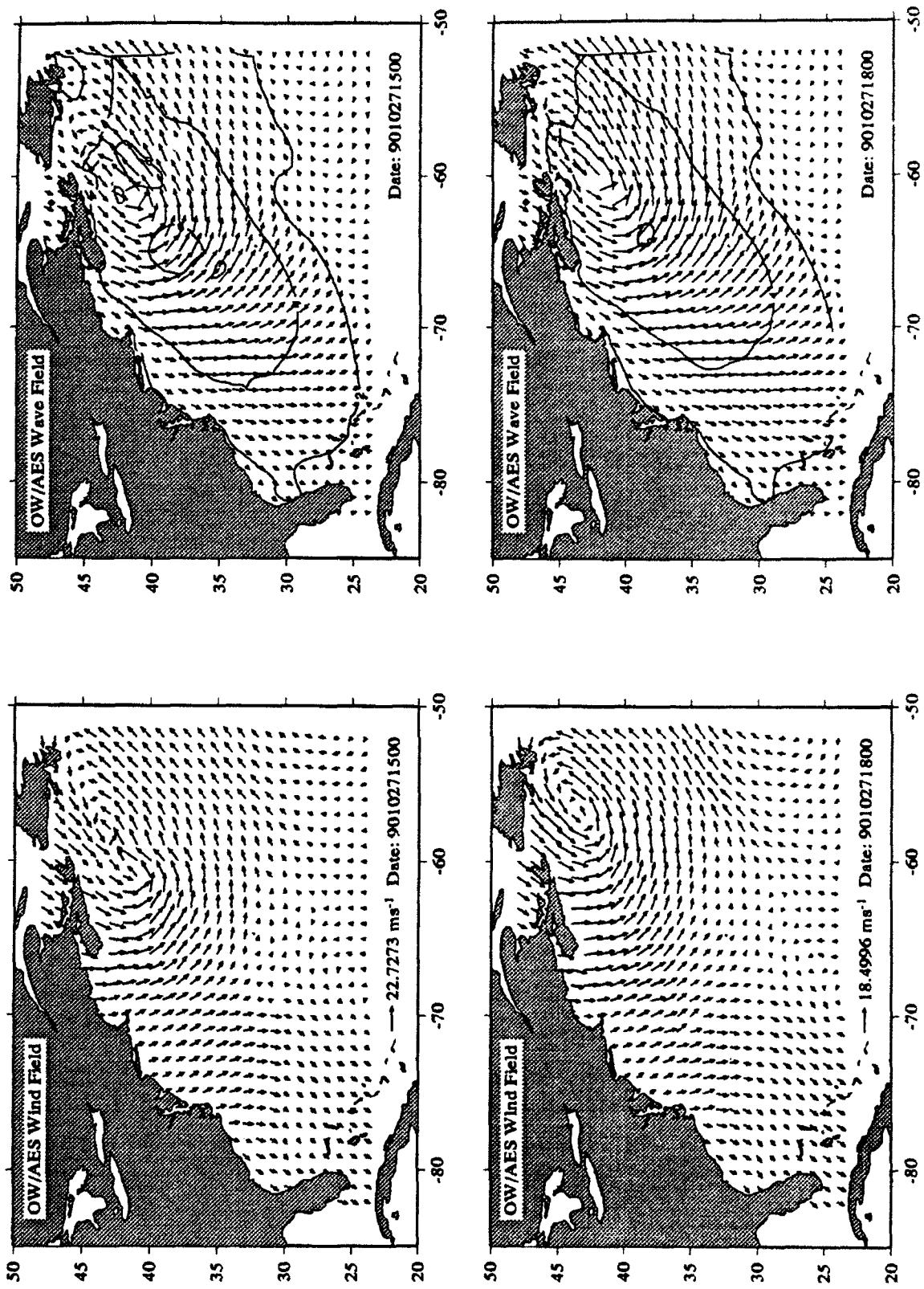


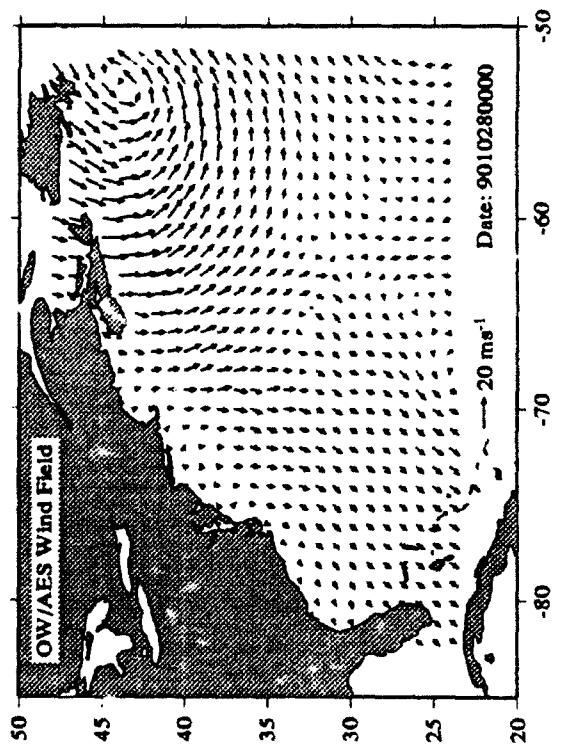
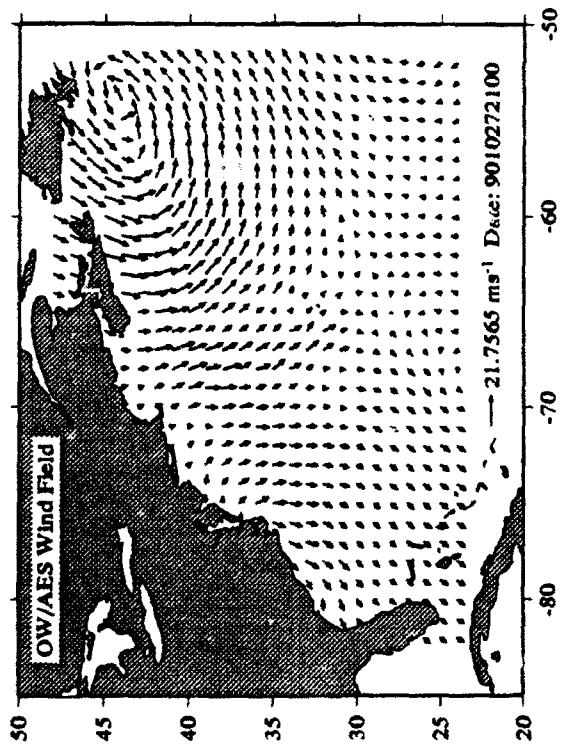
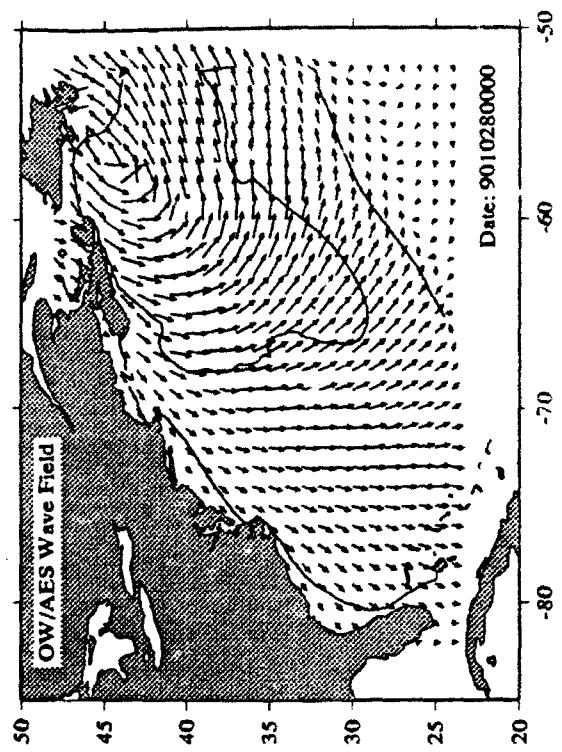
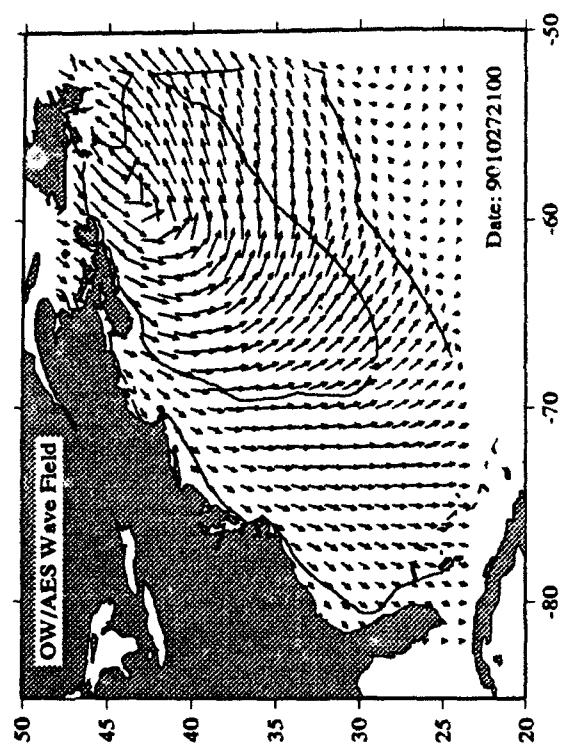


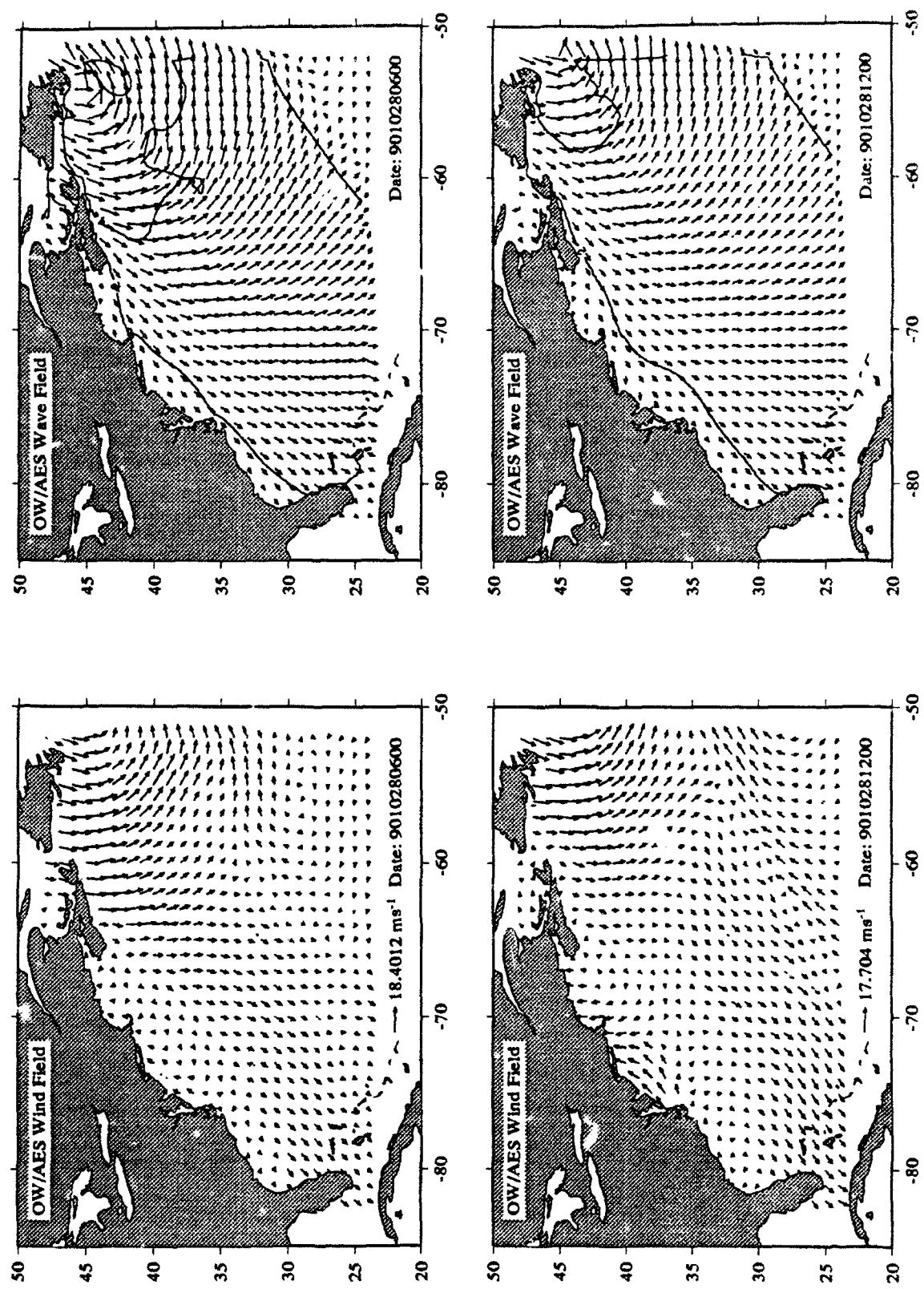


Appendix D Cluster Diagrams of Wind fields and Wave Hindcasts

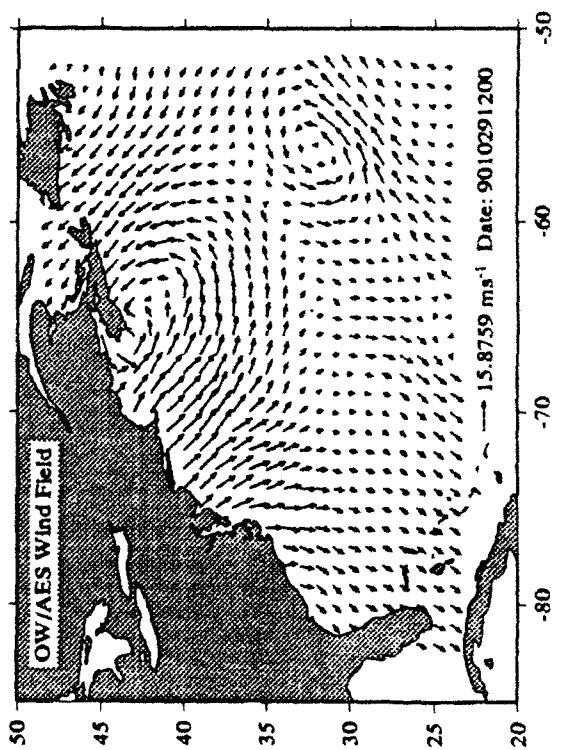
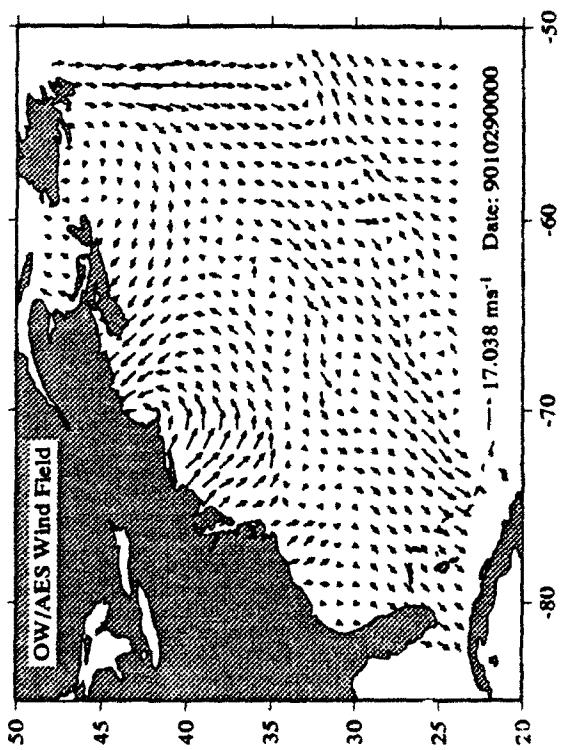
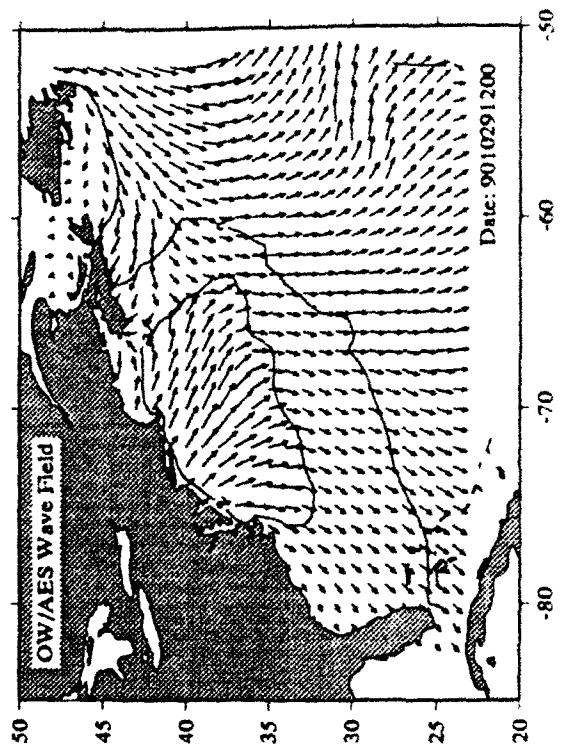
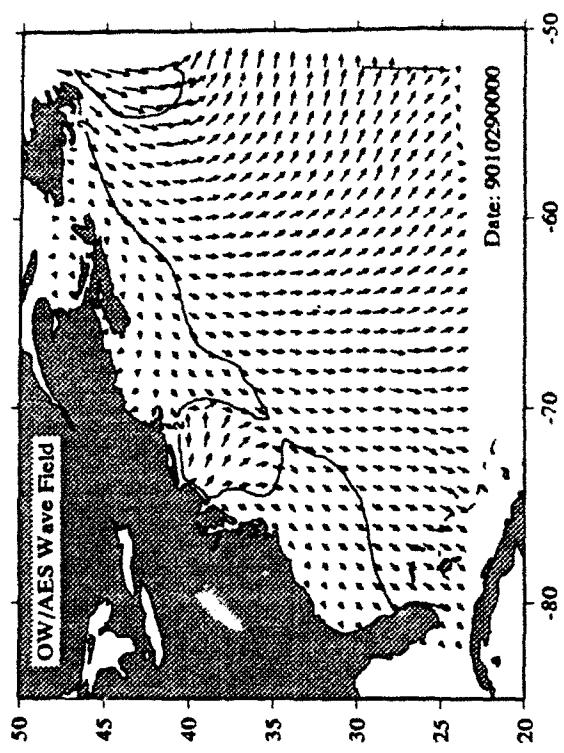


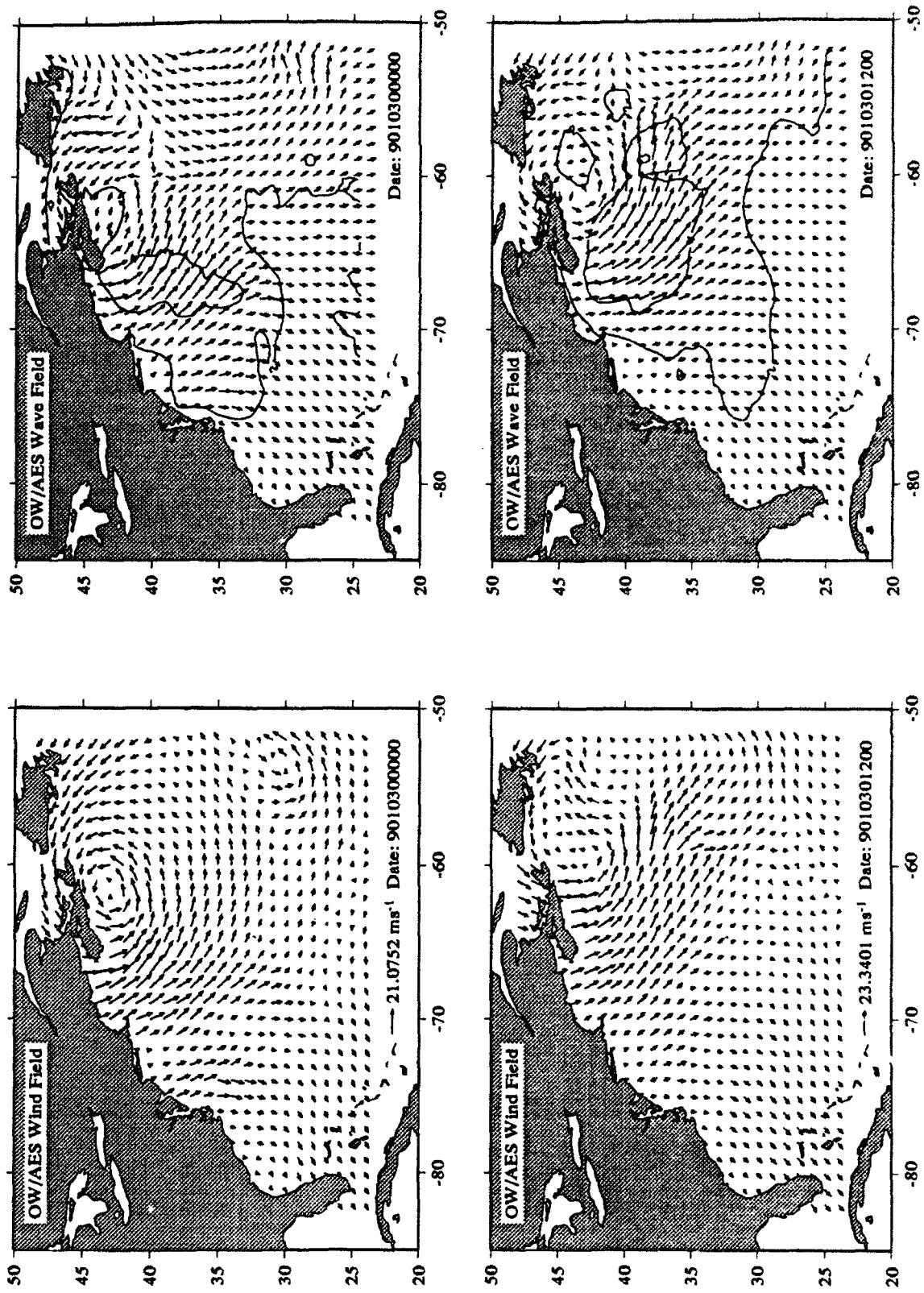


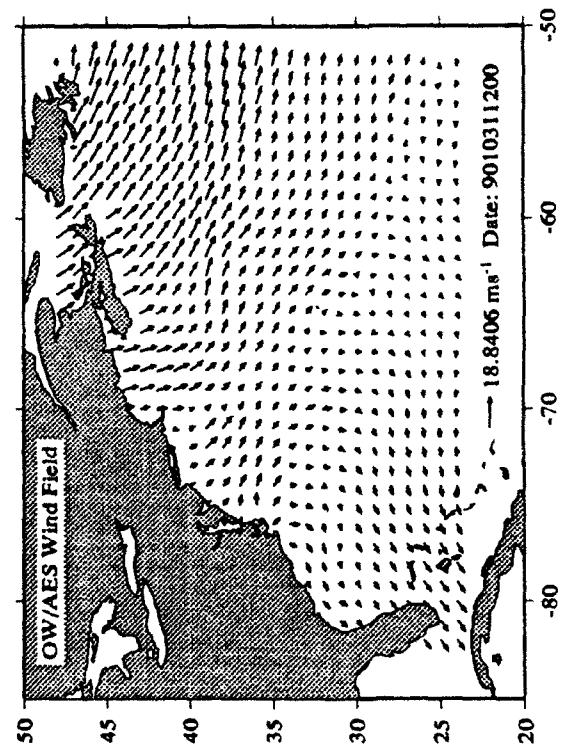
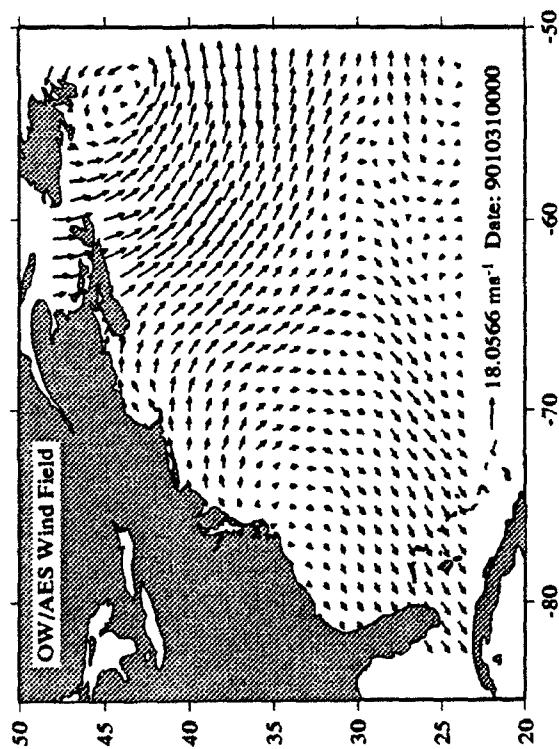
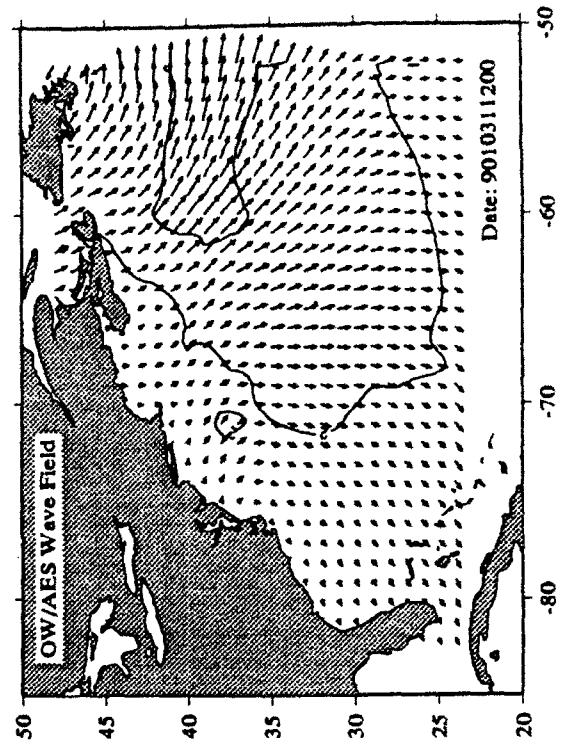
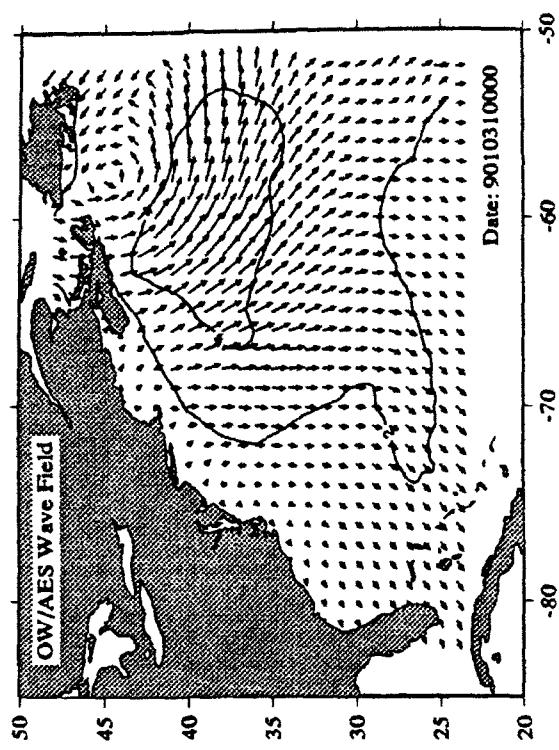




Appendix D Cluster Diagrams of Wind fields and Wave Hindcasts

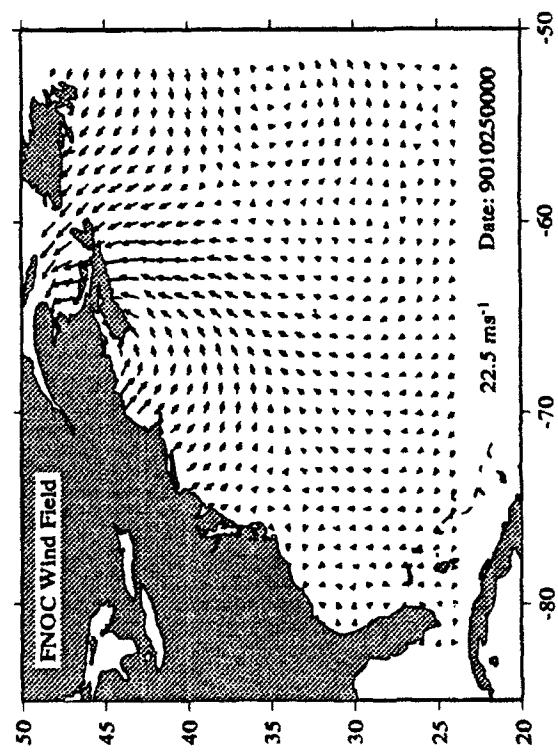
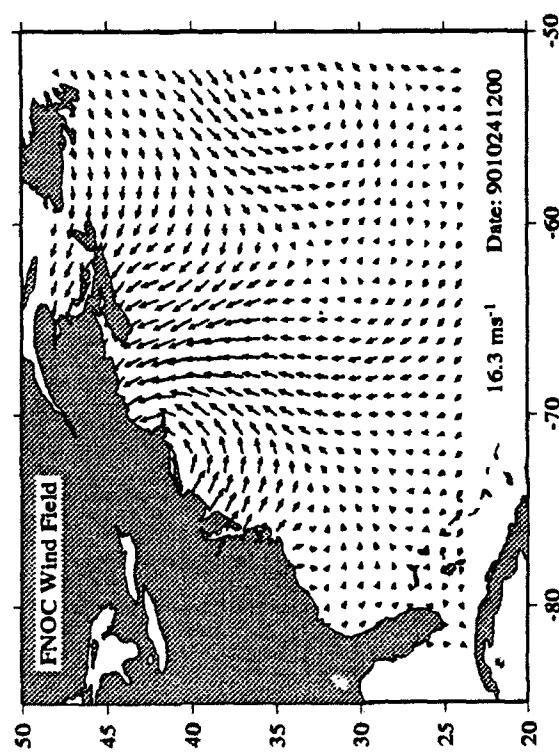
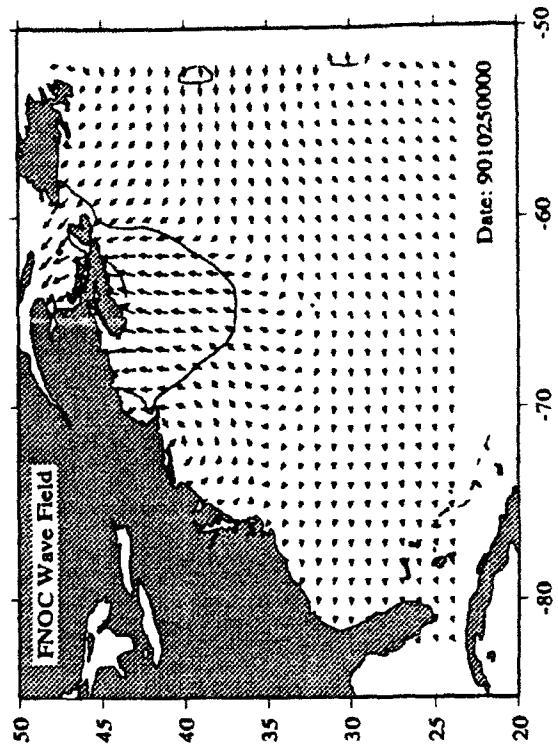
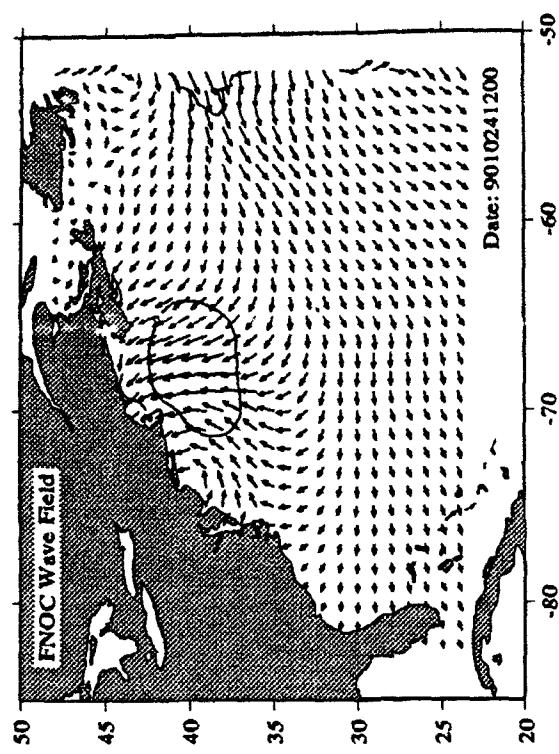


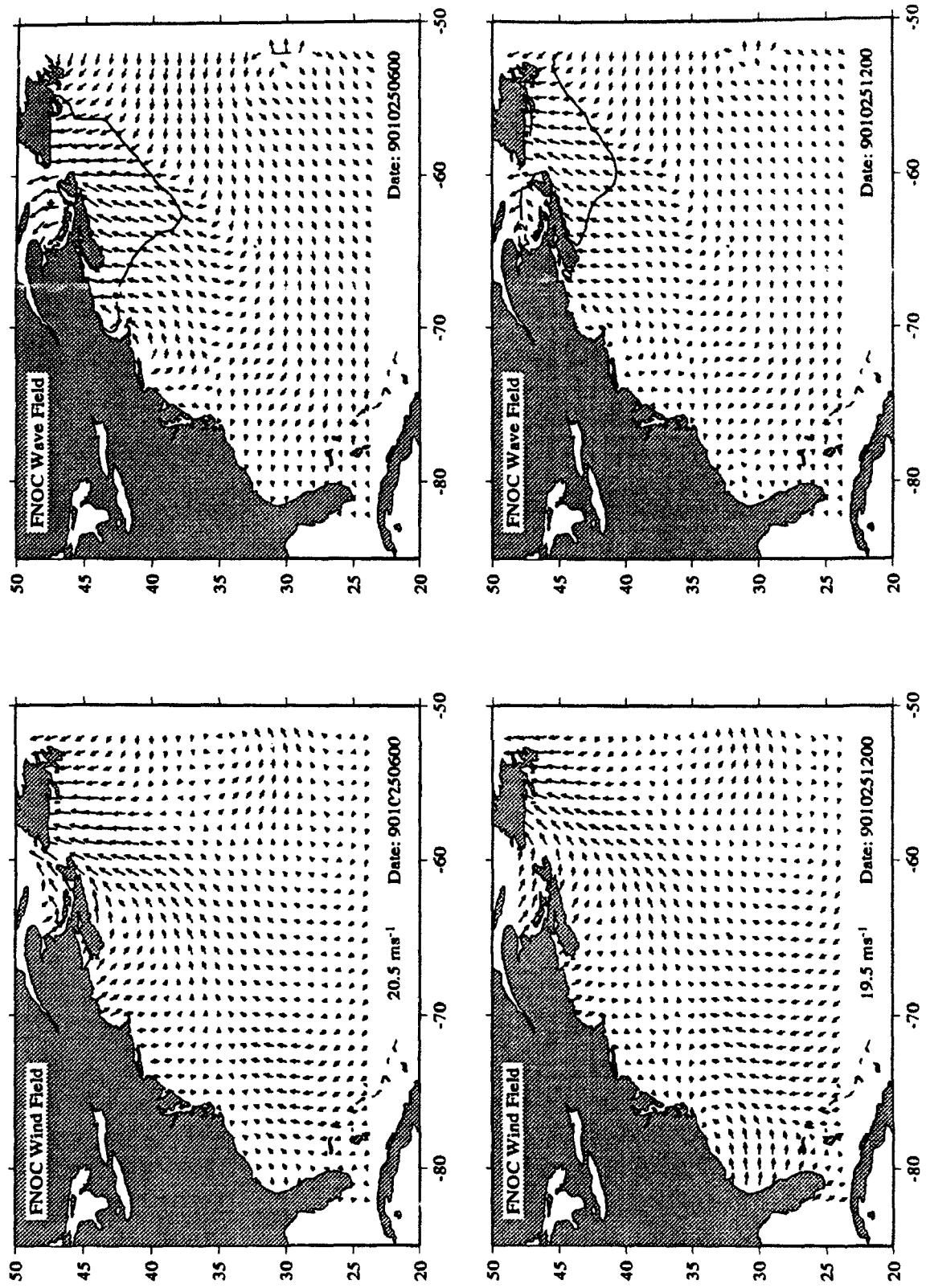


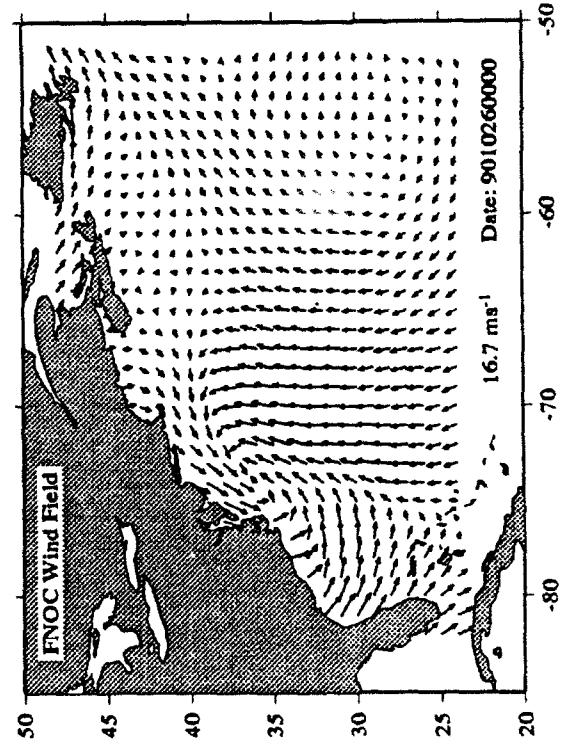
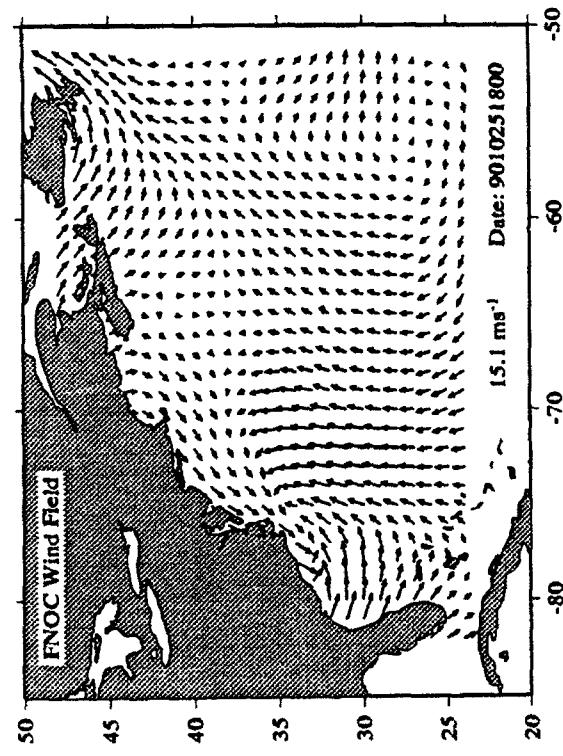
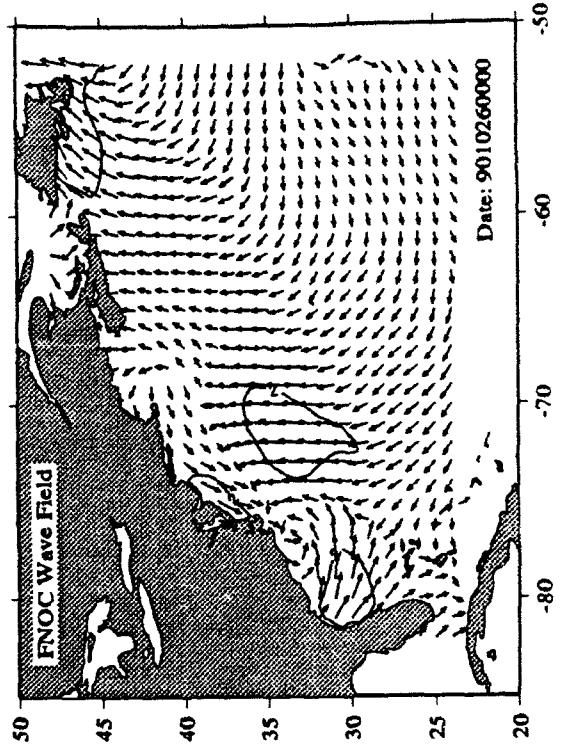
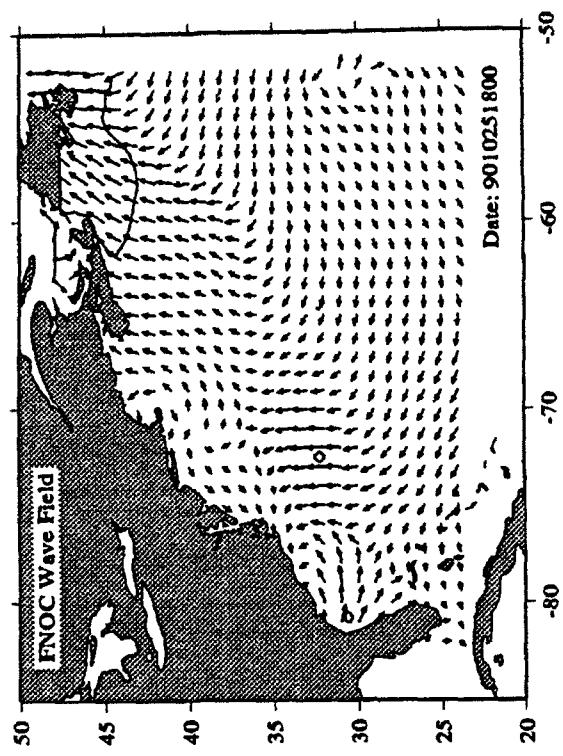


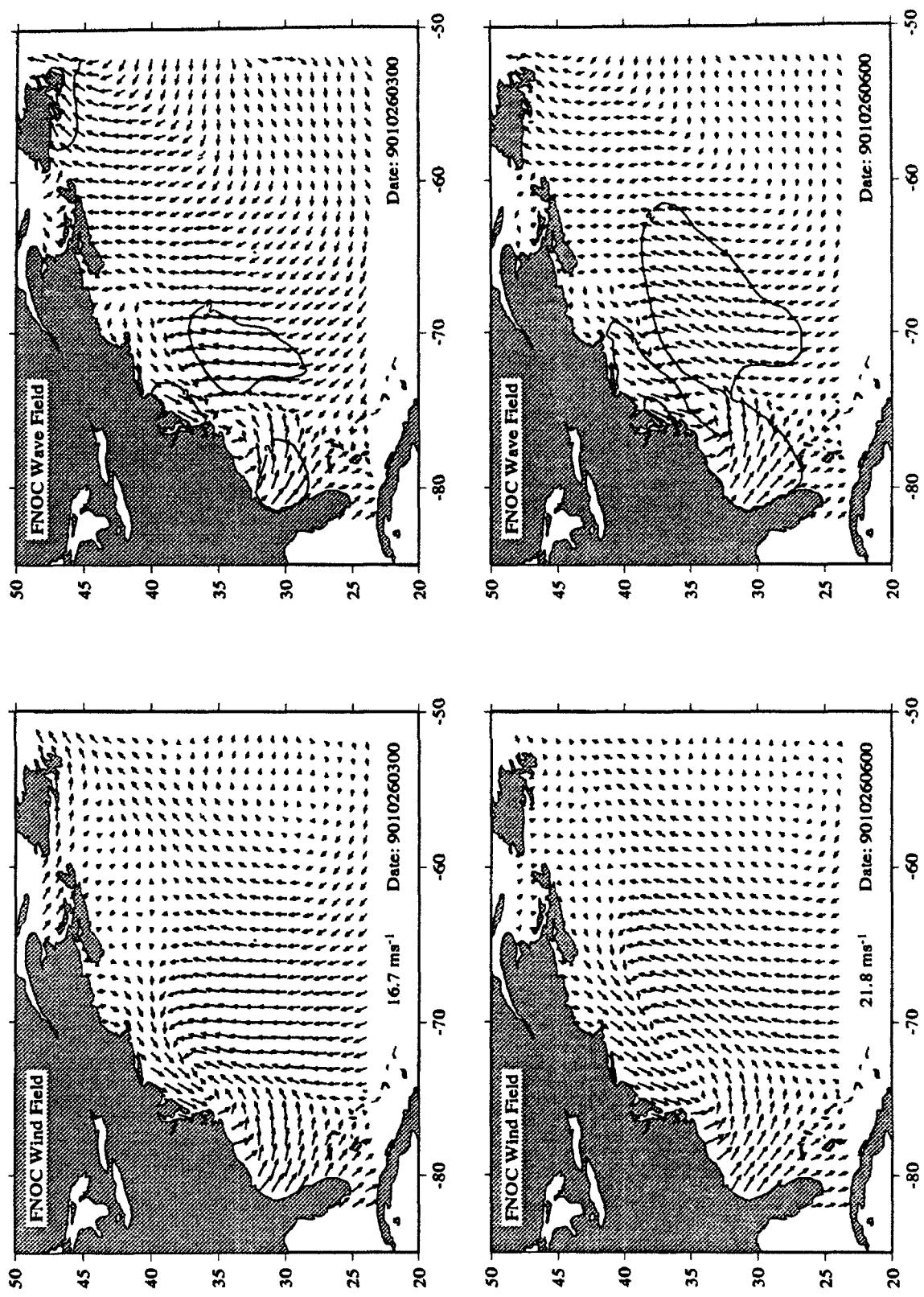
D.2: Fleet Numerical Oceanography Center (FNOC)

Custer diagrams are presented for the time period from 24 October 1990, 12:00 GMT to 28 October 1990, 12:00 GMT of the wind field and corresponding wave hindcasts. Note that the frequency of maps is every 3 hr from 26-28 October, which covers the major storm period.

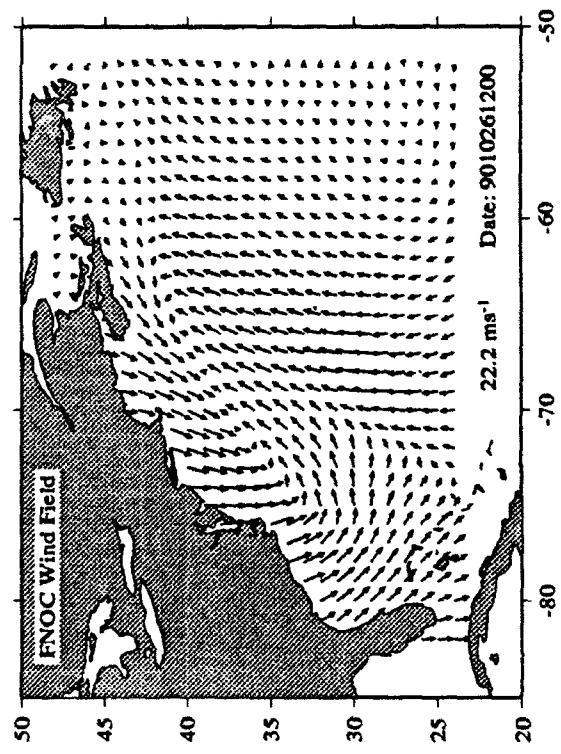
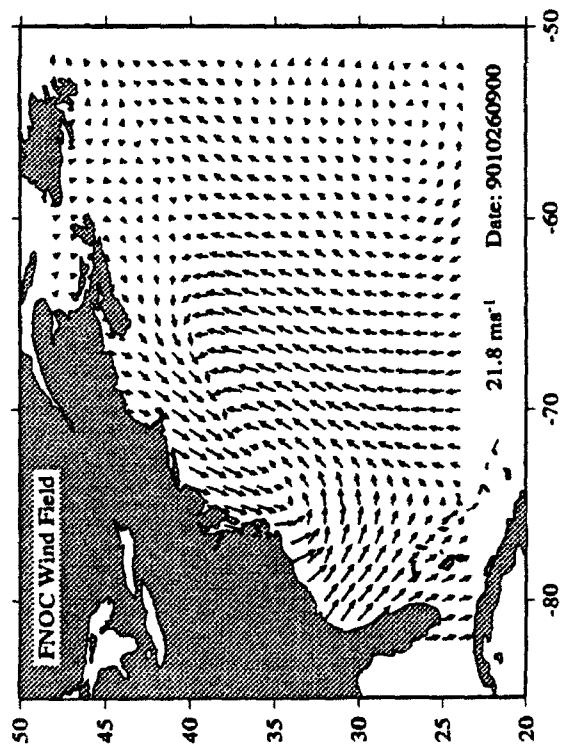
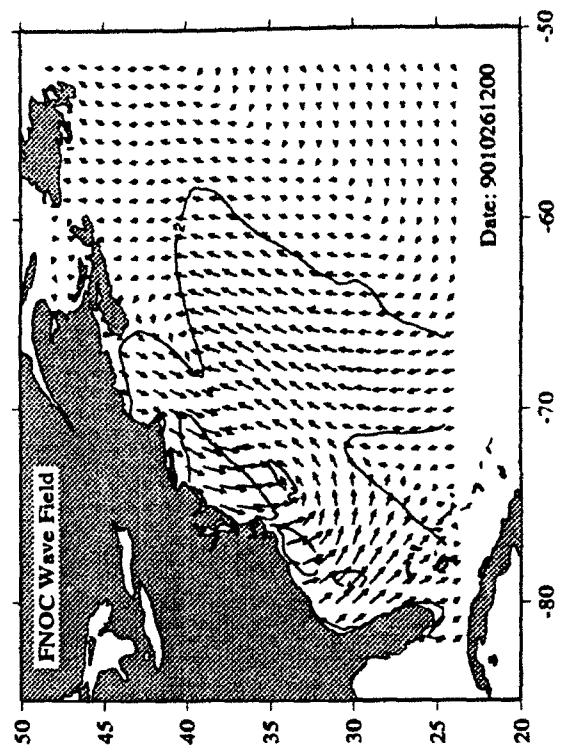
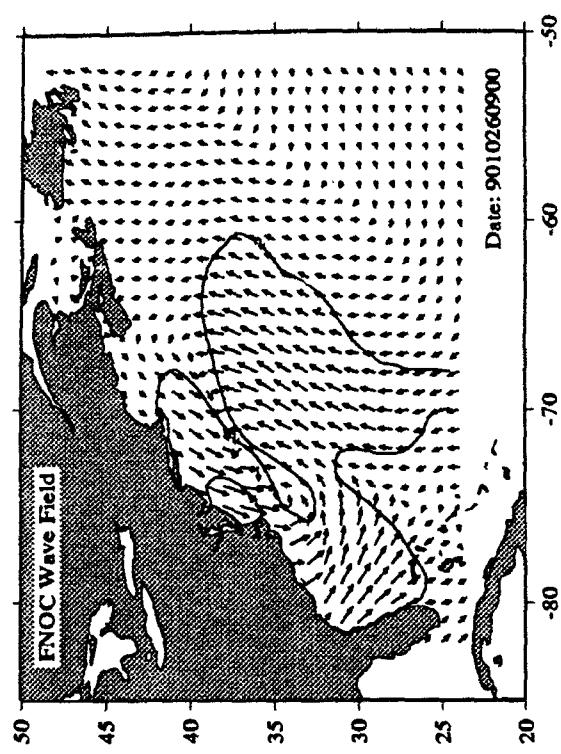


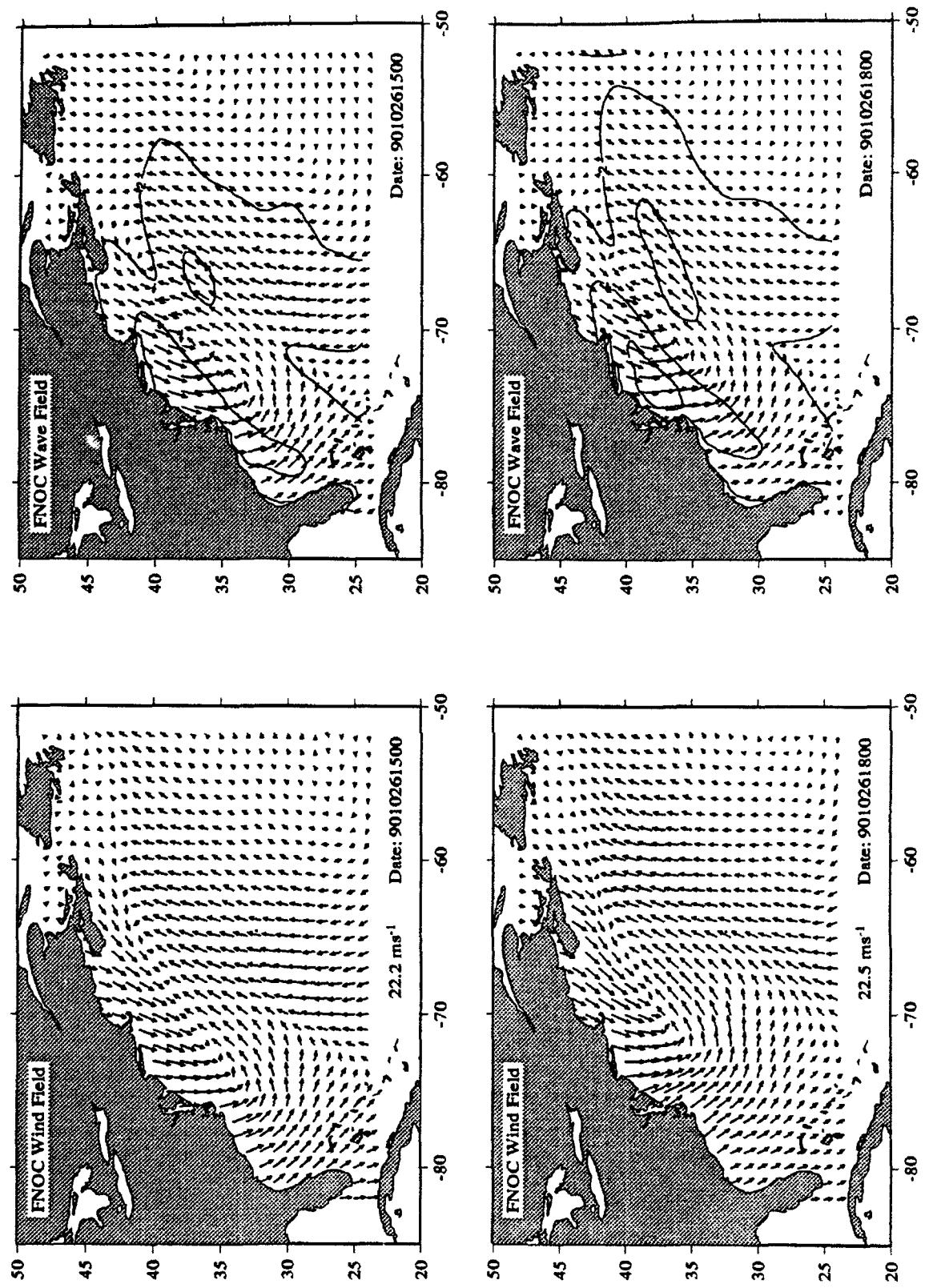




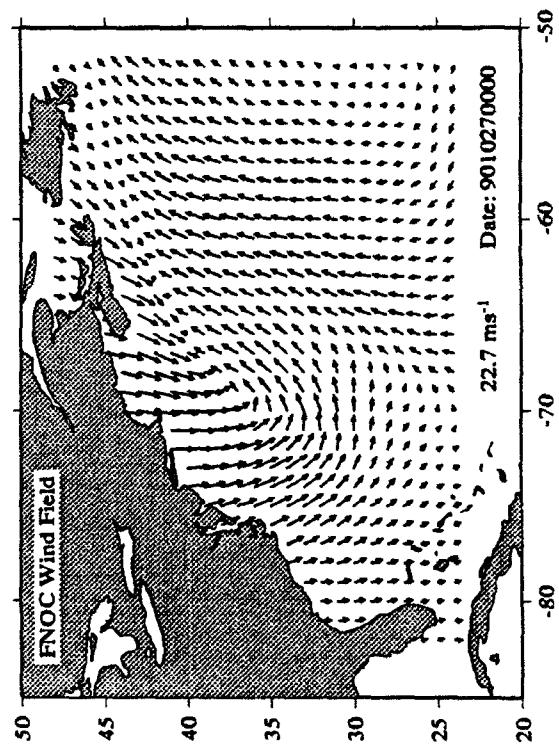
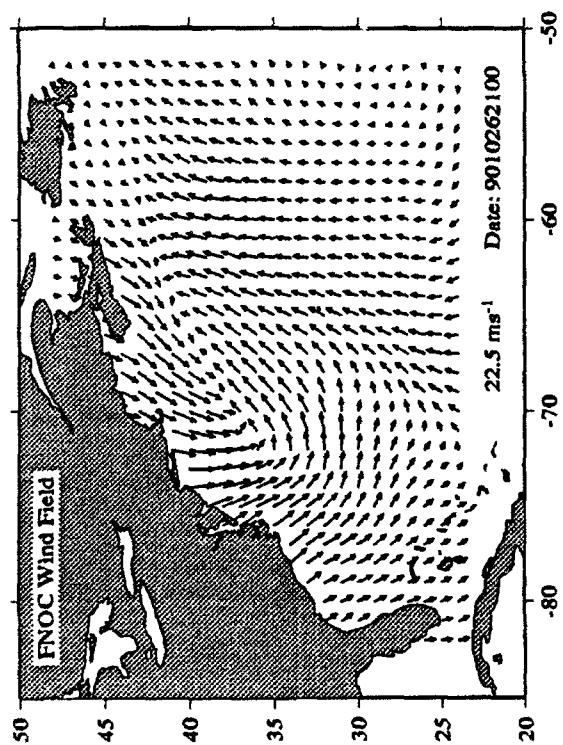
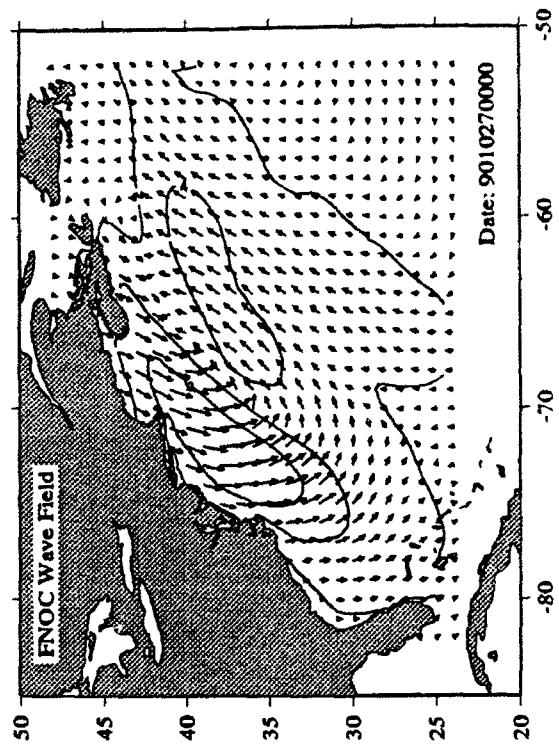
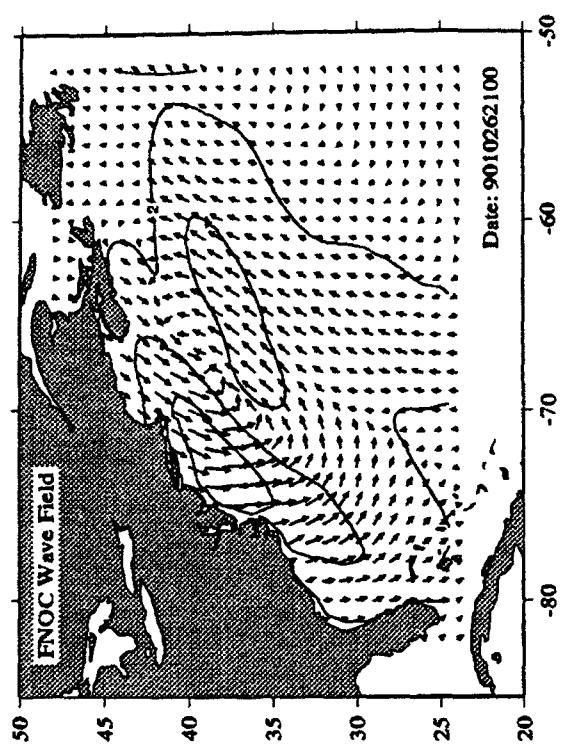


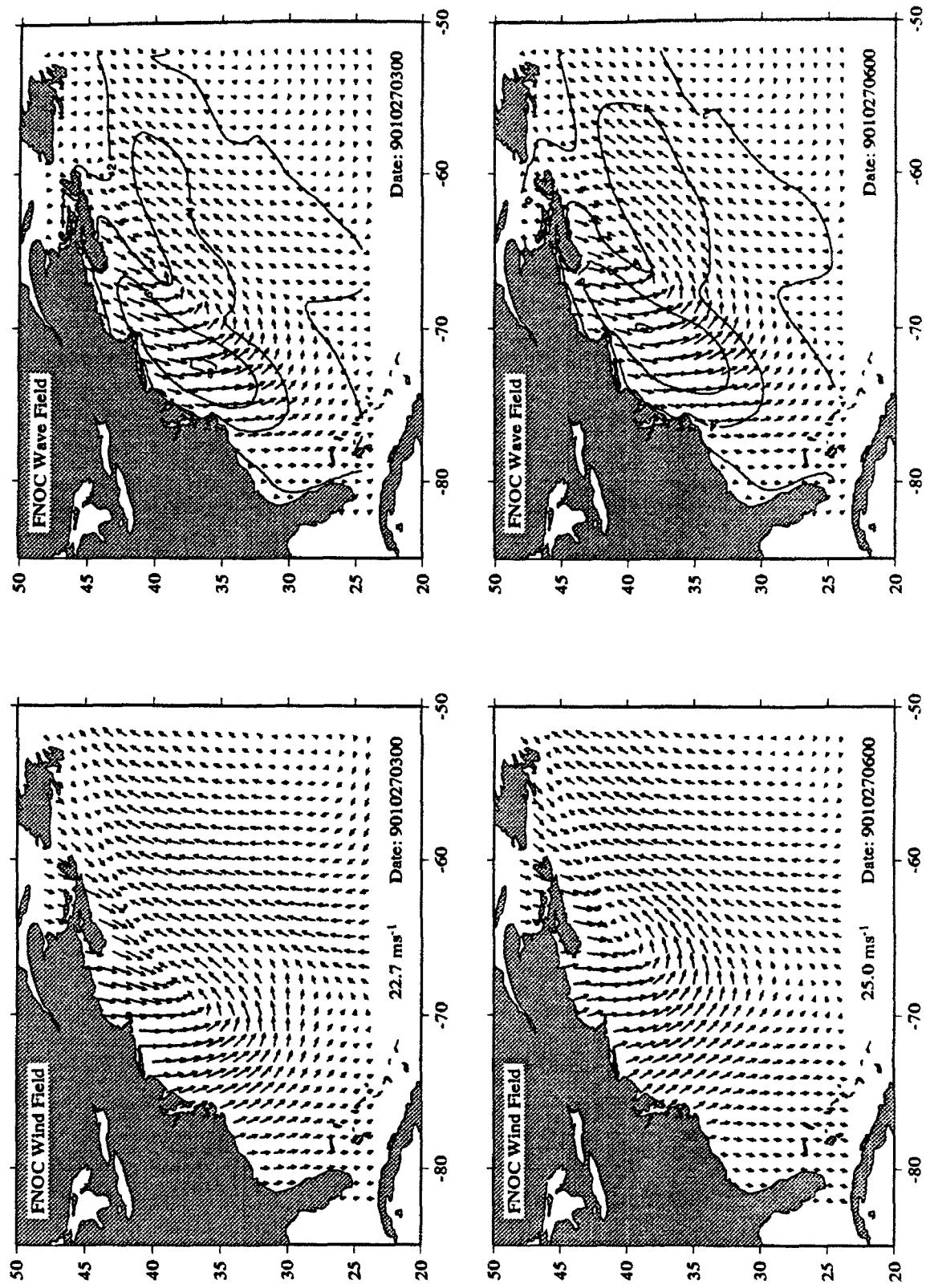
Appendix D Custer Diagrams of Wind fields and Wave Hindcasts

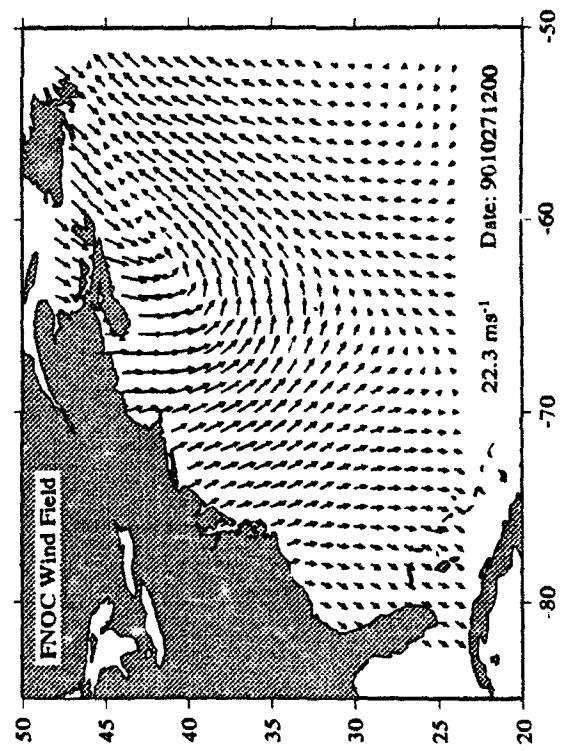
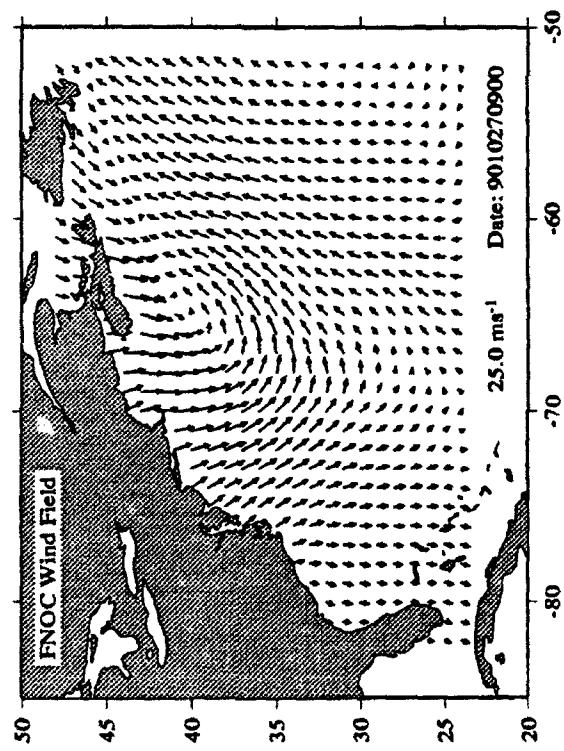
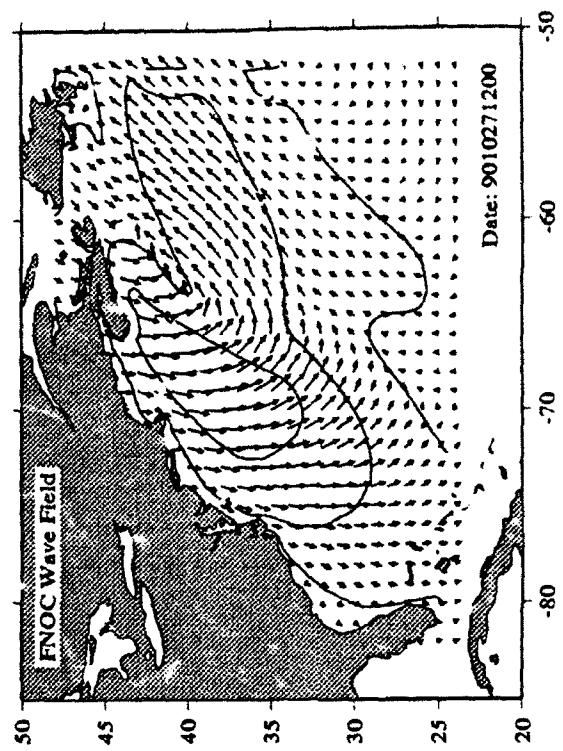
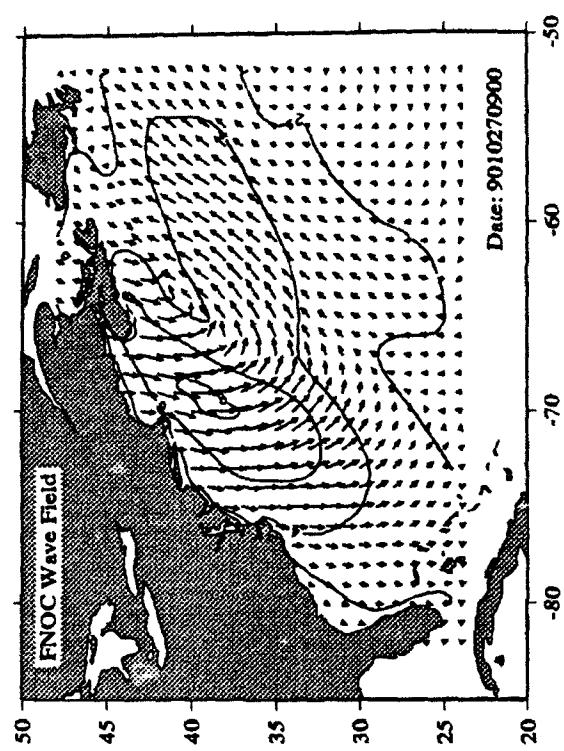


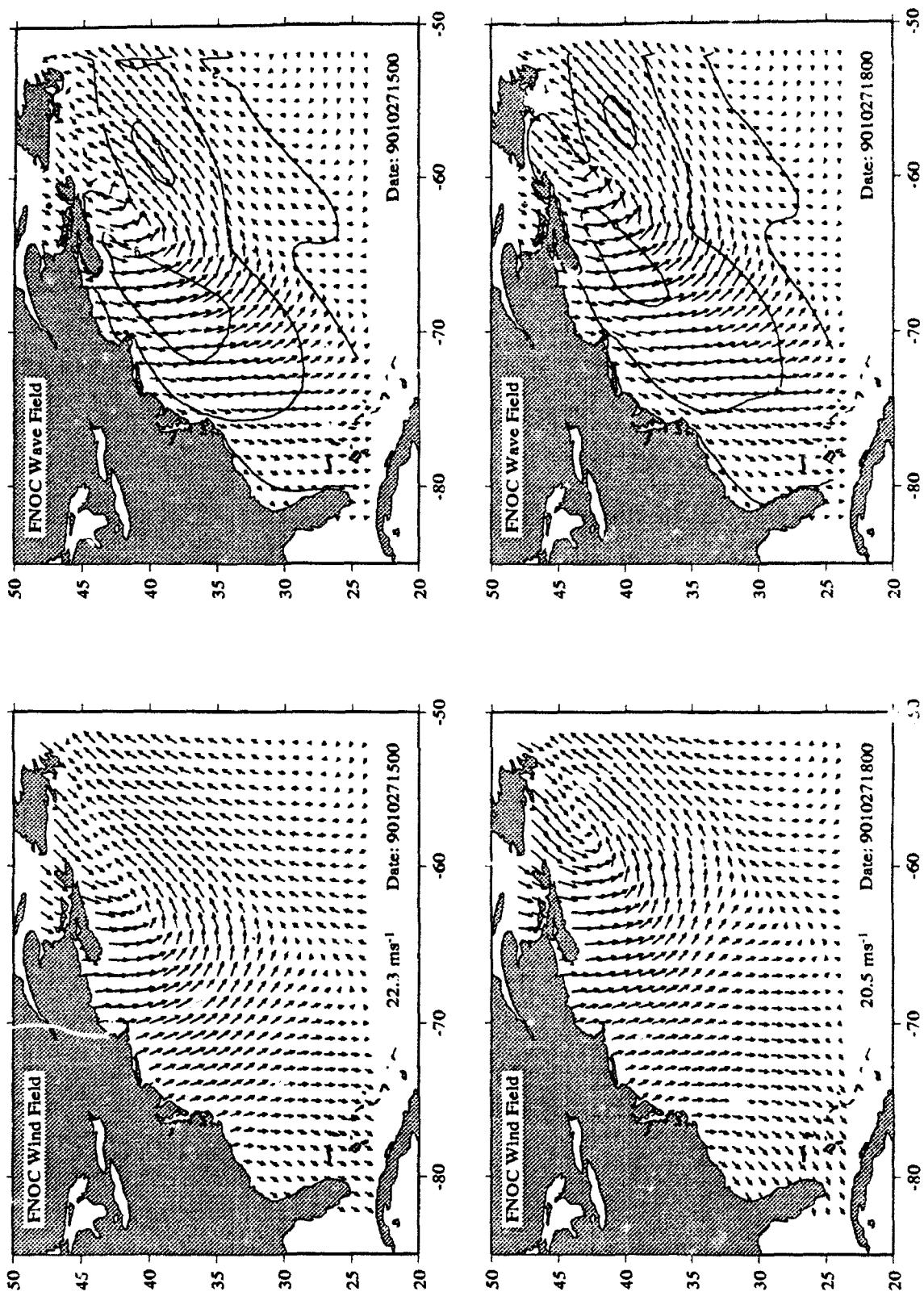


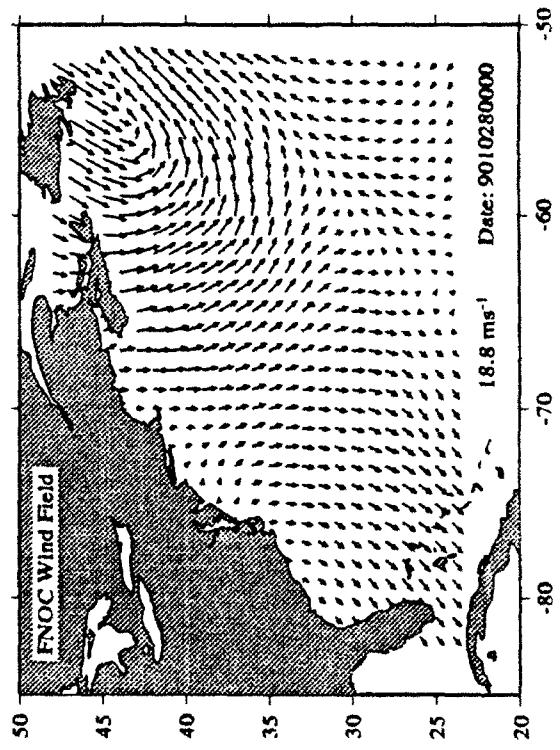
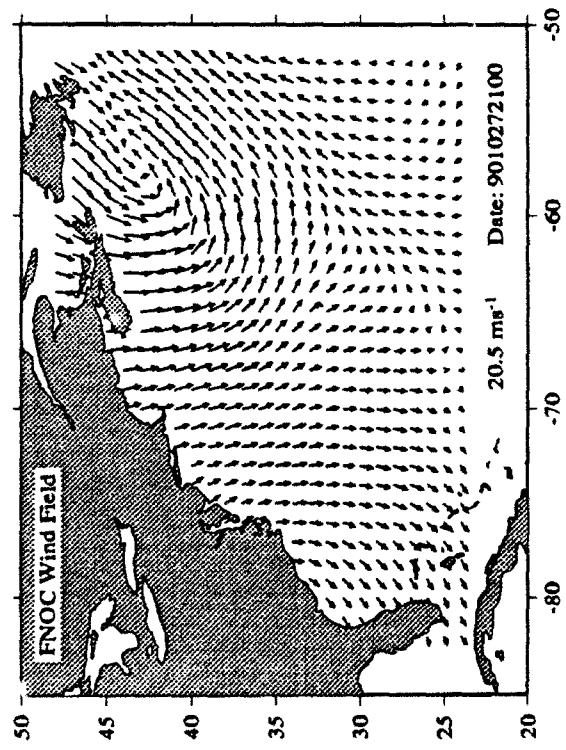
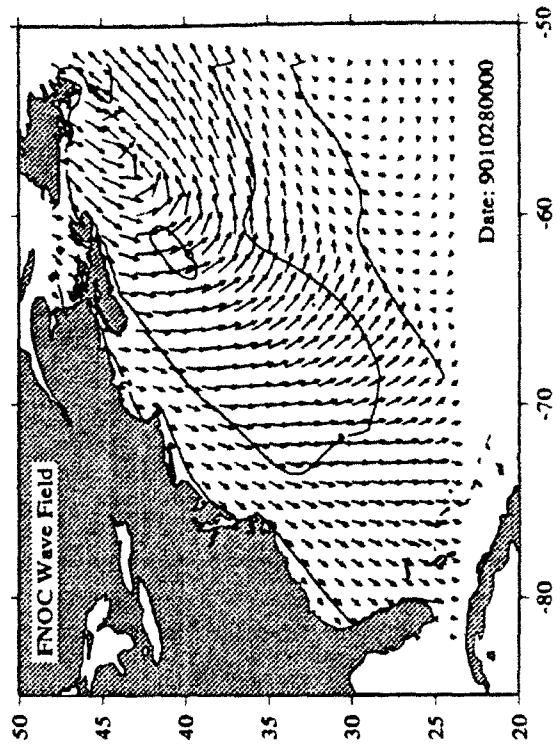
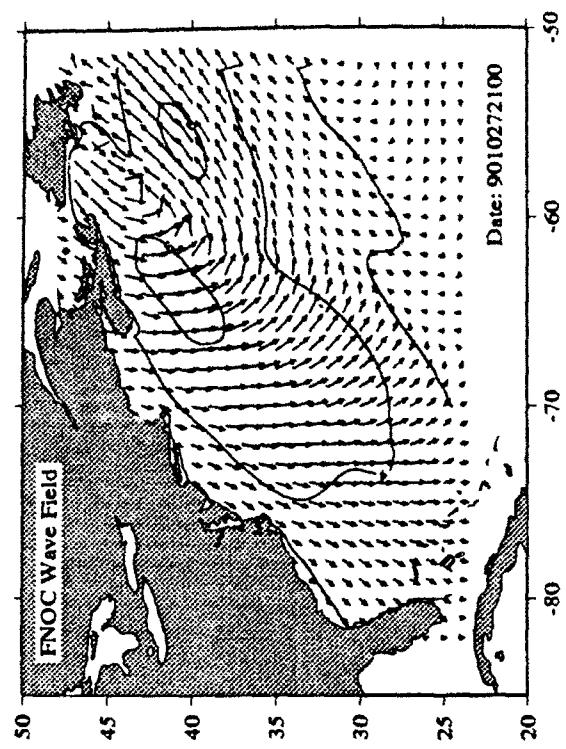
Appendix D Custer Diagrams of Wind fields and Wave Hindcasts

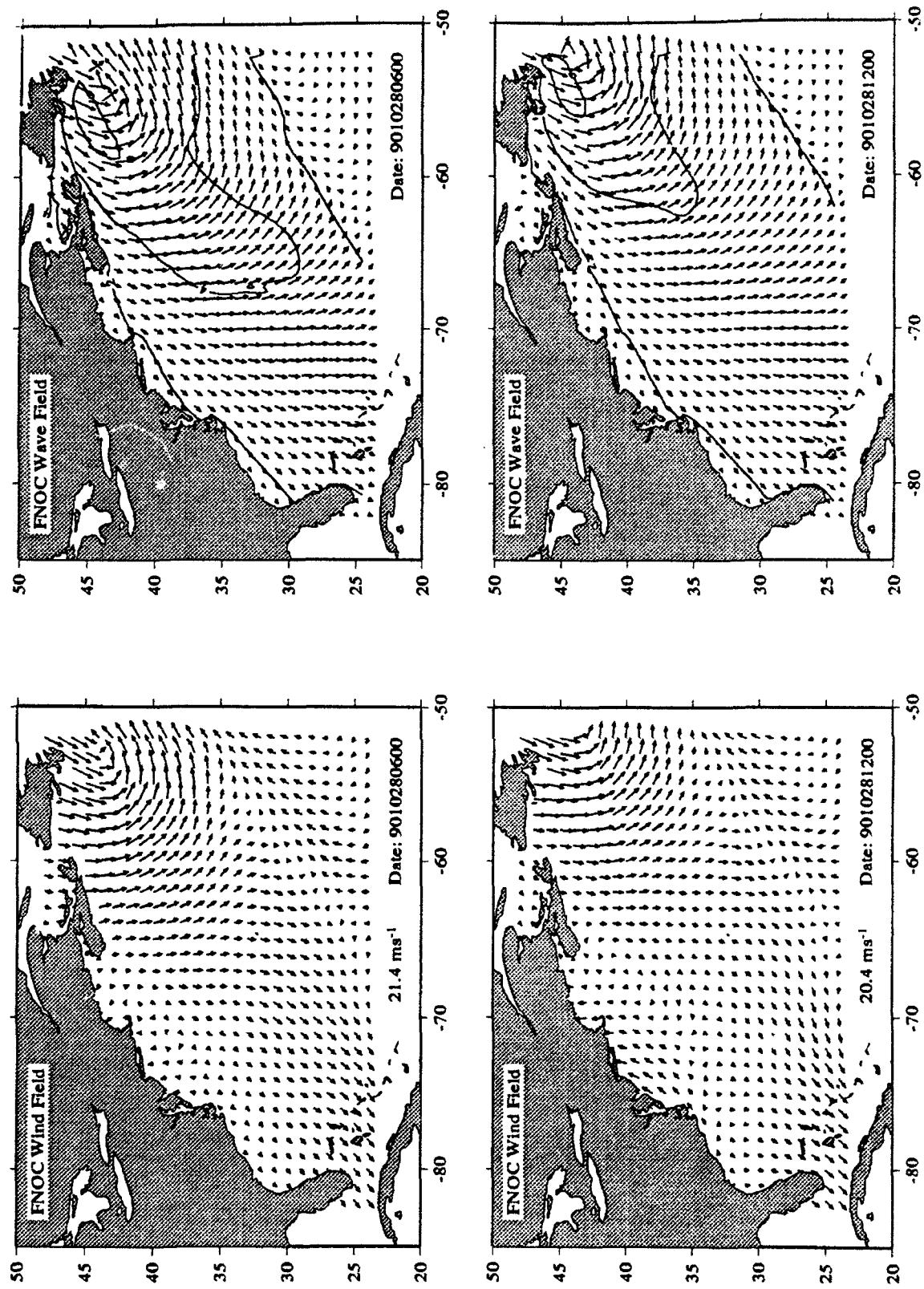








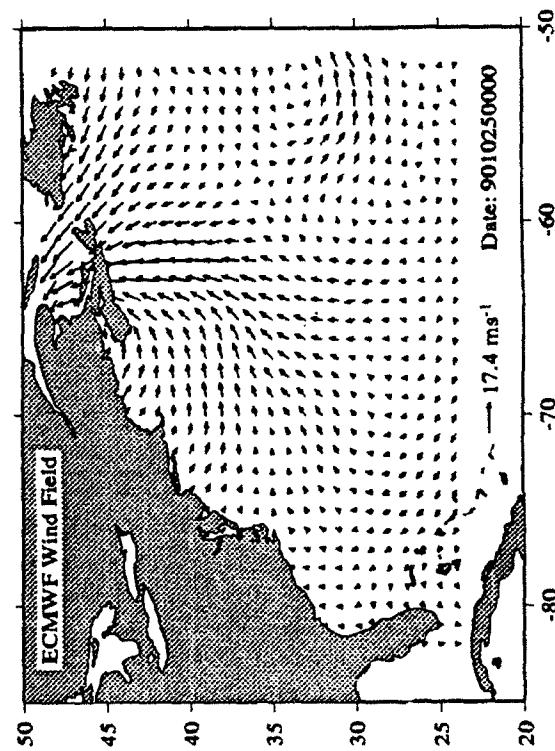
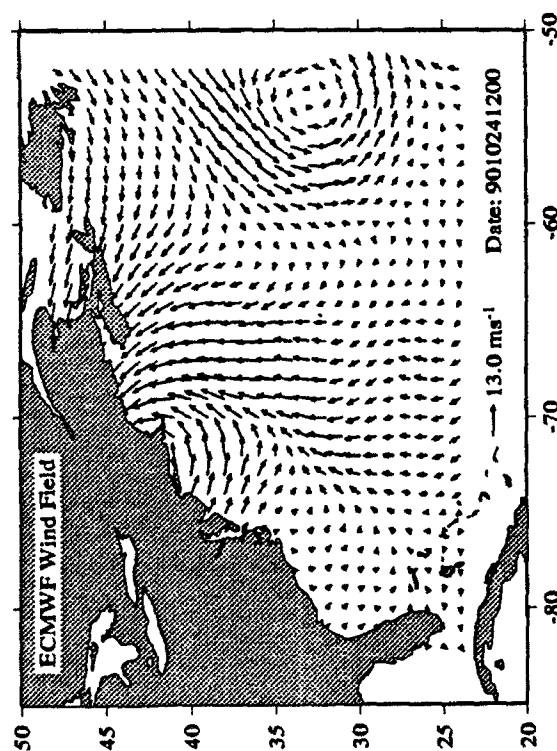
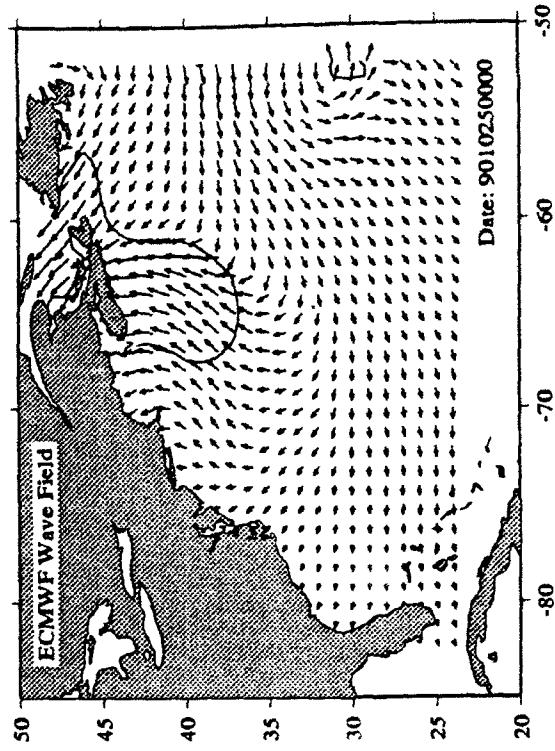
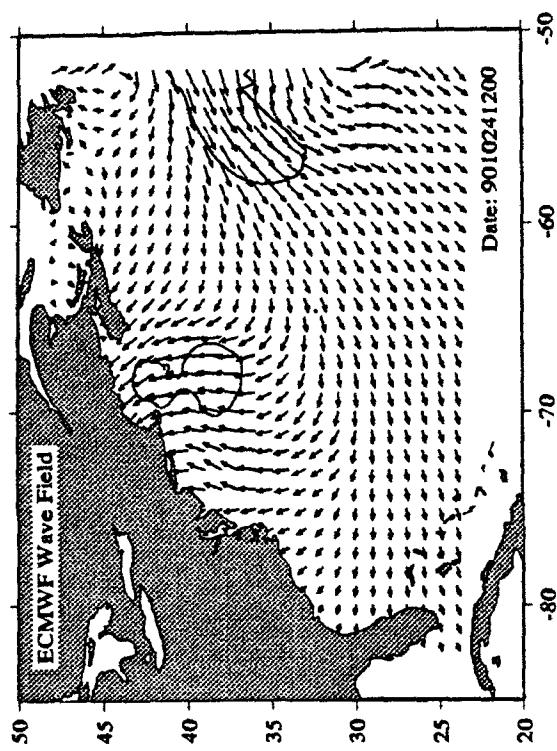


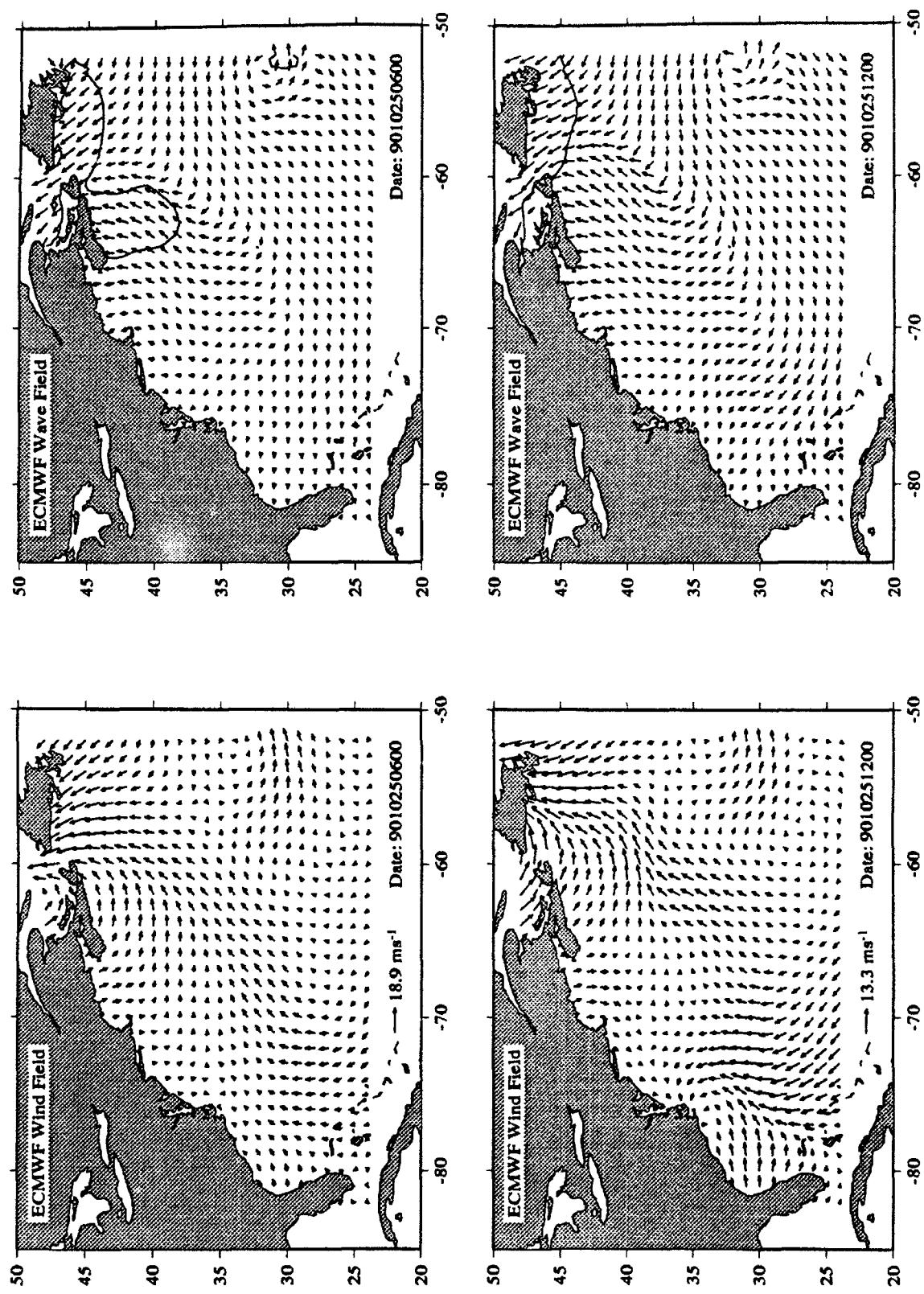


Appendix D Cluster Diagrams of Wind fields and Wave Hindcasts

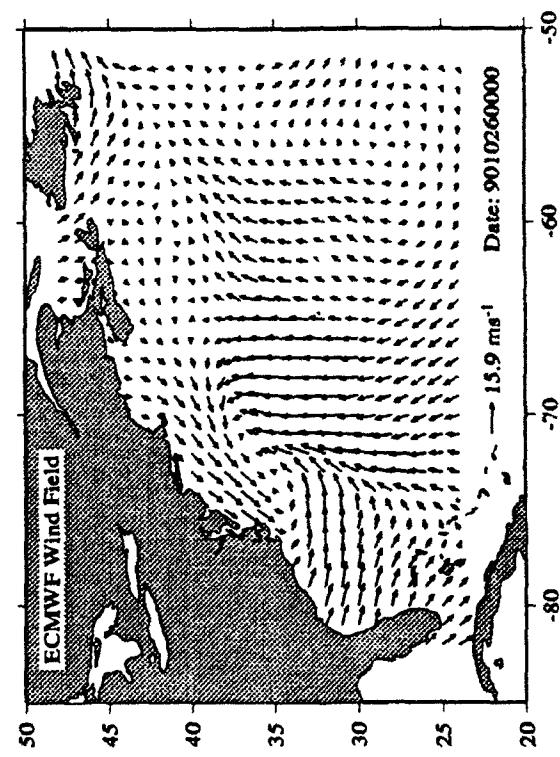
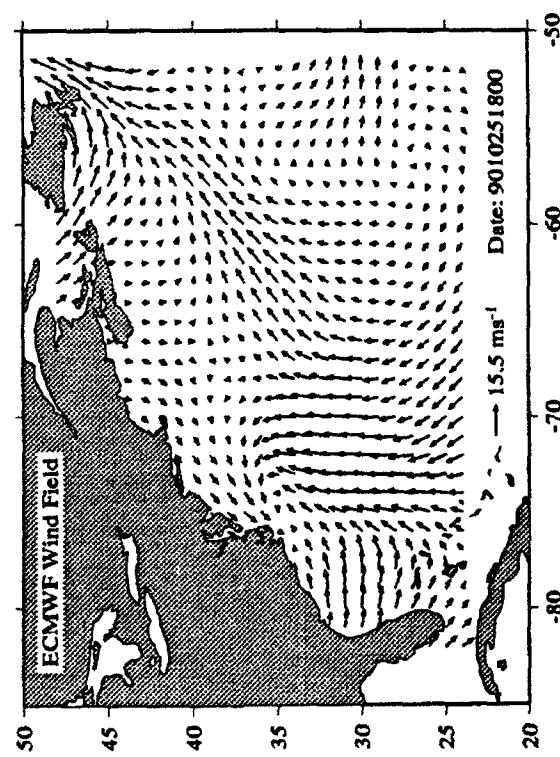
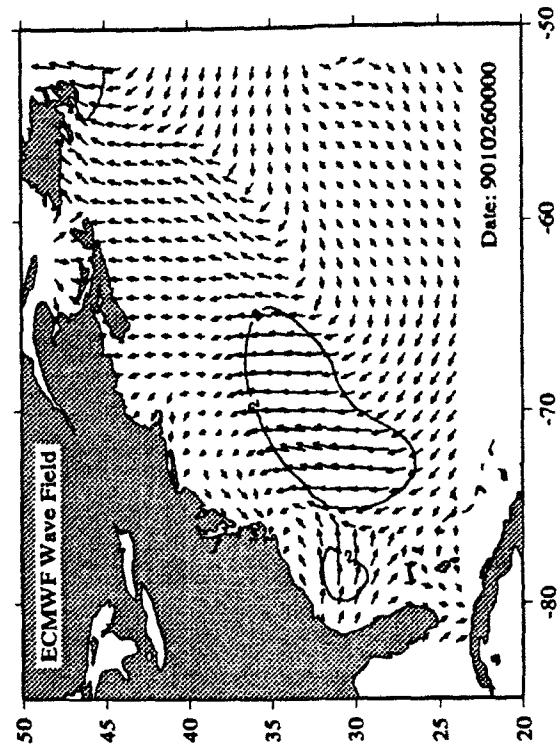
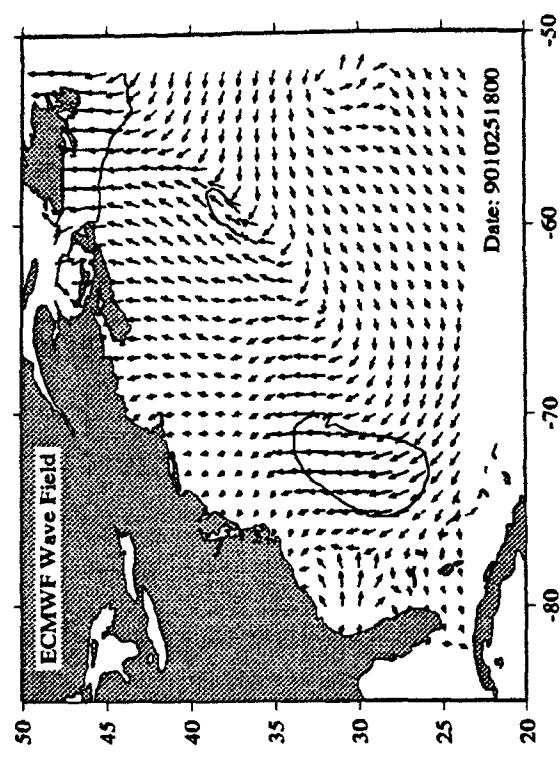
D.3: European Centre for Medium-Range Weather Forecasts (ECMWF)

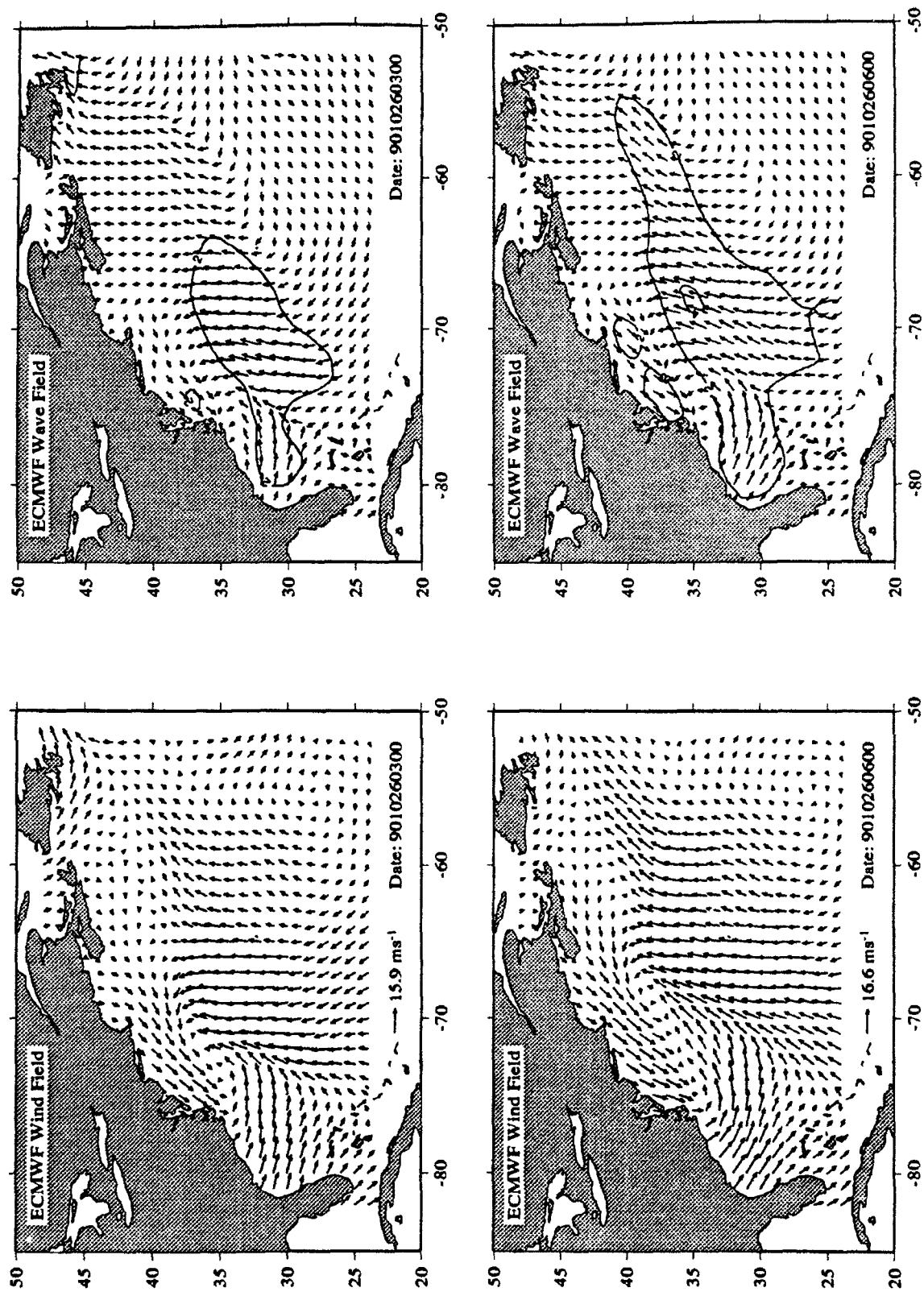
Custer diagrams are presented for the time period from 24 October 1990, 12:00 GMT to 28 October 1990, 12:00 GMT of the wind field and corresponding wave hindcasts. Note that the frequency of maps is every 3 hr from 26-28 October, which covers the major storm period.

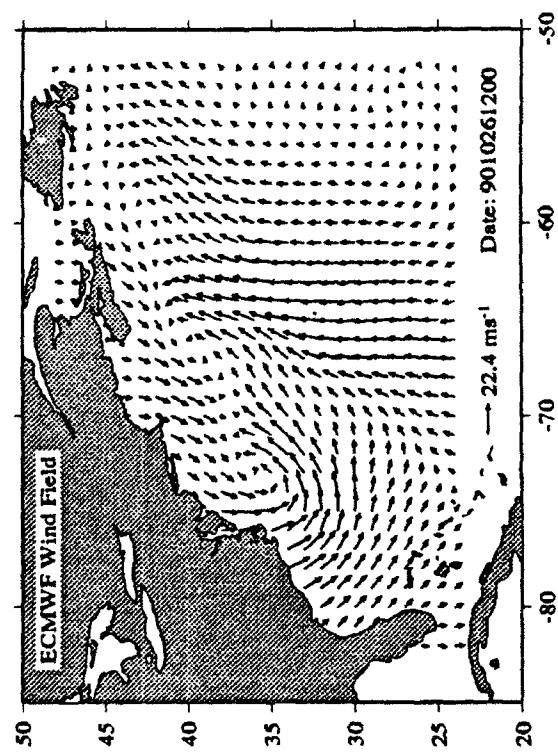
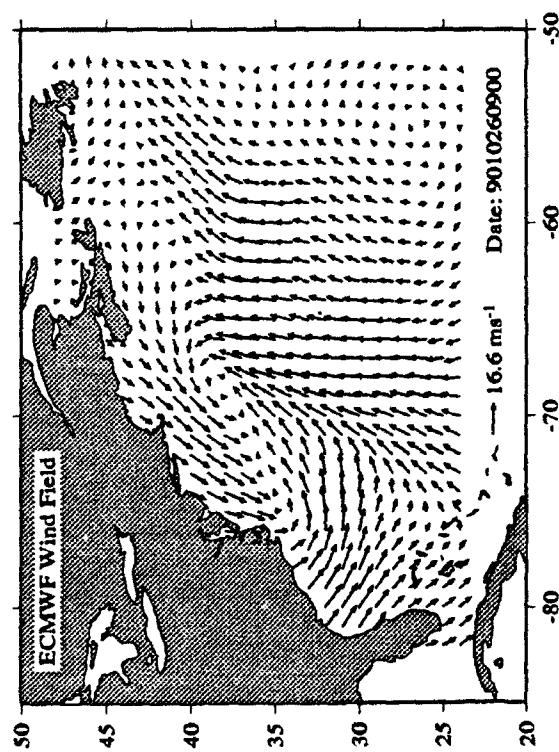
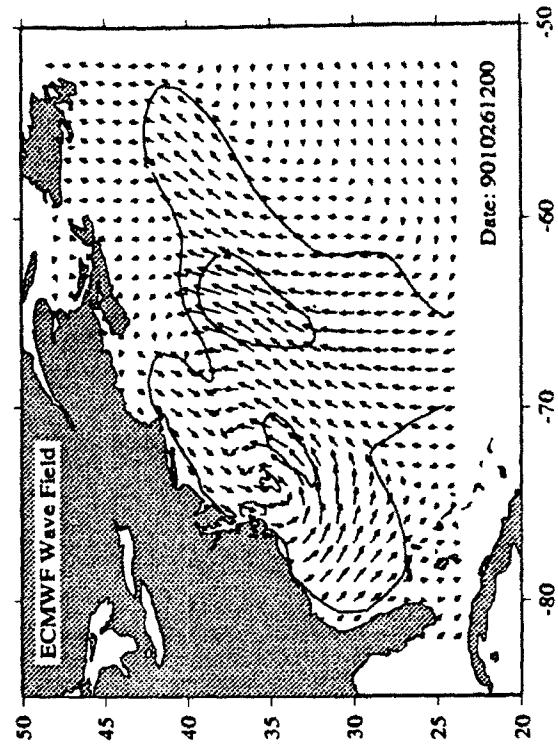
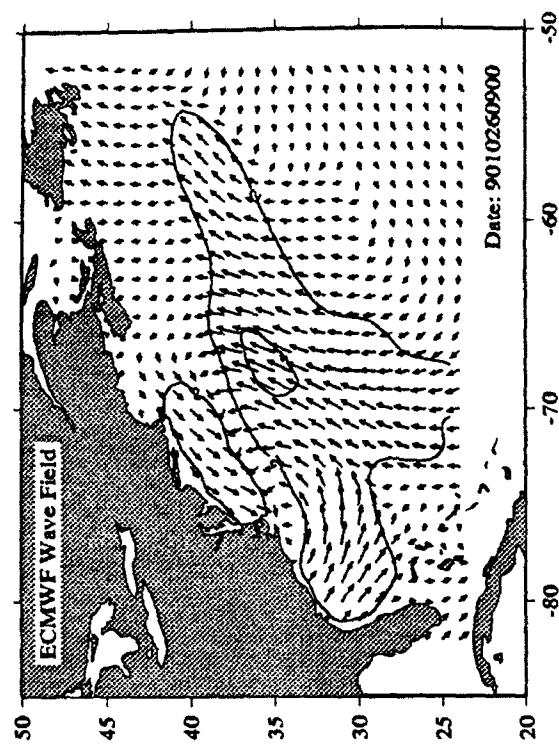


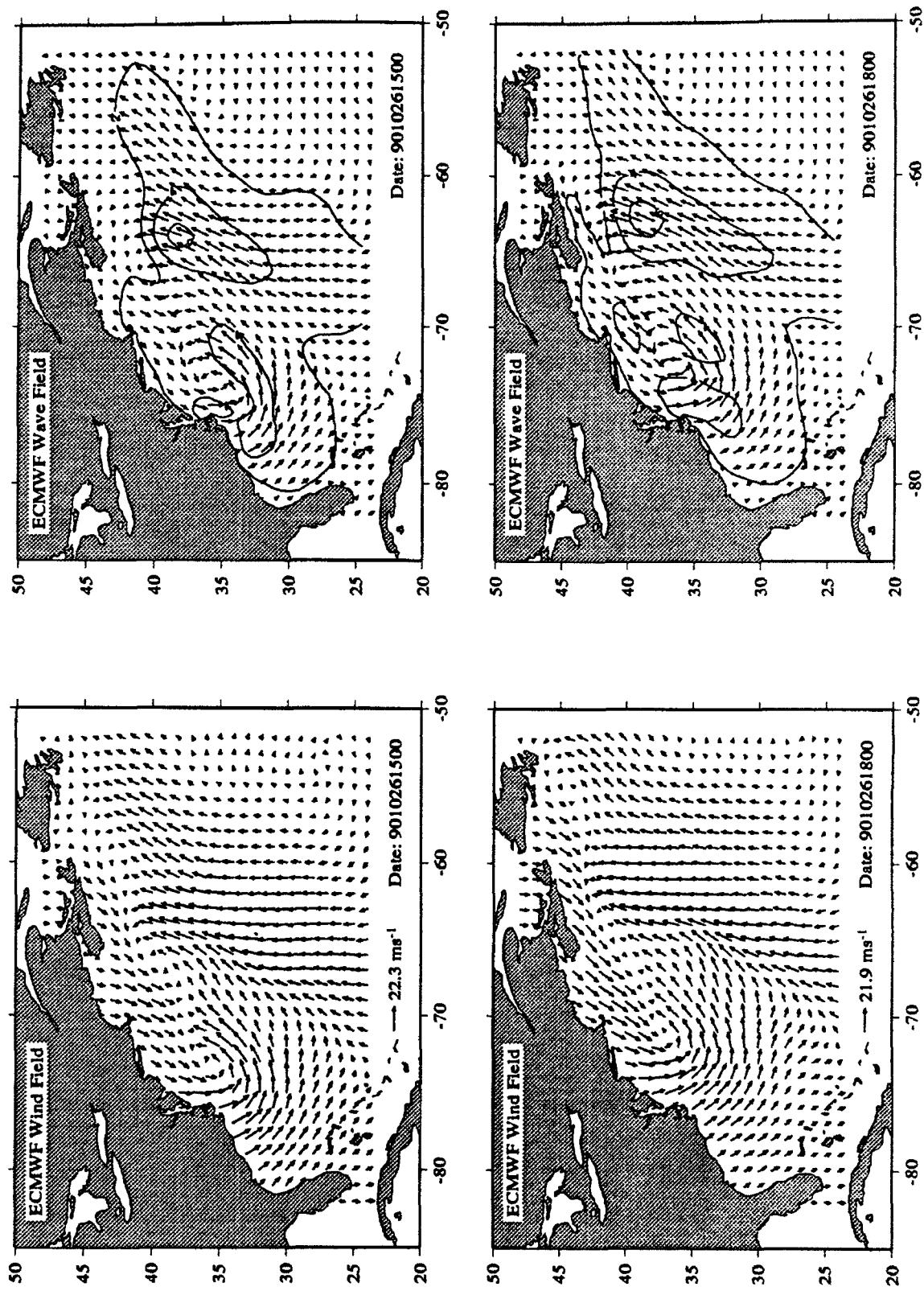


Appendix D Custer Diagrams of Wind fields and Wave Hindcasts

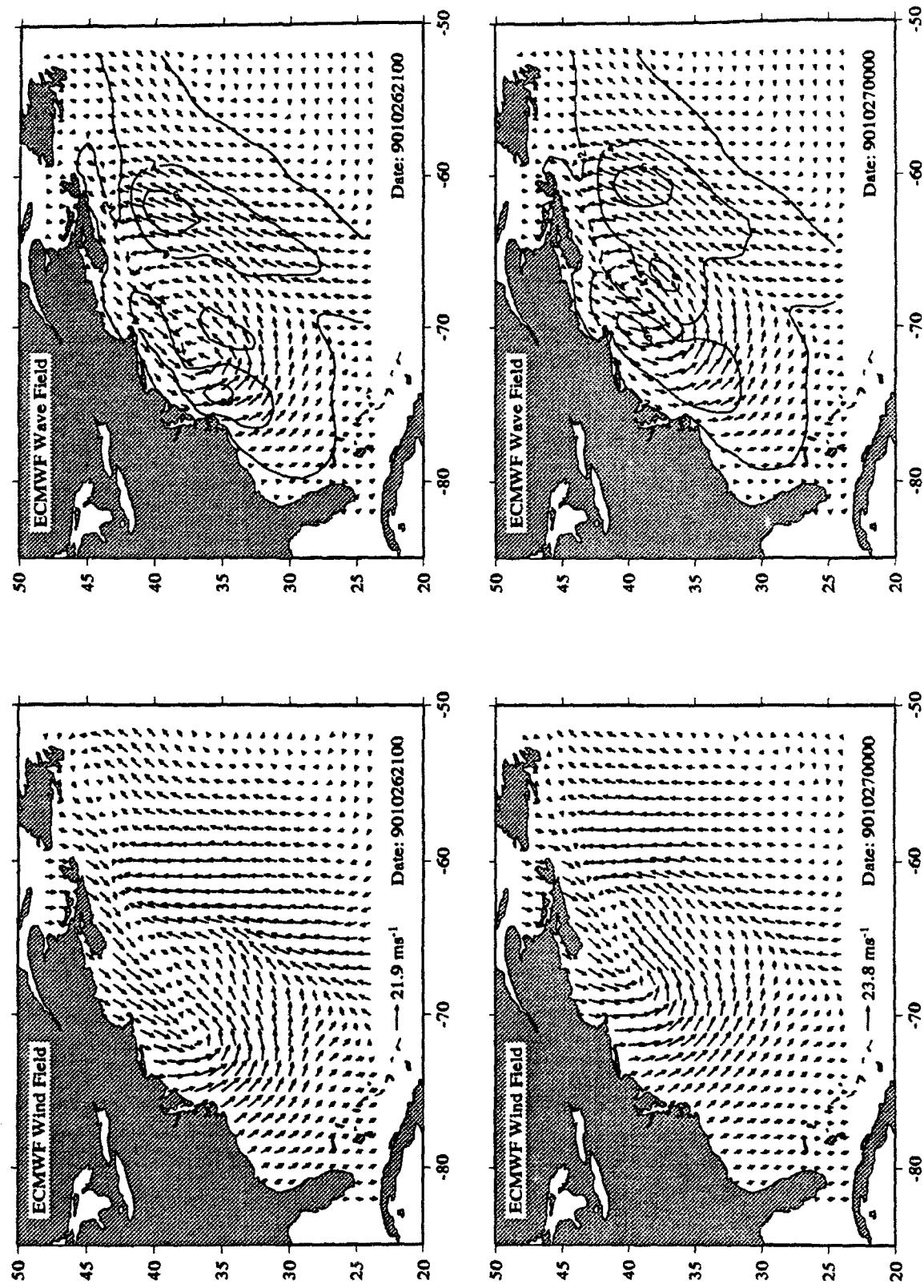


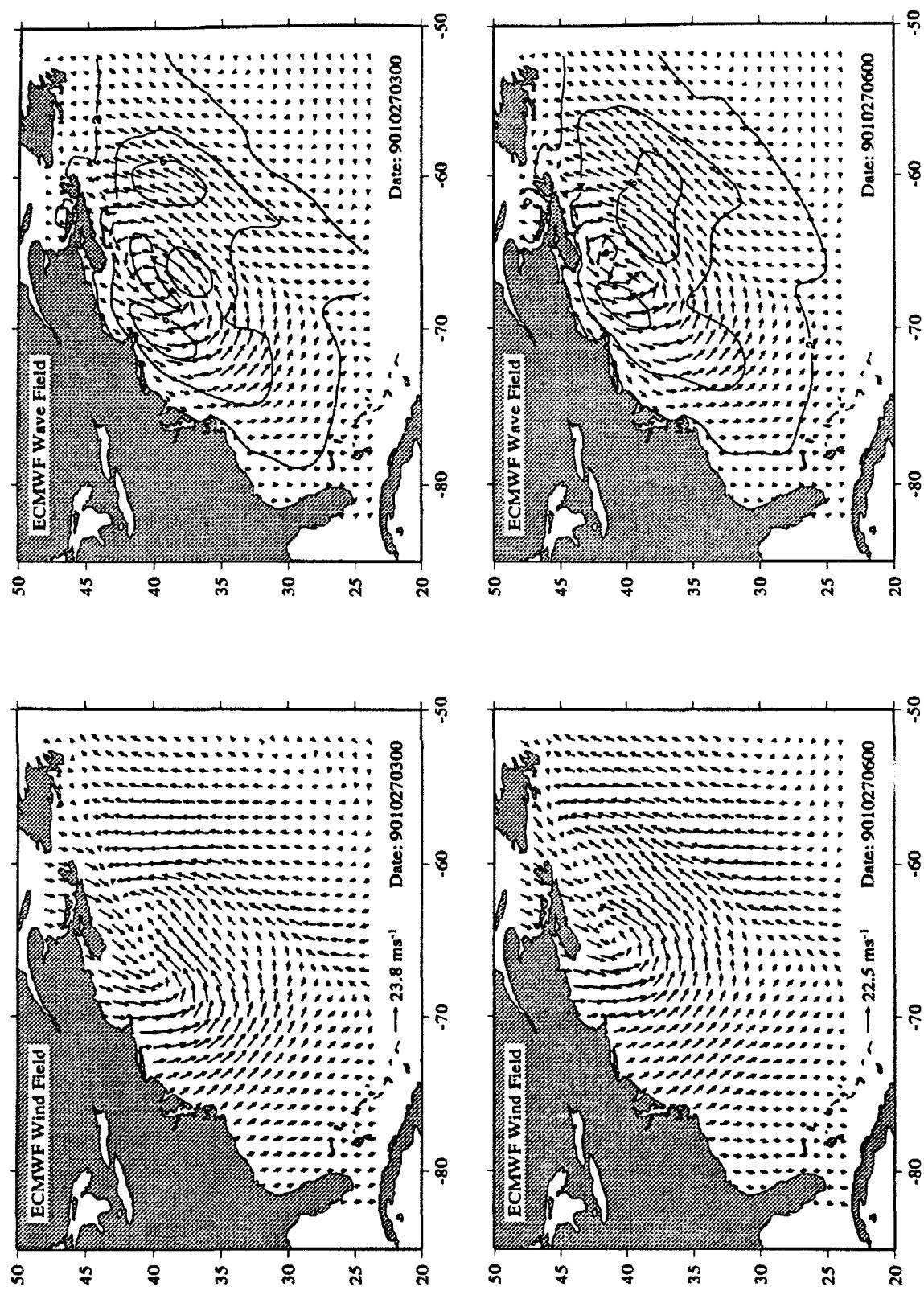




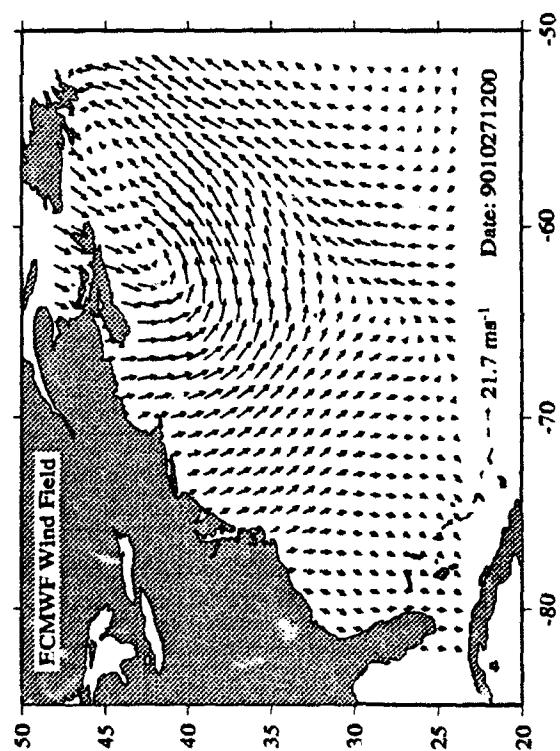
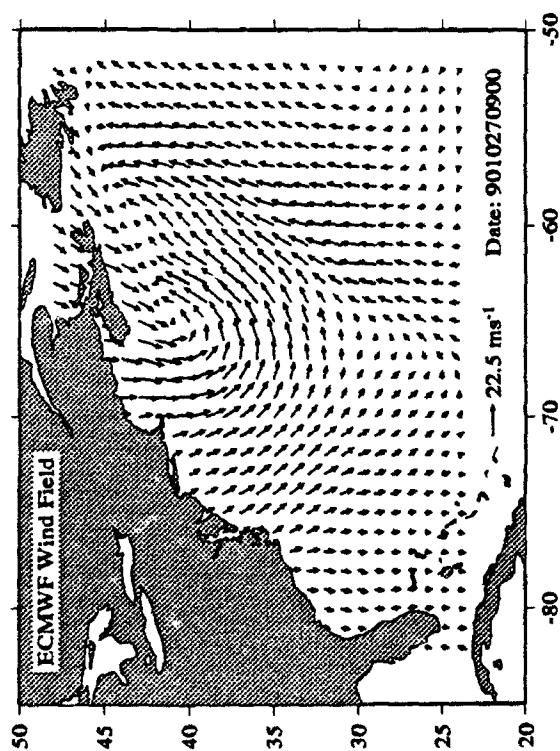
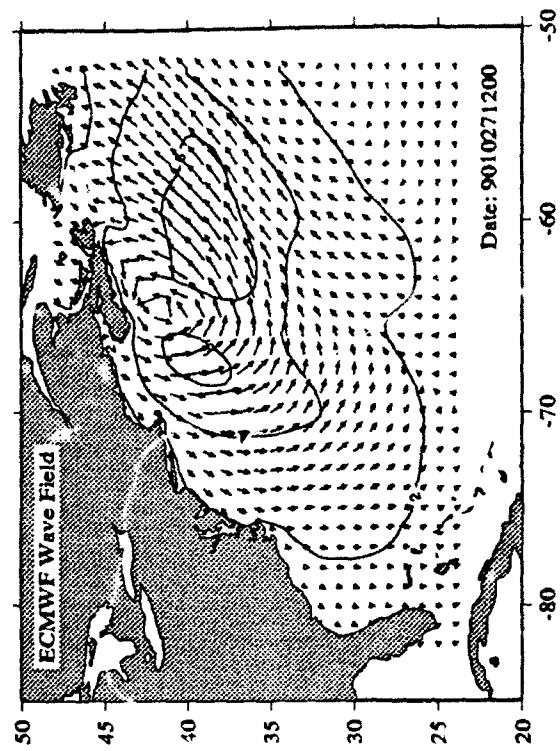
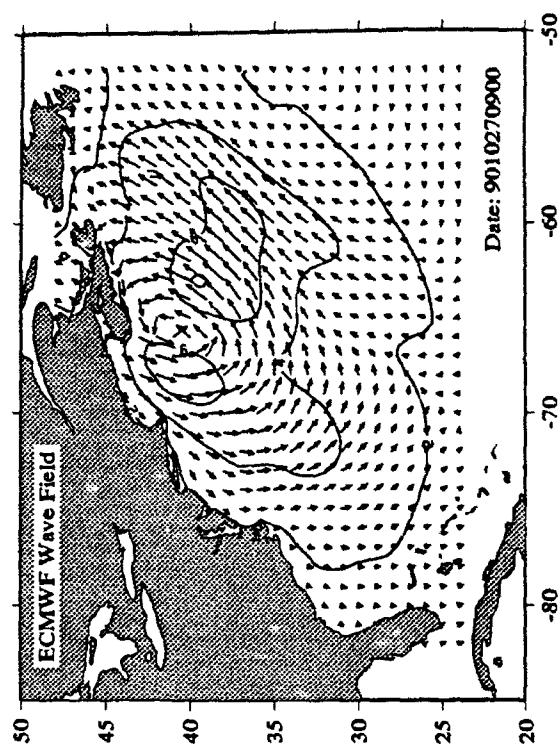


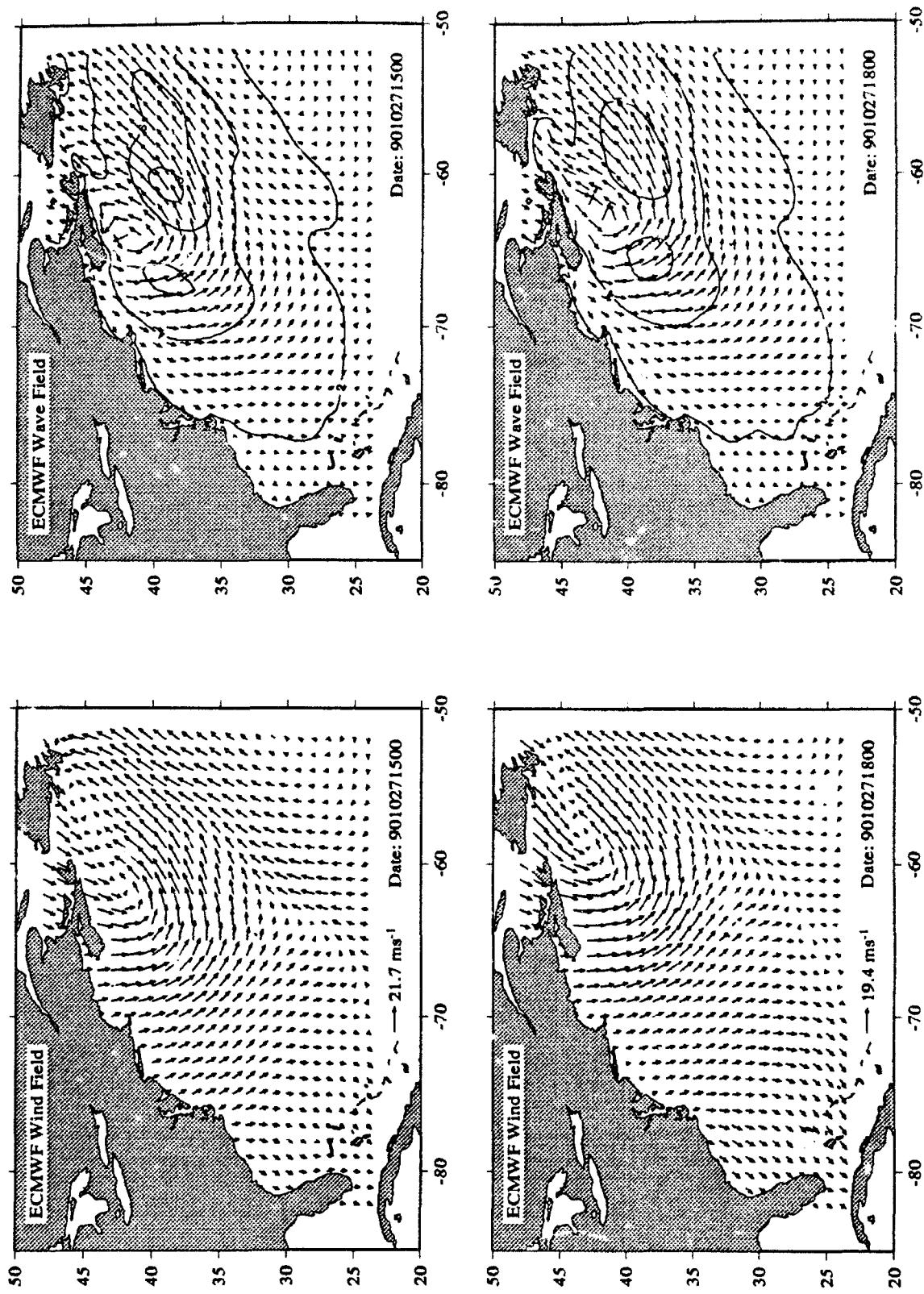
Appendix D Cluster Diagrams of Wind fields and Wave Hindcasts



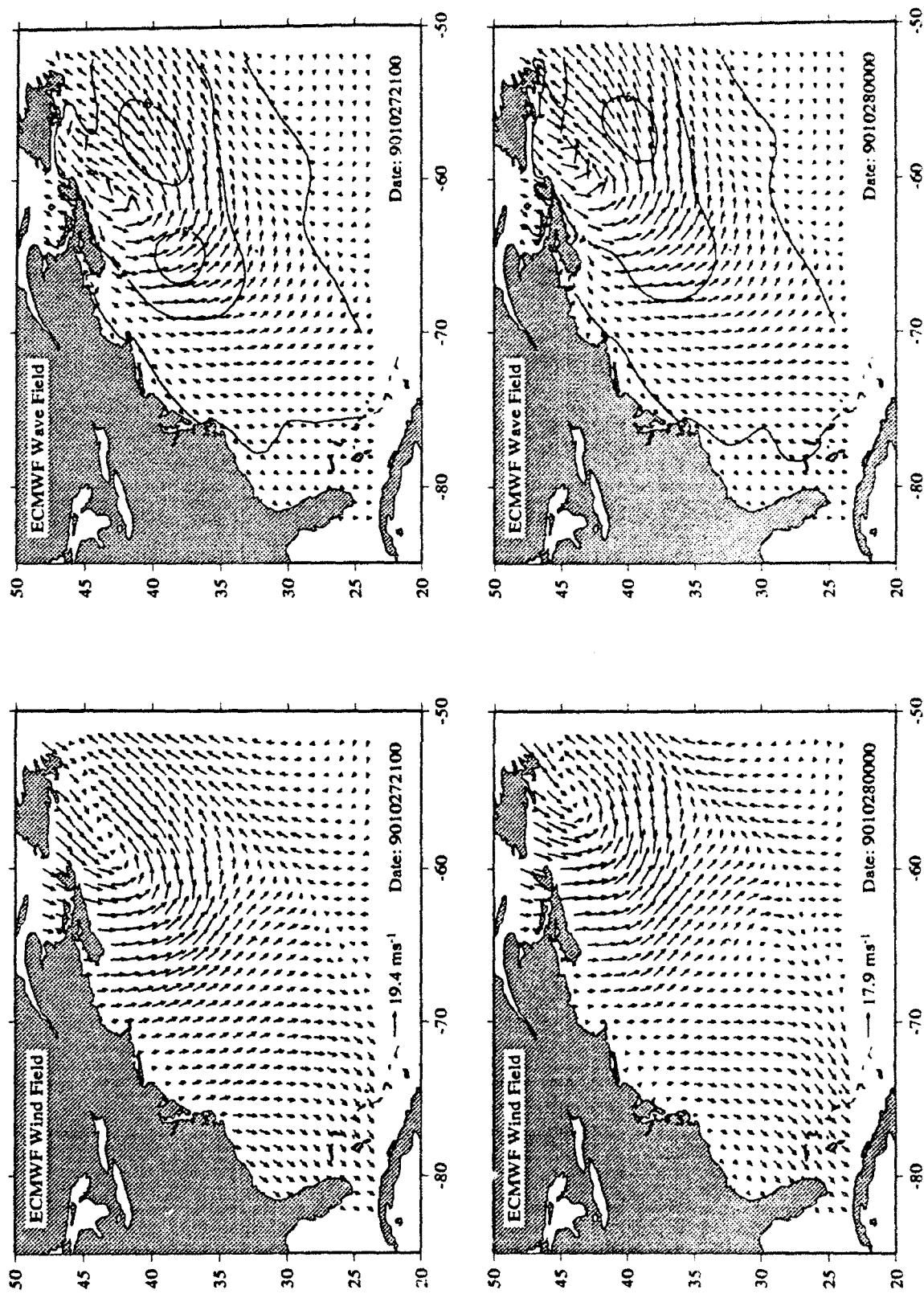


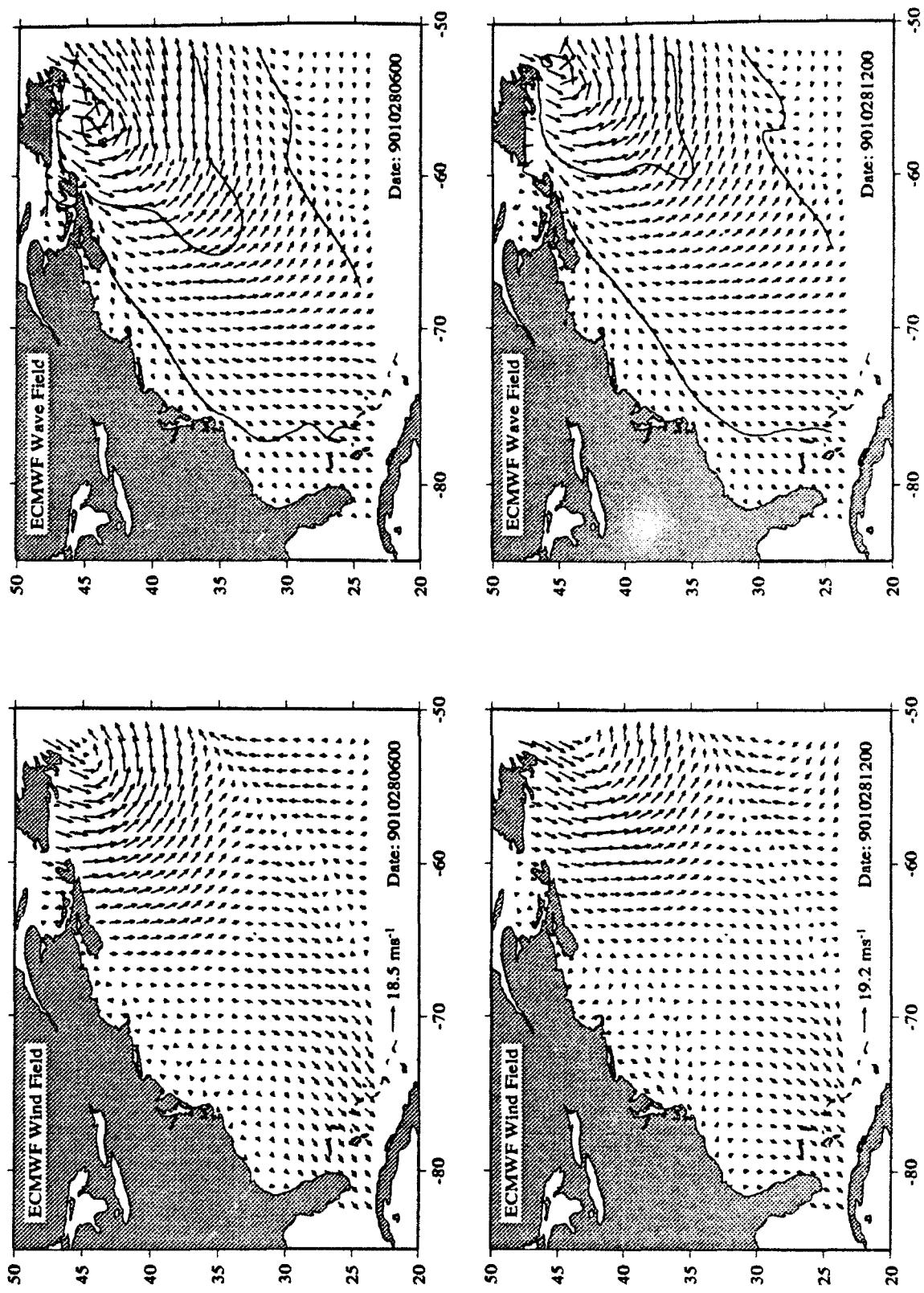
Appendix D Custer Diagrams of Wind fields and Wave Hindcasts





Appendix D Custer Diagrams of Wind fields and Wave Hindcasts

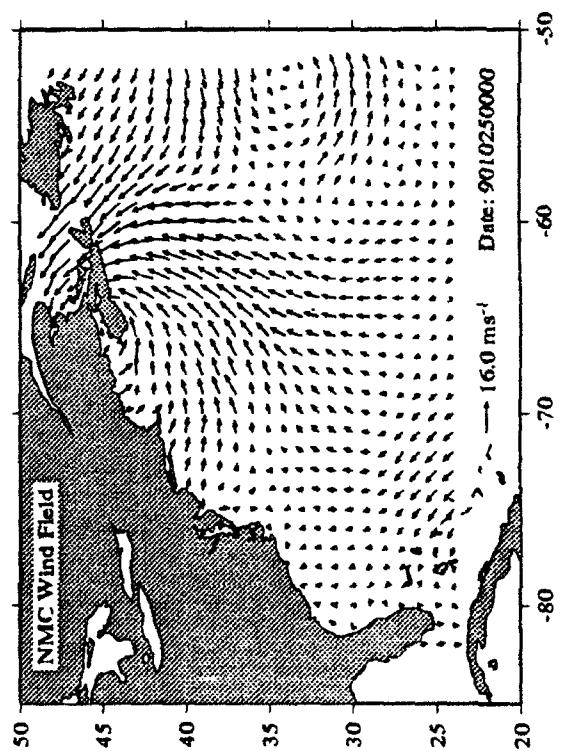
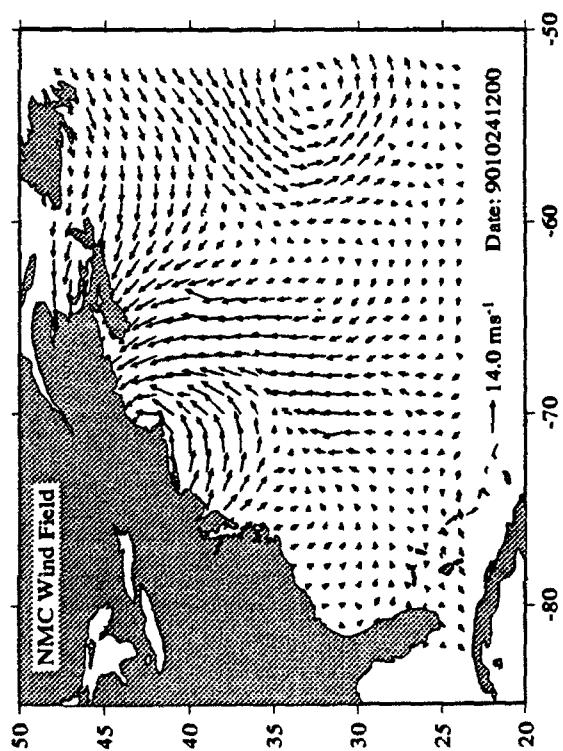
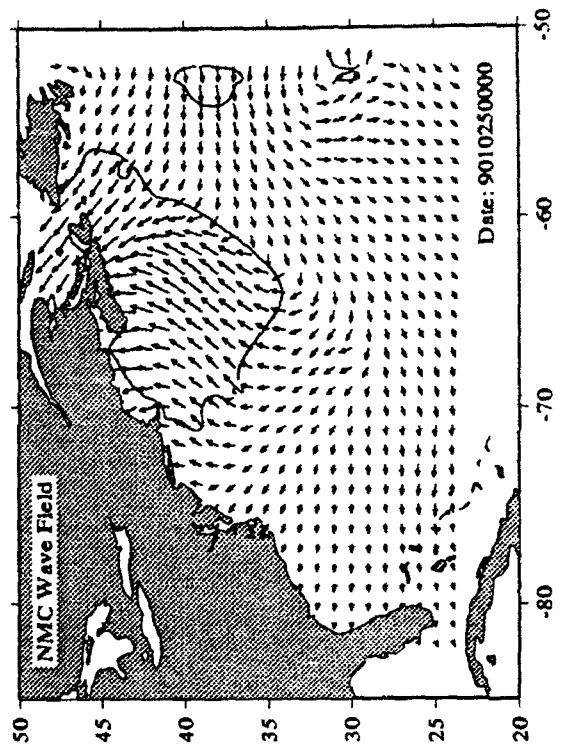
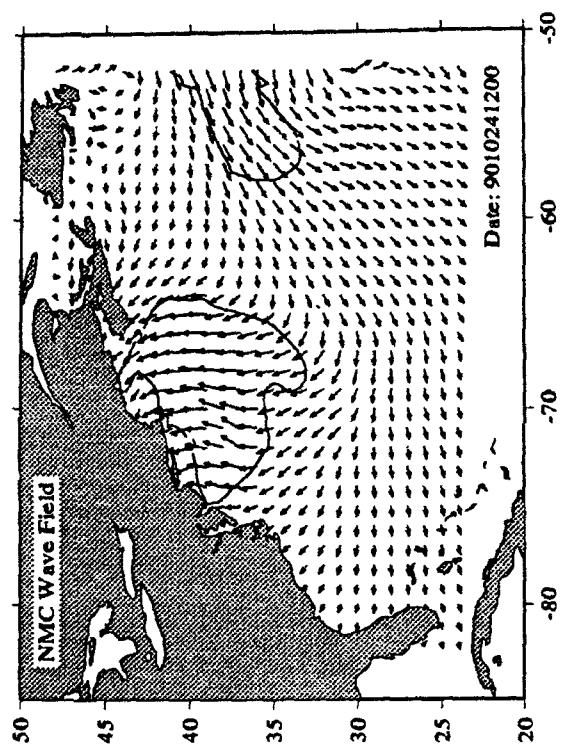


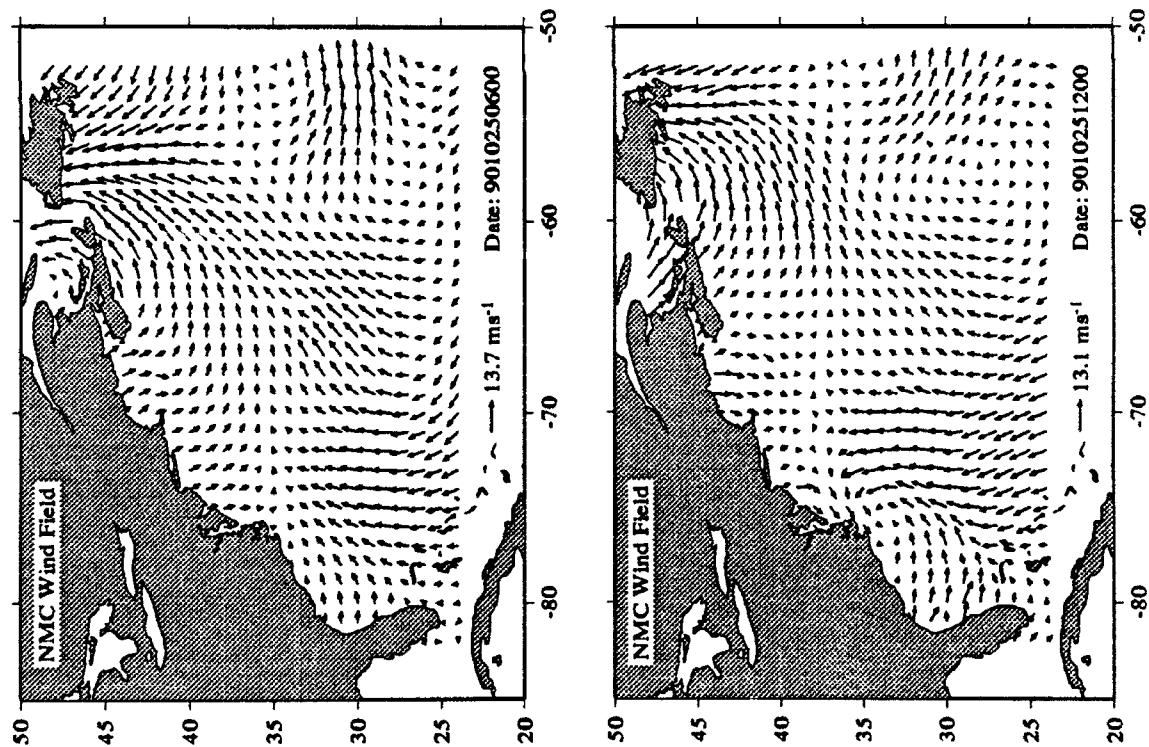
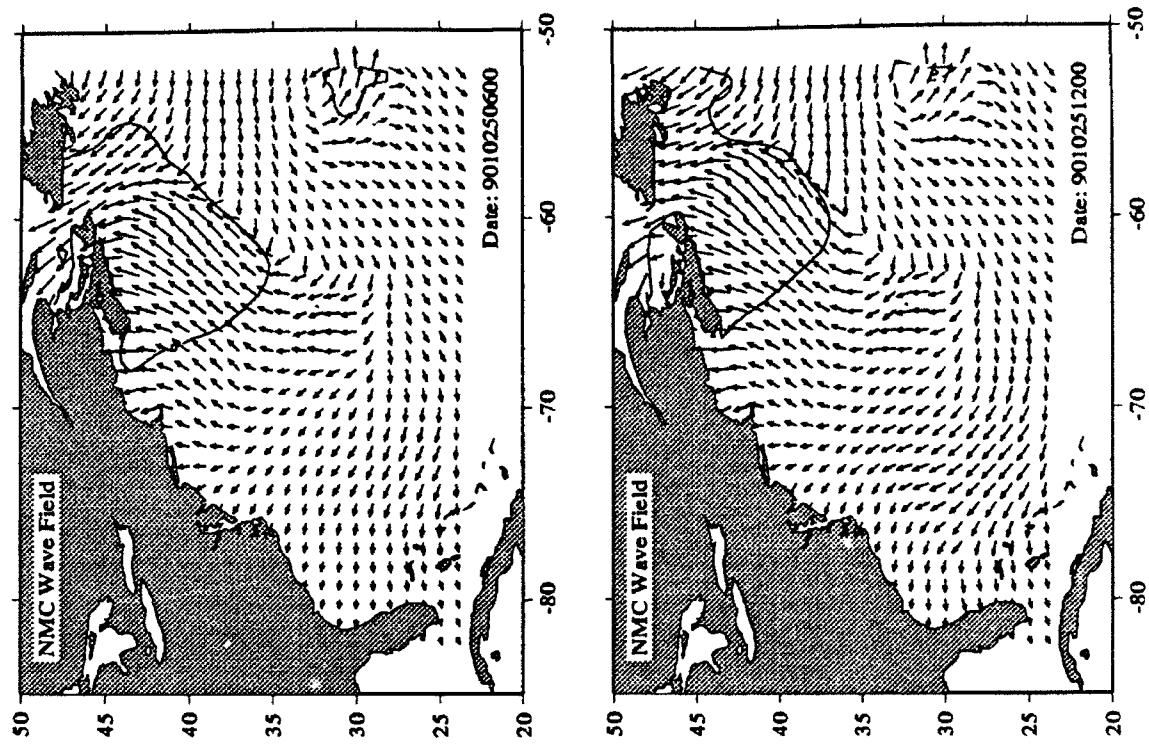


Appendix D Cluster Diagrams of Wind fields and Wave Hindcasts

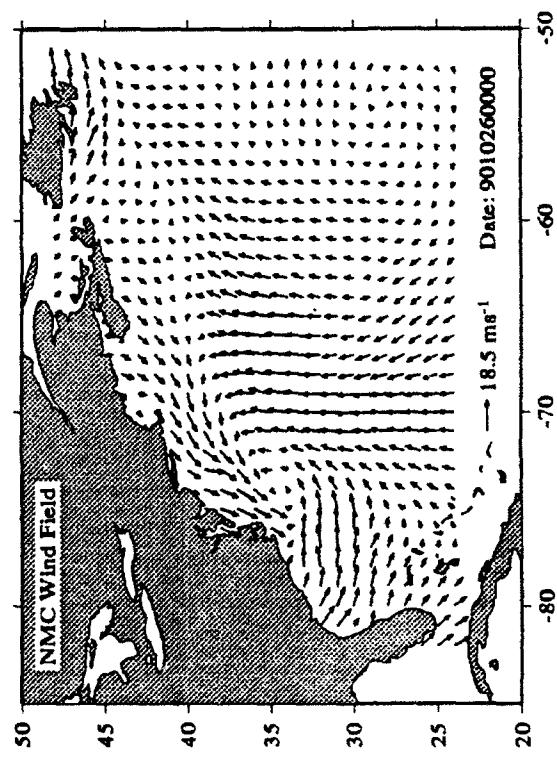
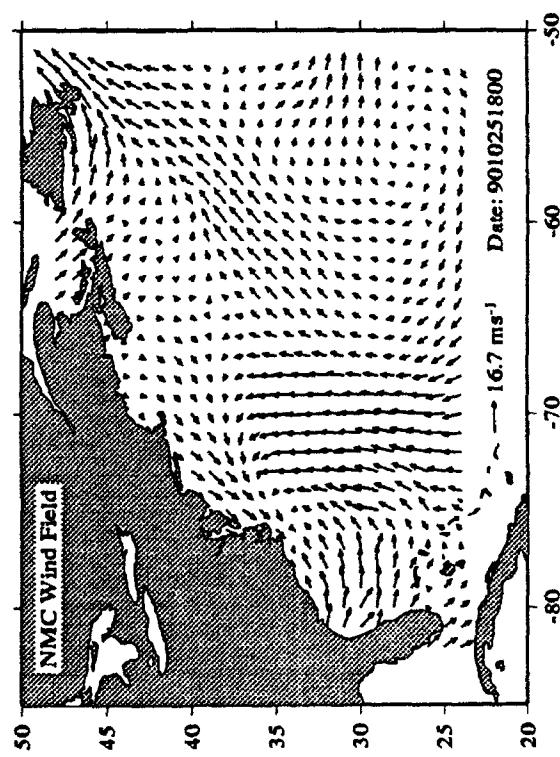
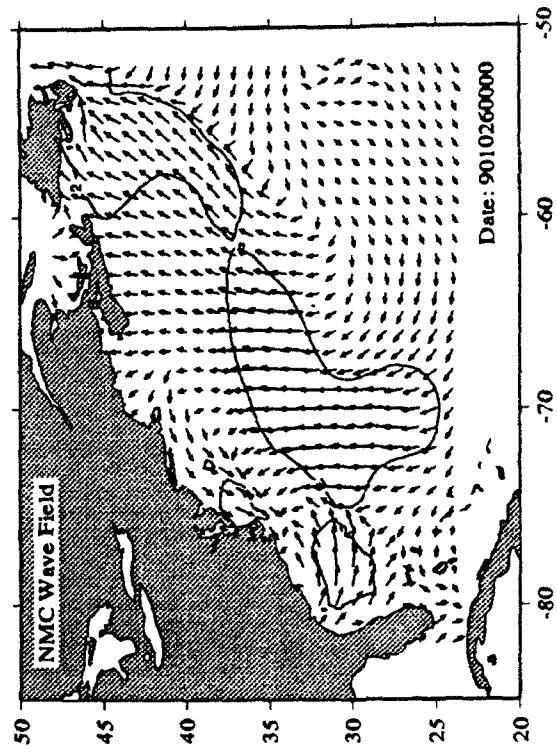
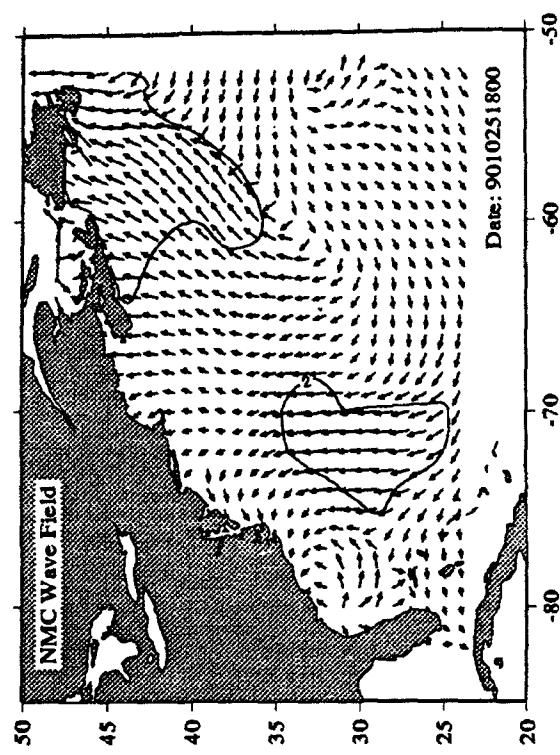
D.4: National Meteorological Center (NMC)

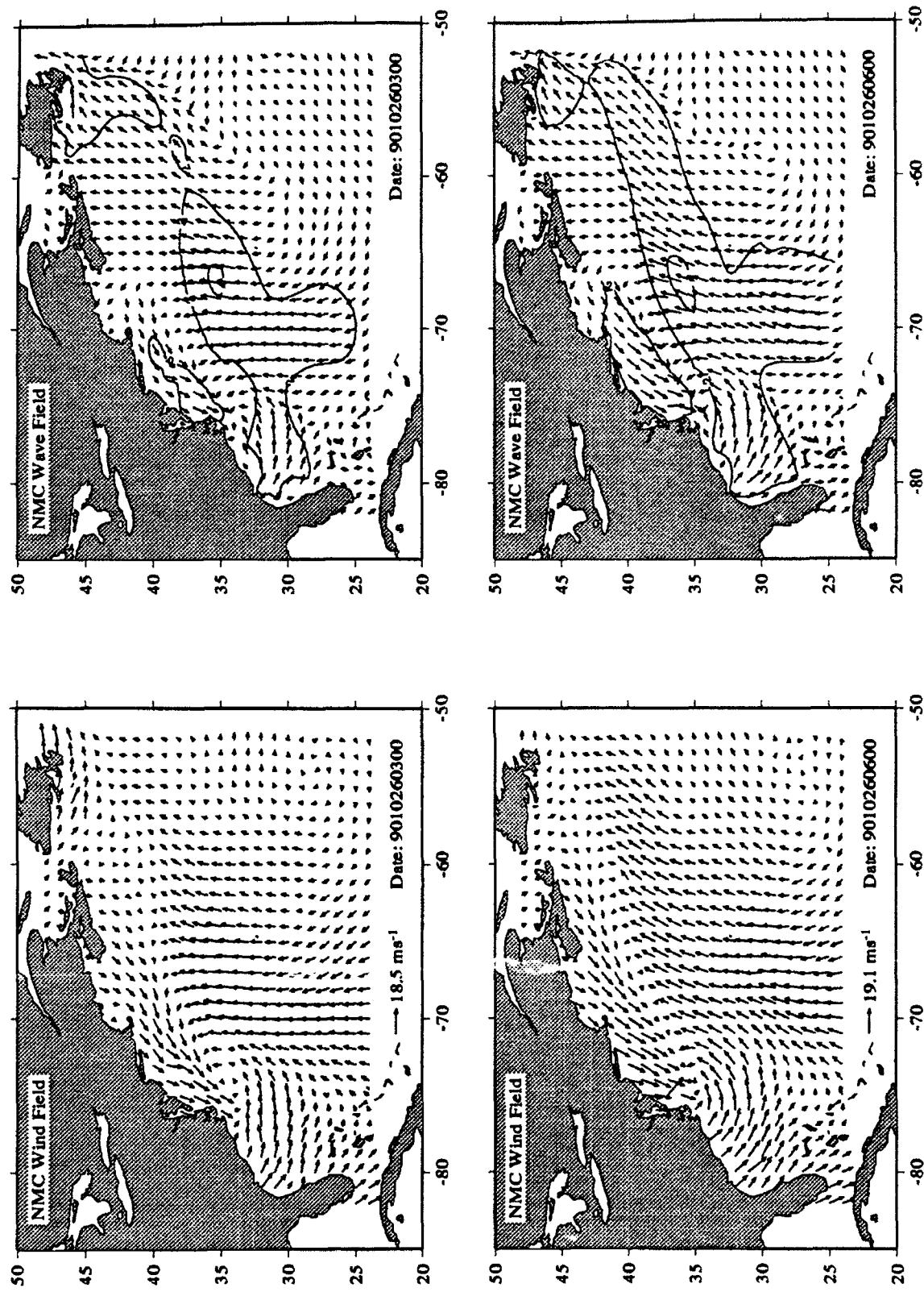
Custer diagrams are presented for the time period from 24 October 1990, 12:00 GMT to 28 October 1990, 12:00 GMT of the wind field and corresponding wave hindcasts. Note that the frequency of maps is every 3 hr from 26-28 October, which covers the major storm period.

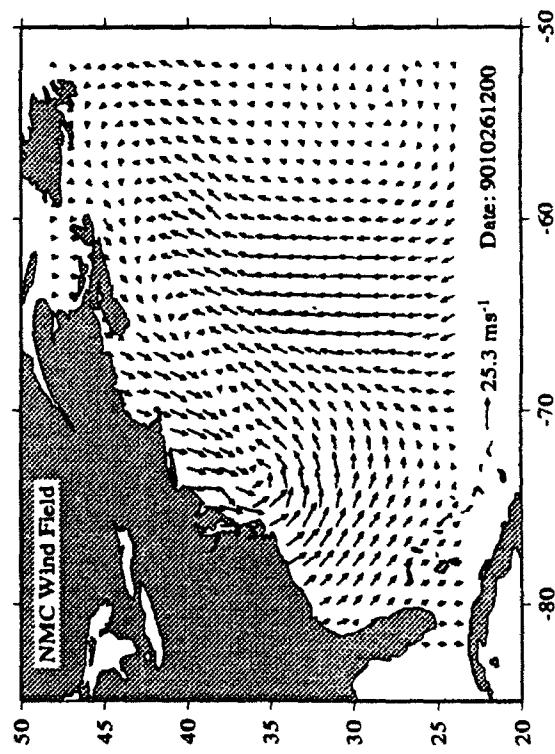
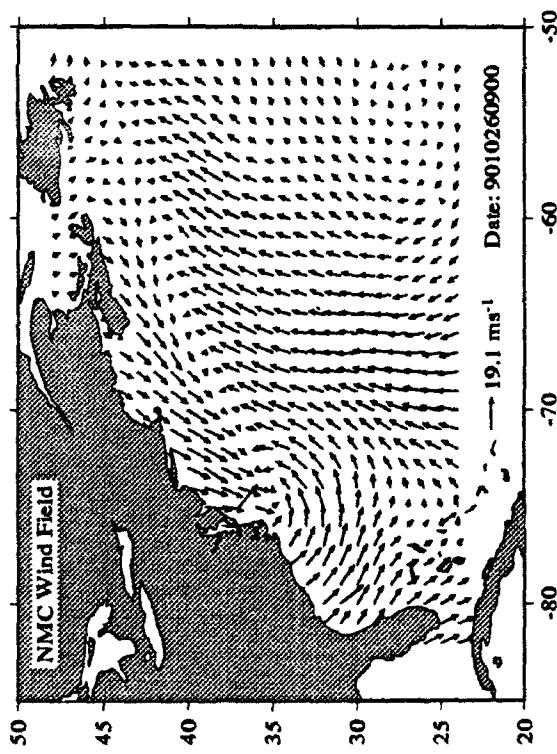
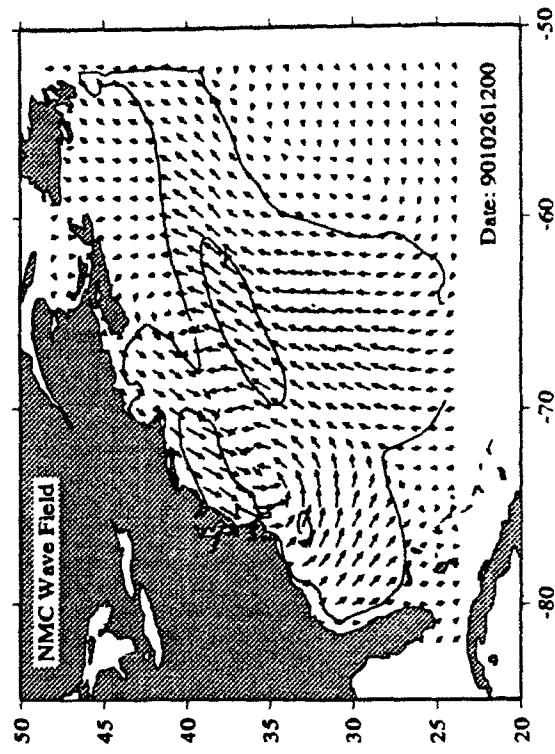
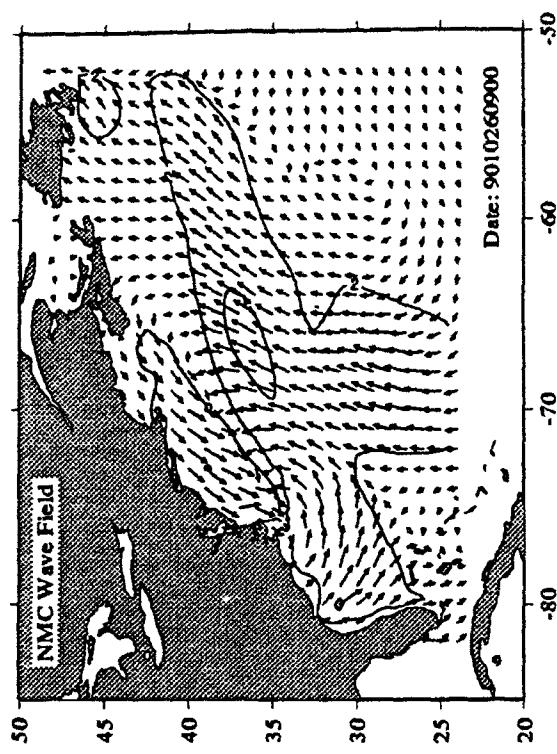


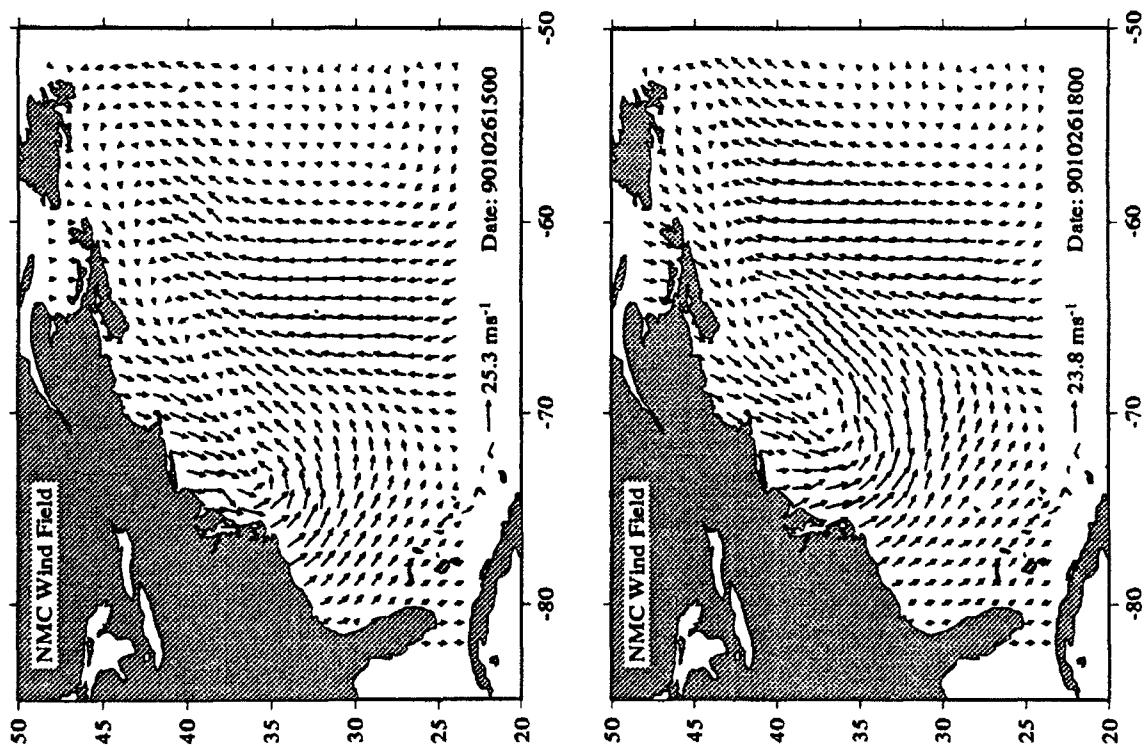
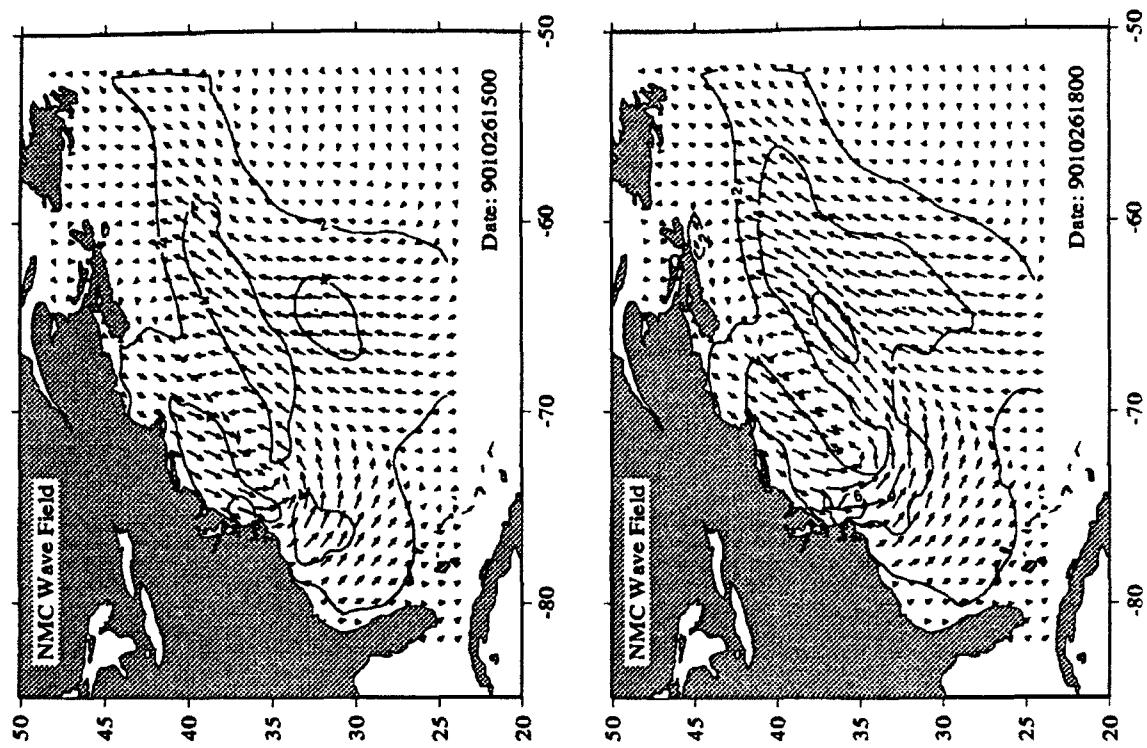


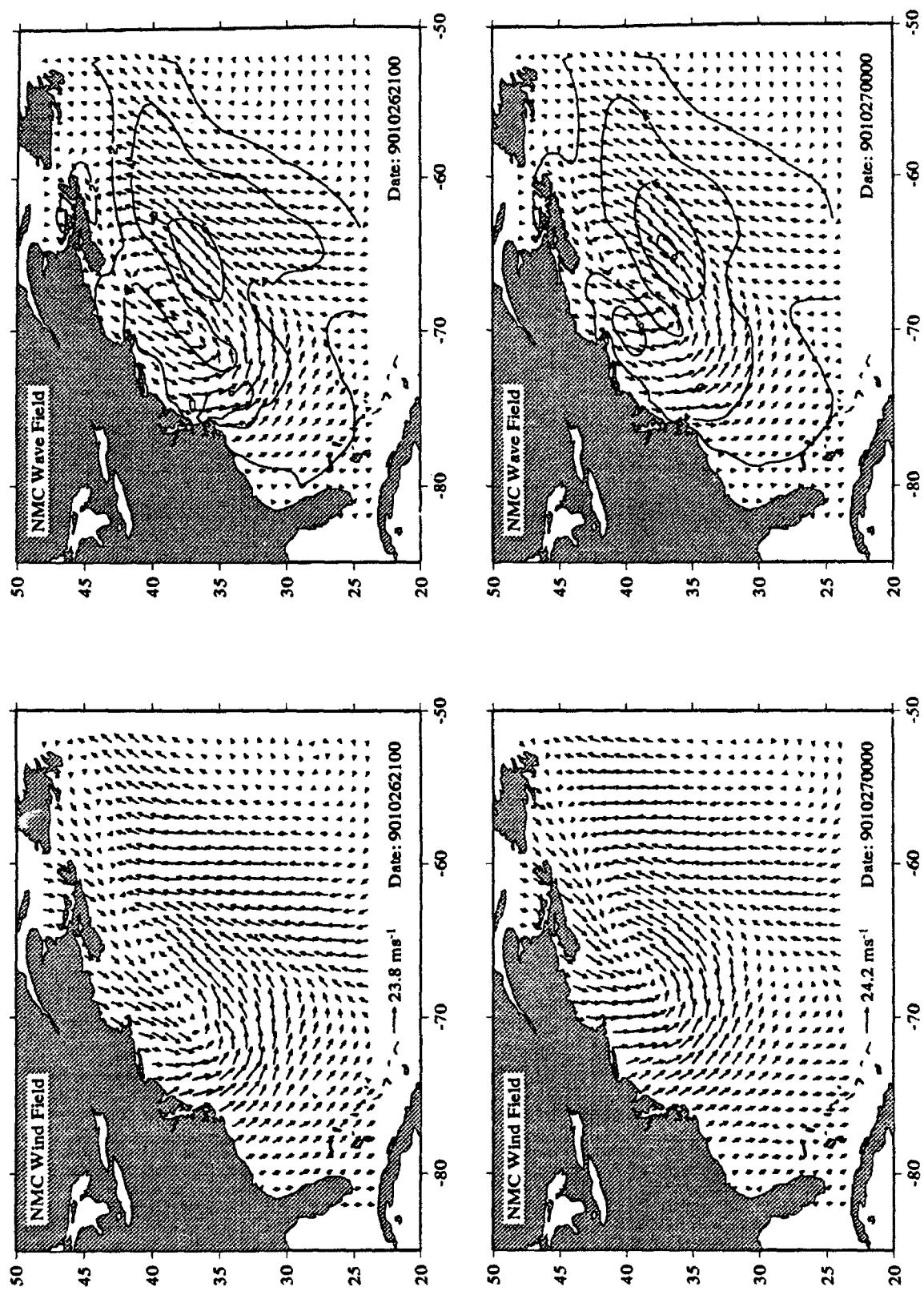
Appendix D Custer Diagrams of Wind fields and Wave Hindcasts

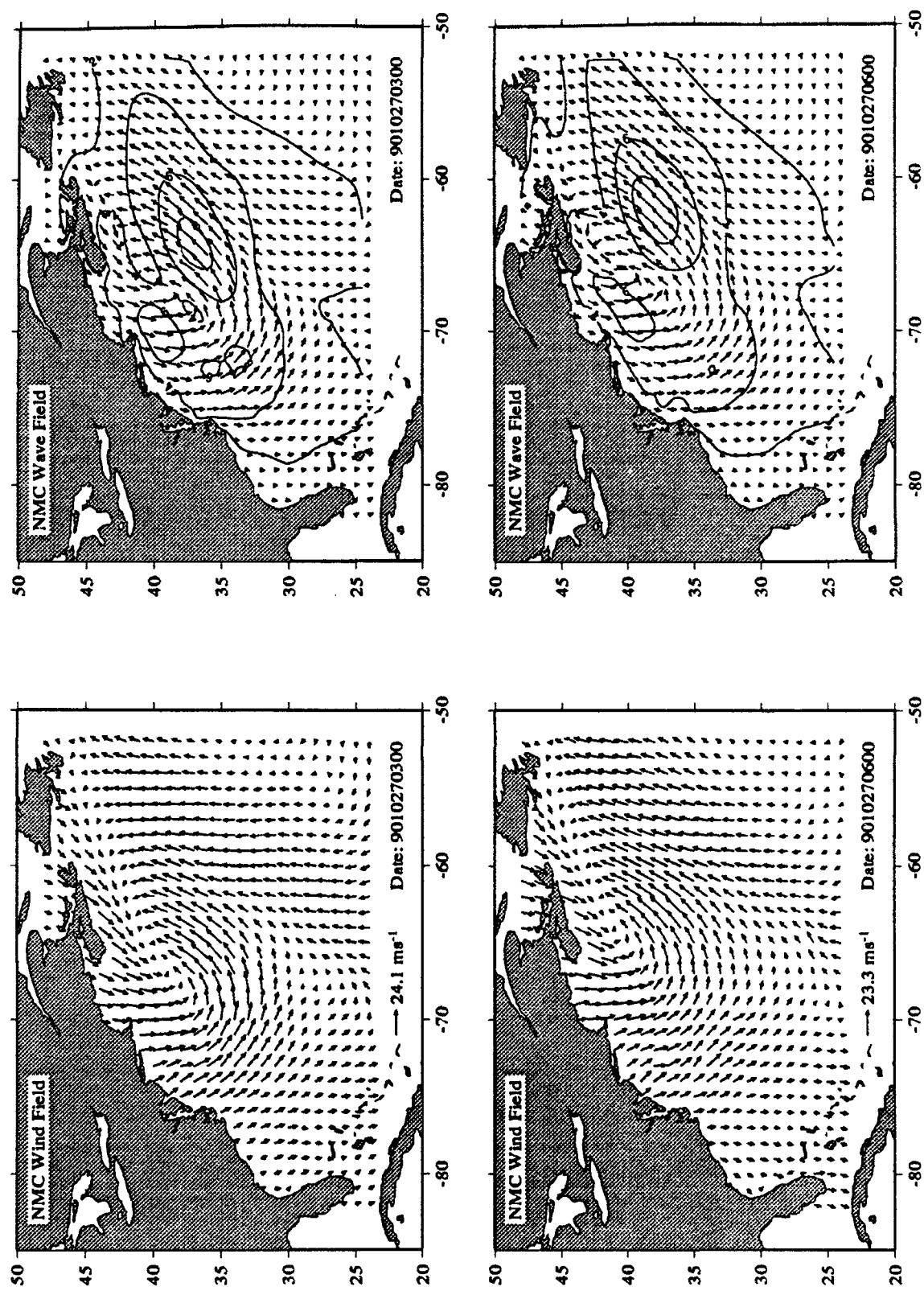




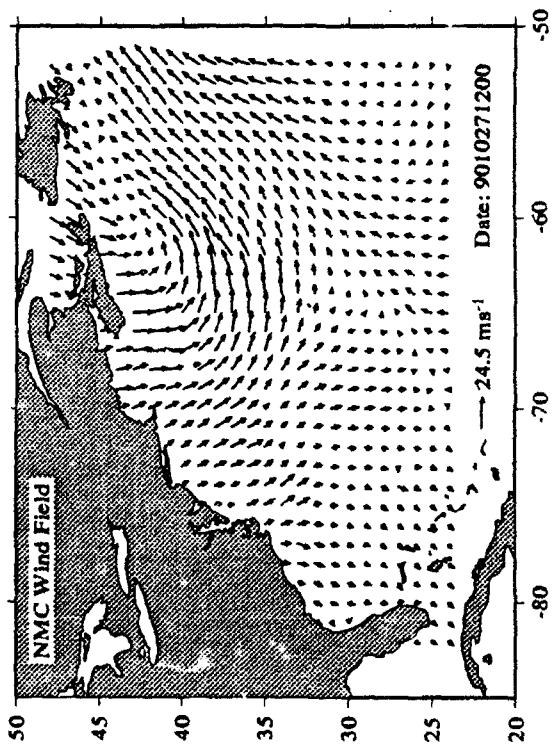
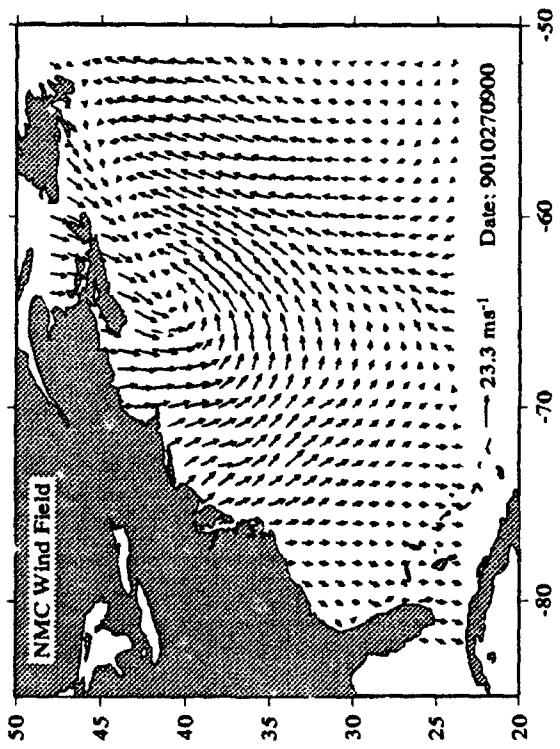
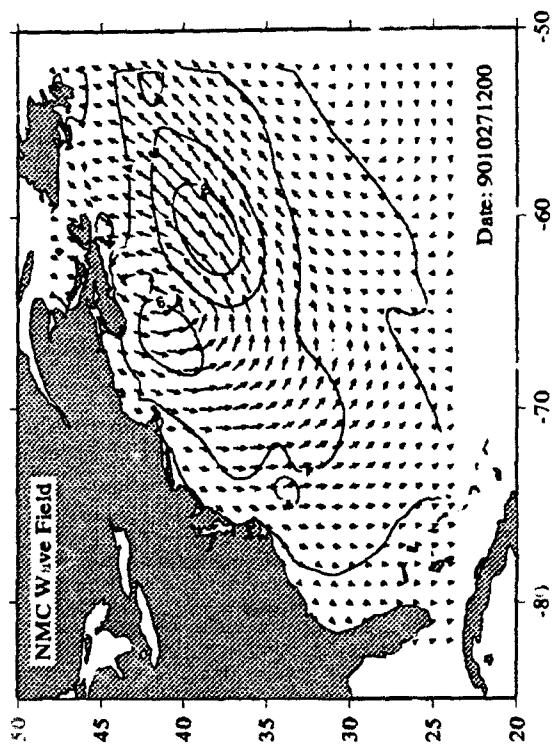
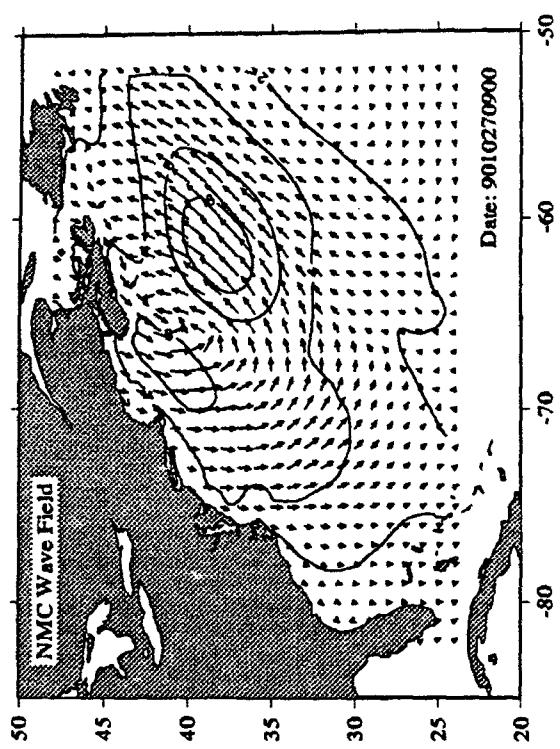


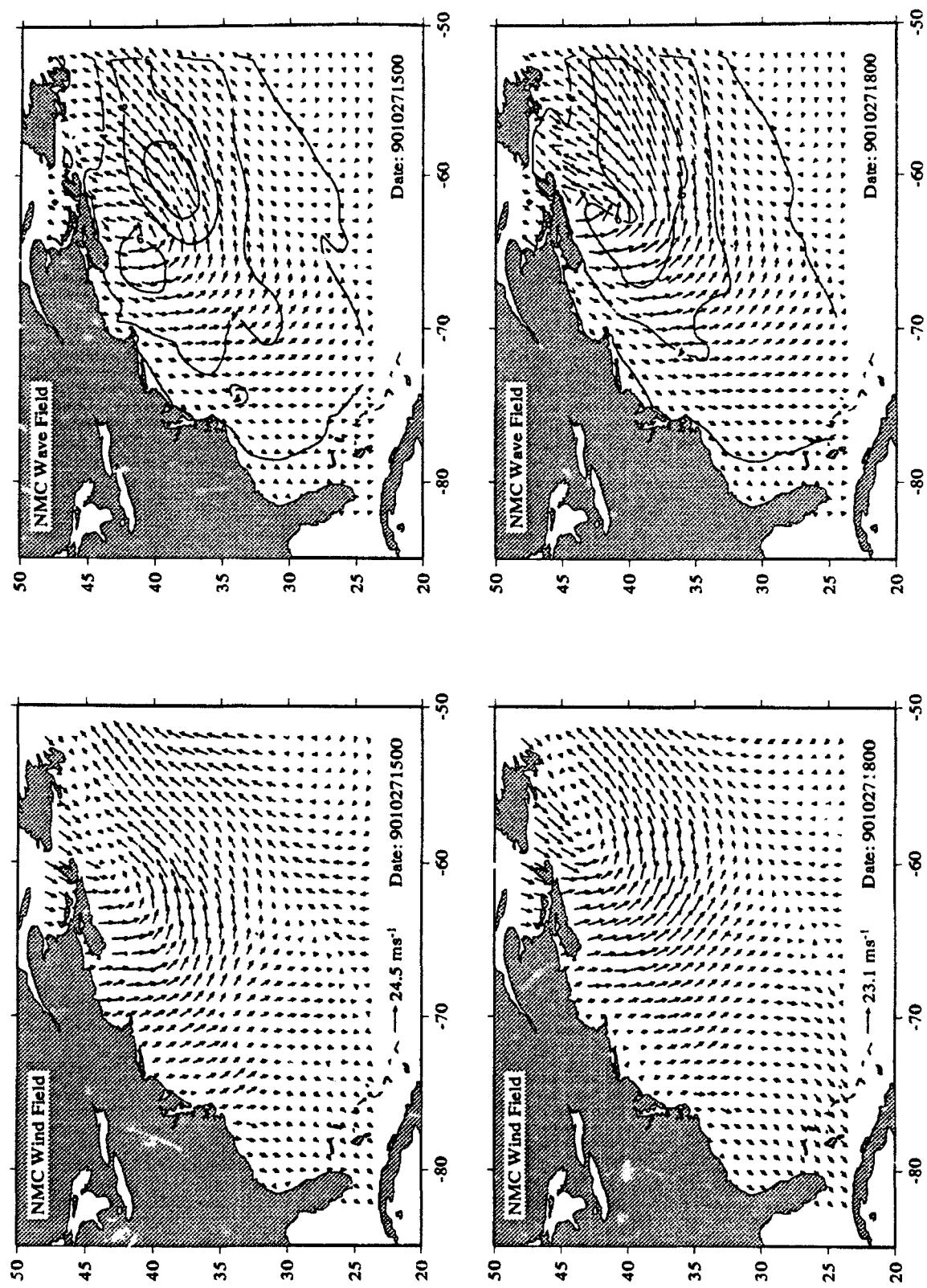


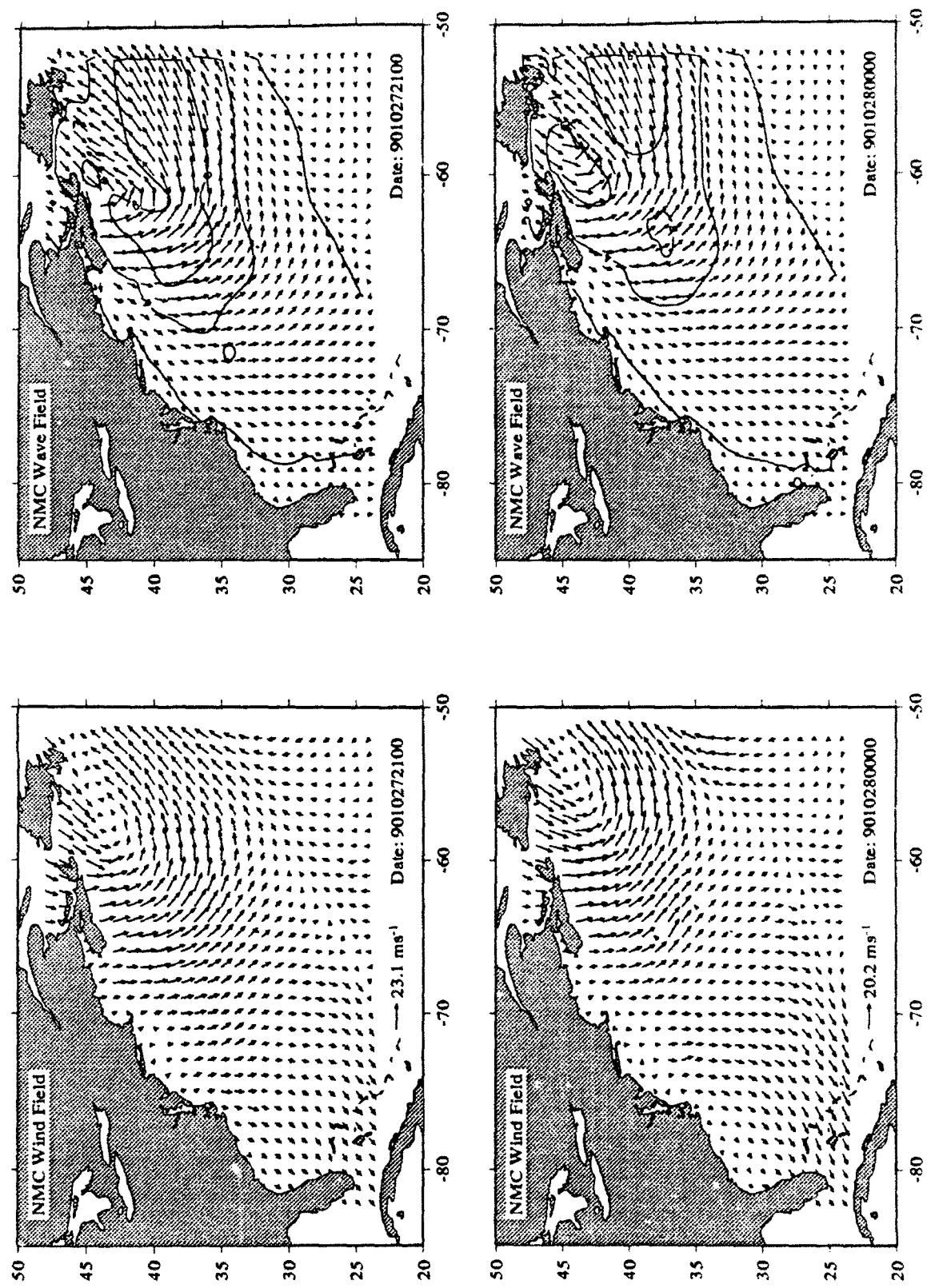


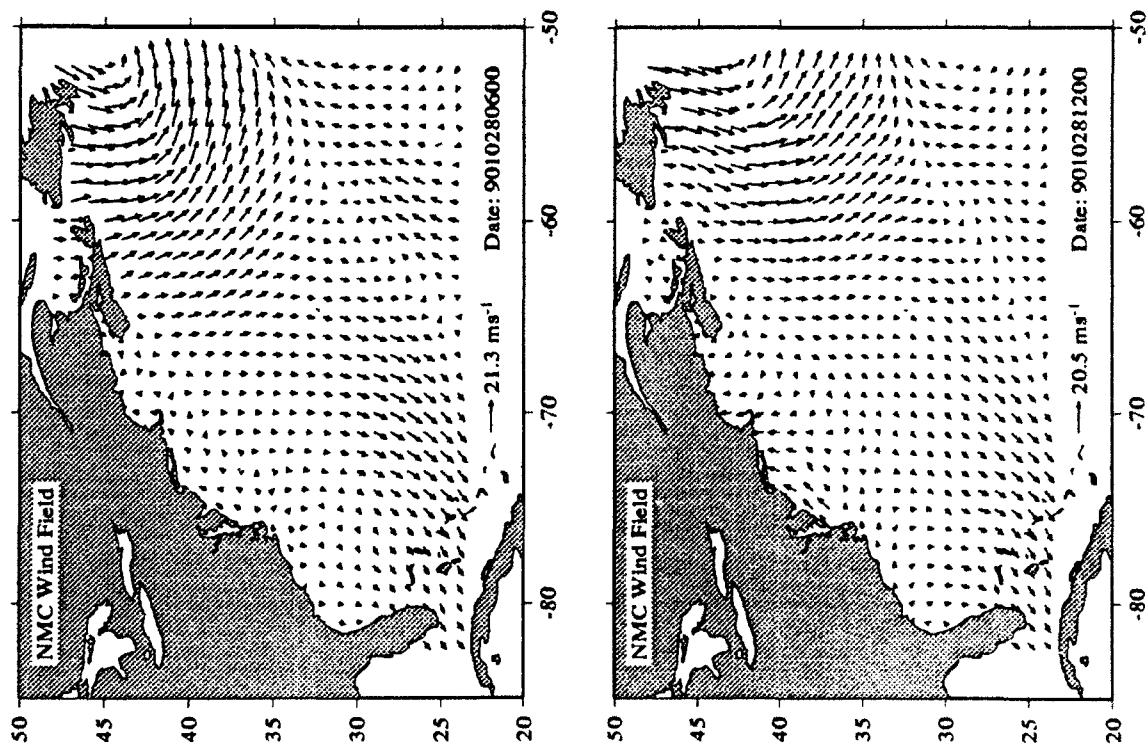
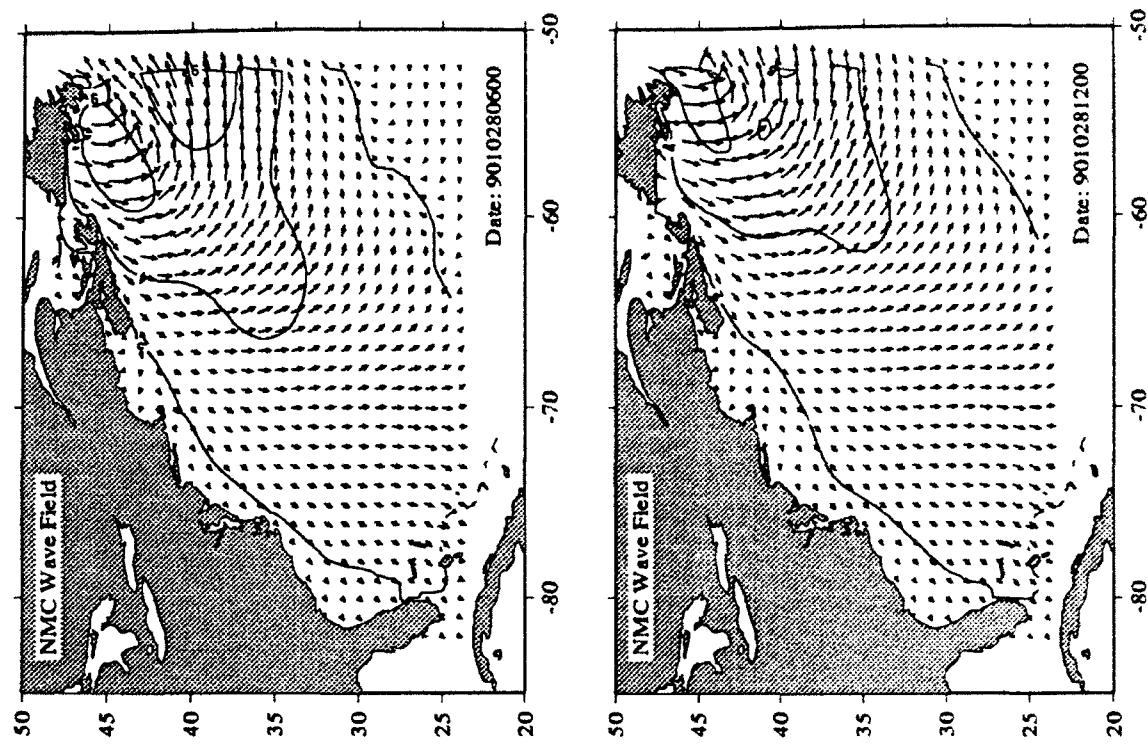


Appendix D Cluster Diagrams of Wind fields and Wave Hindcasts





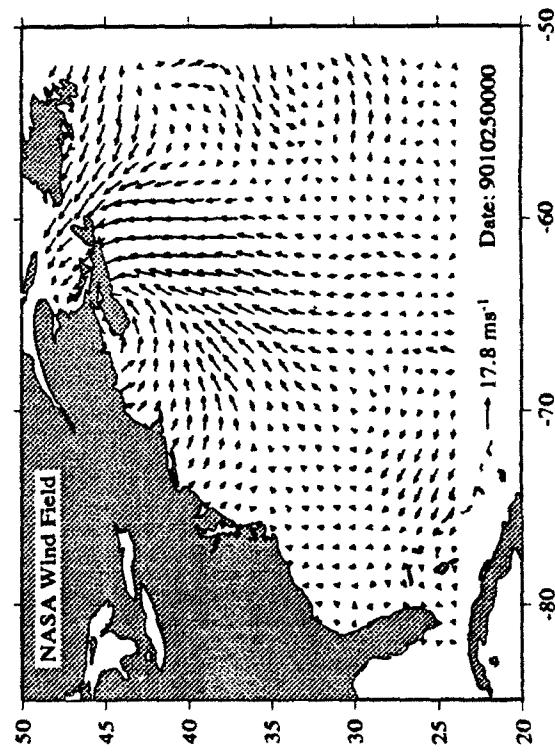
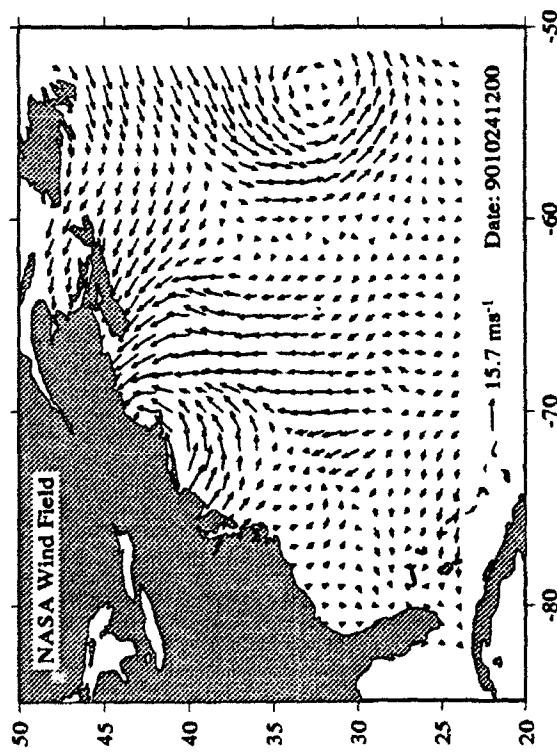
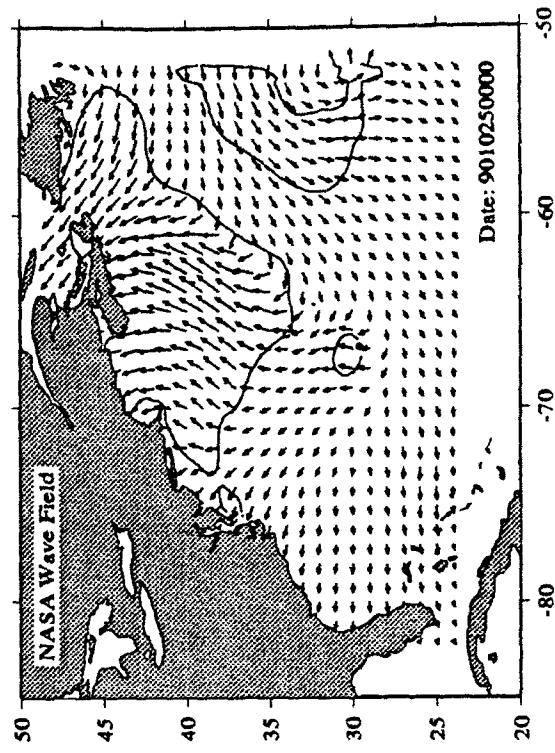
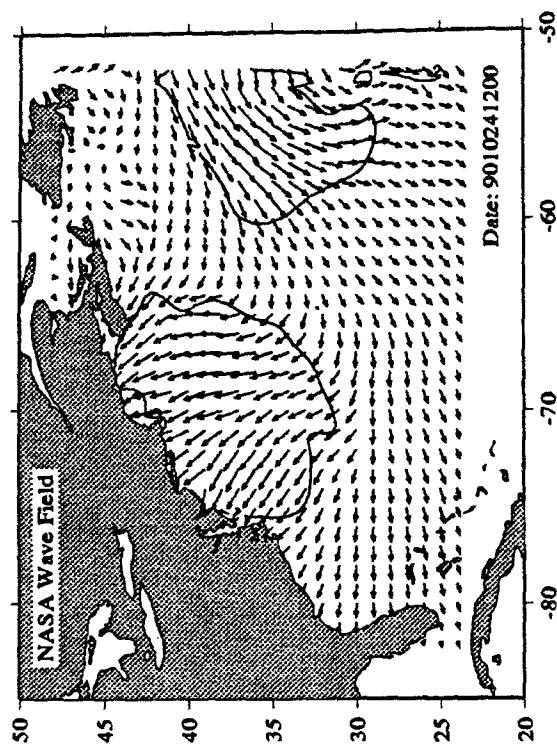


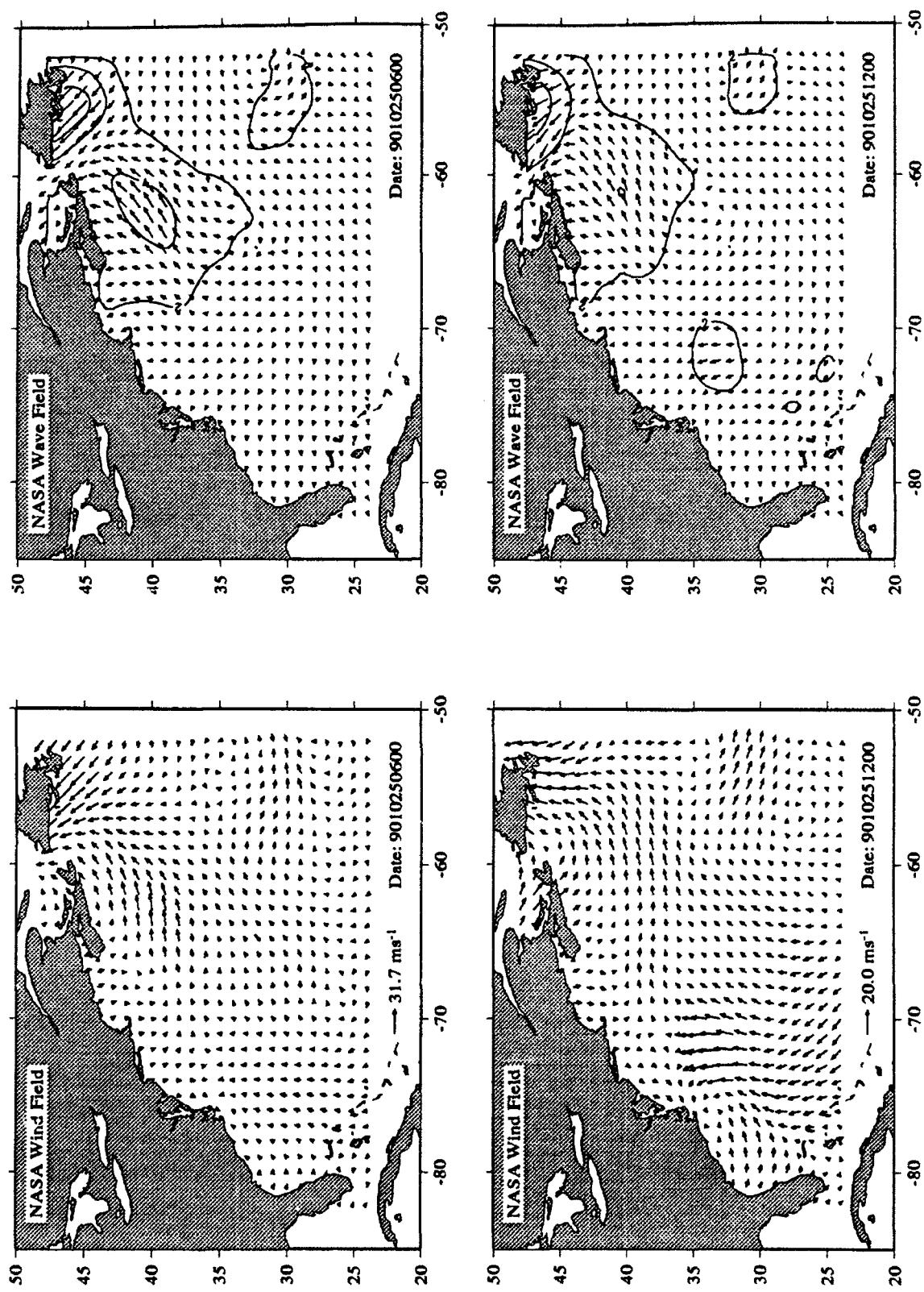


Appendix D Cluster Diagrams of Wind fields and Wave Hindcasts

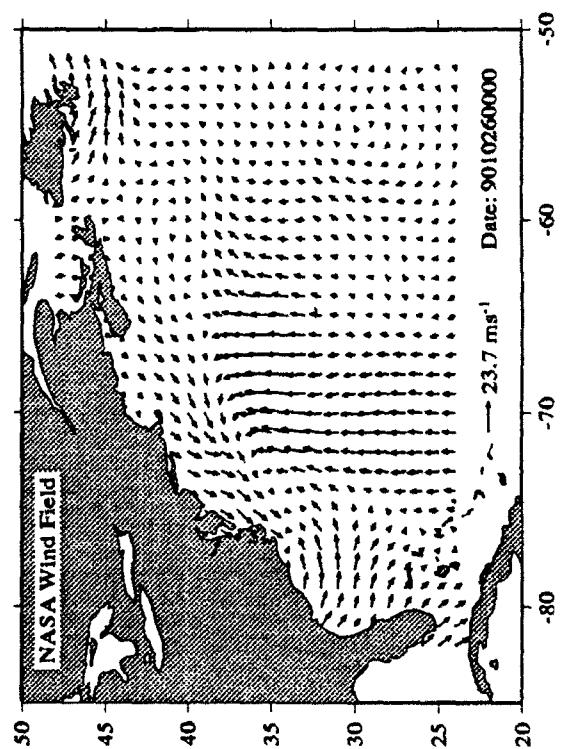
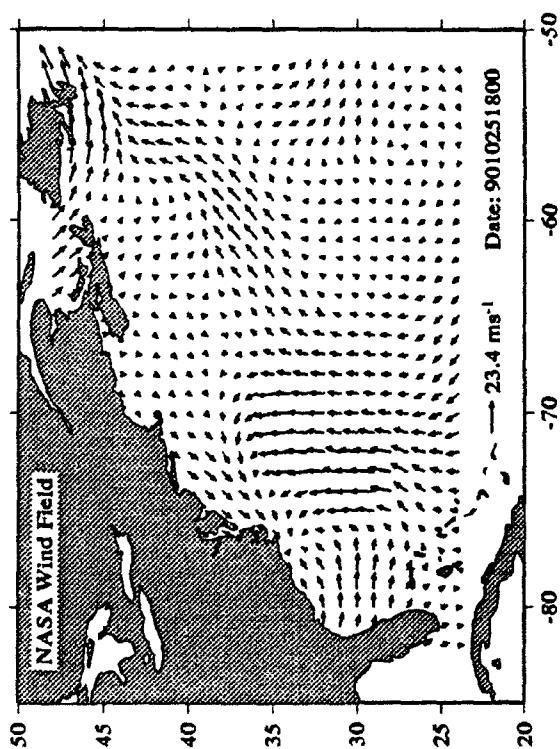
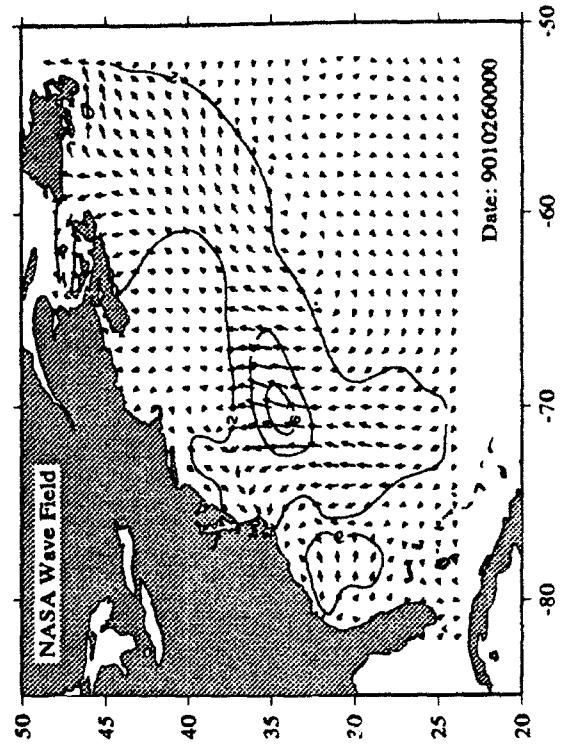
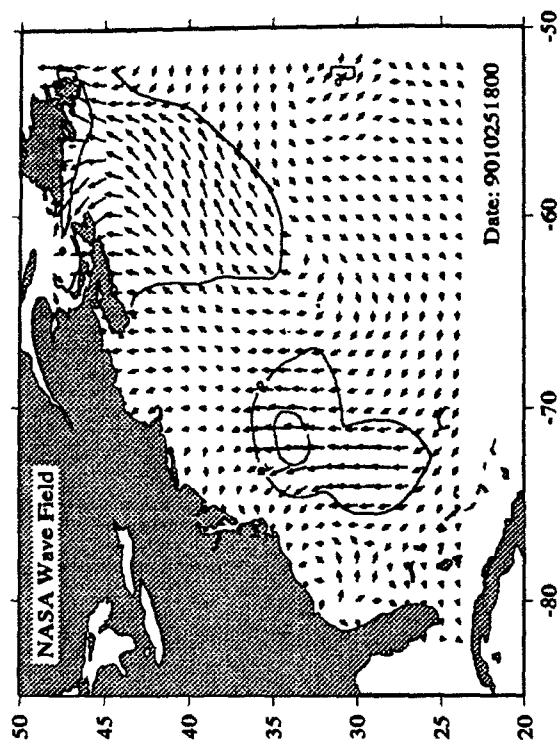
D.5: NASA Goddard Space Flight Facility (GSFC)

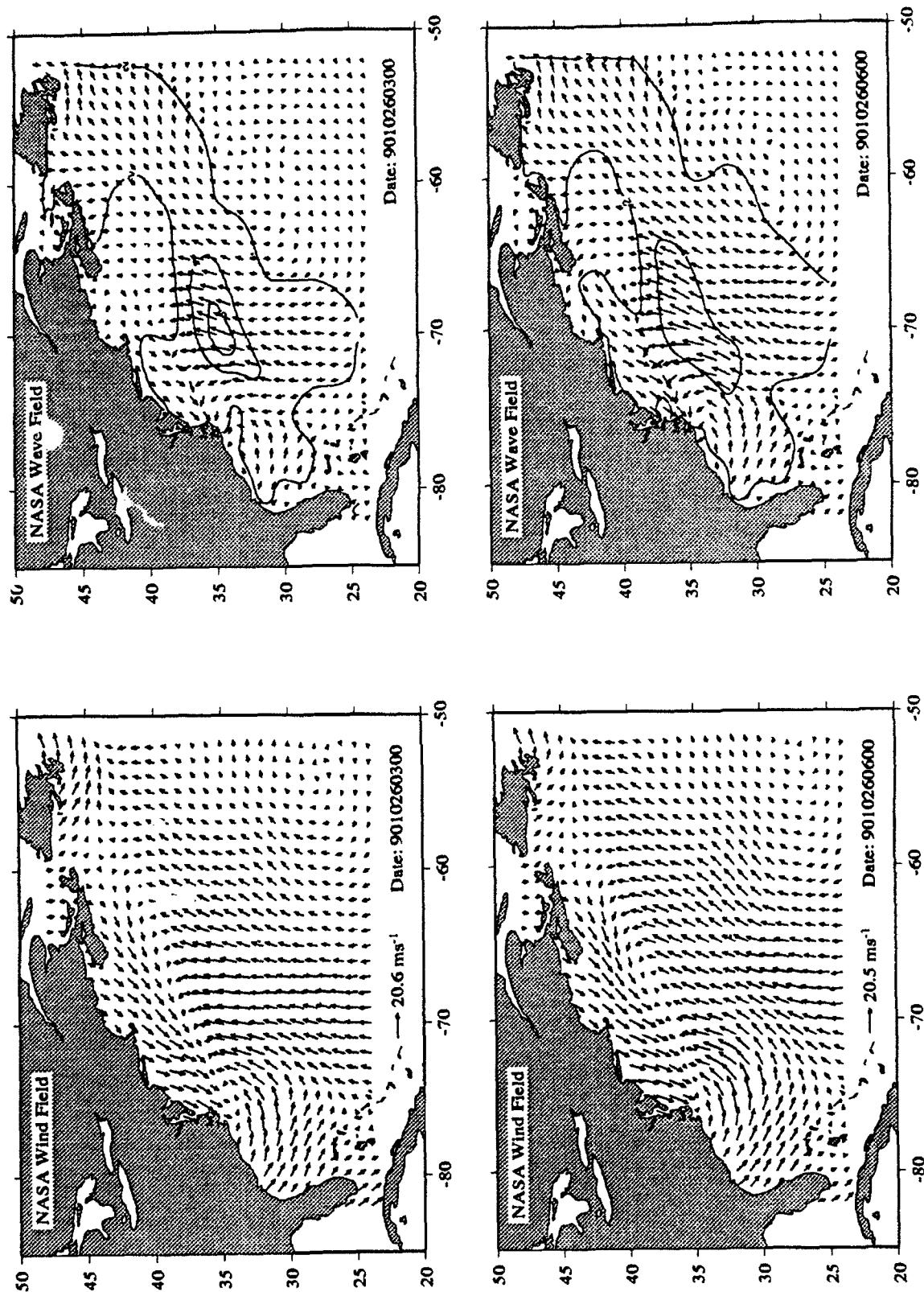
Custer diagrams are presented for the time period from 24 October 1990, 12:00 GMT to 28 October 1990, 12:00 GMT of the wind field and corresponding wave hindcasts. Note that the frequency of maps is every 3 hr from 26-28 October, which covers the major storm period.



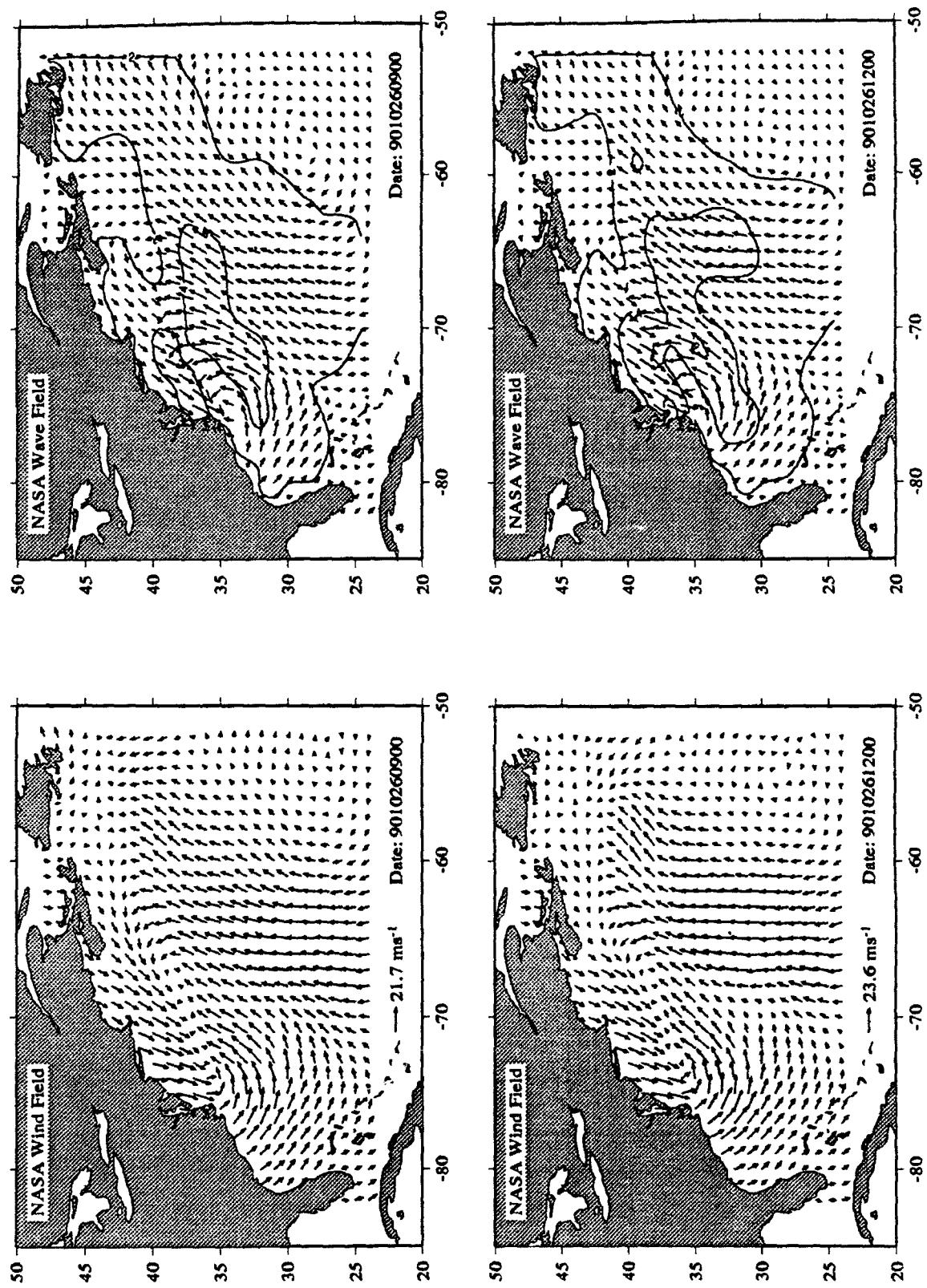


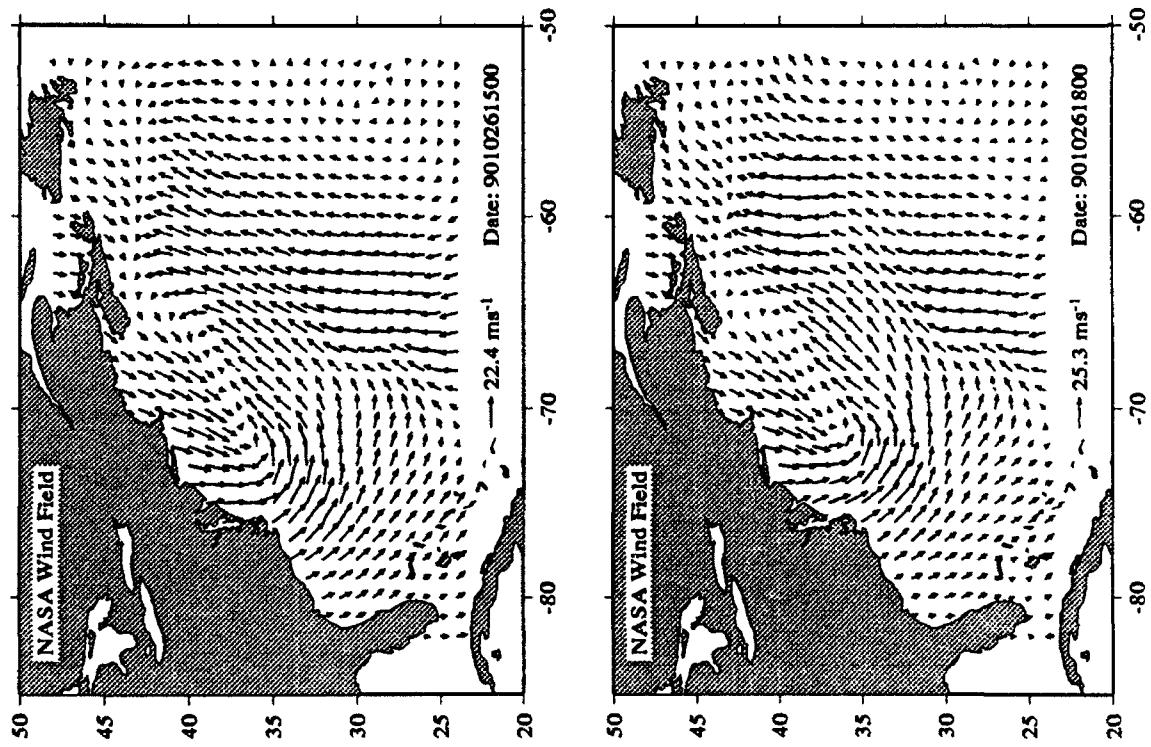
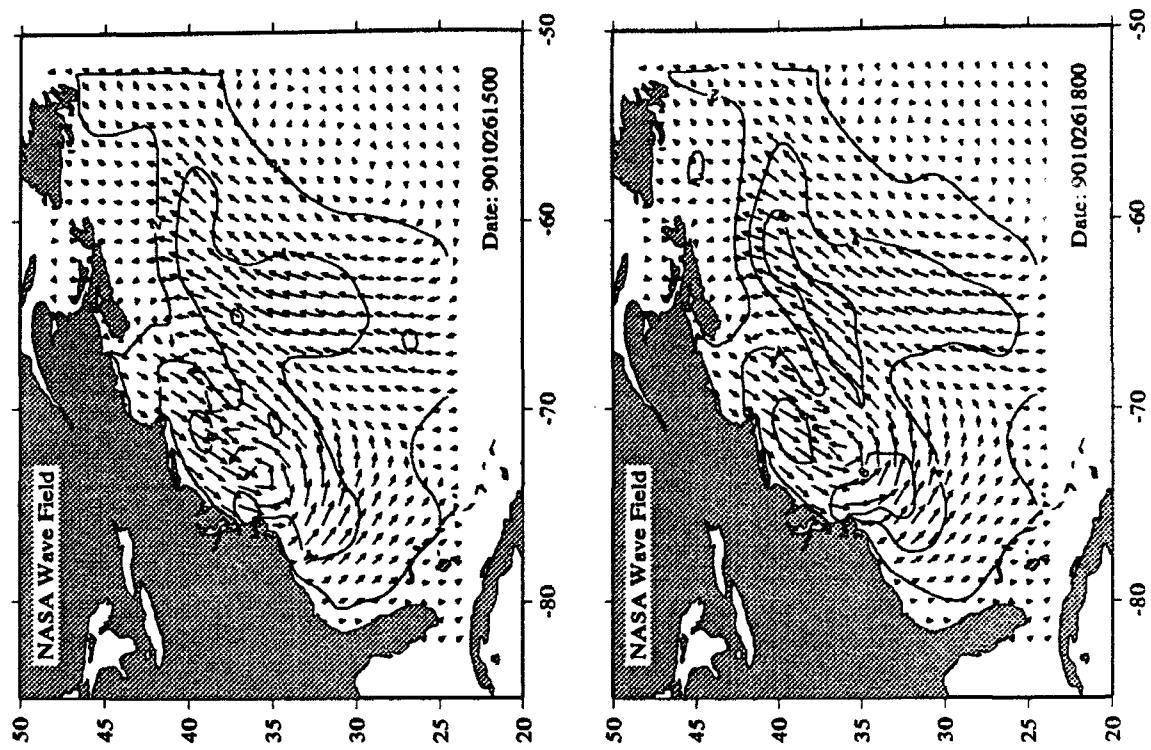
Appendix D Custer Diagrams of Wind fields and Wave Hindcasts

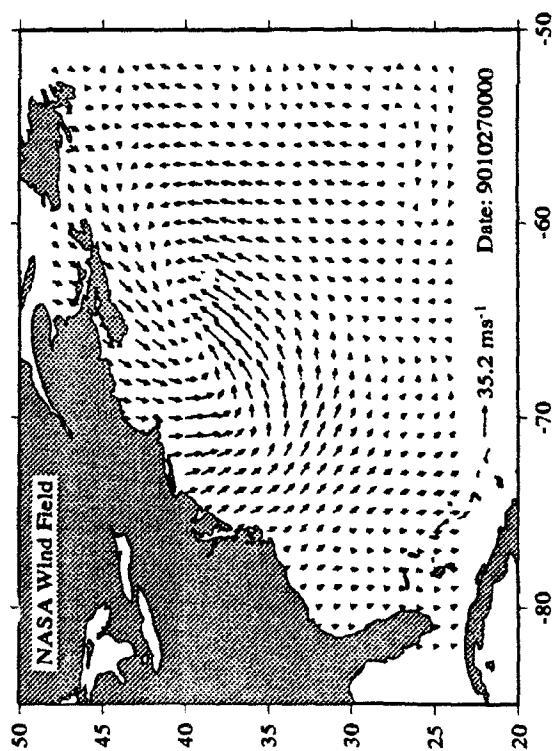
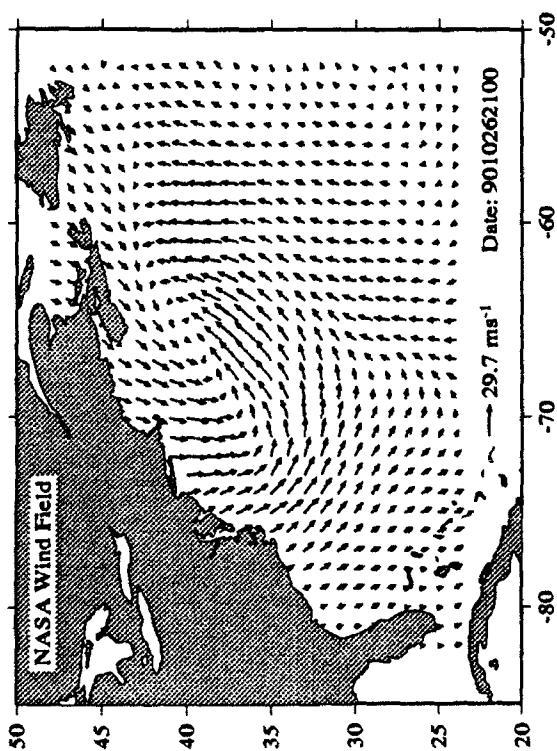
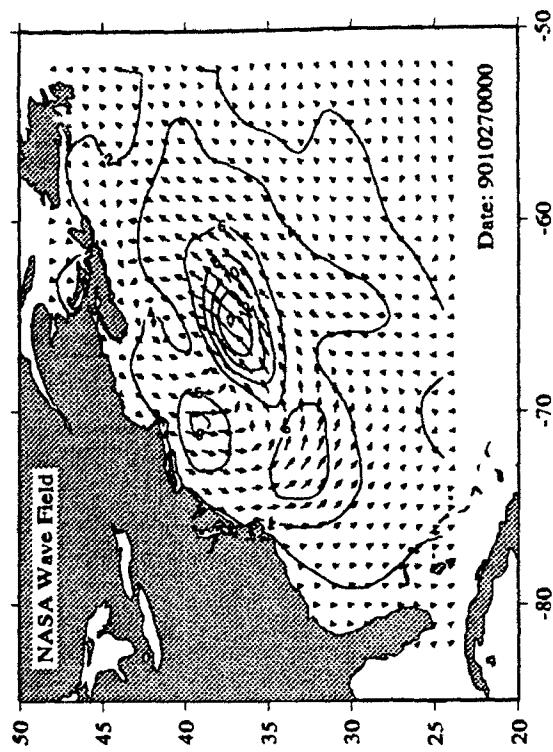
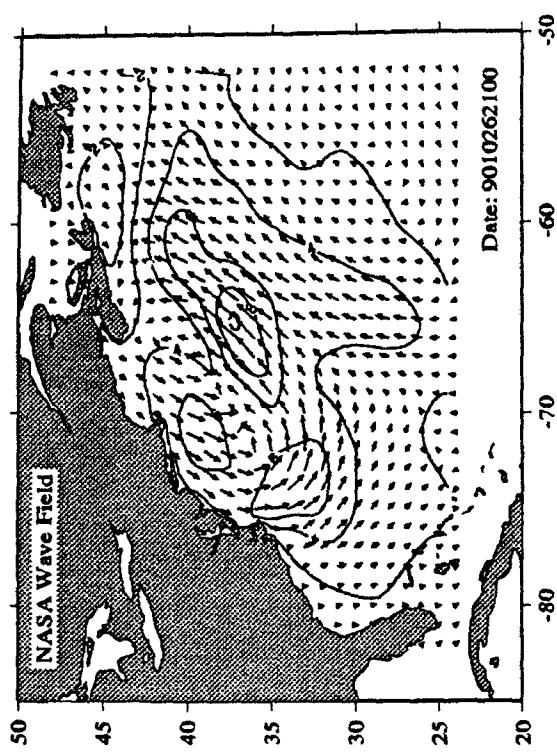


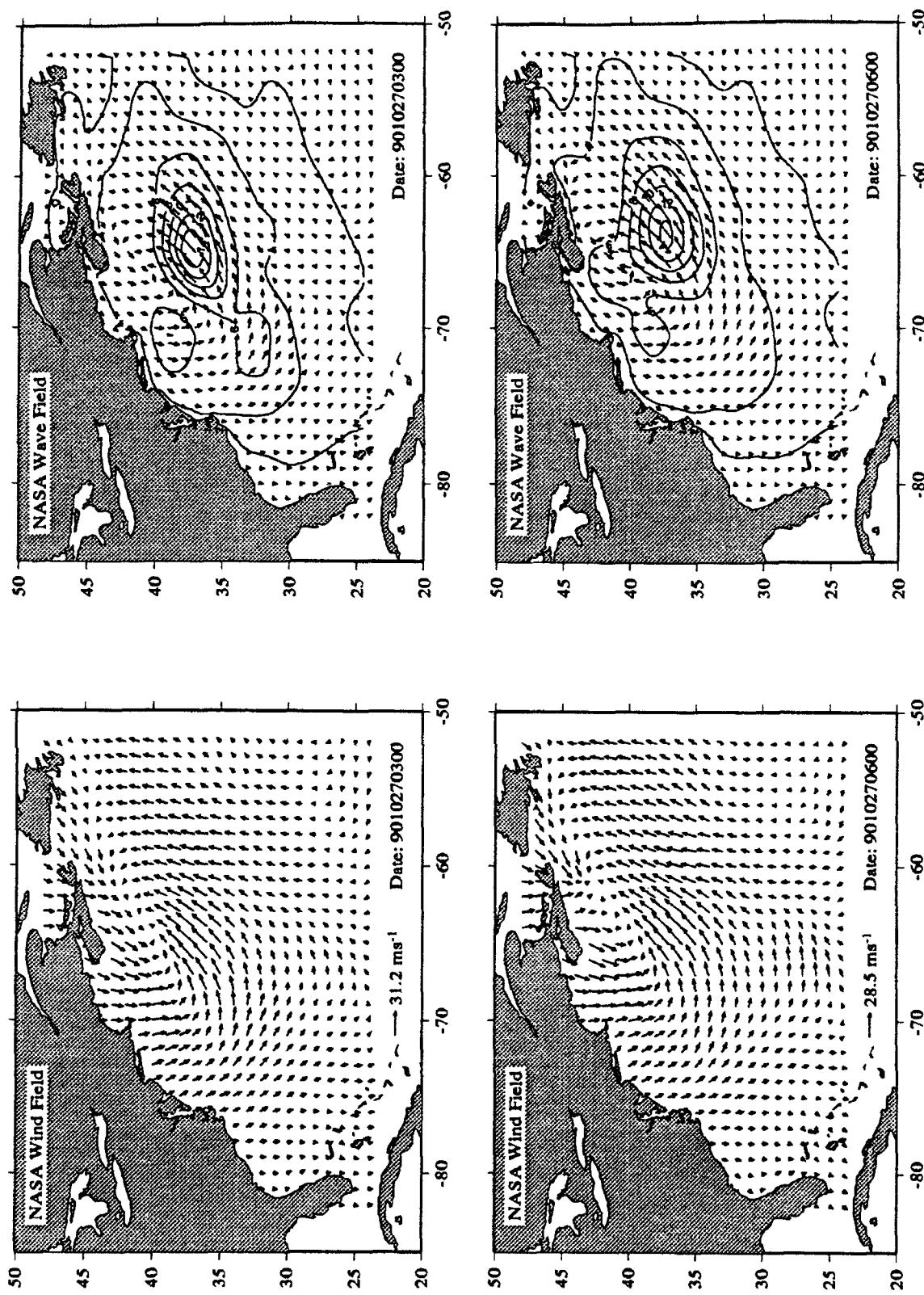


Appendix D Custer Diagrams of Wind fields and Wave Hindcasts

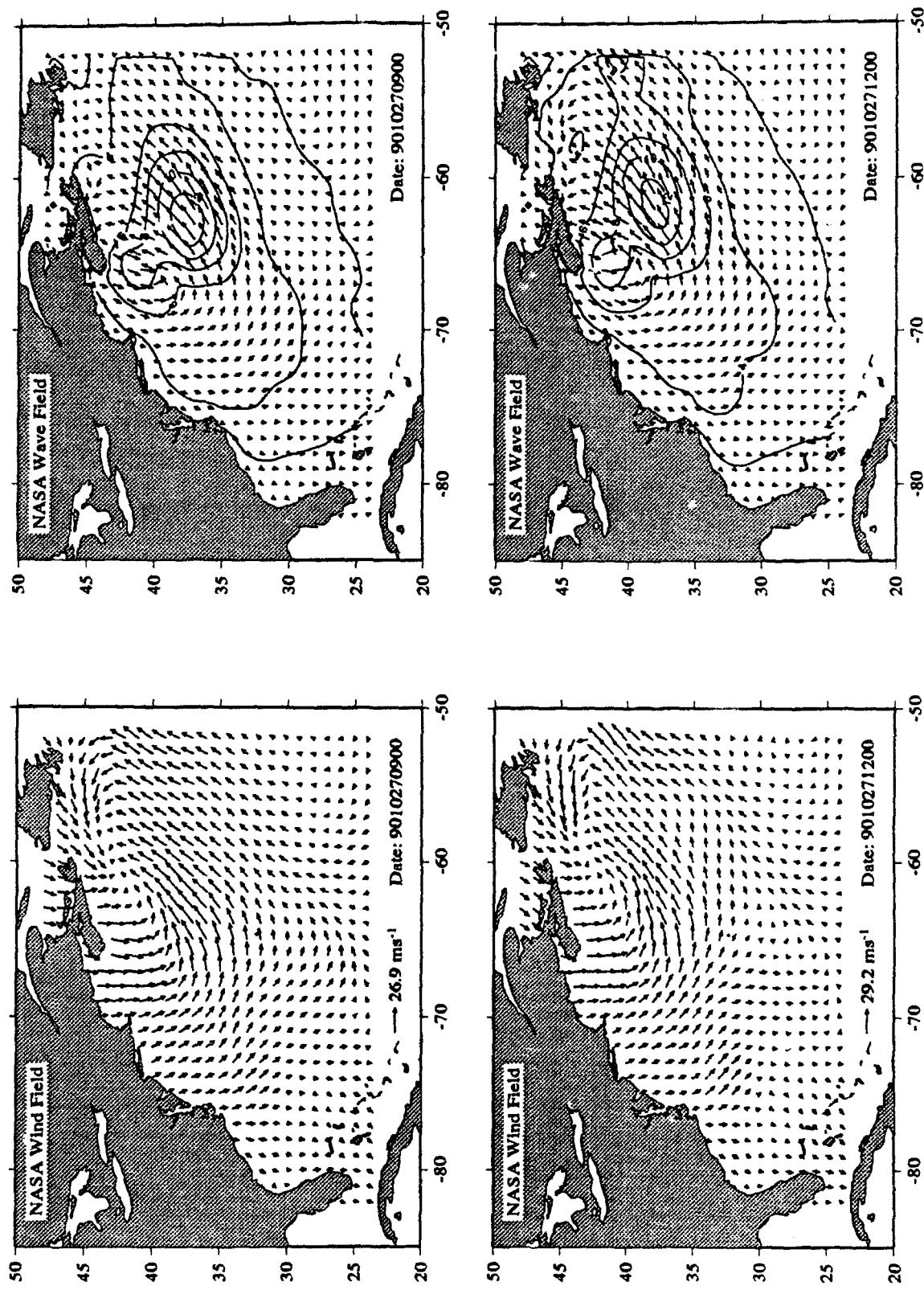


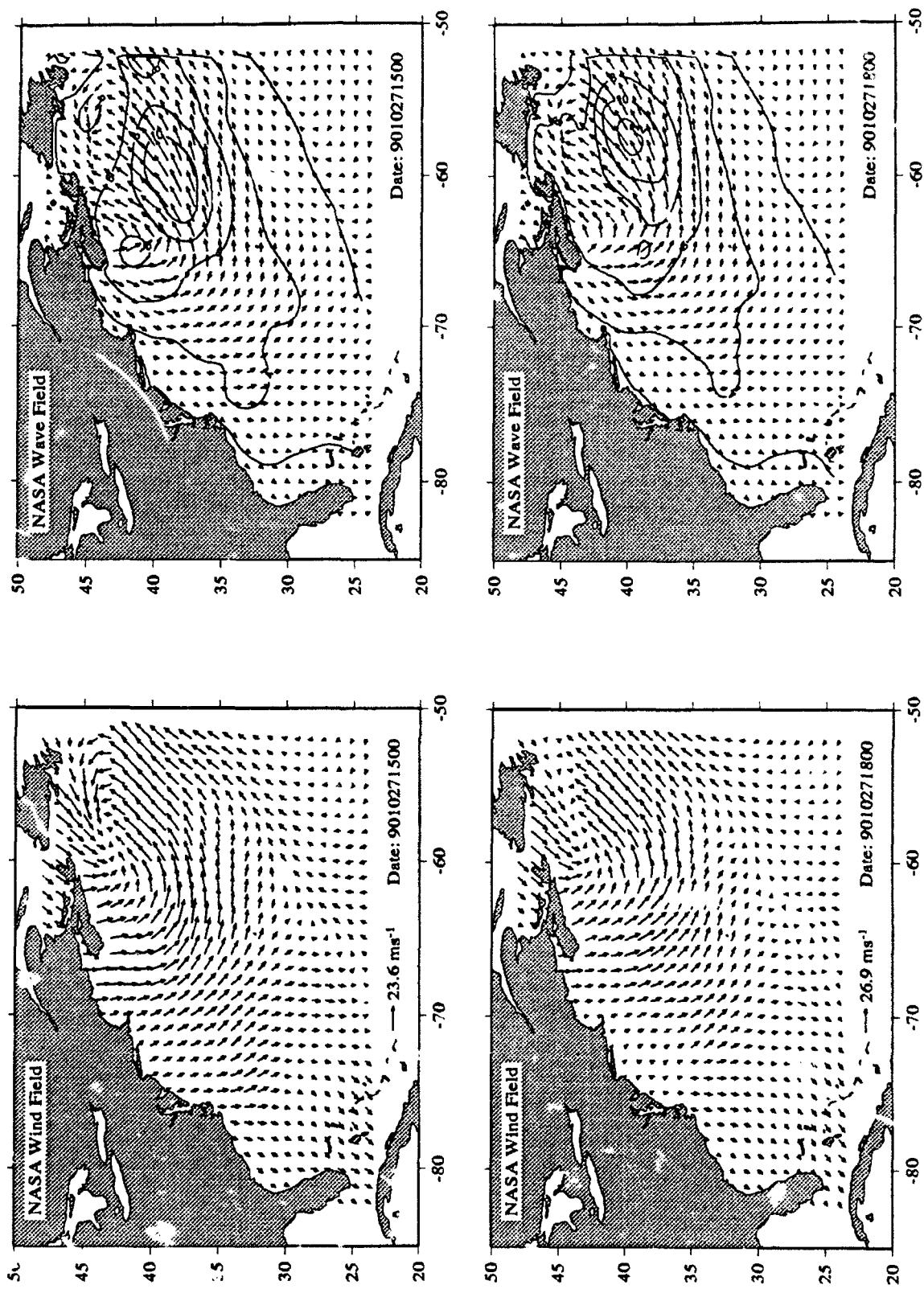


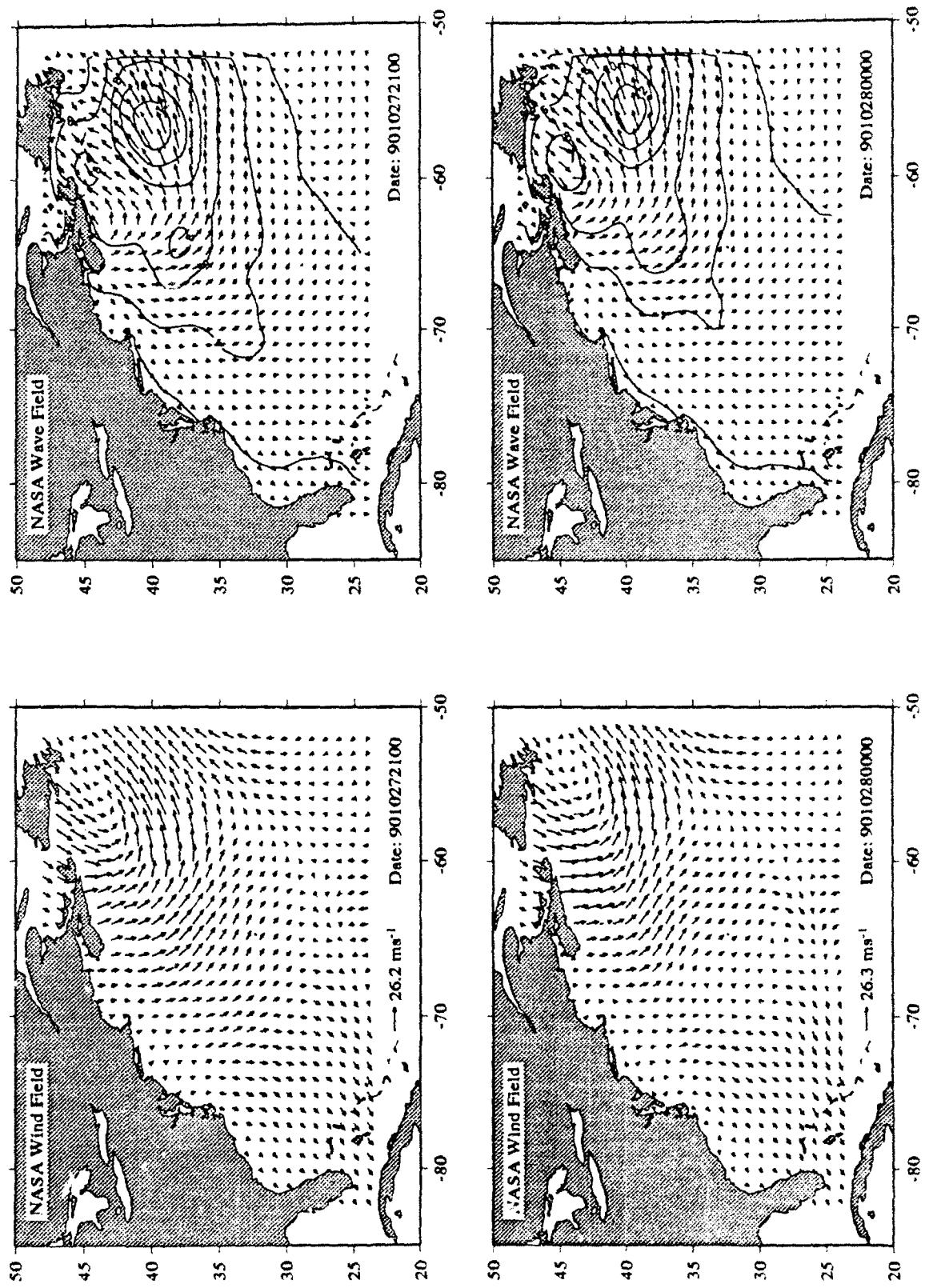


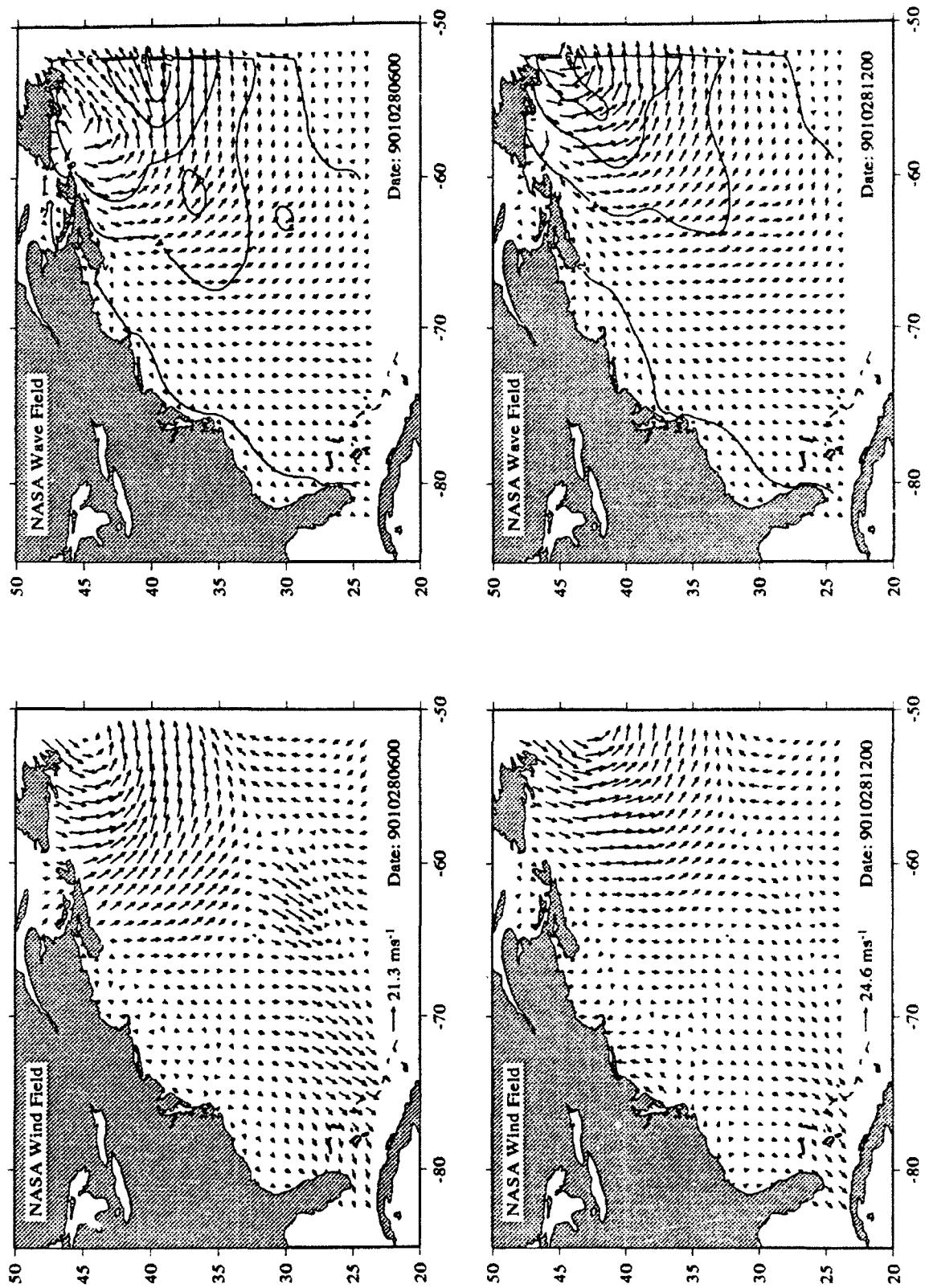


Appendix D Custer Diagrams of Wind fields and Wave Hindcasts





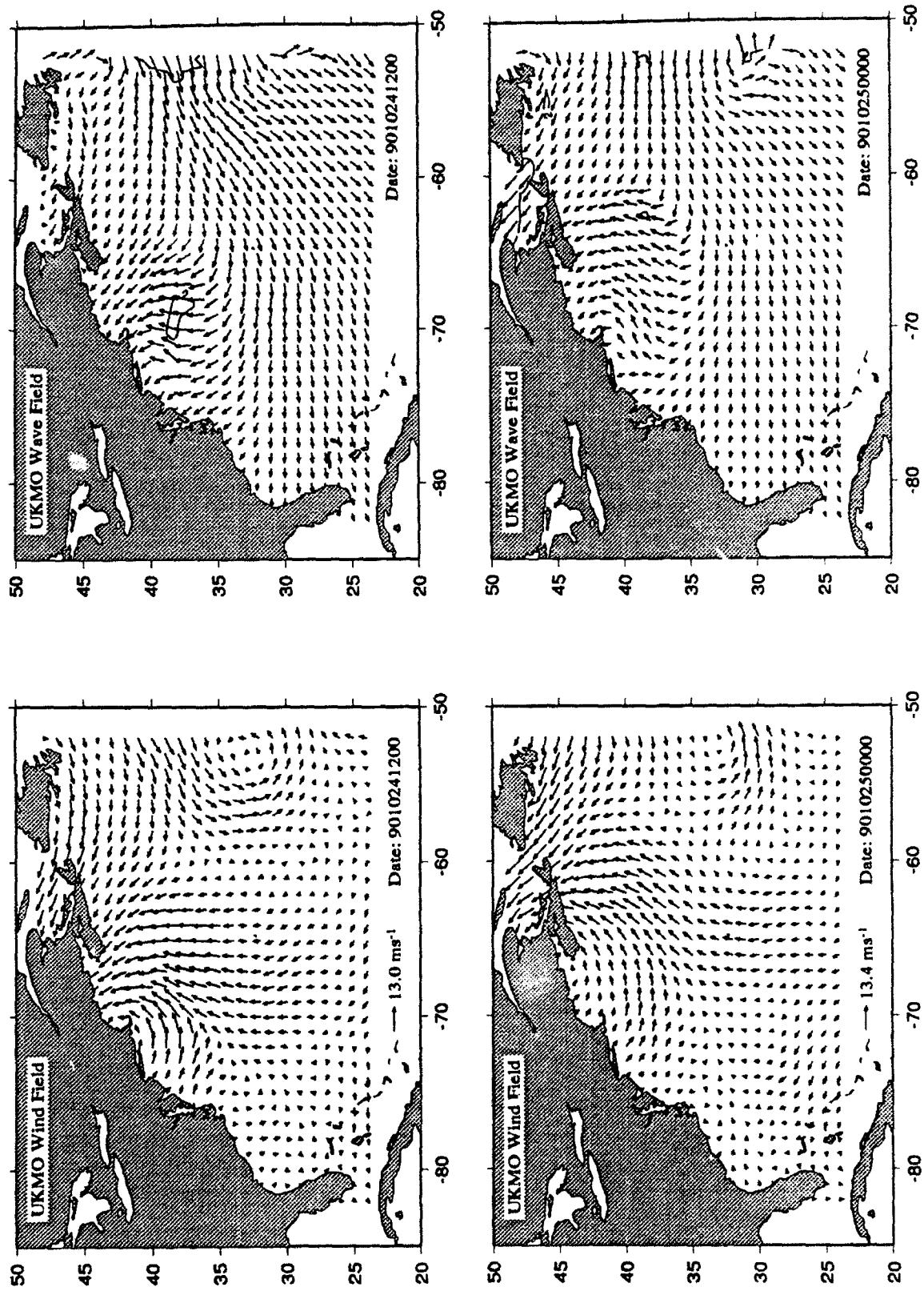


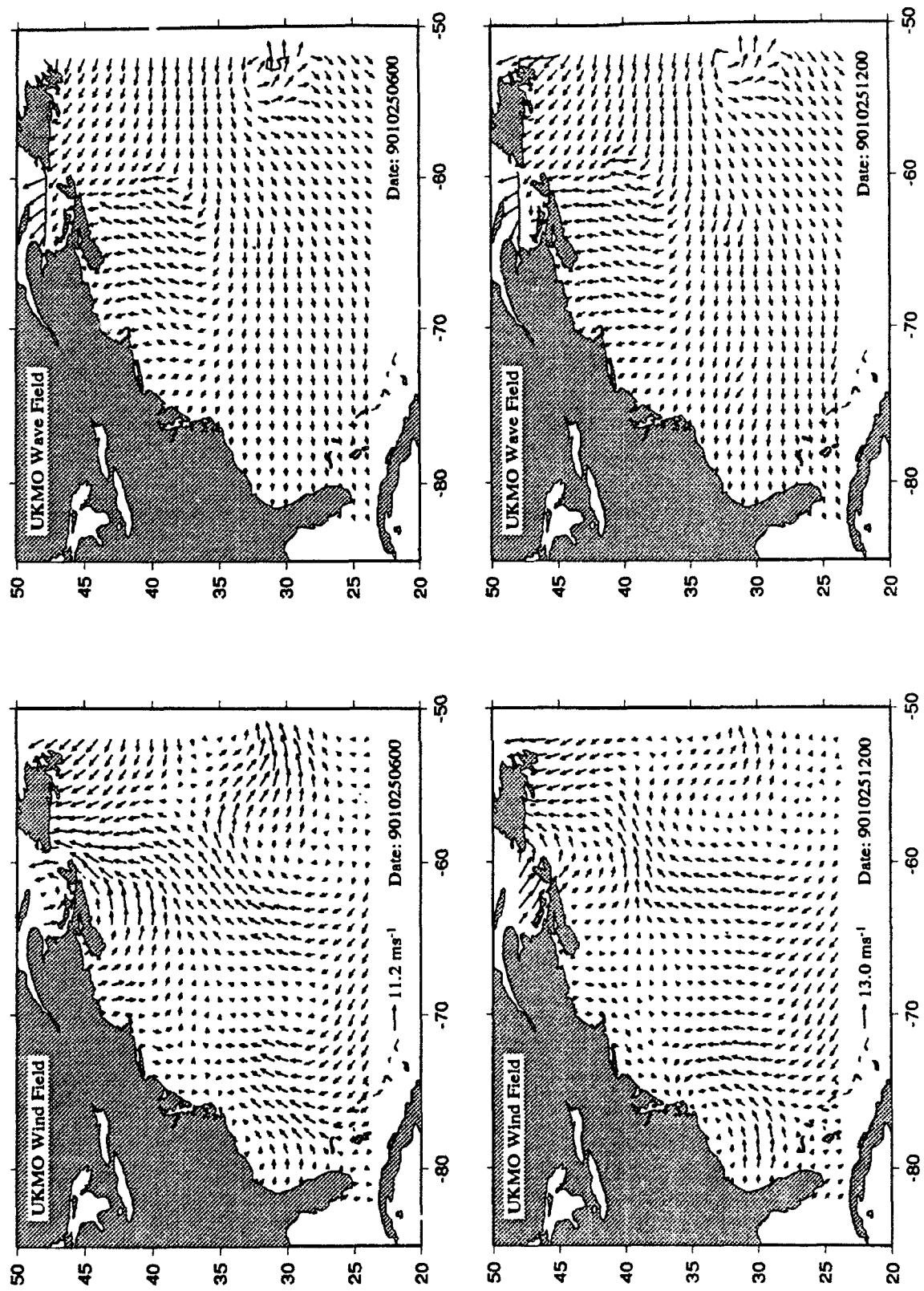


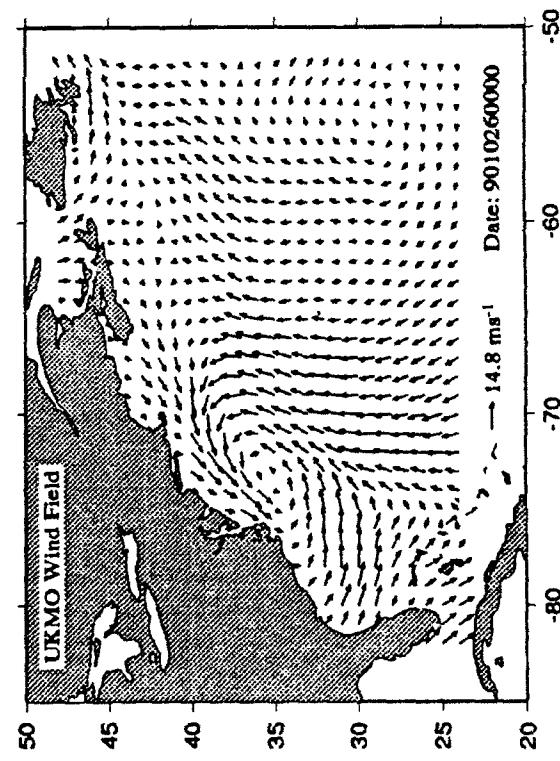
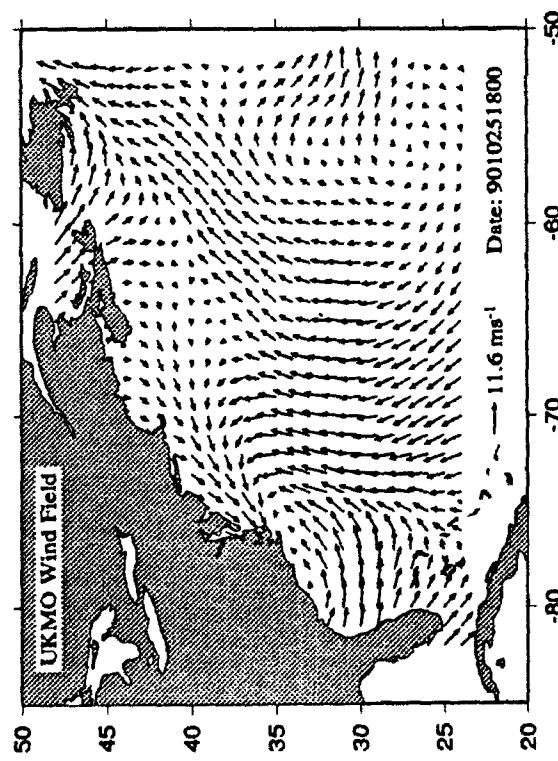
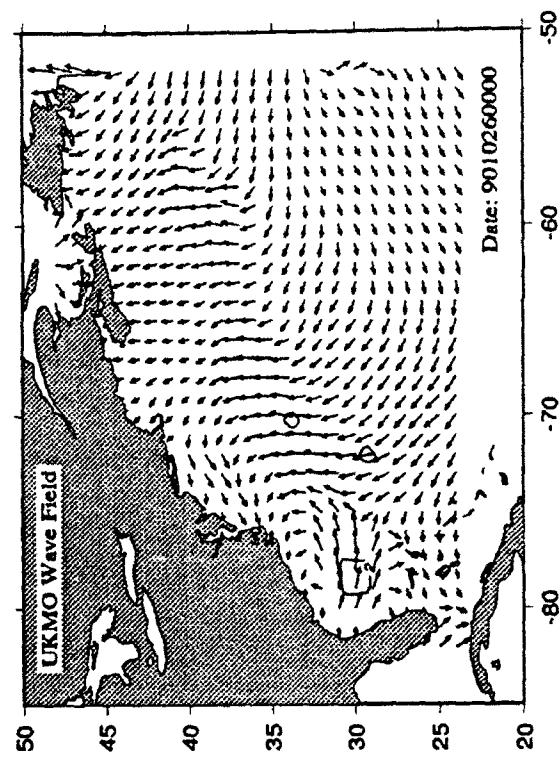
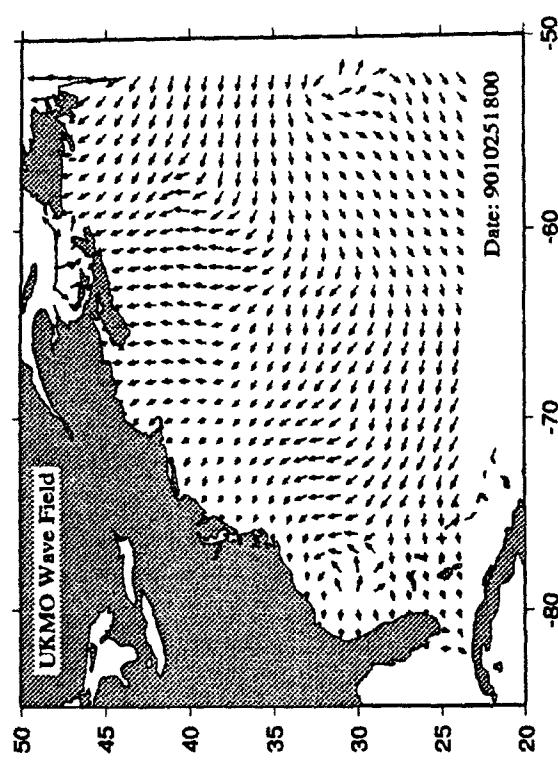
Appendix D Custer Diagrams of Wind fields and Wave Hindcasts

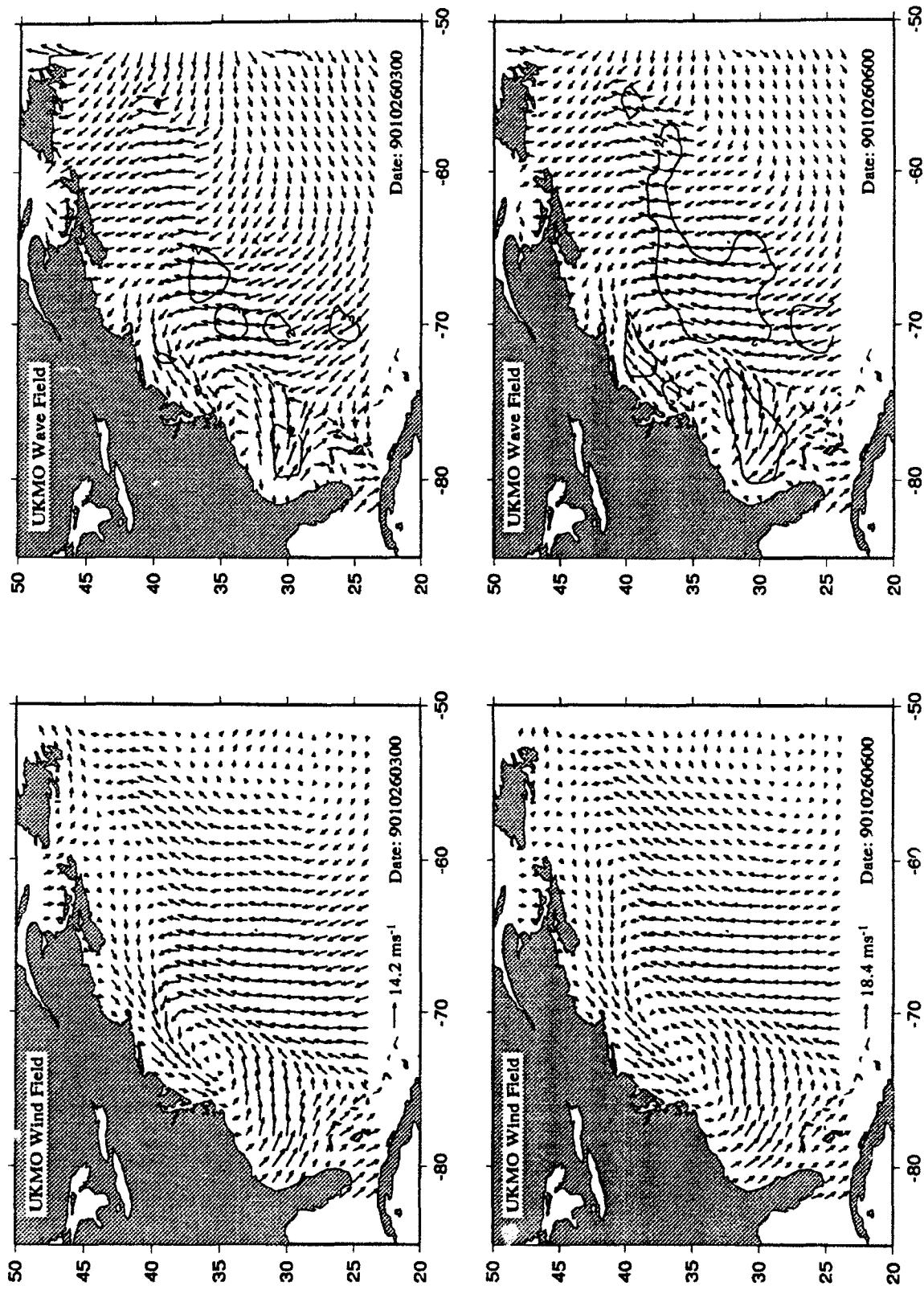
D.6: United Kingdom Meteorological Office (UKMO)

Custer diagrams are presented for the time period from 24 October 1990, 12:00 GMT to 28 October 1990, 12:00 GMT of the wind field and corresponding wave hindcasts. Note that the frequency of maps is every 3 hr from 26-28 October, which covers the major storm period.

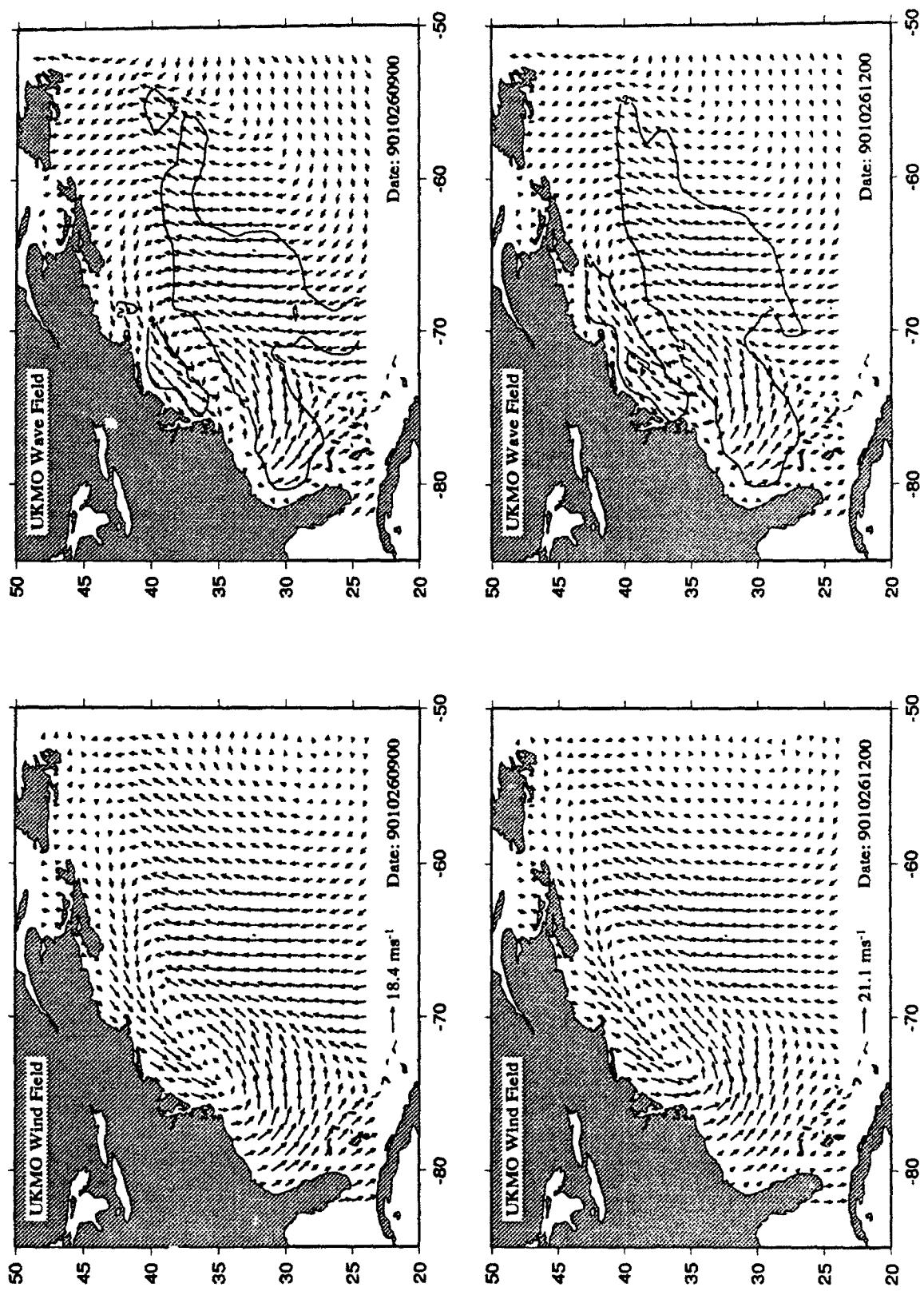


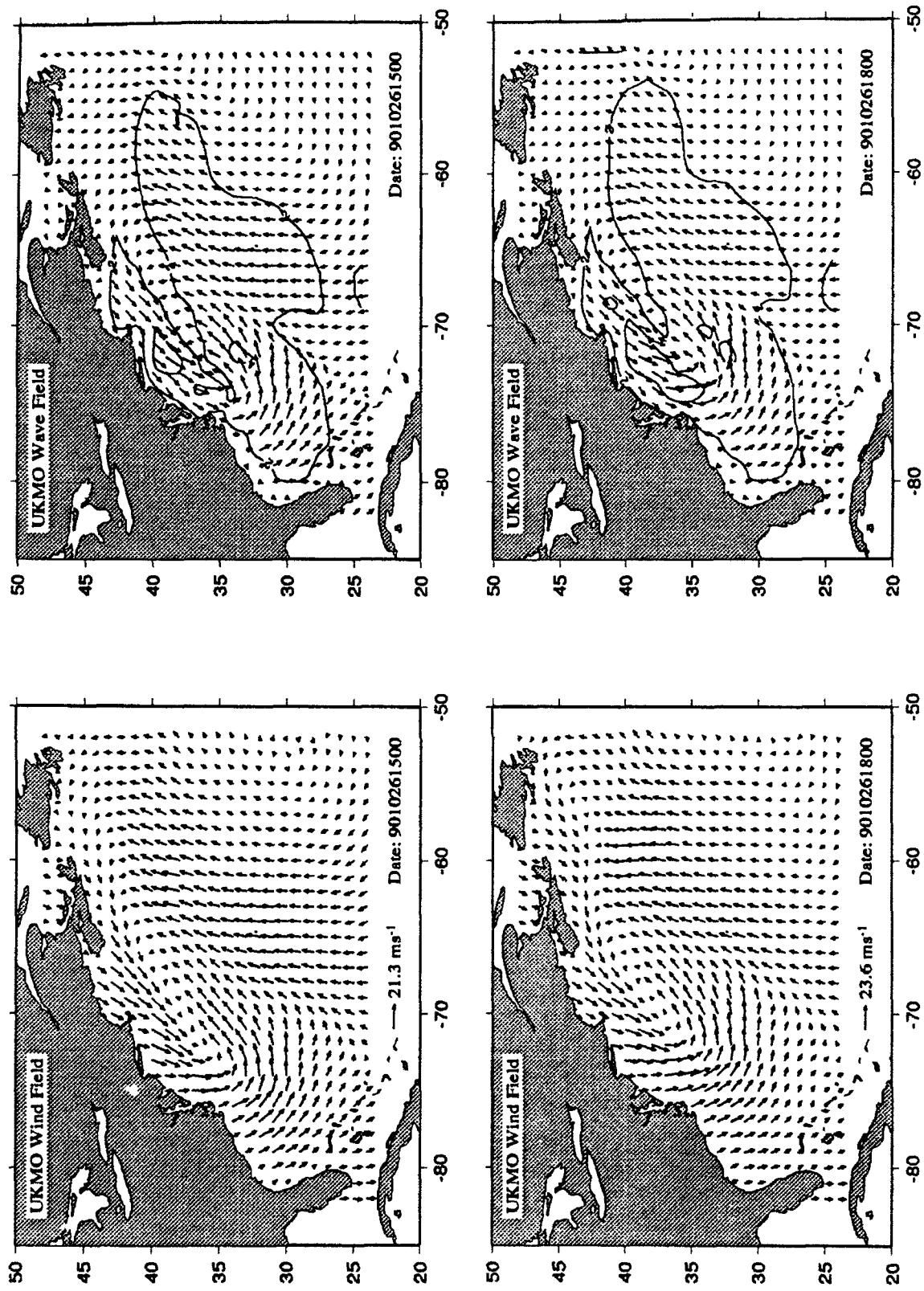


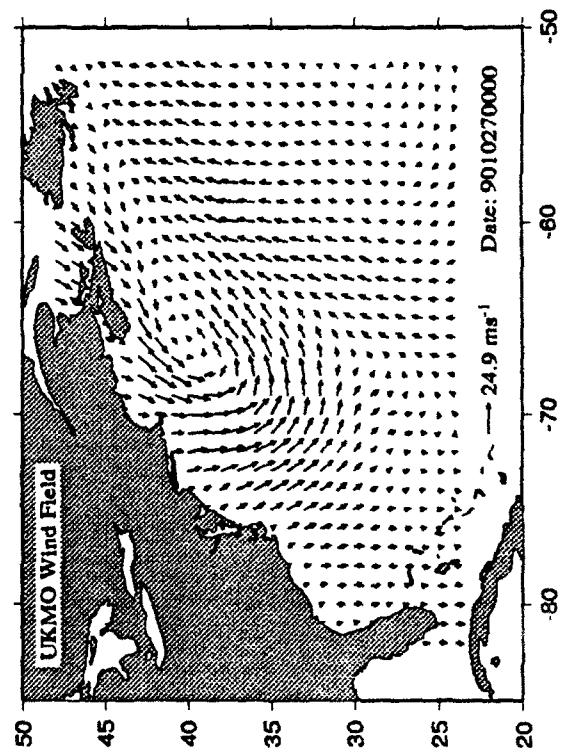
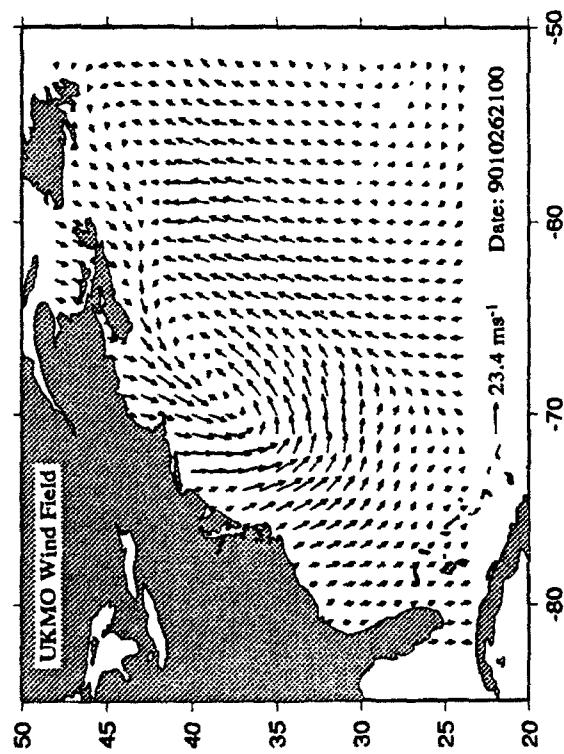
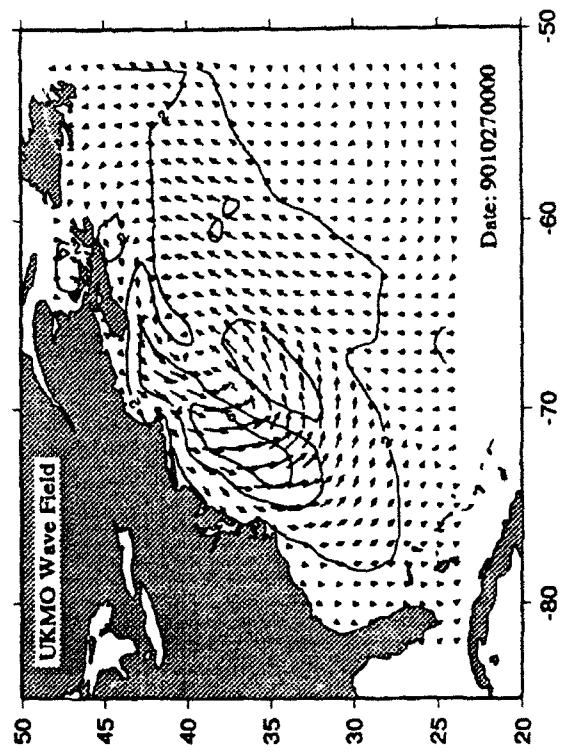
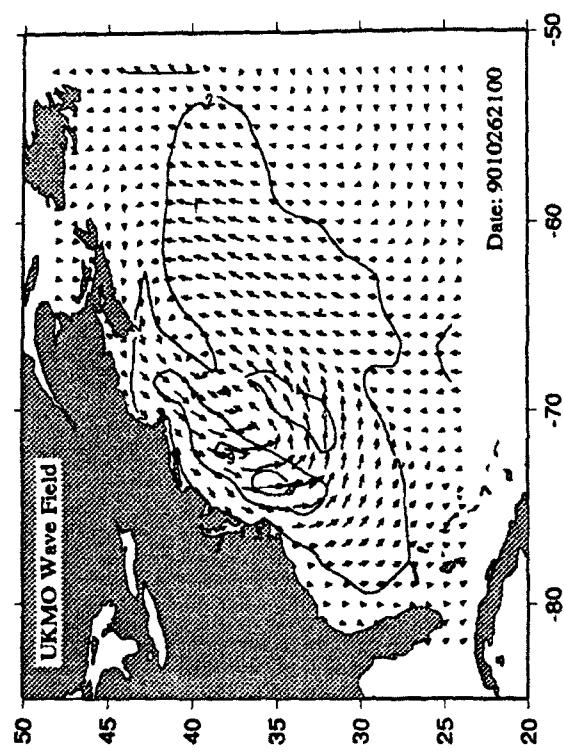


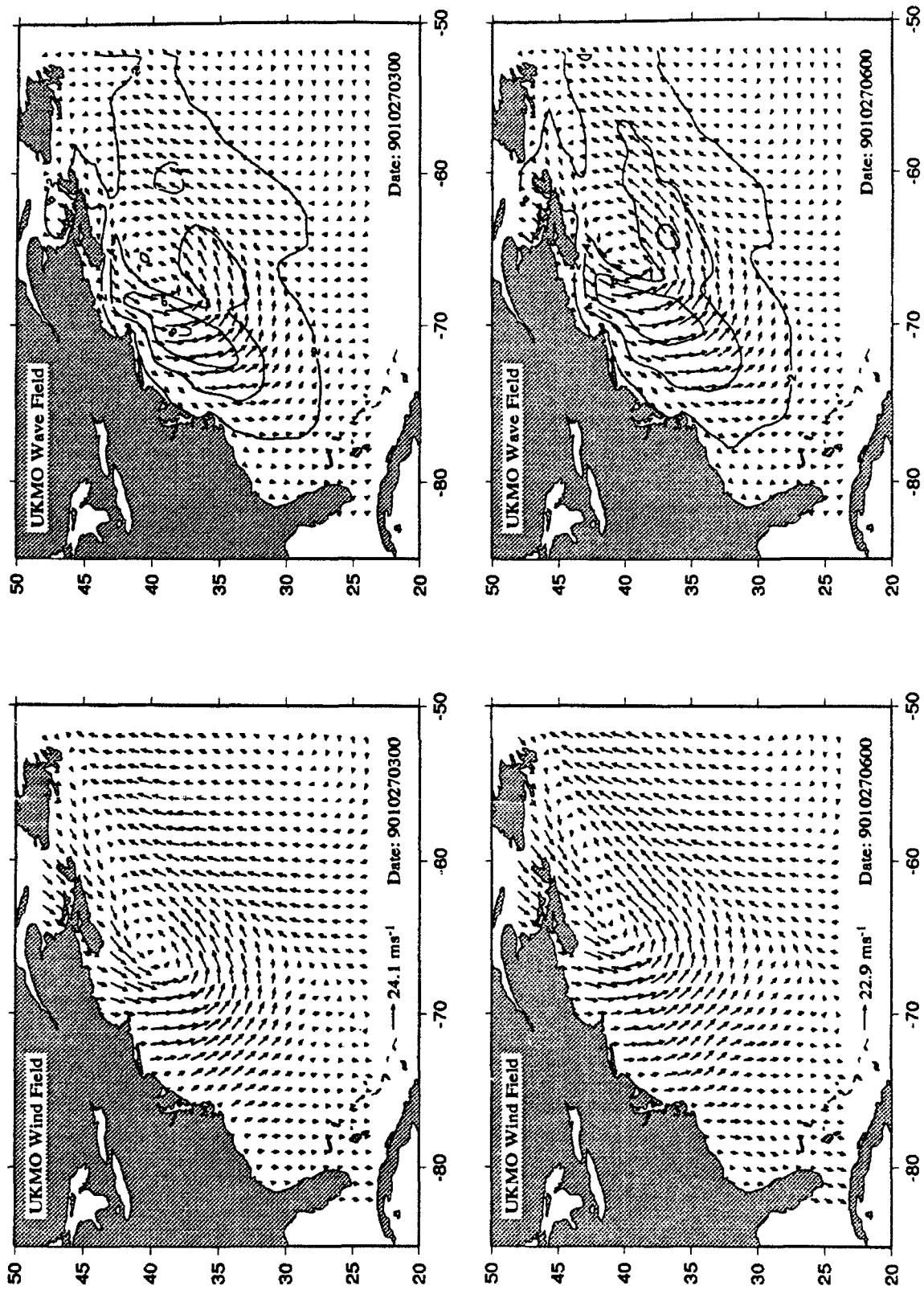


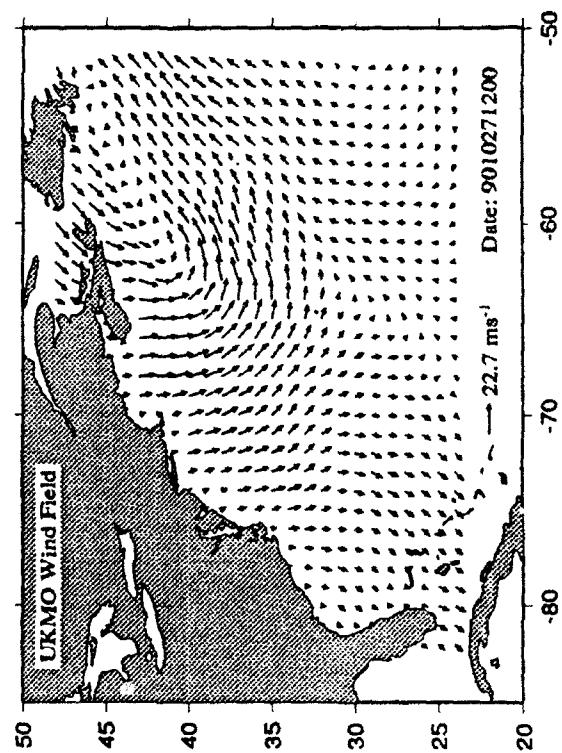
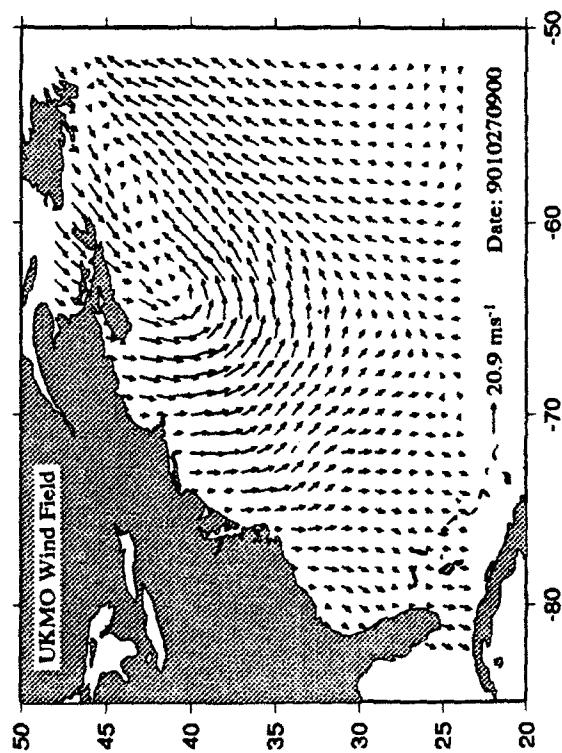
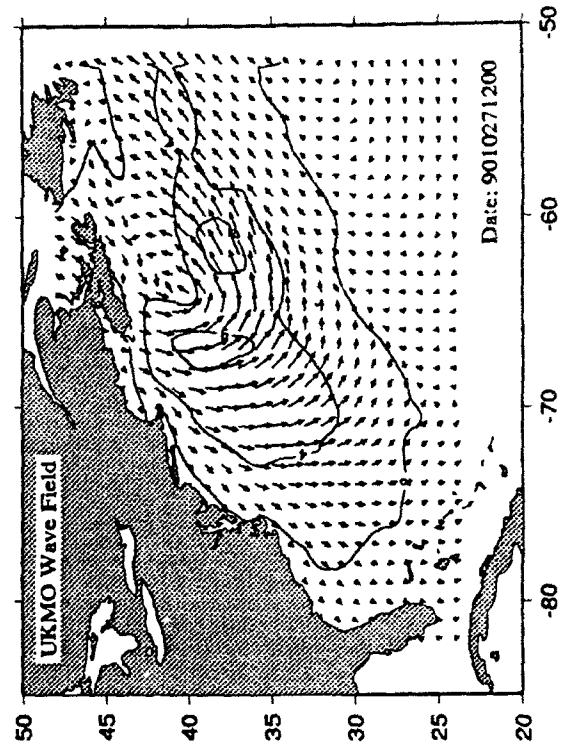
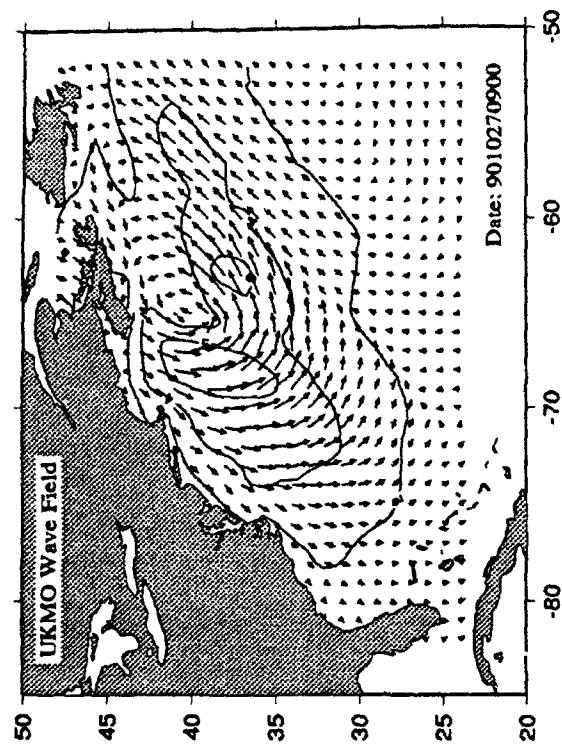
Appendix D Cluster Diagrams of Wind fields and Wave Hindcasts

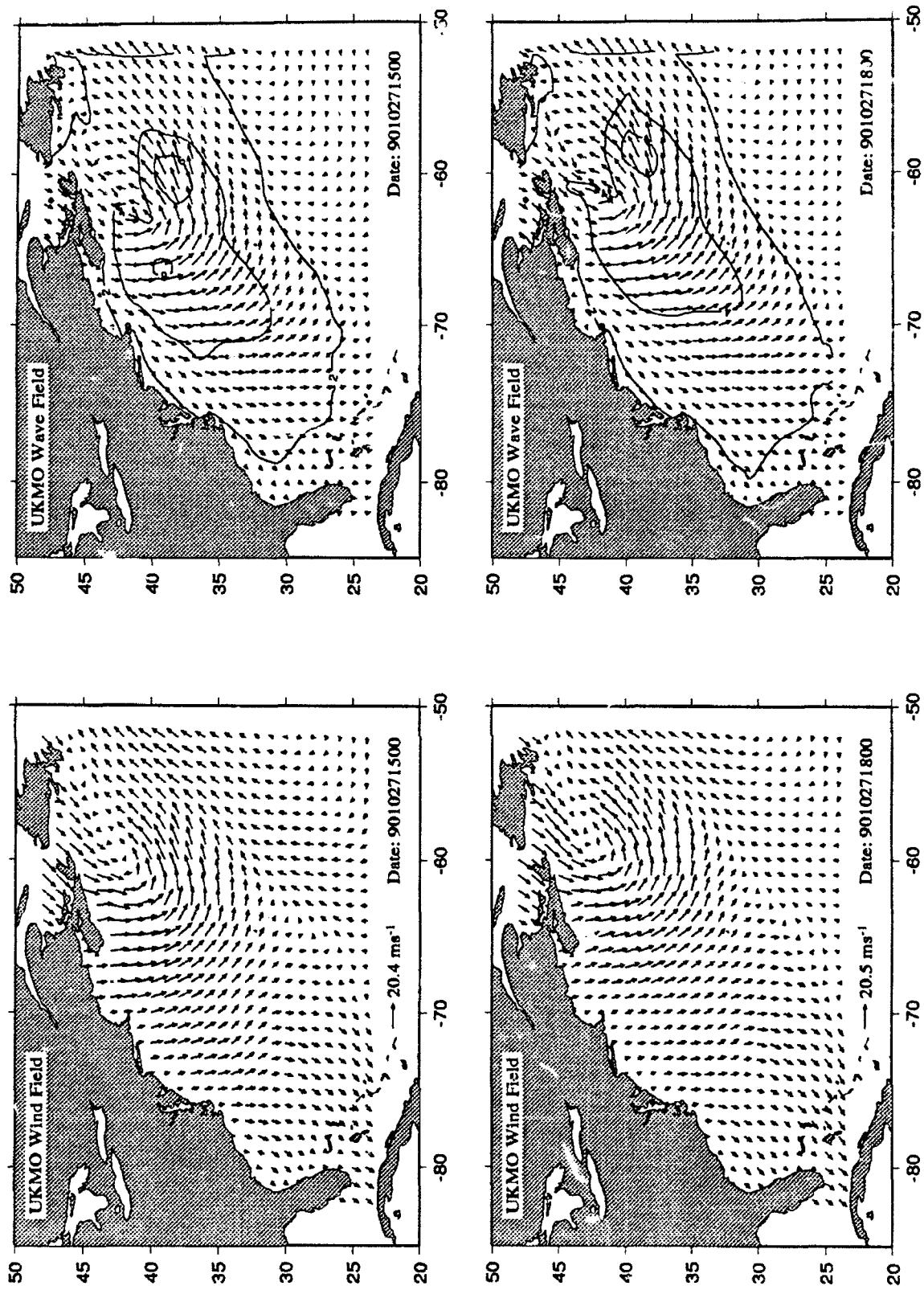




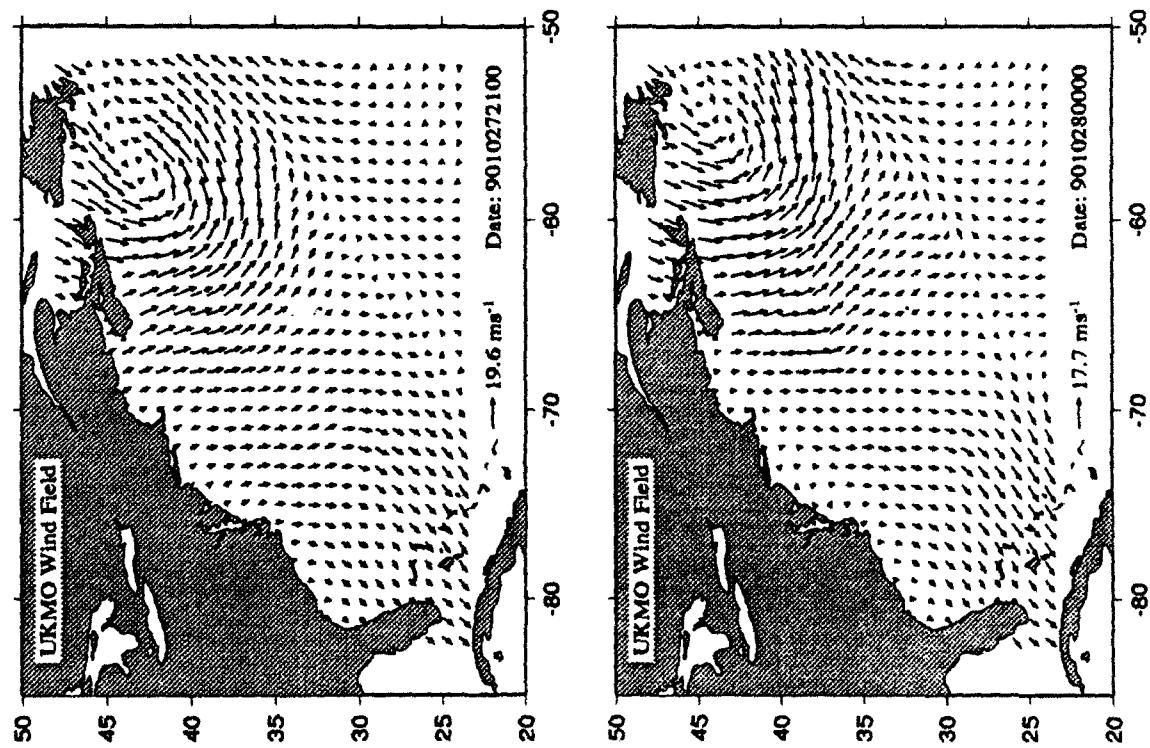
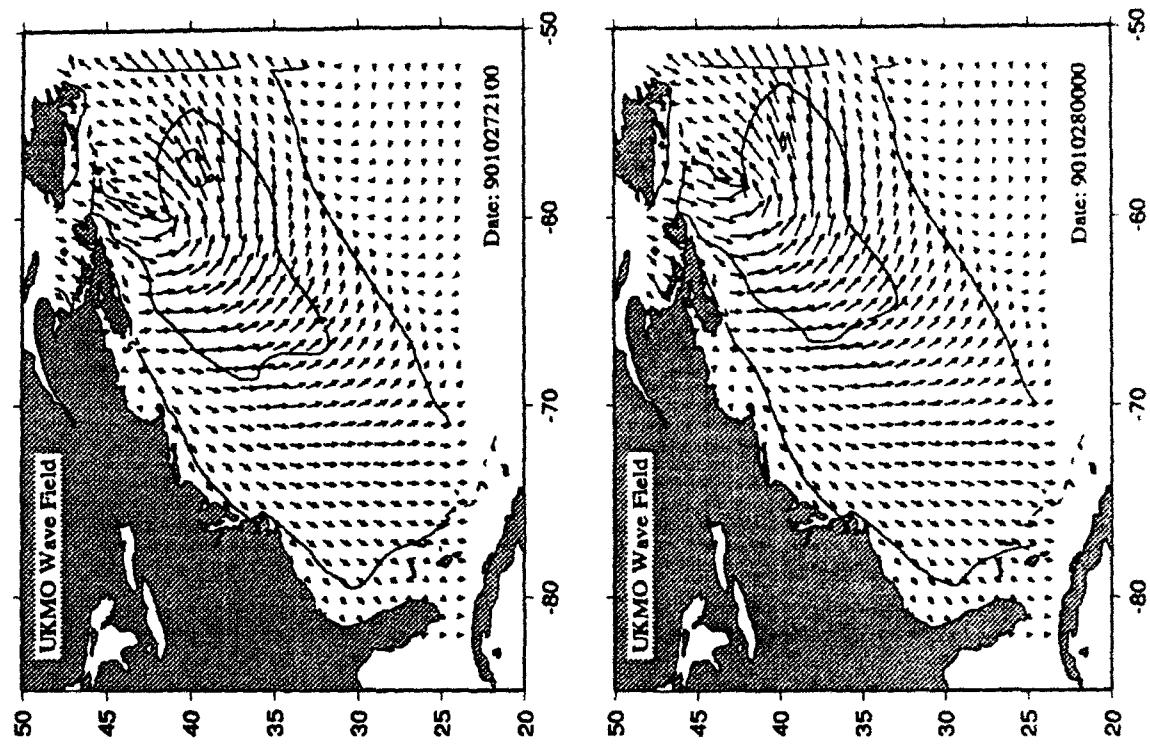


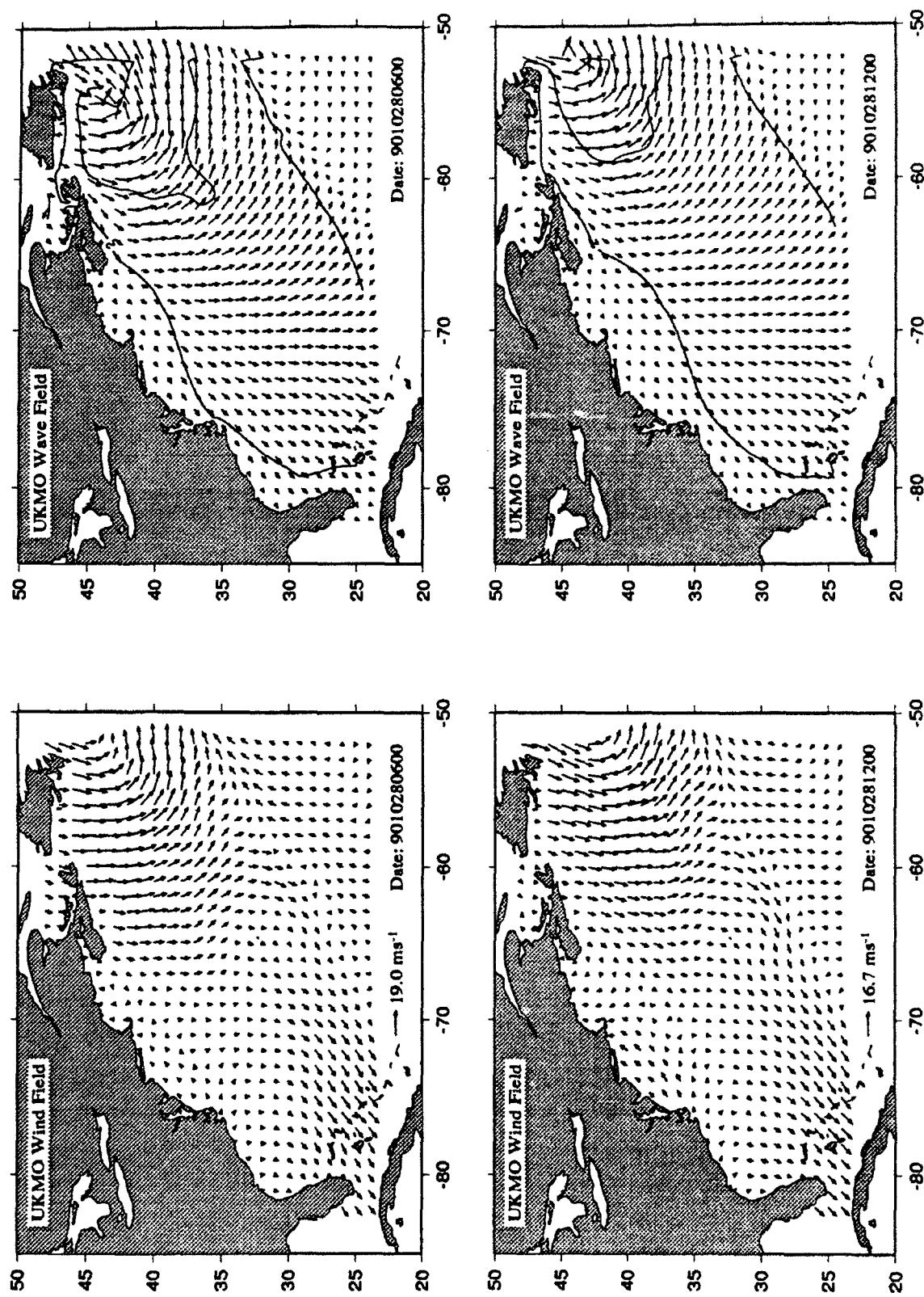






Appendix D Custer Diagrams of Wind fields and Wave Hindcasts

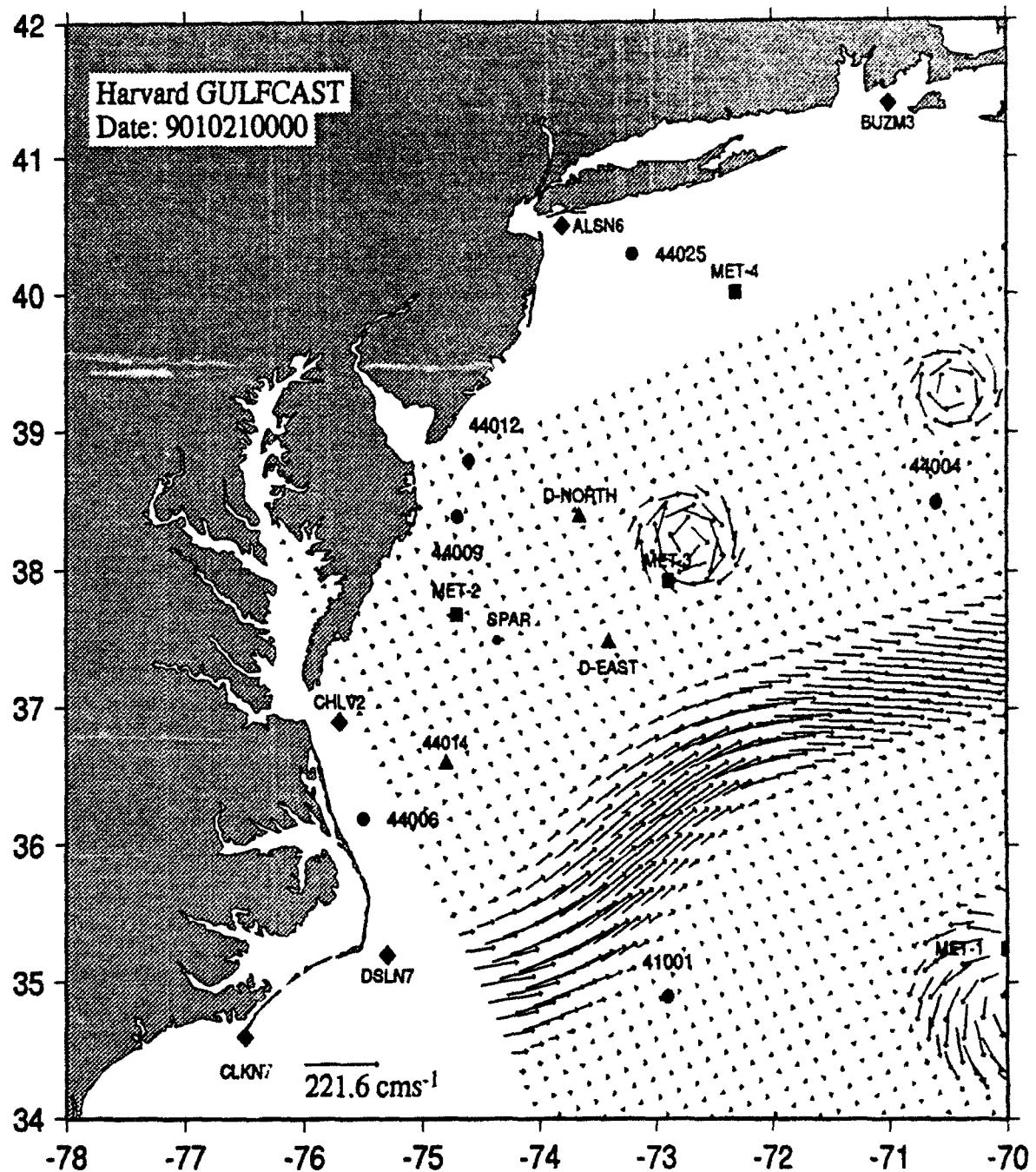


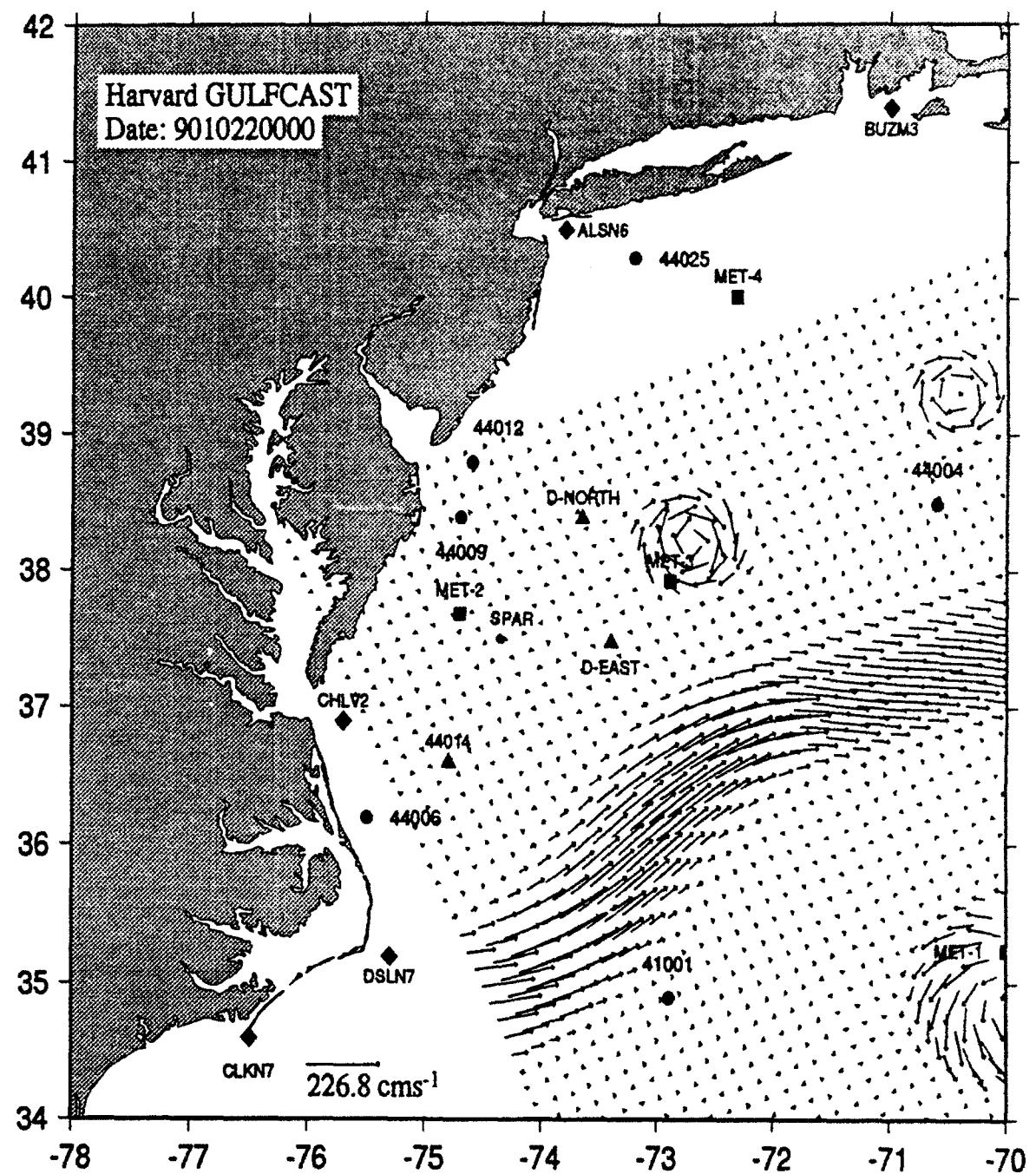


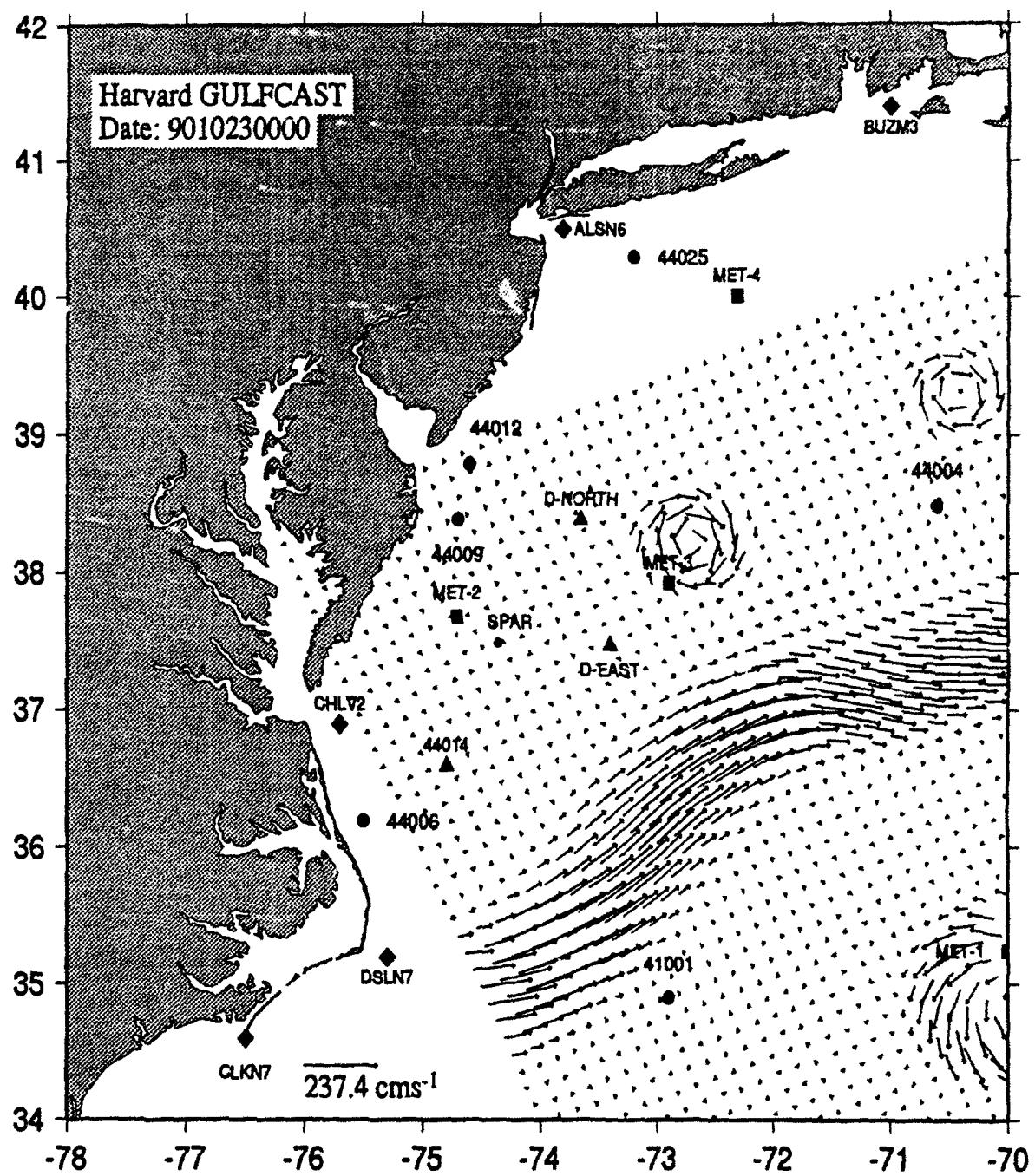
Appendix D Custer Diagrams of Wind fields and Wave Hindcasts

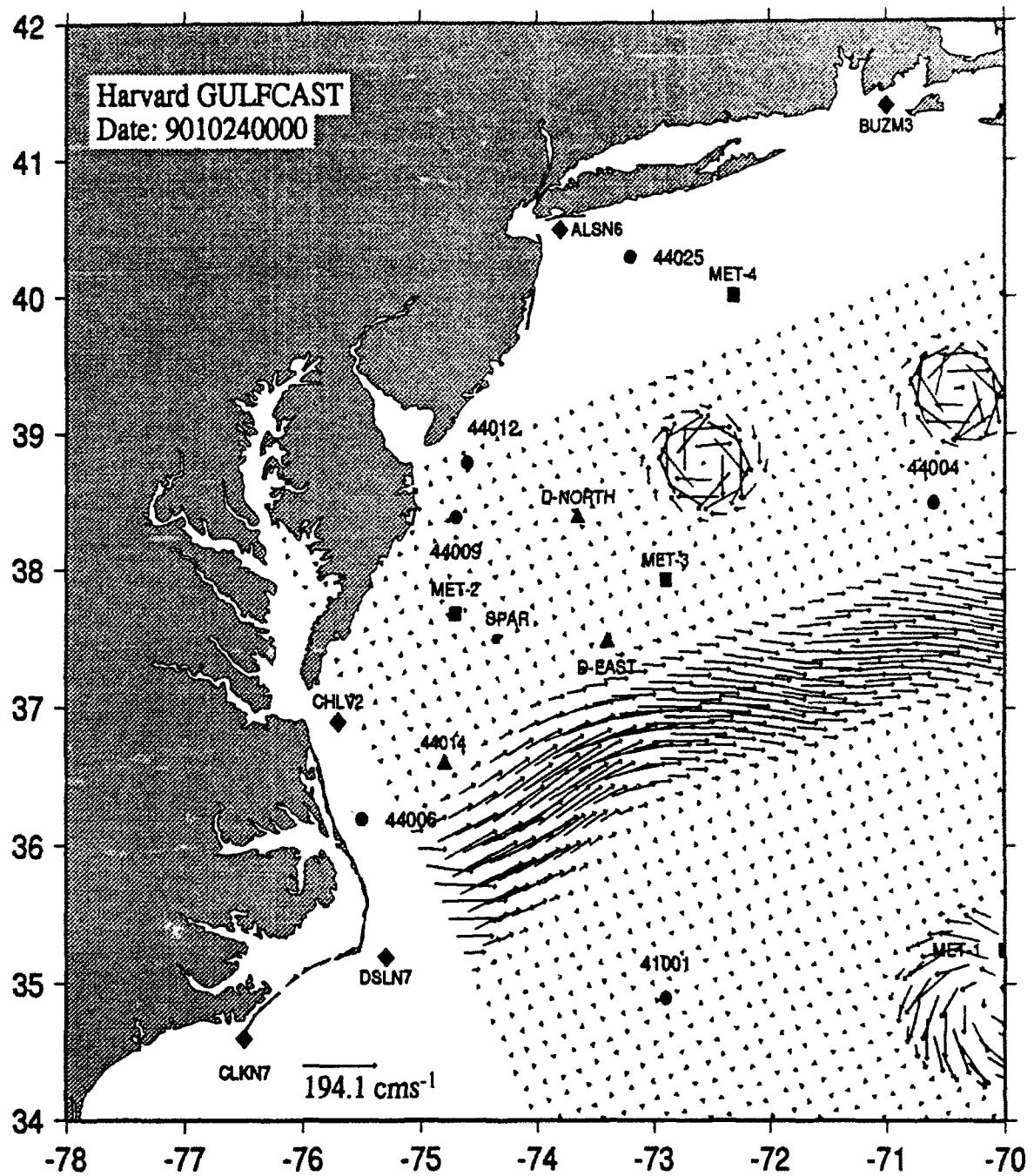
Appendix E: Custer Diagrams of Surface Current Fields

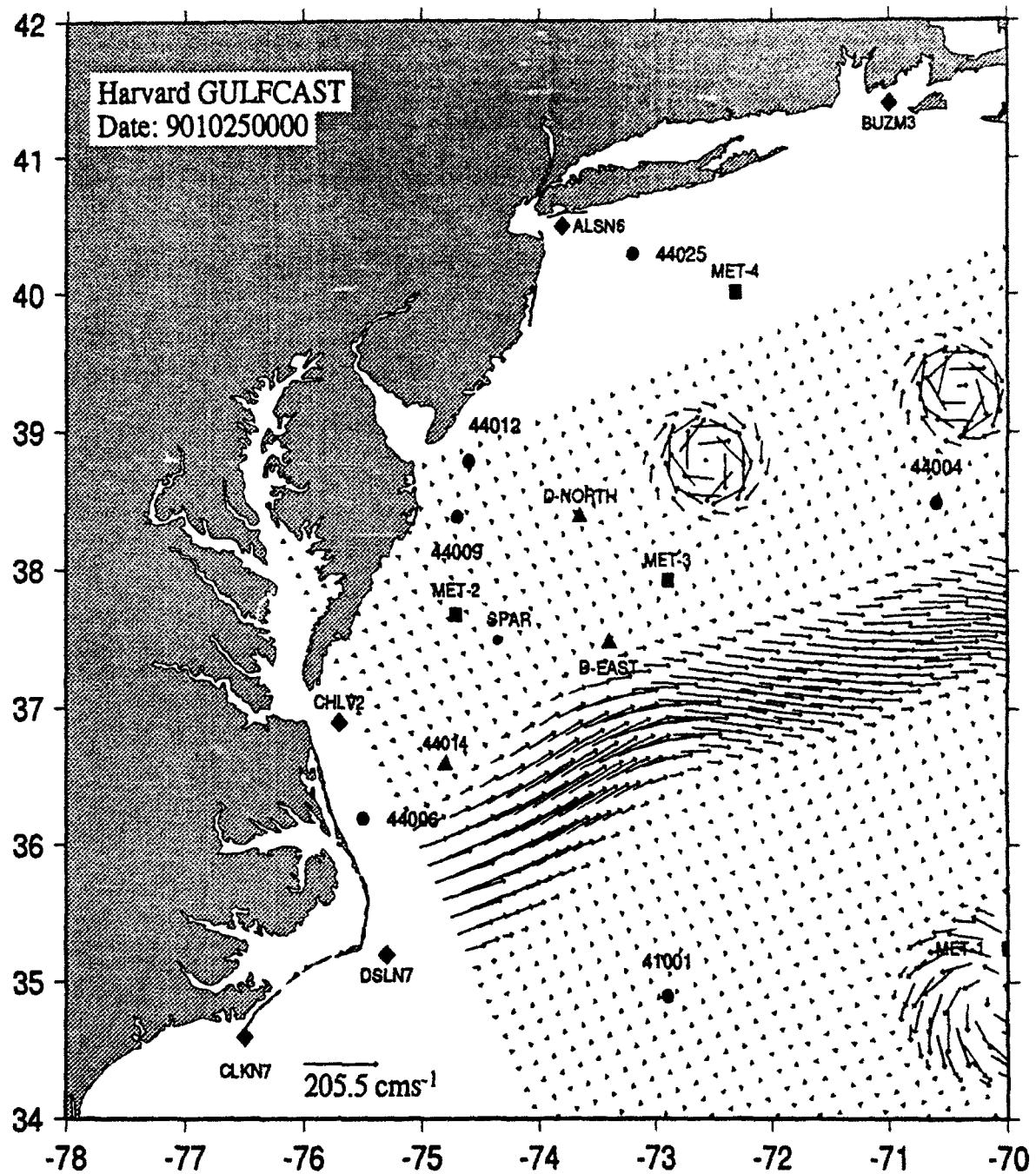
Daily maps of the surface current fields from the Harvard "GULFCAST" feature model are presented in this appendix beginning at 20 October 1990, 00:00 GMT to 31 October 1990, 00:00 GMT.

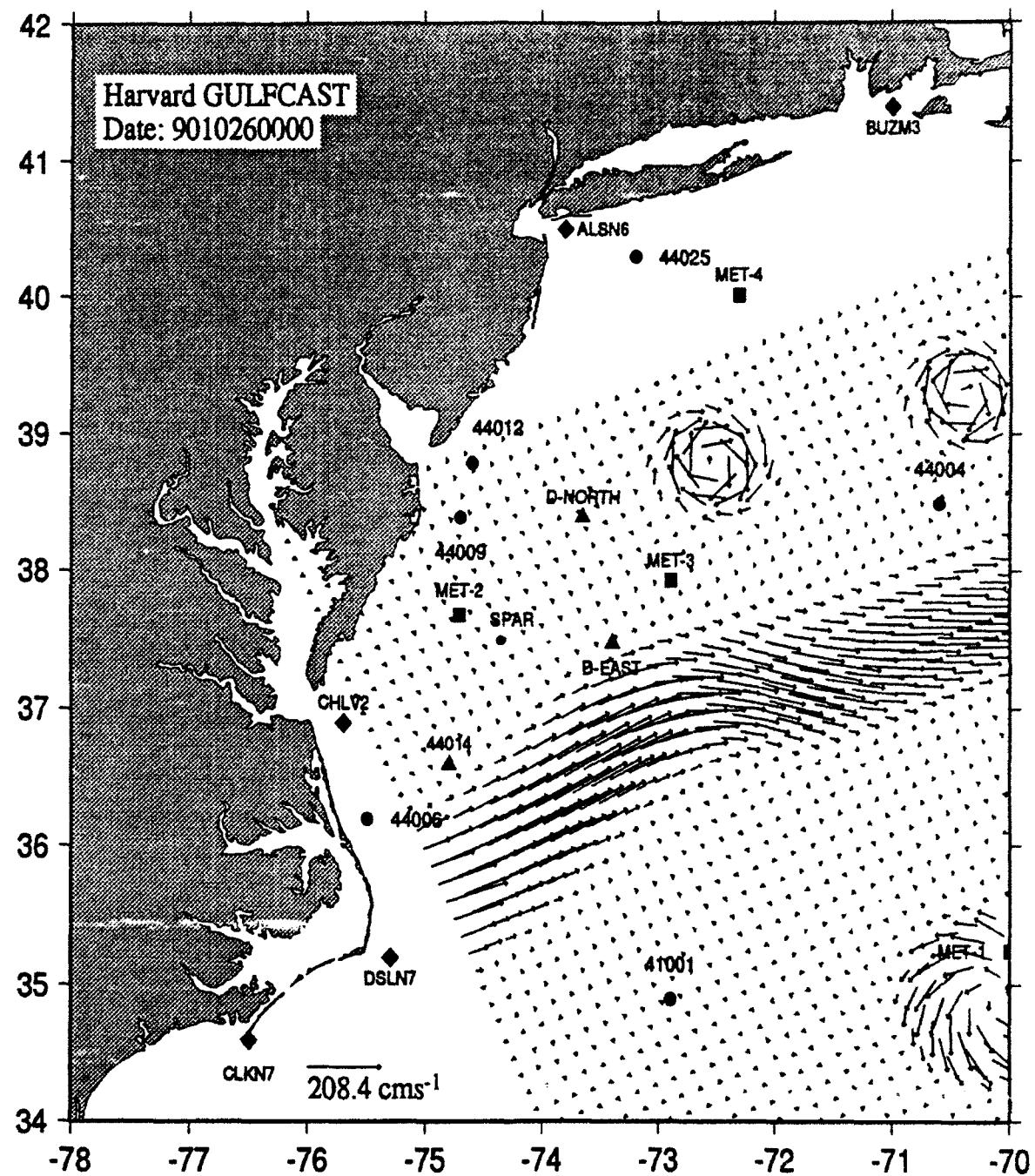


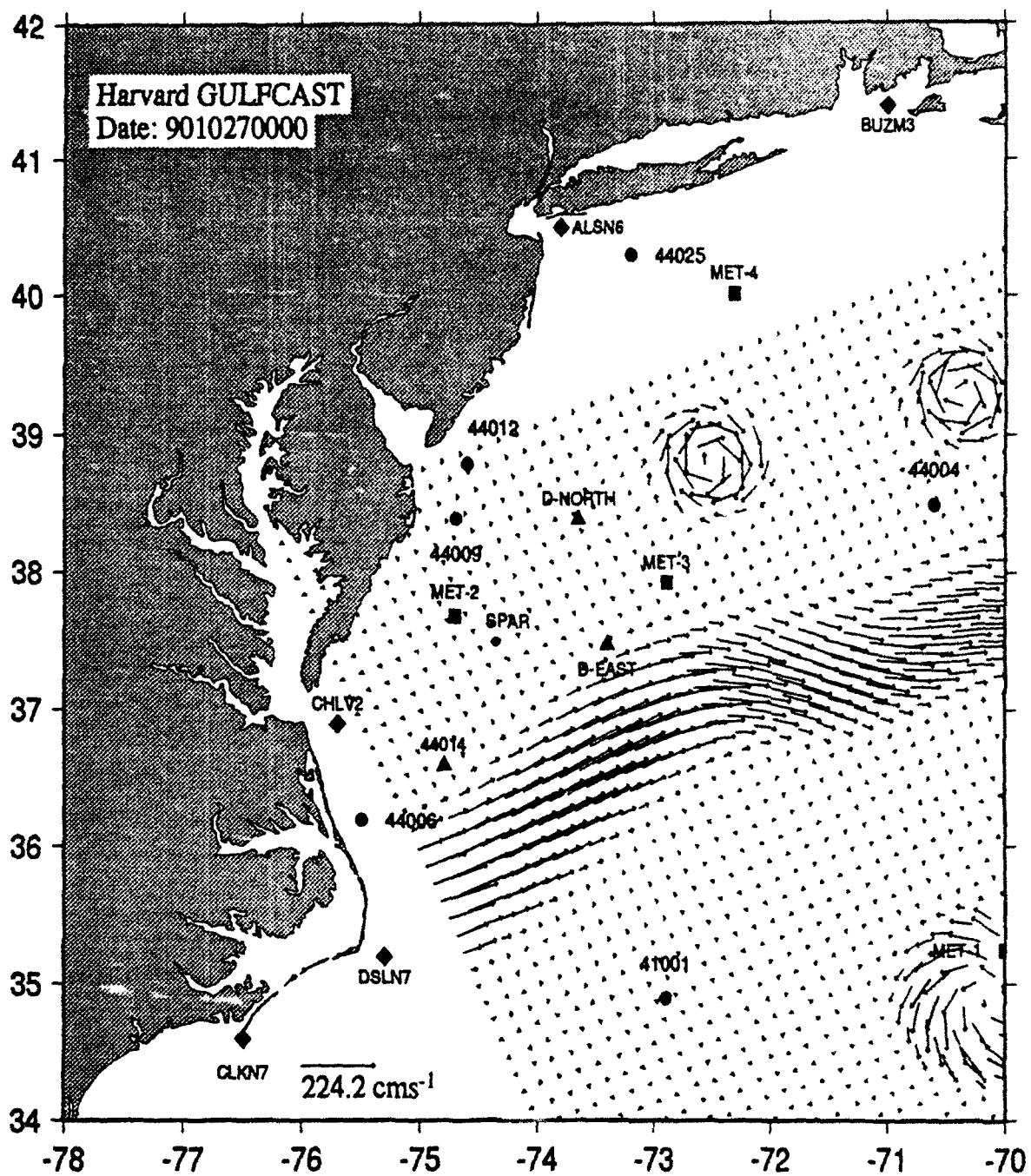


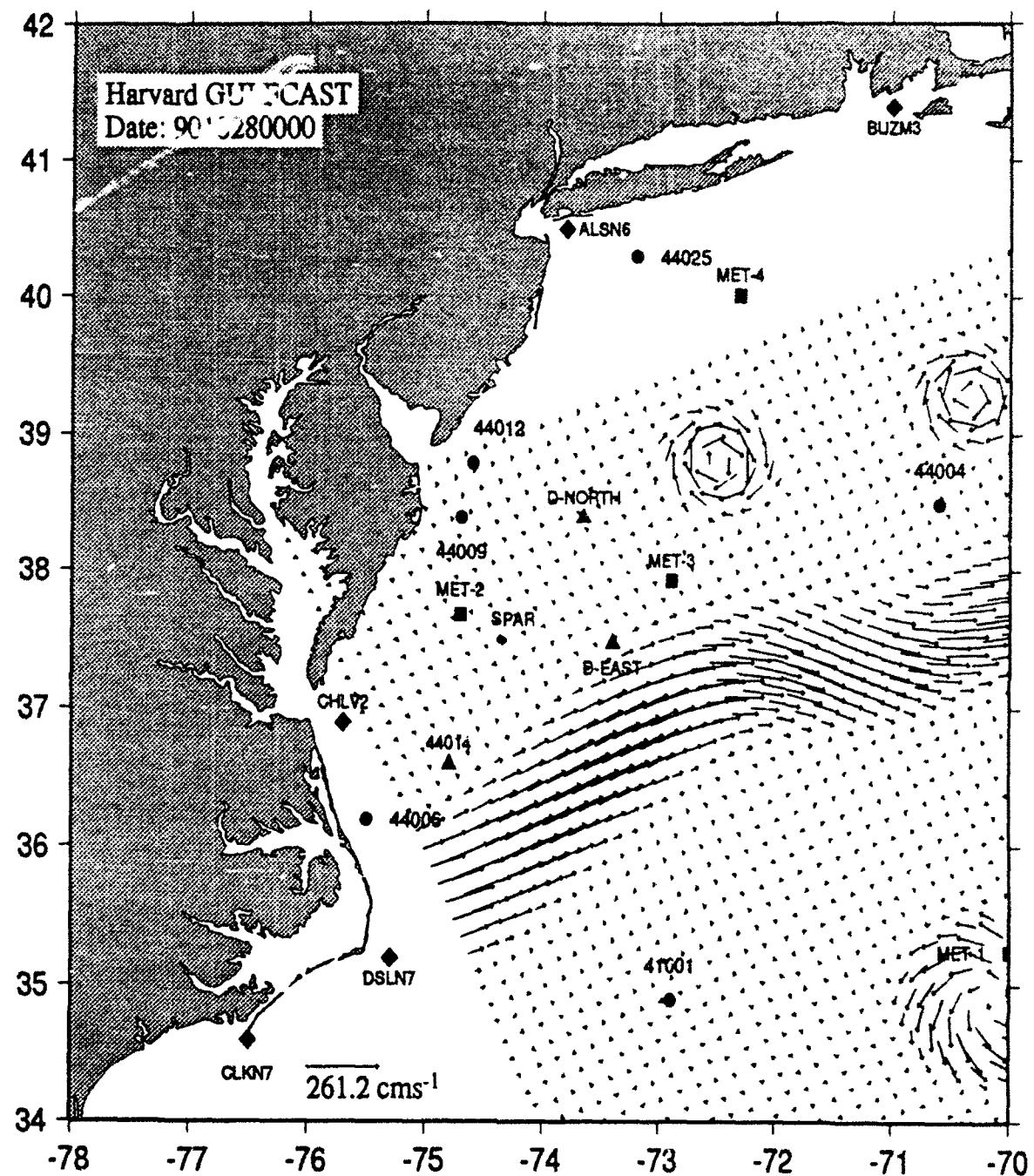


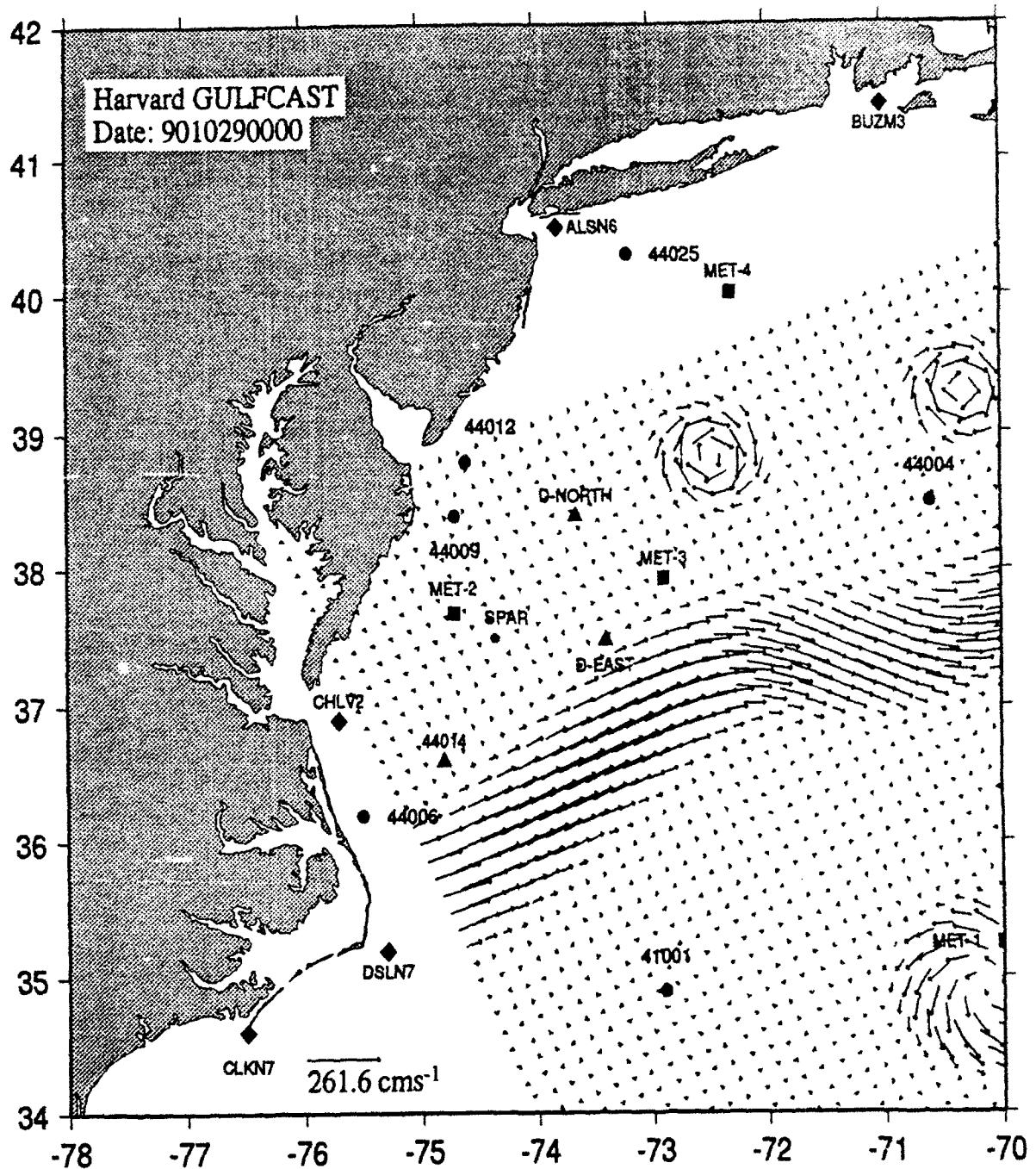


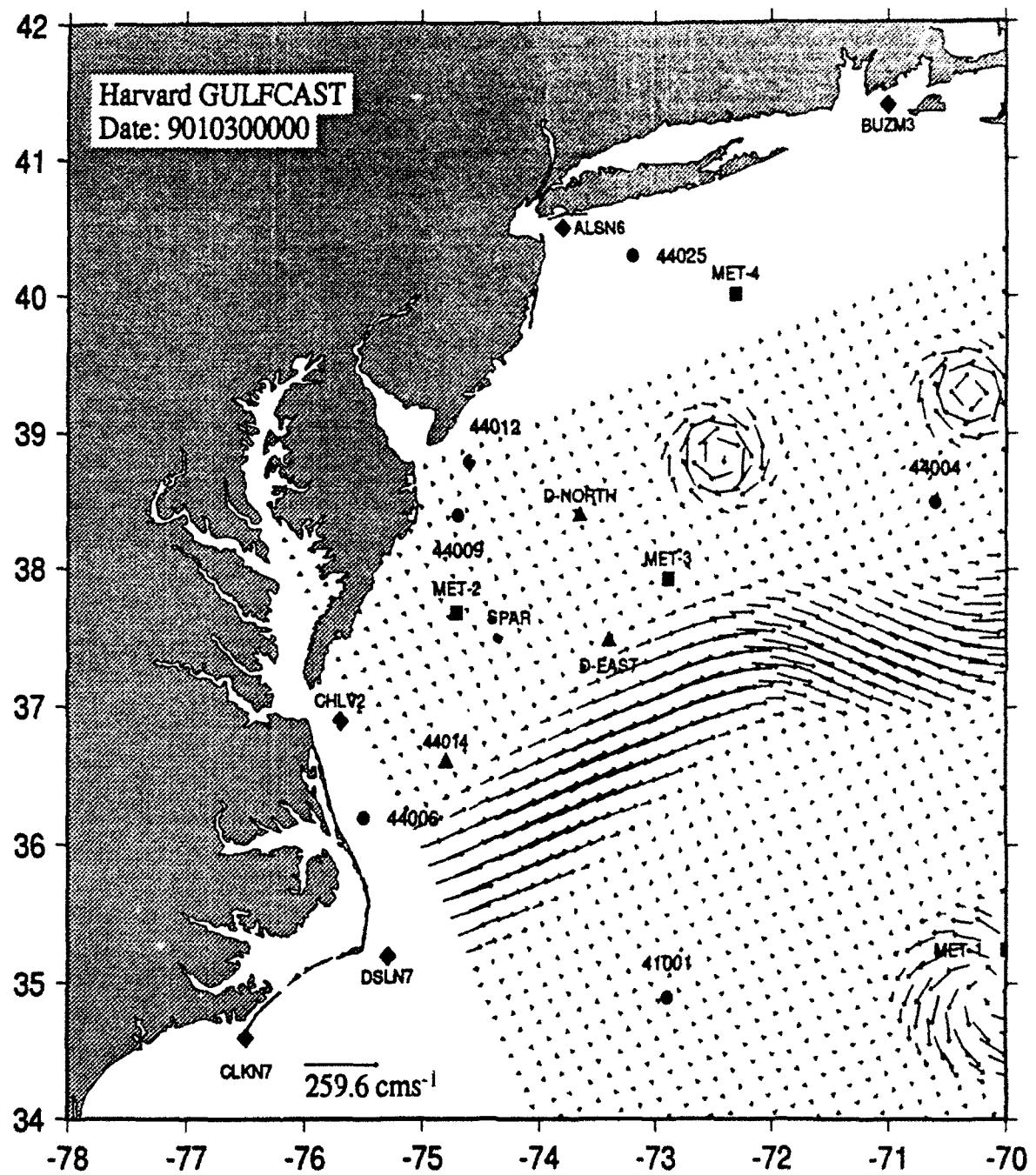


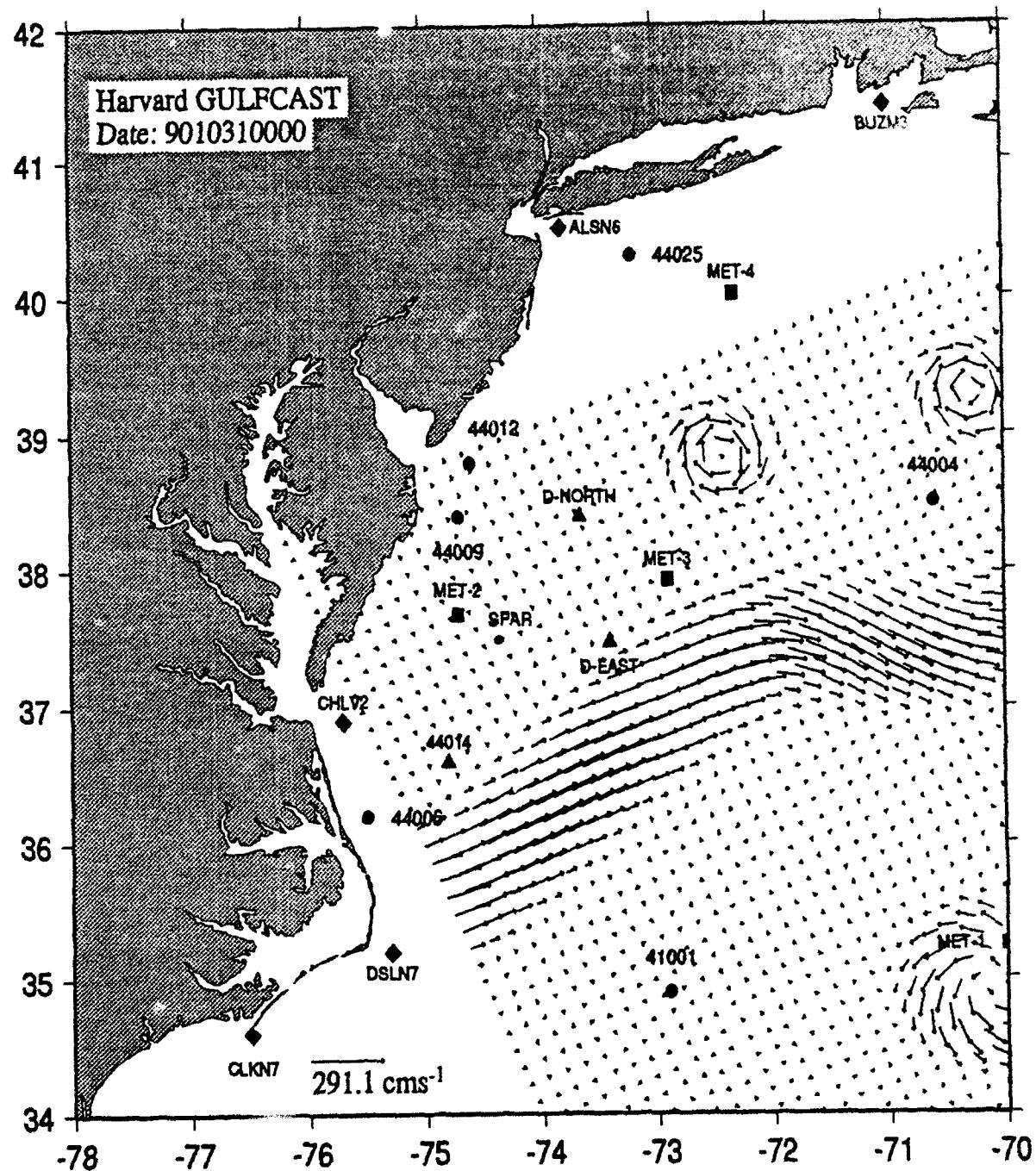












REPORT DOCUMENTATION PAGE

Form Approved
OMB NO. 0704-0188

Public reporting burden for this collection of information is estimated to average 1 hour per response, including the time for reviewing instructions, searching existing data sources, gathering and maintaining the data needed, and completing and reviewing the collection of information. Send comments regarding this burden estimate or any other aspect of this collection of information, including suggestions for reducing this burden, to Washington Headquarters Services, Directorate for Information Operations and Reports, 1215 Jefferson Davis Highway, Suite 1204, Arlington, VA 22202-4302, and to the Office of Management and Budget, Paperwork Reduction Project (0704-0188), Washington, DC 20503.

REPORT DOCUMENTATION PAGE			Form Approved OMB NO. 0704-0188
Public reporting burden for this collection of information is estimated to average 1 hour per response, including the time for reviewing instructions, searching existing data sources, gathering and maintaining the data needed, and completing and reviewing the collection of information. Send comments regarding this burden estimate or any other aspect of this collection of information, including suggestions for reducing this burden, to Washington Headquarters Services, Directorate for Information Operations and Reports, 1215 Jefferson Davis Highway, Suite 1204, Arlington, VA 22202-4302, and to the Office of Management and Budget, Paperwork Reduction Project (0704-0188), Washington, DC 20503.			
1. AGENCY USE ONLY (Leave Blank)	2. REPORT DATE	3. REPORT TYPE AND DATES COVERED	
	April 1993	Report 1 of a series	
4. TITLE AND SUBTITLE		5. FUNDING NUMBERS	
Observations and Modelling of Winds and Waves During the Surface Wave Dynamics Experiment; Report 1, Intensive Observation Period IOP-1, 20-31 October 1990		ORN Contracts N00014-90-J-1464 N00014-92-J-1546 N00014-88-J-1028 WU 32523	
6. AUTHOR(S)		8. PERFORMING ORGANIZATION REPORT NUMBER	
Michael J. Caruso, Hans C. Gruber, Robert E. Jensen, Mark A. Donelan		Technical Report CERC-93-6	
7. PERFORMING ORGANIZATION NAME(S) AND ADDRESS(ES)		9. SPONSORING/MONITORING AGENCY NAME(S) AND ADDRESS(ES)	
See reverse.		U.S. Army Corps of Engineers, Washington, DC 20314-1000; Office of Naval Research, 800 N. Quincy Street, Arlington, VA 22217	
11. SUPPLEMENTARY NOTES		10. SPONSORING/MONITORING AGENCY REPORT NUMBER	
Available from National Technical Information Service, 5285 Port Royal Road, Springfield, VA 22161.			
12a. DISTRIBUTION/AVAILABILITY STATEMENT		12b. DISTRIBUTION CODE	
Approved for public release; distribution is unlimited.			
13. ABSTRACT (Maximum 200 words)			
This report describes the compilation of observed and modelled wind and wave parameters during the first intensive observation period (IOP-1) from October 20-31, 1991, of the Surface Wave Dynamics Experiment. The measurements include wind speeds and directions, wave heights and periods, air and sea temperatures, and atmospheric pressures from three directional wave buoys, four meteorological buoys, and several routinely operated buoys from the National Data Buoy Center (NDBC). In addition, a summary of directional wave spectra is presented for this period. The model data include examples of wind fields from six numerical weather prediction models and the corresponding wave height maps as derived from the 3G-WAM ocean wave model. Estimated surface current velocities and directions from the Harvard quasi-geostrophic model are also presented for this time period.			
14. SUBJECT TERMS		15. NUMBER OF PAGES	
3G-WAM Gulf Stream currents	NDBC wave data SWADE	206	
16. PRICE CODE			
17. SECURITY CLASSIFICATION OF REPORT	18. SECURITY CLASSIFICATION OF THIS PAGE	19. SECURITY CLASSIFICATION OF ABSTRACT	
UNCLASSIFIED	UNCLASSIFIED	20. LIMITATION OF ABSTRACT	

7. (Concluded).

Department of Physical Oceanography

Woods Hole Oceanographic Institution, Woods Hole, MA 02543;

Rosenstiel School of Marine and Atmospheric Science

University of Miami, Miami, FL 33149-1098;

U.S. Army Engineer Waterways Experiment Station,

Coastal Engineering Research Laboratory,

3909 Halls Ferry Road, Vicksburg, MS 39180-6199;

National Water Research Institute

Canada Centre for Inland Waters, Burlington, Ontario L7R 4A6, Canada